

**Oxidative C–H Activation:
Convergent Fragment-Coupling approaches to Spiroacetals and the Total Synthesis of
Clavosolide A**

by

GuangRong Peh

BSc (Hons), National University of Singapore, 2007

Submitted to the Graduate Faculty of the
Dietrich School of Arts and Sciences in partial fulfillment
of the requirements for the degree of
Doctor of Philosophy

University of Pittsburgh

2015

UNIVERSITY OF PITTSBURGH
DIETRICH SCHOOL OF ARTS AND SCIENCES

This dissertation was presented

by

GuangRong Peh

It was defended on

September 30, 2015

and approved by

Dr. W. Seth Horne, Associate Professor, Department of Chemistry

Dr. Kazunori Koide, Associate Professor, Department of Chemistry

Dr. Jeffrey Hildebrand, Associate Professor, Departmental of Biological Sciences

Dissertation Advisor: Dr. Paul E. Floreancig, Professor, Department of Chemistry

Copyright © by GuangRong Peh

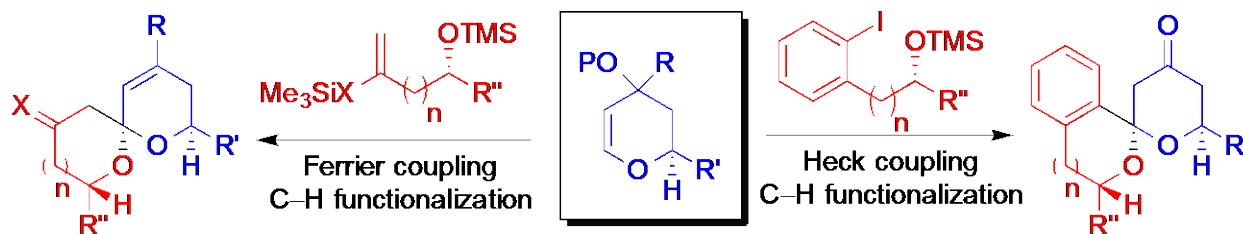
2015

OXIDATIVE C-H ACTIVATION: CONVERGENT FRAGMENT-COUPPLING
APPROACHES TO SPIROACETALS AND TOTAL SYNTHESIS OF
CLAVOSOLIDE A

GuangRong Peh, PhD

University of Pittsburgh, 2015

Two one-pot oxidative cyclization strategies to spiroacetals are described herein. The first approach utilizes a Lewis acid-mediated Ferrier reaction for the initial fragment coupling followed by 2,3-dichloro-5,6-dicyano-1,4-benzoquinone (DDQ)-initiated oxidative carbon–hydrogen bond cleavage and cyclization. The second approach relies on a Heck cross coupling for fragment assembly followed by a DDQ-mediated dehydrogenation of enol ethers into enones and subsequent acid-induced cyclization. These methods provide mild convergent protocols to spiroketal subunits, which are ubiquitous in natural products, medicinal drugs, and chemical libraries.



Cyclopropane-substituted allylic ethers undergo carbon–hydrogen bond cleavage to form stable oxocarbenium ions upon reaction with DDQ. Significantly, in the presence of an appending nucleophile, facile ring closure occurs to yield highly functionalized tetrahydropyrans with no

accompanied cyclopropane scission. This methodology was showcased during the total synthesis of the sponge-derived macrodiolide clavosolide A.

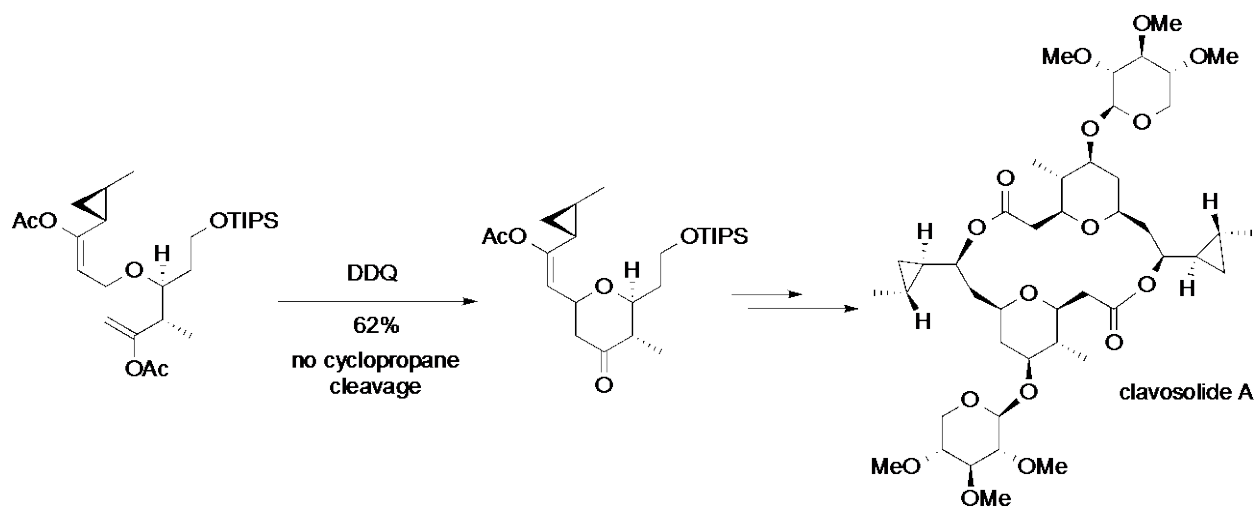


TABLE OF CONTENTS

LIST OF ABBREVIATIONS	XVII
PREFACE.....	XX
1.0 C–H FUNCTIONALIZATION	1
1.1 INTRODUCTION	1
1.2 DEVELOPMENT OF OXIDATIVE C–H BOND FUNCTIONALIZATION (FLOREANCIG GROUP).....	2
1.2.1 Pioneering work by Mukaiyama	2
1.2.2 Floreancig intramolecular oxidative C–H bond approach	4
1.2.3 Oxidative C–H bond activation: Bimolecular coupling	7
2.0 [N+1] APPROACHES TO THE SYNTHESIS OF DIVERSE SPIROACETALS THROUGH OXIDATIVE CATION FORMATION	10
2.1 INTRODUCTION	10
2.1.1 The spiroacetal privileged structure	10
2.1.2 Notable strategies for spiroacetals synthesis	11
2.1.2.1 Acid catalyzed cyclization (Brønsted and Lewis acids)	11
2.1.2.2 Reagent-controlled spiroketalization	14
2.1.2.3 Periphery spiroketal functionalization.....	15
2.1.2.4 Metal-catalyzed hydroalkoxylation.....	17

2.1.2.5	Oxidative radical spiroketalization	19
2.1.2.6	Telescoped cycloaddition and Carbon–Hydrogen activation (Floreancig approach)	22
2.2	TANDEM LEWIS ACID MEDIATED FERRIER COUPLING AND DDQ OXIDATIVE SPIROCYCLIZATION	25
2.2.1	Design principles	25
2.2.2	Exploration of the reaction protocol	26
2.2.3	Design and synthesis of dihydropyrans	29
2.2.4	Design and synthesis of nucleophiles.....	31
2.2.5	Scope of one-pot two component spirocyclization	33
2.2.6	Post cyclization modifications.....	37
2.2.7	Stereoelectronic analysis of Ferrier-coupling and DDQ mediated C-H activation.....	40
2.2.7.1	5'-substituted pyranol	40
2.2.7.2	5' and 6'-disubstituted pyranol systems.....	46
2.2.8	Summary.....	54
2.3	TELESCOPED HECK AND OXIDATIVE COUPLING	55
2.3.1	Design principles	55
2.3.2	Reaction optimization.....	56
2.3.3	Design and preparation of silylated glycals	59
2.3.4	Design and preparation of Heck aryl iodide partner	60
2.3.5	Substrate scope of telescoped Heck coupling with oxidative cyclization	61
2.3.6	Post cyclization modifications.....	64

2.3.7	Stereoelectronic analysis of telescoped Heck-coupling cyclization	67
2.3.7.1	Heck Coupling	67
2.3.7.2	DDQ mediated dehydrogenation	69
2.3.7.3	<i>p</i> -TSA catalyzed spiroketalization	70
2.3.8	Summary	72
3.0	TOTAL SYNTHESIS OF CLAVOSOLIDE A: A SHOWCASE OF OXIDATIVE OXOCARBENIUM CATION COMPATIBILITY WITH CYCLOPROPANE	73
3.1	INTRODUCTION	73
3.1.1	Isolation of clavosolides A-D from marine organism	73
3.1.2	Structural determination of clavosolide A	74
3.1.3	Previous syntheses of (-)-clavosolide A	75
3.1.3.1	Willis's total synthesis of clavosolide A diastereomer	76
3.1.3.2	Smith's total synthesis of clavosolide A	77
3.1.3.3	Lee's total synthesis of clavosolide A	78
3.2	DESIGN PRINCIPLE: STABILIZATION OF CYCLOPROPYL RING THROUGH CONJUGATED OXOCARBENIUM CATION	79
3.2.1	Model substrate design and preparation	80
3.3	RETROSYNTHETIC DISCONNECTION FOR (-)-CLAVOSOLIDE A ..	84
3.3.1	Synthesis of cyclopropyl containing subunit	85
3.3.2	Synthesis of cyclization substrates	87
3.3.3	Oxidative cyclization and completion of the synthesis	90
3.3.4	Summary	94
	APPENDIX A	96

APPENDIX B	156
BIBLIOGRAPHY	182

LIST OF TABLES

Table 1 Selected examples of THP accessible by DDQ C–H bond activation.....	5
Table 2 Optimization of glycal Heck coupling.....	57
Table 3 Further examples of tandem Heck oxa-Micheal fragment coupling	63

LIST OF FIGURES

Figure 1.1 State-of-the-art C–H bond activation	2
Figure 1.2 Mukaiyama’s DDQ-mediated oxidative coupling.....	3
Figure 1.3 DDQ-mediated metal-free C–H bond activation.....	4
Figure 1.4 Bimolecular chromene coupling.....	8
Figure 2.1 Spiroketal containing compounds	10
Figure 2.2 Dehydrative spiroketal strategy	12
Figure 2.3 Intramolecular Sakurai coupling	13
Figure 2.4 Design principle of bimolecular oxidative coupling	25
Figure 2.5 Tandem Ferrier-oxidative annulation	26
Figure 2.6 Proposed pathway for regeneration of TMSOTf.....	28
Figure 2.7 NMR determination of stereochemistry for 2.117	41
Figure 2.8 Negative control for nOe correlation.....	42
Figure 2.9 Positive and negative nOe correlation for Ferrier intermediate 2.117	43
Figure 2.10 Stereochemical outcome of DDQ mediated spirocyclization	44
Figure 2.11 Stereochemical determination of 2.120.....	45
Figure 2.12 Positive nOe correlation between H _f and H _g	45
Figure 2.13 Negative nOe correlation control for alternative isomer	45
Figure 2.14 Negative control for nOe establishment	46

Figure 2.15 Stereochemical determination of Ferrier products: 2.122 and 2.123	47
Figure 2.16 Curtin-Hamett analysis of Ferrier coupling.....	48
Figure 2.17 Stereochemical determination of spiroketals 2.127 and 2.128.....	50
Figure 2.18 Stereochemical analysis of oxidative C–H cyclization	51
Figure 2.19 Stereochemical determination of OTBS Ferrier products	53
Figure 2.20 Stereochemical determination of spiroketals 2.135 and 2.136.....	54
Figure 2.21 Telescoped transition metal cross-coupling with oxidative coupling	56
Figure 2.22 Stereochemical assignment for 2.149.....	64
Figure 2.23 Substrate controlled stereoselective epoxidation.....	66
Figure 2.24 Stereochemical determination of Rubottom oxidation.....	66
Figure 2.25 Stereochemical analysis of glycal-Heck coupling.....	68
Figure 2.26 Stereochemical analysis of Heck intermediate 2.156.....	68
Figure 2.27 DDQ mediated dehydrogenation of glycal.....	69
Figure 2.28 Stereochemical correlation for 2.160b	70
Figure 2.29 Acid catalyzed pseudo oxa-Micheal spiroketalization	71
Figure 2.30 Stereochemical correlation for 2.141	71
Figure 3.1 Members of the clavosolide family	74
Figure 3.2 Selected spectroscopic analysis for 3.1	75
Figure 3.3 Stabilization of cationic cyclopropanes.....	79
Figure 3.4 Nucleophilic addition into conjugated cyclopropyl oxocarbenium.....	80
Figure 3.5 Retrosynthetic analysis of 3.1.....	84
Figure 3.6 Feringa's tandem conjugate addition and cyclopropanation.....	85
Figure 3.7 Stereochemical analysis of intramolecular S _N 2 reaction.....	86

Figure 3.8 Proposed directing group effect by cyclopropane	89
Figure 3.9 Stereochemical model for CBS reduction	93
Figure 3.10 HPLC traces for conjugate addition product of 3.29: Enantioenriched sample (pink) and racemic mixture (black)	165

LIST OF SCHEMES

Scheme 1.1 DDQ mediated transformations of heterocycles	7
Scheme 1.2 Sequential oxidative addition and cyclization.....	9
Scheme 2.1 Acid-catalyzed spiroketalization to the core of ossamycin.....	12
Scheme 2.2 Intramolecular hetero-Micheal addition for spiroketal assembly	13
Scheme 2.3 Reagent-controlled epoxide-opening spirocyclization.....	15
Scheme 2.4 Inverse demand HDA approach to spiroketals.....	16
Scheme 2.5 Spiropyranone approach.....	17
Scheme 2.6 Metal catalyzed hydroalkoxylation	18
Scheme 2.7 Stereoconvergent Au-catalyzed spiroketalization.....	19
Scheme 2.8 Mechanism of oxidative radical cyclization.....	20
Scheme 2.9 Oxidative radical approach to core of bistramide C.....	21
Scheme 2.10 Tandem radical cyclization	22
Scheme 2.11 DDQ mediated oxidative deprotection.....	23
Scheme 2.12 Spiroketal formation: One-pot hetero Diel-Alder addition and C-H functionalization	24
Scheme 2.13 Screening of catalysts for Ferrier coupling	27
Scheme 2.14 TMSOTf catalyzed Ferrier Coupling	27
Scheme 2.15 Optimized Ferrier tandem oxidative cyclization.....	29

Scheme 2.16 Synthesis of pyranones	30
Scheme 2.17 Synthesize of dihydropyranols	30
Scheme 2.18 Synthesize of dihydrothiapyranol.....	31
Scheme 2.19 Preparation of allyl silanes (I)	32
Scheme 2.20 Preparation of allyl silane (II)	33
Scheme 2.21 Substrate scope of DDQ-mediated spiroannulation	35
Scheme 2.22 Debenzylating conditions for spiroketals	38
Scheme 2.23 Attempted hydrozirconation on spiroketal 2.104.....	38
Scheme 2.24 Post cyclization modifications of alkynyl-containing spiroketals (I).....	39
Scheme 2.25 Post cyclization modifications of alkynyl-containing spiroketals (II)	40
Scheme 2.26 Stereochemical analysis of Ferrier reaction	41
Scheme 2.27 Ferrier coupling of 2.121	47
Scheme 2.28 Stereoconvergent oxidative cyclization	49
Scheme 2.29 Ferrier coupling with bulkier substituent	52
Scheme 2.30 Optimized DDQ mediated dehydrogenation and acid catalyzed oxa-Micheal	58
Scheme 2.31 Preparation of Heck glycal acceptors	60
Scheme 2.32 Preparation of Heck donar partner with tethered alcohol	61
Scheme 2.33 Rubottom oxidation of 2.166	65
Scheme 3.1 Willis synthesis of (-)-clavosolide A diastereomer	76
Scheme 3.2 Smith's Petasis-Ferrier rearrangment tactic.....	77
Scheme 3.3 Lee's intramolecular oxa-Micheal cyclization strategy	78
Scheme 3.4 En-route to alkynal propargylic ether 3.18.....	81
Scheme 3.5 Preparation of cyclopropane containing vinyl silanes.....	82

Scheme 3.6 Oxidative cyclization of cyclopropane containing substrates	83
Scheme 3.7 Cyclopropane subunit homologation	86
Scheme 3.8 Fragment coupling and enol acetates formation	88
Scheme 3.9 DDQ mediated oxidative cyclization	90
Scheme 3.10 Glycosidation and reduction of cyclopropyl ketone	91
Scheme 3.11 End game for (-)-clavoslide A	94

LIST OF ABBREVIATIONS

A ^{1,2}	allylic 1,2
BBN	9-borabicyclo[3.3.1]nonane
BOM	benzyloxymethyl acetal
CBS	Corey–Bakshi–Shibata
C–H	carbon-hydrogen
COSY	correlation spectroscopy
CSA	camphorsulfonic acid
DCE	dichloroethane
HDA	hetero Diels-Alder
DDQ	2,3-dichloro-5,6-dicyano-1,4-benzoquinone
DHP	dihydropyran
DMF	dimethylformamide
DOS	diversity-oriented synthesis
DPPF	1,1'-ferrocenediyl-bis(diphenylphosphine)
DtBMP	2,6-di- <i>tert</i> -butylpyridine
HMBC	heteronuclear multiple-bond correlation spectroscopy
IR	infrared
LAH	lithium aluminium hydride

LDA	lithium diisopropylamide
LiDBB	lithium di-tert- butylbiphenyl
LiHMDS	lithium hexamethyldisilazide
<i>m</i> -CPBA	<i>meta</i> -chloroperoxybenzoic acid
MS	molecular sieves
Ms	mesyl
NIS	N-iodosuccinimide
NMR	nuclear magnetic resonance
nOe	nuclear Overhauser effect
NOESY	nuclear Overhauser effect spectroscopy
PMB	<i>para</i> -methoxybenzyl
<i>p</i> -TSA	<i>para</i> -toluenesulfonic acid
RDS	rate-determining step
ROESY	rotating frame nuclear Overhauser effect spectroscopy
rt	room temperature
TBS	<i>tert</i> -butyldimethylsilyl
TEMPO	(2,2,6,6-tetramethylpiperidin-1-yl)oxyl
TES	triethylsilyl
TFA	trifluoroacetic acid
THP	tetrahydropyran
TIPS	triisopropylsilyl chloride
TLC	thin layer chromatography
TMS	trimethylsilyl

TolBINAP 2,2'-bis(di-*p*-tolylphosphino)-1,1'-binaphthyl
TsDPEN *p*-tosyl-1,2-diphenylethylenediamine

PREFACE

I would like to thank my advisor Professor Paul Floreancig for his continuous support and encouragement. I am also thankful for his patience and magnanimous heart for the mistakes I have committed during my Phd candidature. Paul is a walking encyclopedia of organic chemistry and my research projects would not have come to fruition without his intellectual input. I strongly urge current groups members to utilize this valuable source of knowledge while they are still in the group. Committee professors Seth Horne and Kazunori Koide are thanked for their insightful feedback about my research work. Proposal mentor Tara Meyer is acknowledged for the constructive advices during the arduous writing process and the subtle nuances that differentiates an actual NIH/NSF proposal from a research “idea”.

I would like to thank all past and current group members who have contributed to my experience in the Floreancig group. I had unique experience of learning valuable lab techniques from veterans: Lei Liu and Shuangyi Wan, which have been instrumental in the mastery of my hands skills. Chunliang Lu has been of tremendous support both in my academia work and personal life. Xun Han is acknowledged for his wisdom and the laughter shared together. Tyler Rohrs is thanked for his selfless contributions in the maintenance of the lab equipments; the lab would not be functioning without his diligent upkeep. I would also like to thank Professor Hildebrand for agreeing to be my external committee member on such short notice. The electronic version of

this thesis would not be possible without the technical expertise of Mr Richard Hoover (Pitt ETD) during the formatting process.

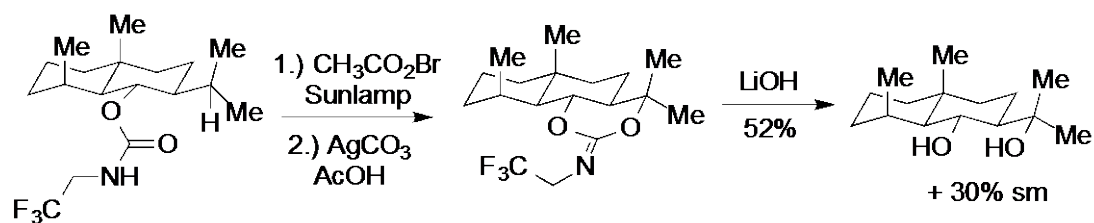
Lastly, I would like to thank my wife for her unrelenting love, trust and patience with me. I am also indebted to my brother for taking care of the family when I am not around.

1.0 C–H FUNCTIONALIZATION

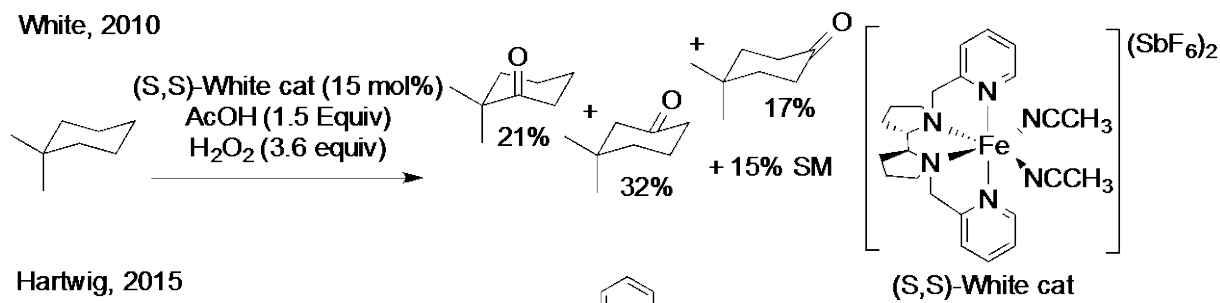
1.1 INTRODUCTION

In recent years, C–H bond activation^[1] has emerged as an important area of research because of its potential to streamline syntheses and reduce waste. Due to the strength of a C–H bond^[2] ($\Delta H \approx 400$ kJ/mol), cleavage of such bonds is not trivial and generally requires a metal catalyst to lower the barrier of activation. Substrates subjected to C–H bond activation also generally require an ancillary group for binding of the catalyst^[3]; to ensure guided regioselective functionalization at the desired site. Notably, Baran^[4] utilized a carbamate-directing group for accessing 1,3-diols via a modified Hofmann-Löffler-Freytag (HLF) reaction (Figure 1.1). In an attempt to mimic remote C–H functionalization displayed by enzyme catalysis, groups such as White^[5] and Hartwig^[6] have designed novel iron catalysts for site-selective functionalization (Figure 1.1). These catalysts differentiate C–H bonds by exploiting intrinsic subtle stereoelectronic variation within the molecules. However, generality in substrate scope is often not obvious and requires further optimization on a case-by-case basis.

Baran, 2009



White, 2010



Hartwig, 2015

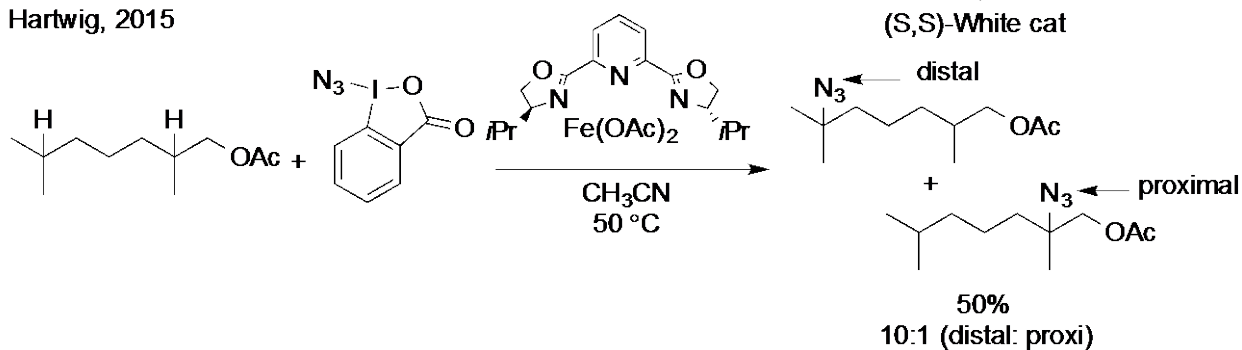


Figure 1.1 State-of-the-art C–H bond activation

1.2 DEVELOPMENT OF OXIDATIVE C–H BOND FUNCTIONALIZATION (FLOREANCIG GROUP)

1.2.1 Pioneering work by Mukaiyama

Oxidation is a one of the key transformations in an organic synthesis. While there are many reagents designed for selective oxidation, there are very few oxidants that can generate cationic species by hydride abstraction. This has significant consequences as these carbocations can be

employed in cascade transformation by reaction with appropriate nucleophiles. As early as the late 1980s, Mukaiyama and co-workers^[7] discovered that 2, 3-dichloro-5, 6-dicyano-1, 4-benzoquinone (DDQ) **1.2** could be used to oxidize allyl ethers **1.1** into their corresponding cationic species which reacted readily with silyl carbon nucleophiles (Figure 1.2).

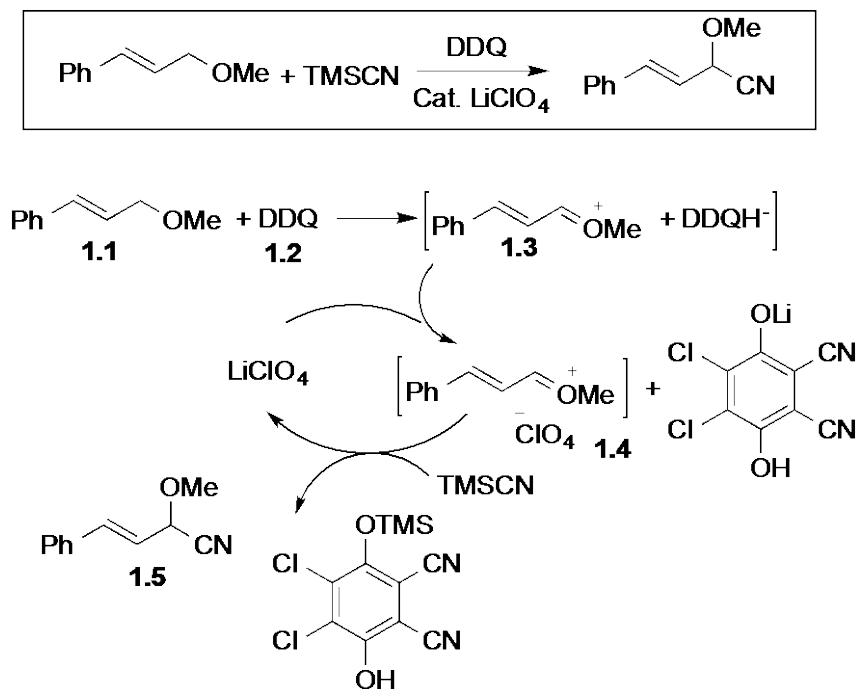


Figure 1.2 Mukaiyama's DDQ-mediated oxidative coupling

A counter ion exchange between the initial DDQH⁻ and LiClO₄ generates a more electrophilic ion pair **1.4** that reacts with TMSCN to afford product **1.5** along with the regenerated LiClO₄. This procedure enabled the oxidation and addition process to be performed in a one-pot manner and the isolation of cationic intermediates unnecessary.

1.2.2 Floreancig intramolecular oxidative C–H bond approach

The Floreancig group has a long-standing interest in oxidative methods used for the formation of carbon-carbon as well as carbon-hydrogen bonds. In an oxidative carbon-bond activation proposal^[8] initiated in 2008, Dr. Tu and Dr. Liu exploited the oxidative nature of DDQ to form aryl-substituted oxocarbenium ions from benzylic ethers. In the presence of an appended enol acetate nucleophile, an intramolecular carbon-carbon bond formation occurred with excellent diastereoselective control (Figure 1.3).

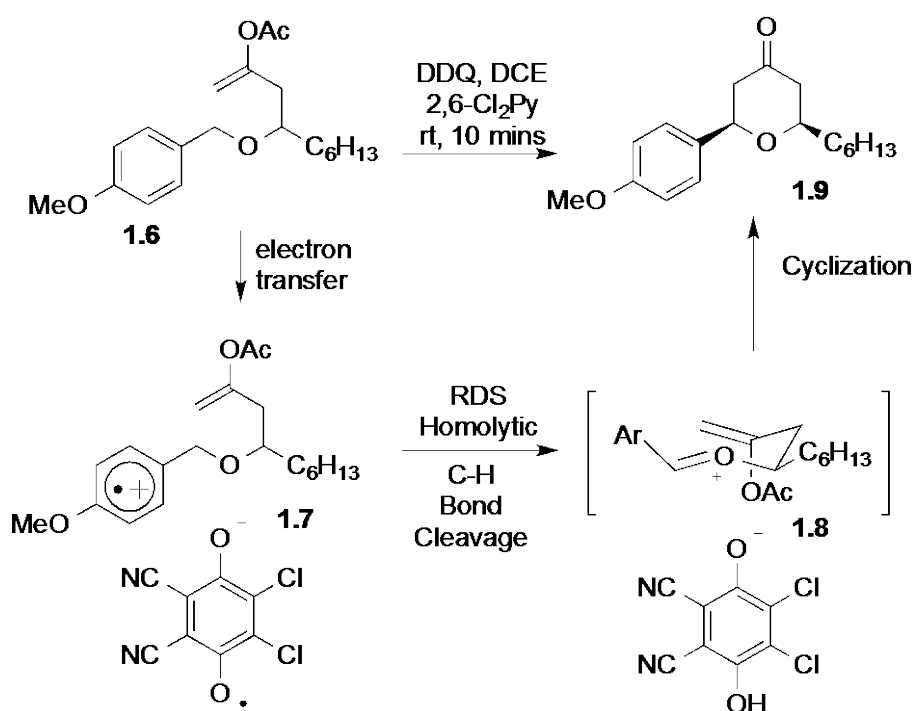
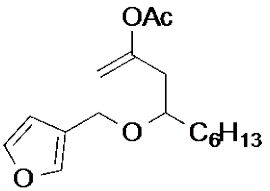
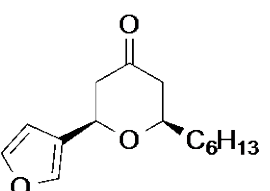
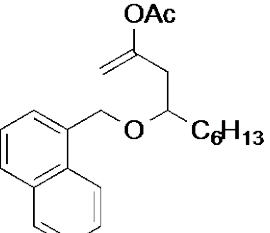
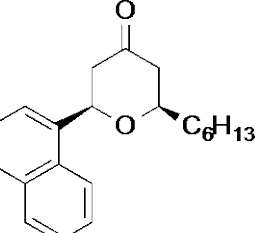
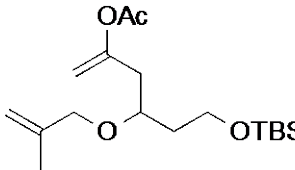
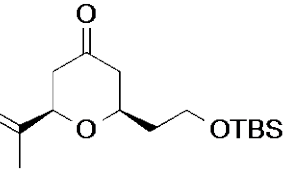
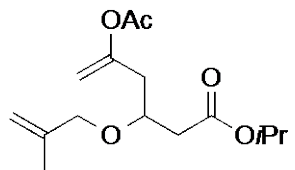
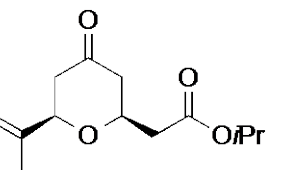


Figure 1.3 DDQ-mediated metal-free C–H bond activation

The proposed mechanism initiates by an initial one-electron oxidation of the PMB group on the enol acetate ether **1.6** into the radical cation **1.7** with the corresponding DDQ- radical counter anion. Due to the decreased bond strength of the adjacent C–H bond, the bond is activated and

undergoes C–H bond cleavage by rate-determining hydrogen atom transfer to give ion-pair **1.8**. Oxocarbenium **1.8** adopts a stable (*E*)-conformation, minimizing potential diaxial interactions with all the substituents adopting the *trans* configuration. Subsequent cyclization and acetyl group cleavage affords **1.9**.

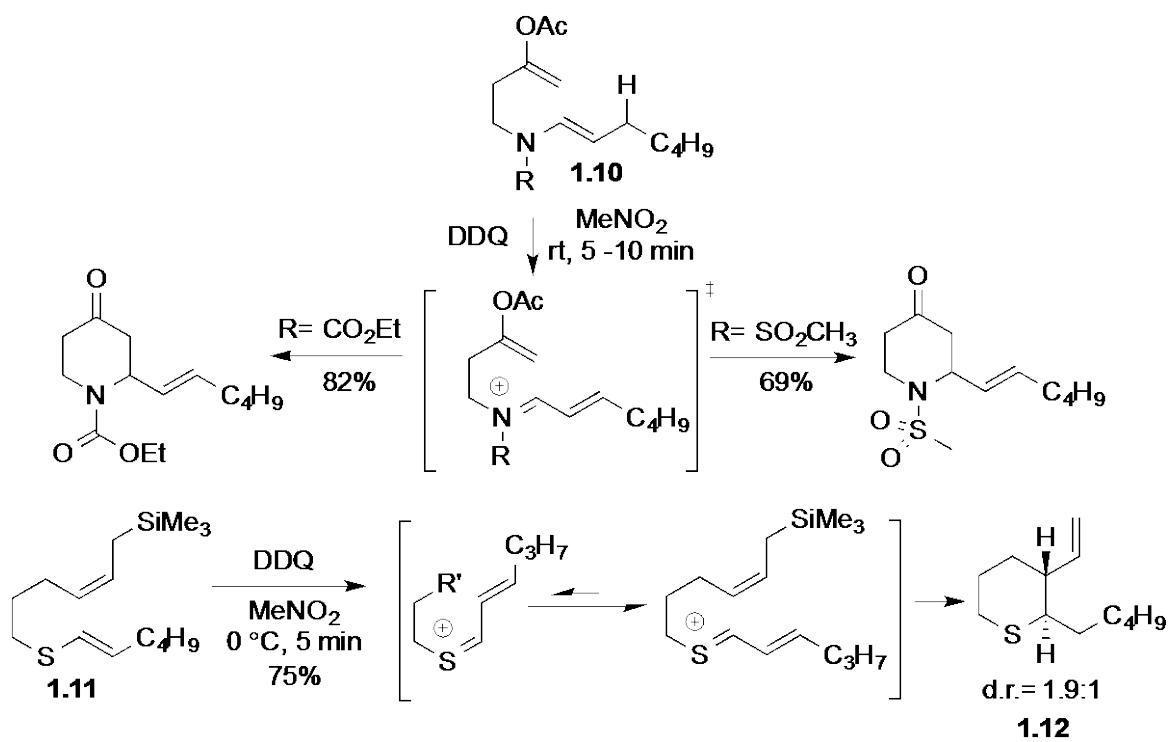
Table 1 Selected examples of THP accessible by DDQ C–H bond activation

Entry	Substrates	Products	t [h]	Yield (%)
1			12	63
2			4	84
3			24	75
4 ^a			12	77

Substrate, 2,6-dichloropyridine (4 equiv), and 4 Å M.S. were stirred in DCE for 15–30 min. DDQ (2 equiv) was then added and the reaction mixture was stirred for the indicated time. [a] Reaction was conducted at 45 °C.

Aromatic substrates (Table 1) generally perform well with electron-donating arenes having the highest reactivity due to lower oxidation potentials and better stability of the intermediate cations. The substrate scope was also expanded to allylic ethers (entries 3 and 4) with adjacent functional groups such as silyl ethers and electrophilic ester groups.

Mr. Brizgys and Dr. Cui further expanded this DDQ-mediated oxidative C–H bond activation protocol into nitrogen^[9]- and sulfur^[10]-containing heterocycles respectively (Scheme 1.1). Some key differences noted were: 1) During the piperidine synthesis, *N*-vinyl amides/sulfonamides **1.10** with lower oxidation potential were used instead as *N*-allyl amides were completely unreactive. 2) Oxidation of vinyl sulfides **1.11** generally gave lower stereoselectivity of the cyclized thiopyran **1.12** than the corresponding allylic ethers. This is due to the lower kinetic barrier to equilibrium between the (*E*)- and (*Z*)-geometry of the thiocarbenium ion caused by the longer carbon–sulfur bond.



Scheme 1.1 DDQ mediated transformations of heterocycles

1.2.3 Oxidative C–H bond activation: Bimolecular coupling

The facile DDQ-mediated C–H bond oxidation and subsequent trapping with a tethered π -nucleophile has allowed for the stereodiversified synthesis of a wide variety of heterocycles. Though attractive, these protocols are not strategically ideal because a highly functionalized fragment must be prepared in advance before the actual oxidative cyclization reaction.

Whitlock defines molecular complexity by the number of rings, stereocenters, functional groups and size as defined by the number of bonds or molecular weight^[11]. As such, bimolecular coupling reactions are inherently advantageous processes for increasing molecular complexity and expediting complex molecules synthesis. The Floreancig group thus embarked on a

program to investigate DDQ mediated oxidative bimolecular coupling. Dr. Clausen succeeded in oxidizing various analogs of chromene into oxocarbenium cation **1.13** and subsequent trapping by external nucleophiles^[12] (Figure 1.4). Interestingly, he noticed that chromene possessing a flanking alcohol moiety could be trapped as spiroketal **1.14** under the oxidative DDQ conditions.

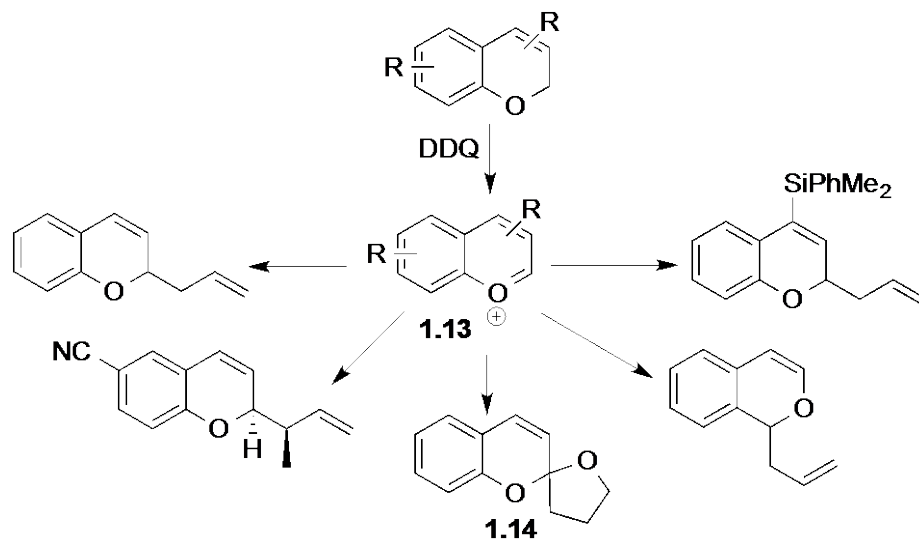
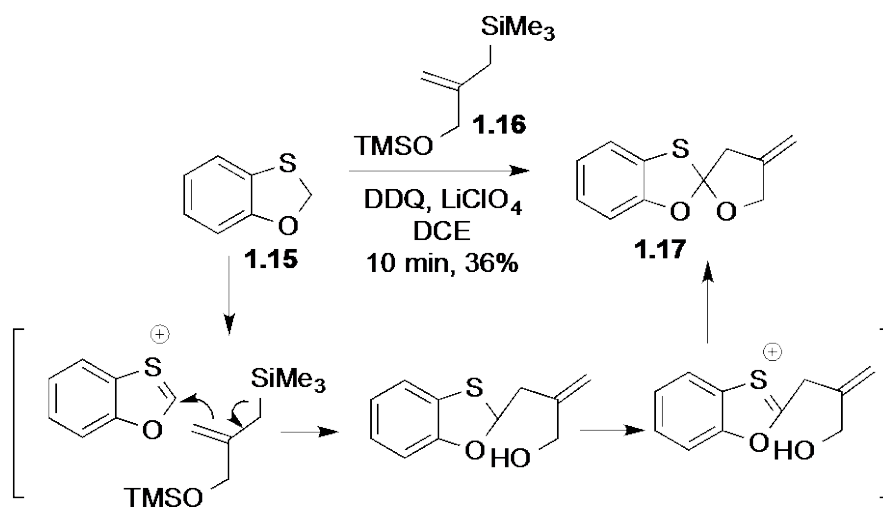


Figure 1.4 Bimolecular chromene coupling

Mr. Villafane also managed to access spiro-heterocycle **1.17** via a sequential one-pot fragment coupling of benzo[*d*][1,3]oxathiole **1.15** with allyl silane **1.16** (Scheme 1.2)^[13]. These two examples are key precedents, which eventually led to the development of the current Ferrier oxidative spirocyclization project.



Scheme 1.2 Sequential oxidative addition and cyclization

2.0 [N+1] APPROACHES TO THE SYNTHESIS OF DIVERSE SPIROACETALS THROUGH OXIDATIVE CATION FORMATION

2.1 INTRODUCTION

2.1.1 The spiroacetal privileged structure

Oxygen-containing spirocycles are important motifs in nature as evident in their abundance in natural products (Figure 2.1). The x-ray structure of the bistramide A **2.1** complex with actin reveals that the spiroketal subunit directly participates in the stabilization of the small molecule-protein interaction affecting regulation of metastatic cancer cells via H-bonding and hydrophobic effects^[14].

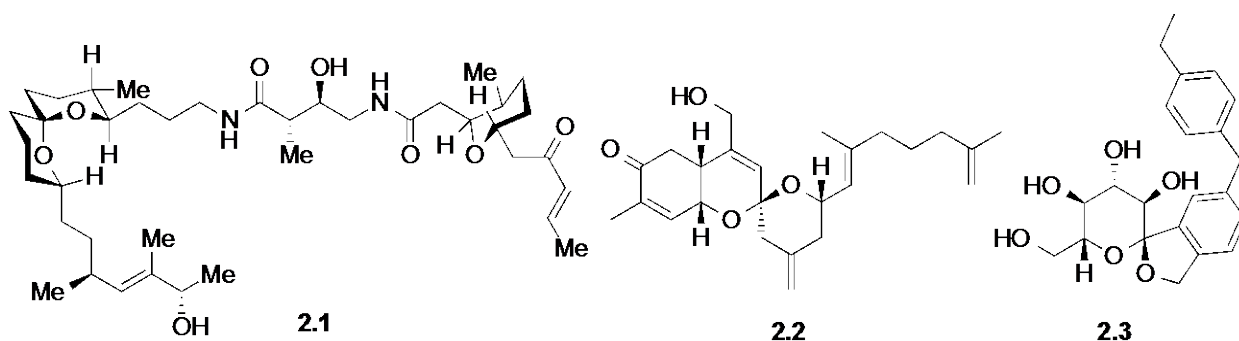


Figure 2.1 Spiroketal containing compounds

Alotaketal A **2.2** is an important activator of the cAMP-signaling pathway vital for daily life processes^[15]. The spiroketal subunit possessing a rigid, stereochemical defined sp^3 stereocenter is also an excellent candidate for fragment-based drug design (FDBB). It has a more sp^3 -enriched structure that can reach out and access previously uncharted chemical spaces^[16]. For instance, Tofogliflozin (CSG452) **2.3**, a synthetic compound with an *O*-spiroketal *C*-arylglucoside core combined with another aromatic sp^2 appendage, resulted in a highly potent phase III clinical lead for type 2 diabetes mellitus^[17].

2.1.2 Notable strategies for spiroacetals synthesis

This section will highlight some well-established as well as novel tactics for accessing spiroketals.

2.1.2.1 Acid catalyzed cyclization (Brønsted and Lewis acids)

The most commonly used protocol for spiroketal formation is based on a dehydrative approach^[18] (Figure 2.2), which requires the preparation of a generic ketone-diol **2.4**. In the presence of a catalytic acid, **2.4** cyclizes to form pyranol **2.5**, followed by the loss of water to form the oxocarbenium ion intermediate **2.6**, which readily undergoes ring closure to yield spiroketal **2.7**. The entire process is reversible and the final conformation of the spiroketal is driven by thermodynamics.

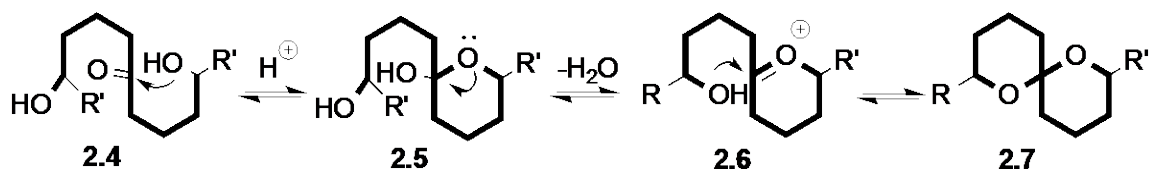
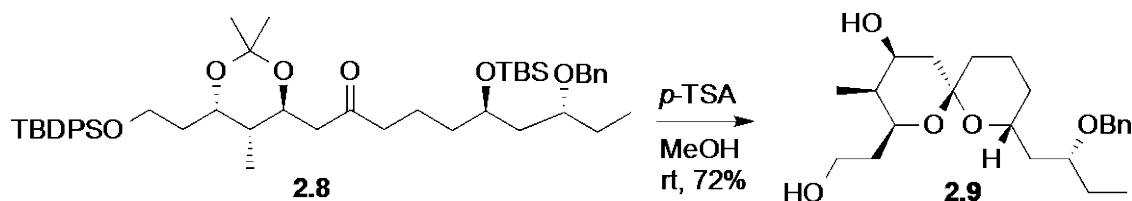


Figure 2.2 Dehydrative spiroketal strategy

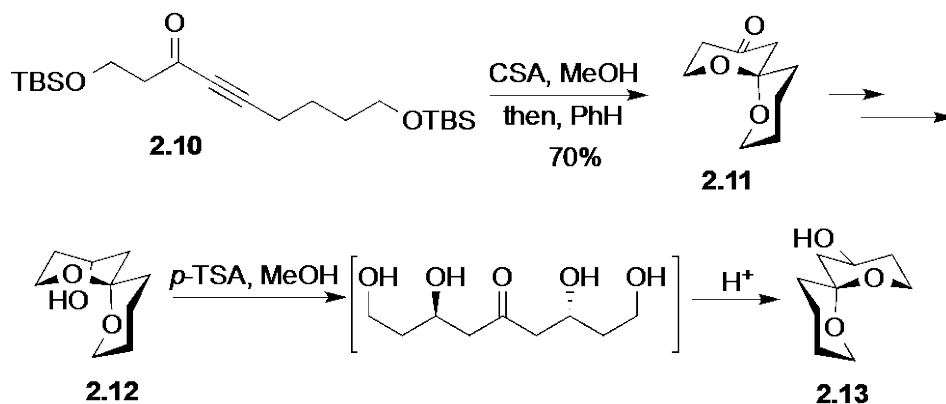
Recently, Yadav and co-workers applied this tactic during the synthesis of the spiroketal portion of ossamycin^[19] (Scheme 2.1). The highly functionalized intermediate **2.8** underwent a one-pot concomitant silyl-group deprotection and cyclization in the presence of *p*-TSA to afford the 6,6-spiroketal **2.9**.



Scheme 2.1 Acid-catalyzed spiroketalization to the core of ossamycin

Forsyth and co-workers^[20] utilized a double intramolecular hetero-Michael addition reaction for the racemic synthesis of a *Dacus oleae* olive fly pheromone **2.13** by the clever design of dihydroxy ynone **2.10** (Scheme 2.2). Treatment of ketone **2.10** with camphorsulfonic acid (CSA) in MeOH resulted in the cleavage of the silyl ether protecting groups followed by a solvent switch to benzene for facilitation of the bis-conjugate additions into the alkyne. Spiroketal **2.11** was subsequently reduced with NaBH₄ to give a mixture of alcohols, favoring the axially disposed alcohol **2.12**. Nevertheless, in the presence of *p*-TSA-catalyzed equilibration, spiroketal **2.12** was able to interconvert into the lower energy equatorial alcohol **2.13**. This method

possesses the added advantage of providing a useful ketone handle for further manipulation following post-cyclization.



Scheme 2.2 Intramolecular hetero-Michael addition for spiroketal assembly

Markó and co-workers^[21] reported a highly facile tactic of synthesizing spirocycles exploiting an intramolecular Hosomi-Sakurai between a bis-silylated reagent with either an acetal **2.14**, ketone or aldehyde to afford spiroketal **2.16**, spirocycle or THP respectively (Figure 2.3). The process is catalyzed by TMSOTf and is proposed to involve the oxocarbenium ion intermediate **2.17**.

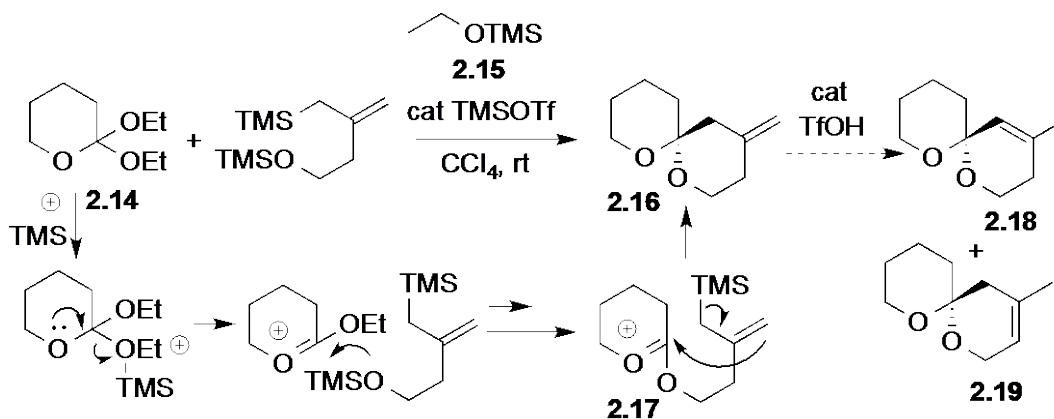
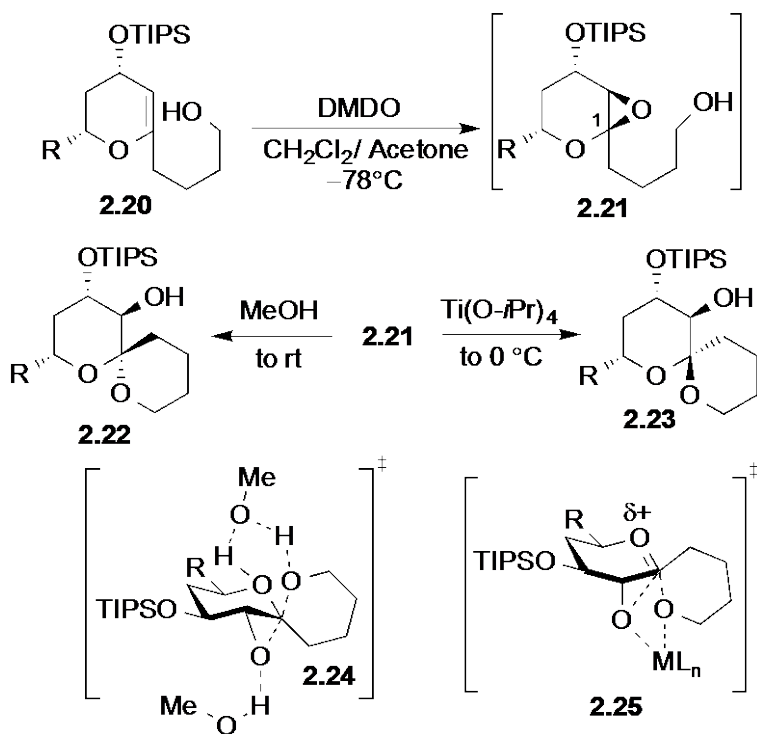


Figure 2.3 Intramolecular Sakurai coupling

They noted that by addition of another silyl ether **2.15** as an additive, they were able to quench any residual TfOH that might be formed by reaction with adventitious water. This was crucial because an even trace amount of this acid promoted undesired isomerization into *exo* isomers **2.18** and **2.19**. This protocol provides a simple yet adept, modular entry into the family of spirocycles.

2.1.2.2 Reagent-controlled spiroketalization

Tan and co-workers were able to utilize epoxide-opening spirocyclization (Scheme 2.3) to access a diverse library of spiroketals. Starting from glycol **2.20**, a mild *in-situ* epoxidation with DMDO produced intermediate **2.21** which could undergo either a) methanol-assisted kinetic spiroketalization^[22] to give **2.22** with stereochemical retention at the anomeric center or b) Ti(O-*iPr*)₄ catalyzed spirocyclization^[23] to yield the opposite diastereomer **2.23** with stereochemical inversion of the C1 atom. The methanol-controlled epoxide opening transition state **2.24** is postulated to be under H-bonding catalysis with one molecule of methanol coordinating to the oxygen of the THP ring and directing the trajectory of the OH nucleophile and another molecule of methanol activating the epoxide electrophile via H-bonding. The Ti(O-*iPr*)₄ catalyzed process is postulated to follow a chelation-controlled early transition state model **2.25**, leading to the thermodynamic product **2.23**. The ability to employ simple and widely available reagent-control to supersede any inherent thermodynamic bias in product formation makes this an extremely useful method for the rapid construction of stereodiversified spiroketals.

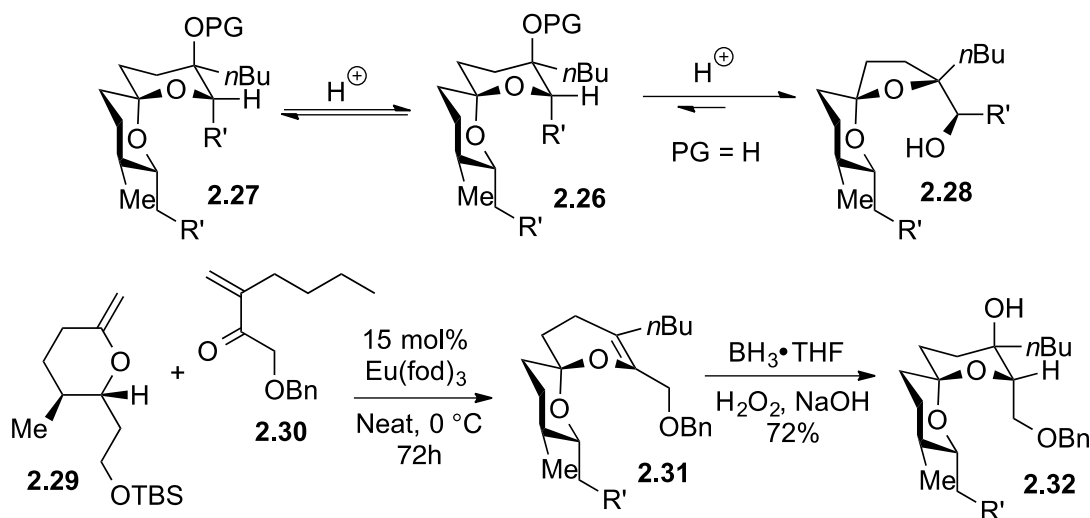


Scheme 2.3 Reagent-controlled epoxide-opening spirocyclization

2.1.2.3 Periphery spiroketal functionalization

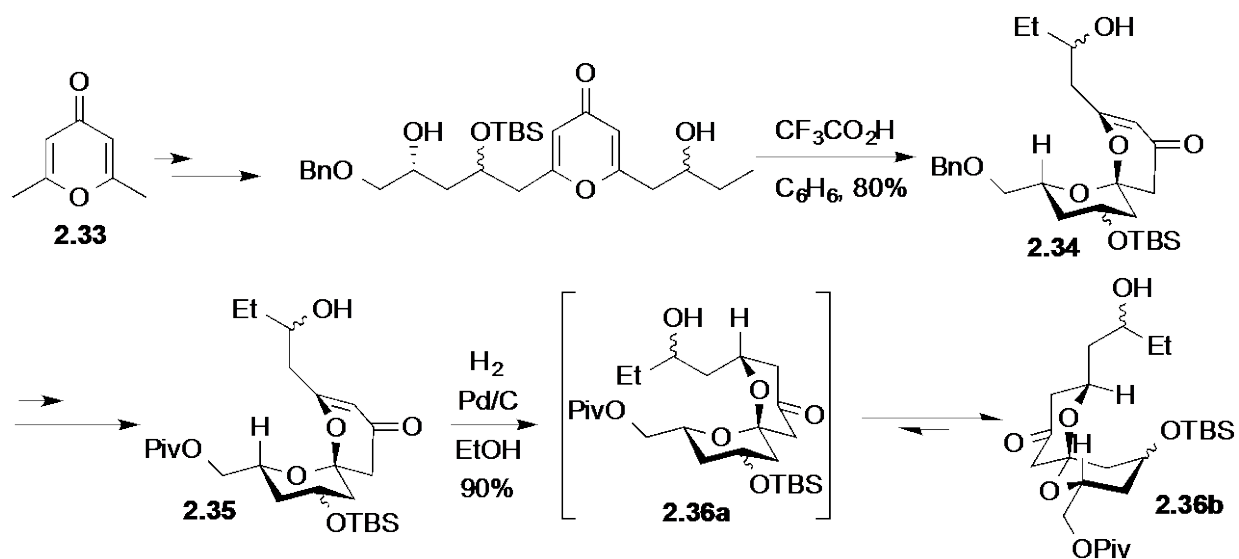
Spiroketals with double anomeric effects are usually the most stable products in spirocyclization reactions. However, stereoelectronic and steric effects of substituents may also play an important role in dictating the final stereochemical outcome of some spiroketals. This is highlighted during the total synthesis of (–)-reveromycin A. Rizzacasa and co-workers^[24] recognized that the 6,6-spiroketal core **2.26** cannot be synthesized using conventional acid-mediated methods because the desired spiroketal **2.26** has an unfavourable *syn*-pentane interaction (Scheme 2.4). To relieve the steric strain, **2.26** is prone to a ring flip into an alternative axial-equatorial arrangement **2.27** at the expense of sacrificing one anomeric effect. In addition, if a naked OH moiety is present, **2.27** also has a propensity to revert to a more thermodynamic 5,6-spiroketal form **2.28**. All these

combined effects resulted in complex mixtures as previously reported. Rizzacasa and co-workers worked around this issue by utilizing a convergent inverse demand HDA reaction between **2.29** and **2.30** to establish the stereochemistry of spiroketal **2.31** followed by a hydroboration/oxidation sequence to finally arrive at the core **2.32** of (-)-reveromycin A.



Scheme 2.4 Inverse demand HDA approach to spiroketals

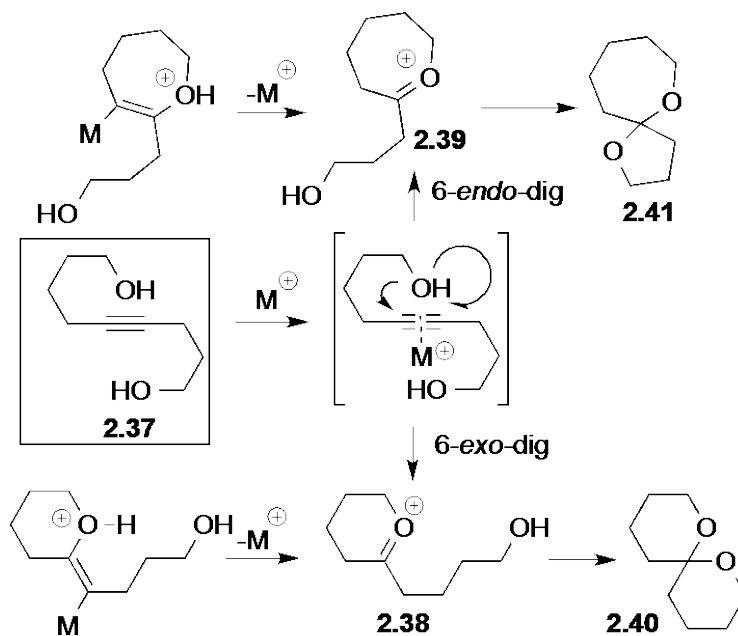
There are also examples of natural products, which possess unique axial-equatorial spiroketals subunits, which are inaccessible by direct acid-catalyzed spiroketalization due to the energetic penalty of losing anomeric stabilization. During the synthesis of altohyrtin A (Scheme 2.5), Crimmins and co-workers^[25] deployed a pyrone approach by sequential addition of the lithiated pyrone **2.33** to aldehydes, followed by an acid-induced spirocyclization to give **2.34**. Spiropyranone **2.35** was then hydrogenated on the less hindered face to yield **2.36a**, which flips to the axial-equatorial spiroketal **2.36b** due to unfavorable 1,3-diaxial interactions. By identifying and exploiting steric interactions within functionalized spiroketals, Crimmins and co-workers were able to establish the spiroketal stereochemistry of altohyrtin A.



Scheme 2.5 Spiropyranone approach

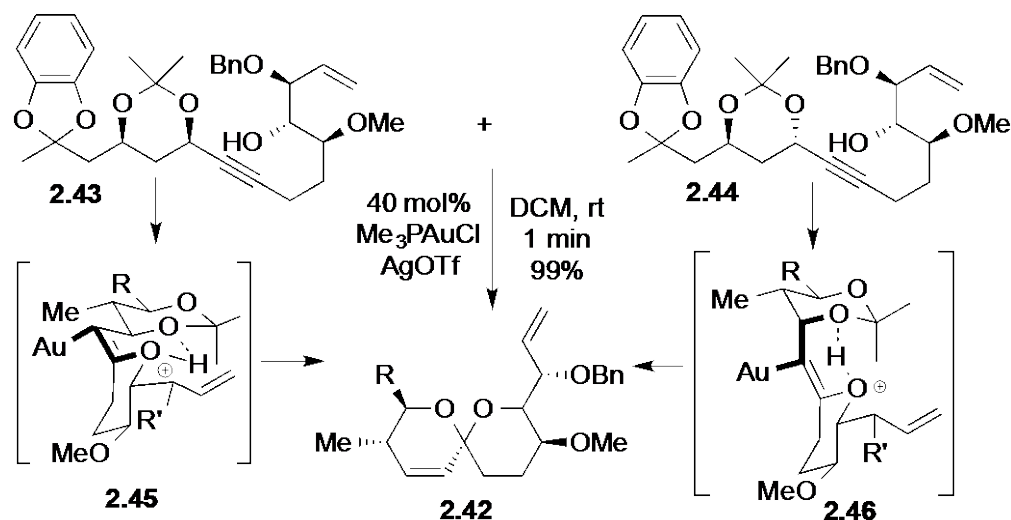
2.1.2.4 Metal-catalyzed hydroalkoxylation

The most atom-economical and efficient route to spiroketal is the direct sequential addition of oxygen nucleophiles across an unsaturated alkyne **2.37** (Scheme 2.6). However, due to the relatively high enthalpy cost of cleaving the O-H sigma bond and the relatively weak nucleophilicity of OH groups, hydroalkoxylation requires the facilitation of a metal catalyst for overcoming the associated activation barriers. Metal complexes capable of mediating intramolecular dihydroalkoxylation include Pt complexes such as Zeise's dimer^[26], Rh^[27] and Ir complexes^[28]. There are many parameters including metal ligands, solvent and substituents' steric that determines whether the addition goes through an *exo*-dig **2.38** or *endo*-dig **2.39** transition state which ultimately leads to the 6,6-spirocycle **2.40** or the 5,7-spirocycle **2.41** respectively.



Scheme 2.6 Metal catalyzed hydroalkoxylation

Recently, gold halides complexes have also proved to be versatile and mild catalysts for effecting such transformations. The Aponick group was able to identify that a key spiroketal intermediate **2.42** within the spirastrellolide family can be constructed using an Au-catalyzed spiroketalization^[29] (Scheme 2.7). By masking the 1,3-diol moiety as the acetonide, they were able to regulate the sequence and resultant regioselectivity of the spiroketalization event.



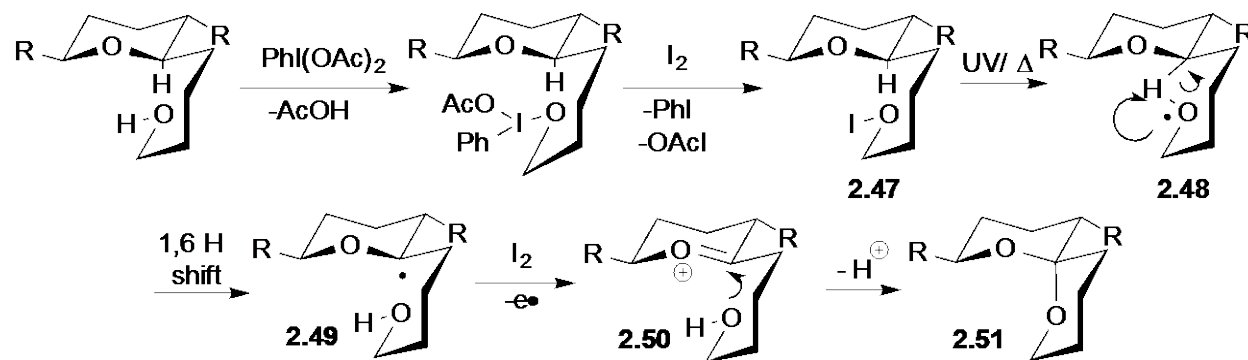
Scheme 2.7 Stereoconvergent Au-catalyzed spiroketalization

Importantly, regardless of the stereochemistry at the pro-gargylic position, both diastereomers **2.43** and **2.44** were able to convert to the desired spiroketal **2.42** due to the excellent periplanar alignment of the gold complex sigma bond **2.45/2.46** with the OH leaving group. This process is facilitated by H-bonding and entropically driven by the extrusion of acetone, exposing the 2nd OH group for spiroketalization.

2.1.2.5 Oxidative radical spiroketalization

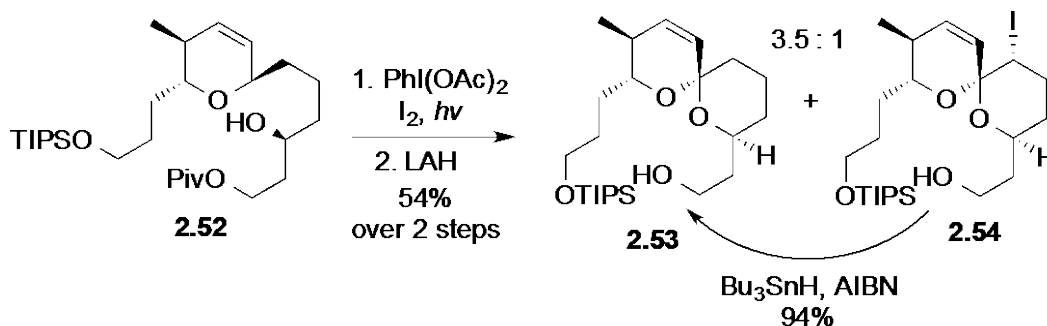
Oxidative methods of generating radicals through intramolecular hydrogen abstraction (IHA) are well documented^[30] and provide a complementary approach for accessing non-anomeric stabilized kinetic spiroketals, which are prone to equilibration in the presence of acids (Scheme 2.8). The reagents of choice for promoting this oxidative cyclization have evolved from combinations of $\text{Pb}(\text{OAc})_4 / \text{I}_2$ to HgO / I_2 and more recently to $\text{PhI}(\text{OAc})_2 / \text{I}_2$ due to its higher reactivity (stoichiometric equivalents) and lower toxicity. This mechanism involves the

generation of alkyl-hypodite species **2.47**, which is cleaved in the presence of UV light or heat to form an alkoxide radical **2.48**. **2.48** then undergoes a 1,6-H shift to give **2.49**, which is oxidized in the presence of iodine to the oxocarbenium species **2.50**. Subsequent intramolecular attack by the hydroxyl group onto the oxocarbenium gives spiroketal **2.51**.



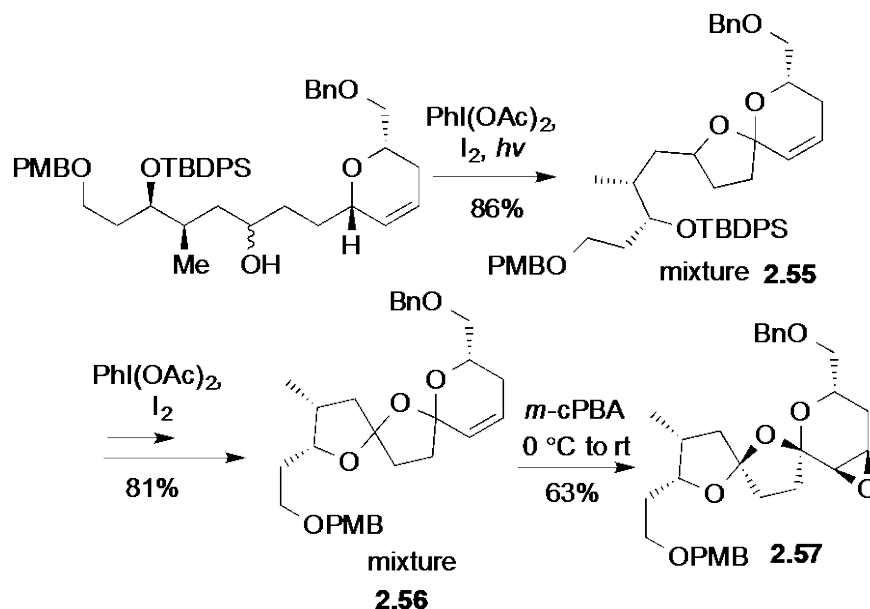
Scheme 2.8 Mechanism of oxidative radical cyclization

During the total synthesis of bistramide **C** by Wipf and co-workers^[31] (Scheme 2.9), they assembled the core of the spiroketal **2.53** by subjecting alcohol **2.52** under oxidative radical cyclization conditions. A 3.5:1 mixture of **2.53**: **2.54** was obtained. Nevertheless, **2.54** could be readily converted into **2.53** using tin hydride reduction. Importantly, they noted a significant improvement in the cyclization step as compared to the saturated analog of **2.52**, indicating that the double bond within the THP ring facilitates the formation of a stable oxocarbenium ion/radical species for facile cyclization.



Scheme 2.9 Oxidative radical approach to core of bistramide C

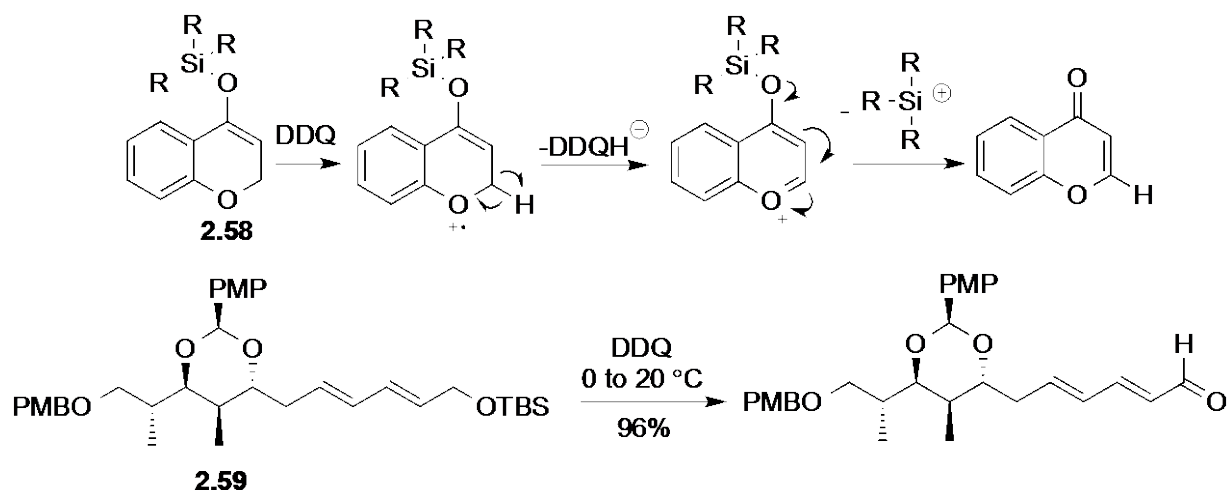
Brimble and co-workers^[32] also utilized this oxidative protocol in their synthesis of the triad of spirocycles found within the shellfish toxins spirolide family (Scheme 2.10). In an exceptional showcase of thermodynamic equilibration under substrate control, they were able to carry forward diastereomeric mixtures **2.55** and **2.56** through two sequence of oxidative spiroketalization and eventually perform a one-pot epoxidation/ chlorobenzoic acid-mediated (present in *m*-CPBA) stereo-convergent transformation of four possible diastereomer into a single desired isomer **2.57**.



Scheme 2.10 Tandem radical cyclization

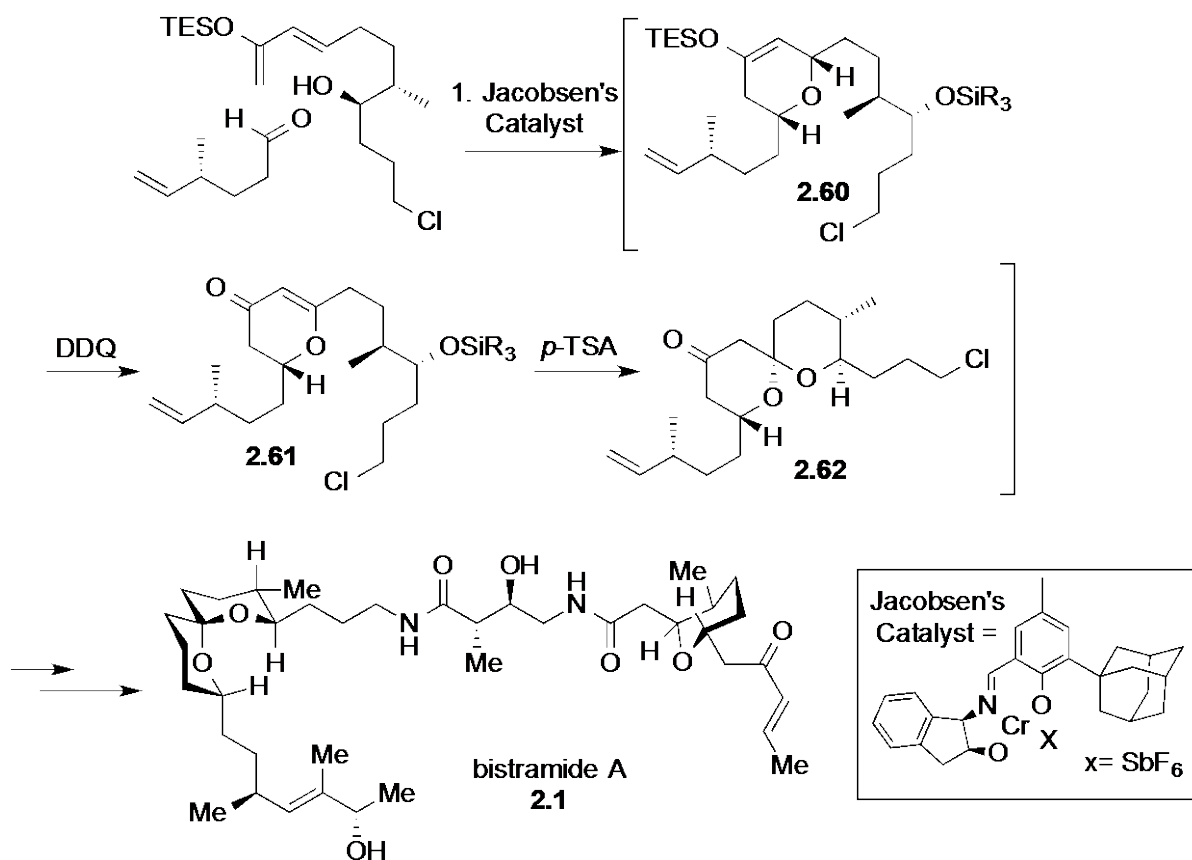
2.1.2.6 Telescoped cycloaddition and Carbon–Hydrogen activation (Floreancig approach)

During the DDQ mediated bimolecular coupling study, Dr. Clausen documented the facile decomposition of chromenes **2.58** substituted at the 4-position as enol silane or vinyl acetate before it can be trapped by an external nucleophile (Scheme 2.11). Similarly, Paterson had previously reported the facile oxidative cleavage of electron rich vinyl silyl ether **2.59** in the presence of DDQ^[33] (Scheme 2.11).



Scheme 2.11 DDQ mediated oxidative deprotection

Based on these results, the Floreancig group subjected the intermediate enol silane THP adduct **2.60** derived from the HDA reaction under the oxidative conditions with DDQ to obtain the dehydrogenated enone **2.61** (Scheme 2.12). In the presence of *p*-TSA, the silyl group undergoes cleavage and liberates the tethered alcohol. Subsequently, this alcohol underwent an acid catalyzed intramolecular oxa-Michael cyclization to yield the desired cyclized spiroketal **2.62**. Under optimized conditions, this transformation was carried out in a one-pot manner with sequential addition of reagents. Isolation of intermediates was unnecessary, with only one column chromatography purification performed towards the end. Two rings and three bonds were constructed in a highly stereoselective reaction. This telescoped cycloaddition and C–H functionalization protocol was eventually utilized as a key step during the convergent synthesis of bistramide A **2.1** (Scheme 2.12).



Scheme 2.12 Spiroketal formation: One-pot hetero Diel-Alder addition and C–H functionalization

As discussed earlier, despite the vast repertoire of strategies available for construction of spirocycle motif, most of these methods require the pre-installation of highly elaborated intermediates in a linear fashion.

Our DDQ-mediated oxidative protocol has proved viable and extremely useful in bimolecular annulation reactions for rapid generation of molecular complexity. Besides facilitating intermolecular C–C bond formation in chromene substrates (section 1.2.3), the incorporation of a C–H functionalization step (mediated by DDQ) in tandem with another fragment-coupling reactions (e.g., cycloaddition) also demonstrated the inherent versatility of our oxidative strategy.

2.2 TANDEM LEWIS ACID MEDIATED FERRIER COUPLING AND DDQ OXIDATIVE SPIROCYCLIZATION

2.2.1 Design principles

We have previously shown that the oxidative C–H bond activation of chromene systems occurs readily in the presence of DDQ (Figure 2.4). However, we were uncertain whether the THP ring **2.63** with a single degree of unsaturation was capable of forming an oxocarbenium cation under our oxidative conditions. Once generated, a suitable coupling partner **2.64** of sufficient nucleophilicity must be present to drive the equilibrium towards **2.65**. Upon the addition of a second equivalent of DDQ, we postulate that **2.66** will undergo a facile intramolecular annulation to yield spiroketal **2.67**.

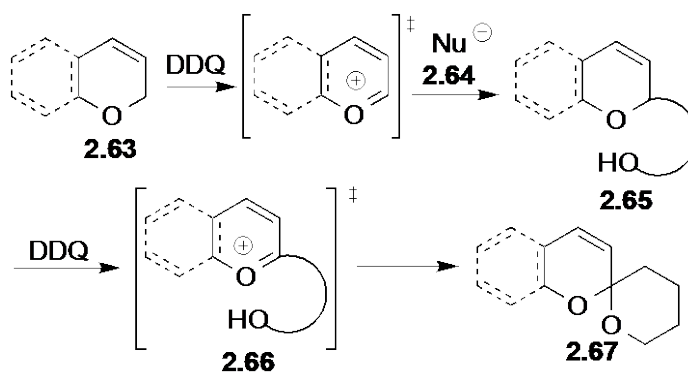


Figure 2.4 Design principle of bimolecular oxidative coupling

From the studies of Mr. Villafane (Scheme 1.2), we noticed that a sequential intermolecular followed by an intramolecular fragment coupling is feasible, despite only achieving a modest yield. Nevertheless, the second spirocyclization gave slightly higher yields than the first

intermolecular coupling, potentially due to the higher nucleophilicity of the alcohol moiety to thermodynamically trap the reversibly generated oxocarbenium cation and the faster rate of intramolecular annulation compared to intermolecular addition. Hence, we decided to utilize a type-I Ferrier rearrangement reaction^[34] for the initial robust coupling of a glycal **2.68** with the protected allyl silane **2.69** (Figure 2.5). The resultant transposition of the double bond from the C2–C3 to C3–C4 bond also stabilizes the resultant oxocarbenium cation **2.70** by conjugation, which subsequently cyclizes in the presence of a pendent hydroxyl group.

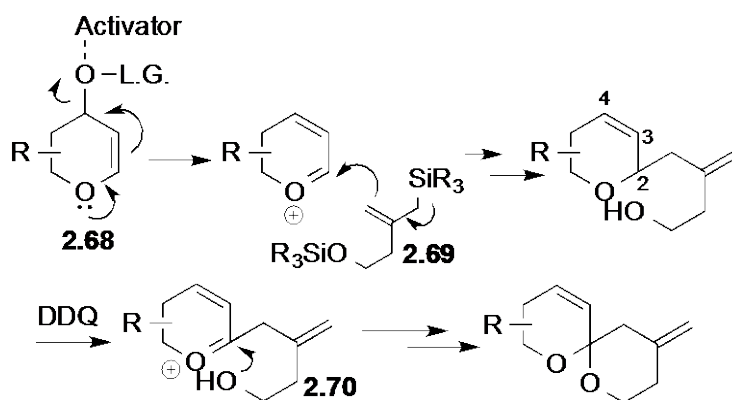
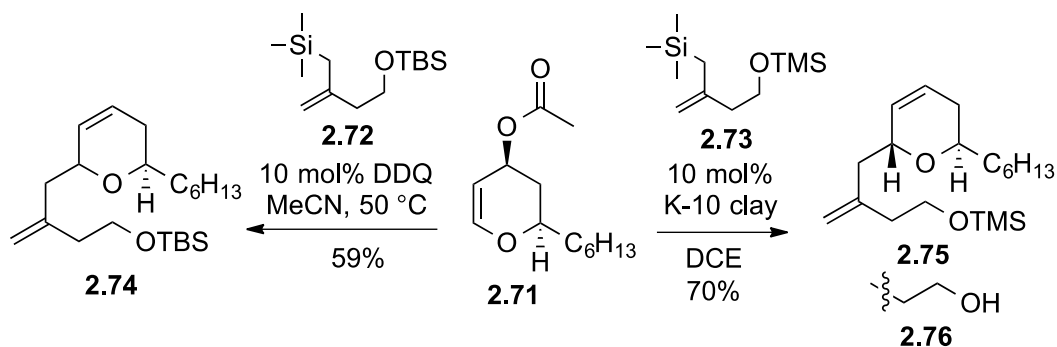


Figure 2.5 Tandem Ferrier-oxidative annulation

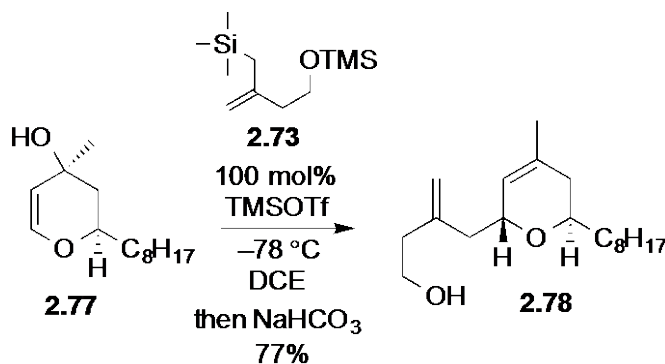
2.2.2 Exploration of the reaction protocol

We screened various promoters such as DDQ^[35] and K-10 montmorillonite clay^[36] for the initial Ferrier coupling reaction and obtained moderate yields of 59% and 70% respectively (Scheme 2.13). The disadvantages of these protocols include: 1.) an additional concession step is needed to convert the pyranol into the pyranol acetate **2.71** with a better leaving acetate group and 2.) the resultant tethered homoallylic alcohol is obtained primarily as the protected silyl form **2.74/2.75**, which prohibited the subsequent spirocyclization step.



Scheme 2.13 Screening of catalysts for Ferrier coupling

Toshima and co-workers^[37] reported the use of TMSOTf for the *C*-glycosidation of unprotected glycols with allyl silanes (Scheme 2.14). Upon stirring pyranol **2.77** with allyl silane **2.73** and TMSOTf, the desired product **2.78** was obtained with concomitant OTMS deprotection upon quenching with aqueous NaHCO₃.



Scheme 2.14 TMSOTf catalyzed Ferrier Coupling

After further optimization, the catalytic loading of the TMSOTf was reduced to 1-5 mol% without significant reduction in yield. The reduced loadings also circumvented the low temperature requirement. The proposed cycle for substoichiometric TMSOTf promoted Ferrier

coupling is depicted in Figure 2.6. We hypothesized that the combination of the allyl silane used in the reaction has a beneficial synergistic effect on the catalytic cycle because the departing TMS group from allylic oxocarbenium cation intermediate can combine with the triflate counter-anion to regenerate the active TMSOTf catalyst. Upon quenching with aqueous NaHCO₃, trace amounts of TMSHCO₃ (carbonic acid derivative) formed after basic hydrolysis yield the desilylated alcohol.

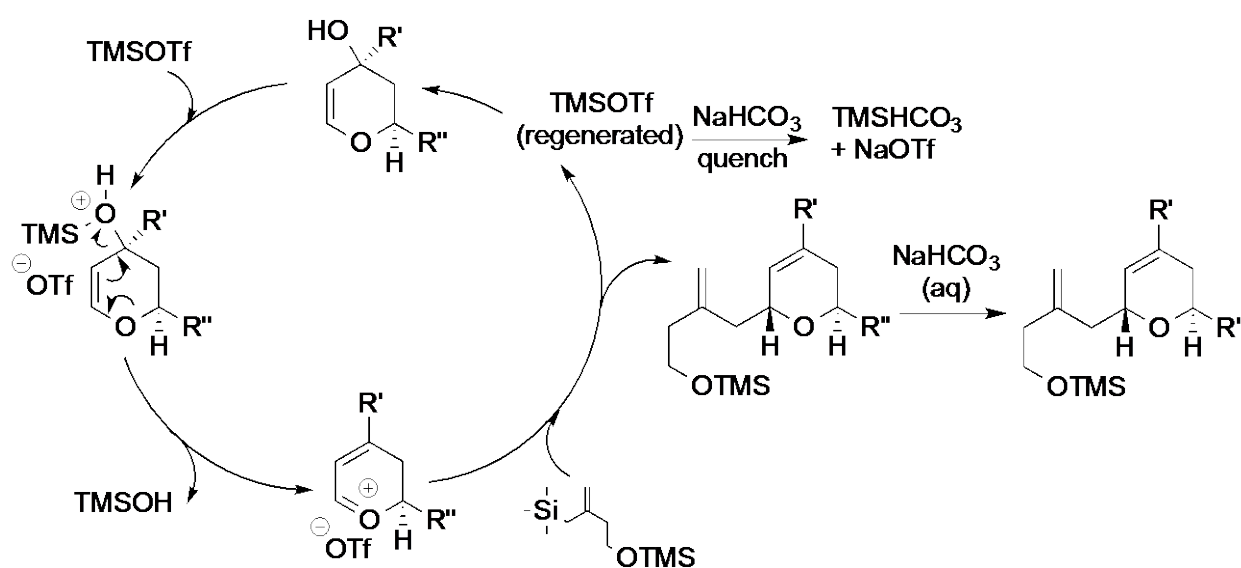
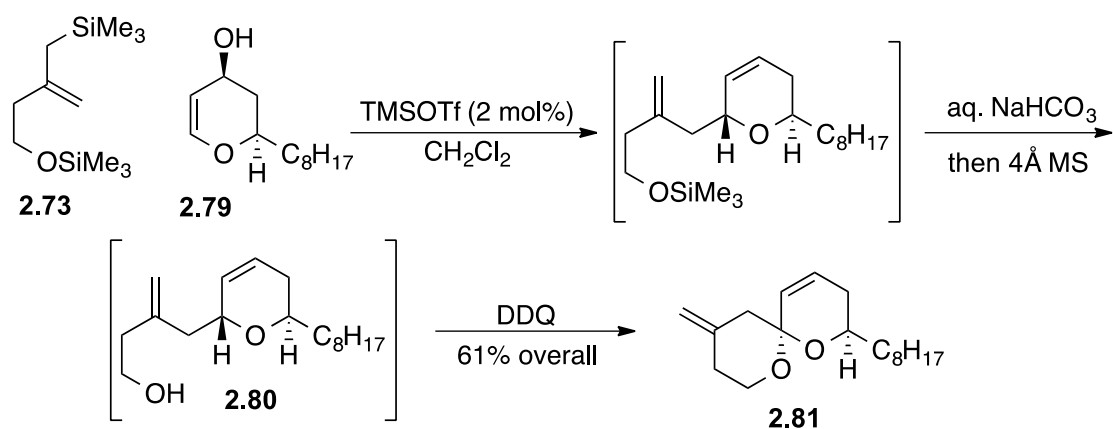


Figure 2.6 Proposed pathway for regeneration of TMSOTf

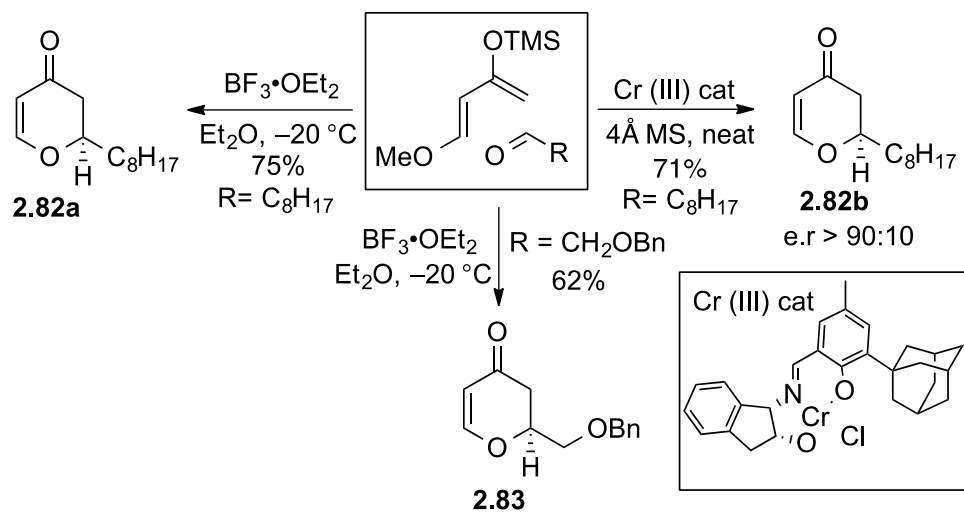
Under the new optimized protocol, **2.81** was obtained in 61% moderate yield (Scheme 2.15). This catalytic one-pot two-component Ferrier coupling can be conveniently conducted at room temperature with no significant deleterious effects on yield. The small amount of TMSOTf can be quenched efficiently with saturated NaHCO₃ to yield intermediate **2.80**. The final oxidative spirocyclization mediated by DDQ is performed under neutral conditions and is highly compatible with adjacent functional groups.



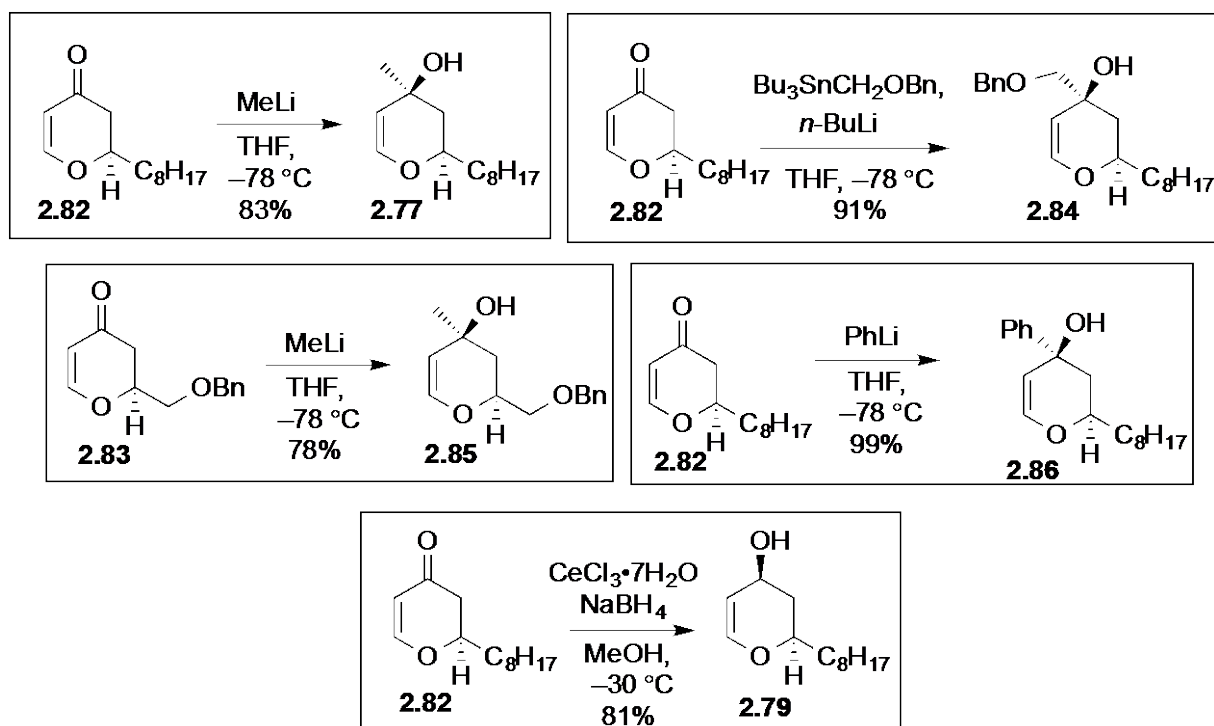
Scheme 2.15 Optimized Ferrier tandem oxidative cyclization

2.2.3 Design and synthesis of dihydropyrans

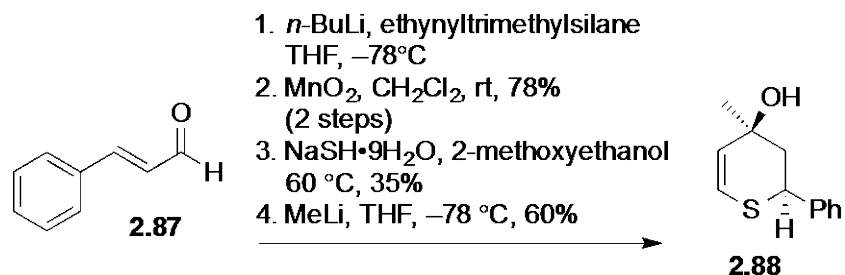
The dihydropyranols were accessed by a hetero HDA reaction between Danishefsky's diene^[38] and the appropriate aldehyde (scheme 2.16), followed by an appropriate organometallic addition into the respective dihydropyranones (Schemes 2.17). Asymmetric versions of dihydropyrans such as pyranone **2.82b** were analogously prepared using Jacobsen's Cr(III)-salen complex^[39] instead of $\text{BF}_3 \cdot \text{Et}_2\text{O}$ in the HDA reaction. Pyranol **2.84** with a planar sp^2 benzyloxymethyl appendage is an attractive candidate for diversity-orientated synthesis (DOS) when coupled together with the sp^3 -rich fragments of spiroketals. This is significant because current DOS libraries have been mostly limited to planar sp^2 -heteroaromatic fragments^[40]. Dihydropyranol **2.85** with a benzyloxy substituent at the 6-position was prepared to demonstrate the compatibility of our DDQ-mediated protocol with common functional groups. Similar to pyranol **2.77**, pyranol **2.86** with a phenyl substituent at the 4-position will have a higher oxidative potential to form the allylic oxocarbenium cation due to the increased conjugation stability. This could potentially enhance the rate of spirocyclization. Dihydrothiapyranol **2.88** was prepared in a four-step sequence from cinnamaldehyde **2.87** via a double thia-Michael reaction^[41] (Scheme 2.18).



Scheme 2.16 Synthesis of pyranones



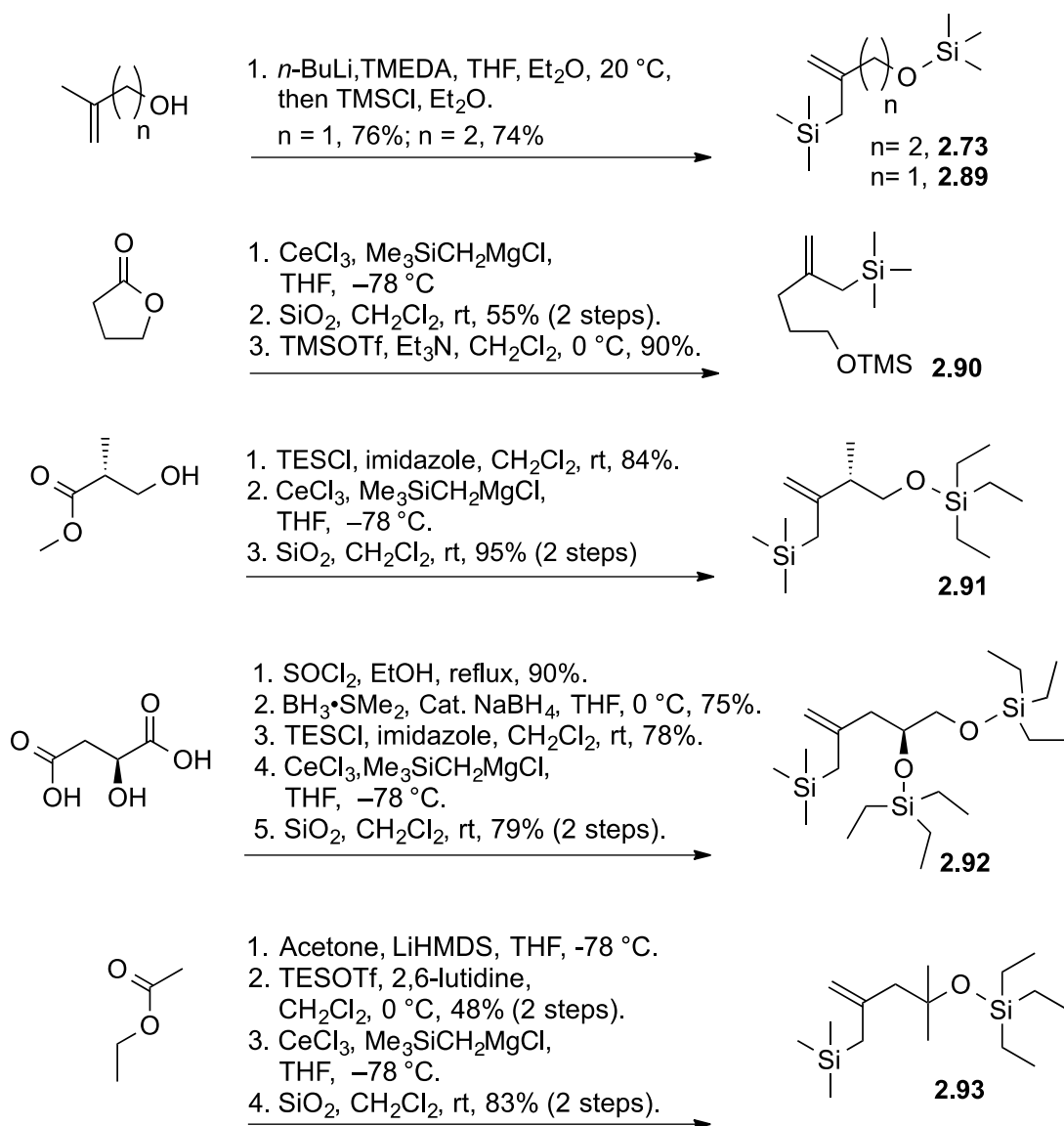
Scheme 2.17 Synthesis of dihydropyransols



Scheme 2.18 Synthesis of dihydrothiapyranol

2.2.4 Design and synthesis of nucleophiles

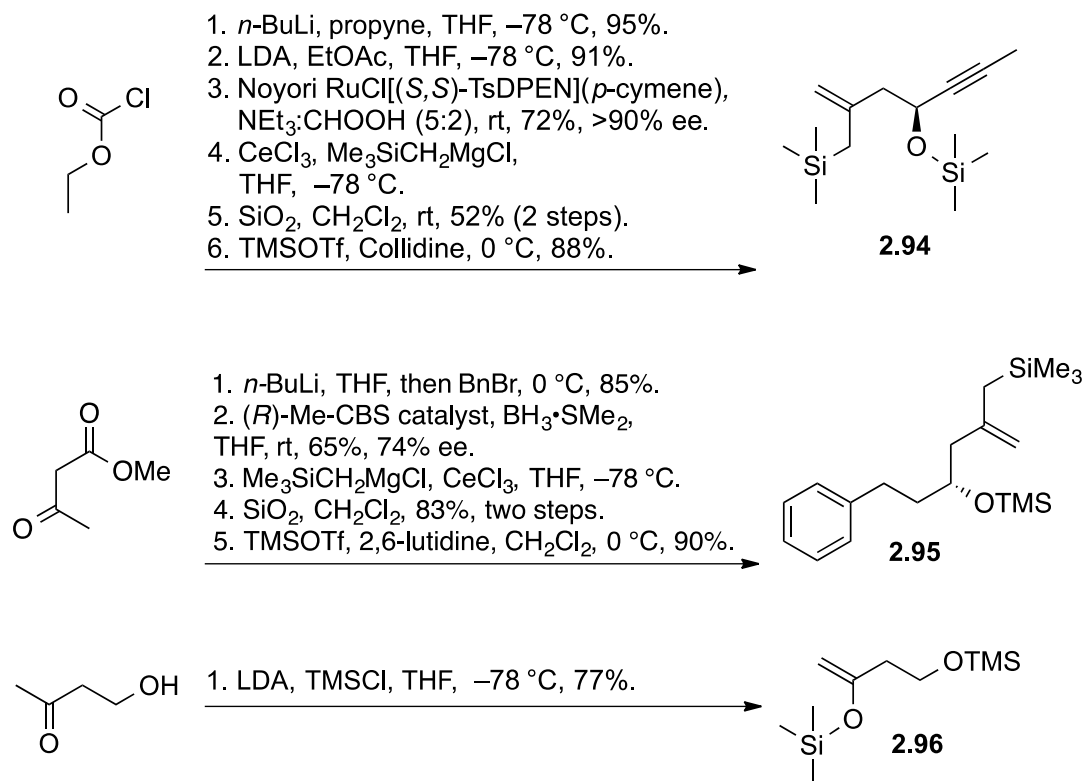
The highly modular nature of our fragment coupling approach allows for easy diversification of the spiroketal portion by simply varying of the allyl silane fragment (scheme 2.19). Allyl silanes were selected as the nucleophilic partner based on their benign chemical toxicity relative to allyl stannanes and also its facilitation in the regeneration of TMSOTf. Allyl silanes **2.73** and **2.89** were prepared through a metallated dianion intermediate following Carlson's procedure^[42]. The seven-membered allyl silane **2.90** was prepared from the corresponding lactone by a CeCl_3 mediated addition of $\text{TMSCH}_2\text{MgCl}$ (Bunnell^[43] protocol) into the lactone followed by silylation of the terminal alcohol. Allyl silane **2.91** was derived from a commercial chiral ester by initial silylation of the terminal alcohol followed by the Bunnelle-Peterson process. Similarly, allyl silane **2.92** was derived from *L*-malic acid by first capping the terminal acidic ends followed by a regioselective reduction of the methyl ester at the 1-position, silylation of the diols and finally conversion of the terminal ethyl ester into allyl silane. Allyl silane **2.93** containing a sterically challenging alcohol was prepared by an initial aldol reaction between ethyl acetate and acetone, followed by capping of the tertiary alcohol with TESOTf and finally conversion into the allyl silane.



Scheme 2.19 Preparation of allyl silanes (I)

Allyl silane **2.94** (Scheme 2.20) was synthesized from ethyl chloroformate by initial insertion of lithiated propyne, followed by nucleophilic acyl substitution with the enolate of ethyl acetate. The resulting β -keto ester was reduced by Noyori's asymmetric transfer hydrogenation^[44] into the alcohol, which was subsequently silylated and converted to the desired allyl silane. Silyl ether **2.95** was prepared by a methylacetoacetate dianion alkylation with benzyl bromide. The resulting β -keto ester was subjected to asymmetric CBS reduction^[45] to yield the alcohol in 74%

ee, which was subsequently converted to the allyl silane. Enol silane **2.96** was prepared from 4-hydroxybutanone in one step by kinetic deprotonation of the α -hydrogen and terminal alcohol altogether in one step followed by quenching with TMSCl.

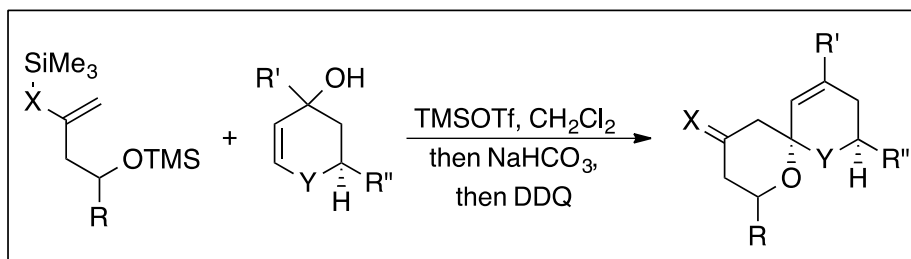


Scheme 2.20 Preparation of allyl silane (II)

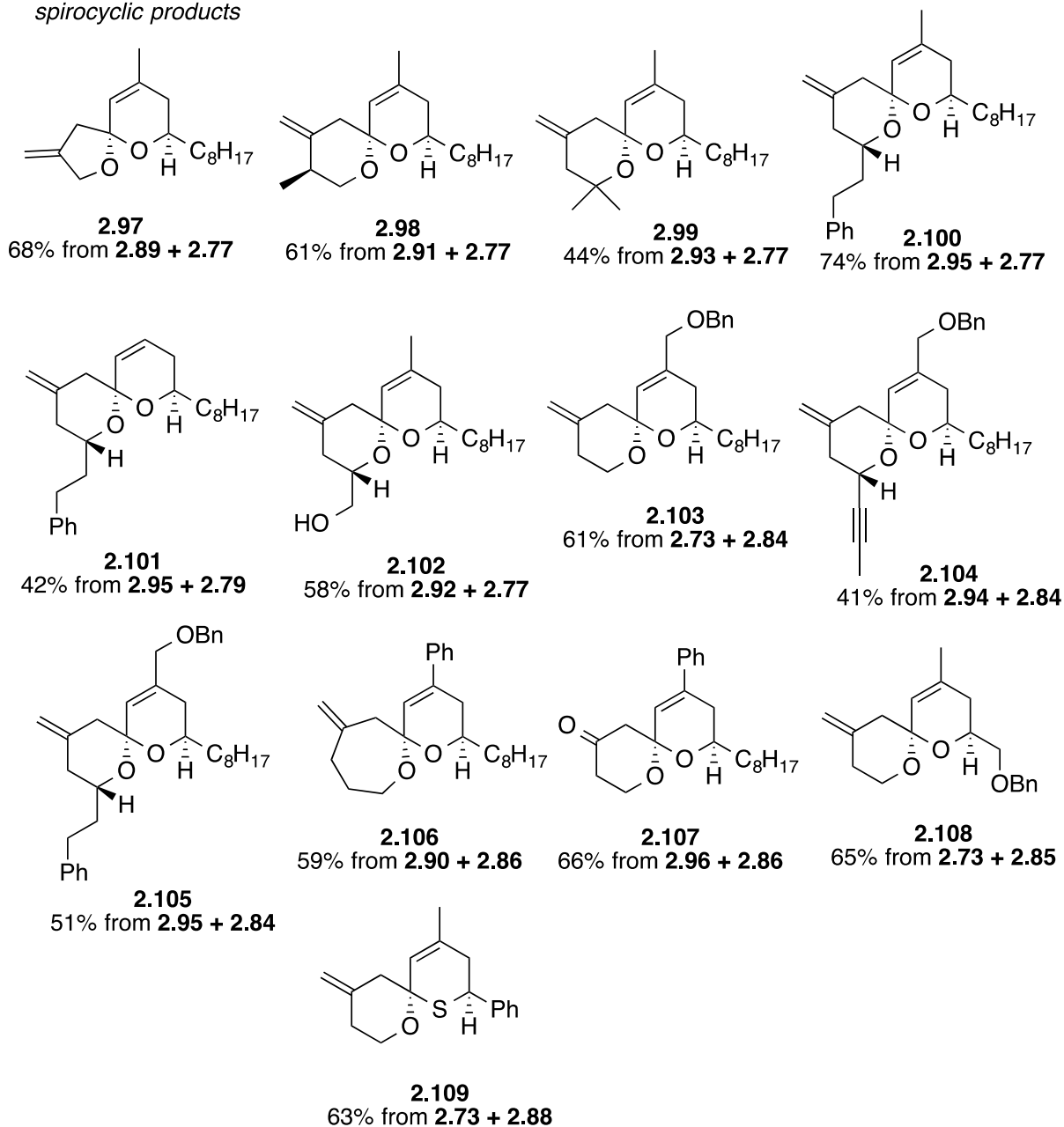
2.2.5 Scope of one-pot two component spirocyclization

The scope of the one-pot TMSOTf mediated fragment coupling followed by DDQ-promoted oxidative cyclization is shown in Scheme 2.21. For the [5.6] spiroketal **2.97**, the 5-*exo*-trig cyclization of the tethered alcohol onto the allylic oxocarbenium cation was extremely facile at room temperature and eventually lead to undesired decomposition pathways. To overcome this, the reaction was performed at $0\text{ }^{\circ}\text{C}$ with portion-wise addition of the oxidant. This exceedingly

facile ring closure in comparison to the 6-membered spiroketals can be attributed to the lower entropic penalty encountered in the transition state for ring closure due to its lower degrees of freedom^[46].



spirocyclic products



Scheme 2.21 Substrate scope of DDQ-mediated spiroannulation

The fragment coupling protocol is compatible with various substitution patterns in the allyl silane partner as demonstrated by the formation of spiroketal **2.98** with a methyl branch at the allylic position, spiroketal **2.99** with a tertiary ether and spiroketal **2.102** with a functionalized ether. Particularly, for **2.99** the sterically hindered tertiary alcohol nucleophile does not seem to encounter much difficulty inserting into the allylic oxocarbenium cation. This example seems to indicate that the electronics of the tethered nucleophile may play a more dominant role over its inherent steric hindrance during the oxidative cyclization event. The mild and neutral conditions of the DDQ-mediated cyclization also allowed for the smooth spiroketalization to **2.102**. Over-oxidation of the terminal alcohol was not observed. This example also revealed that in the presence of two competing alcohol tethers, formation of the [6.6] spiroketal is favored over the [7.6] spiroketal.

Spiroketals **2.100**, **2.101**, **2.102** and **2.104** resulting from the corresponding tethered secondary alcohols, cyclized smoothly during the oxidative spiro-annulation process. The coupling of enantiomerically pure pyranol **2.82** with allyl silane **2.95** (74% ee) gave **2.100** as a 6:1 mixture of diastereomers. In comparison, **2.101** without the 4-methyl stabilizing group, was obtained in 41% yield. Spiroketals **2.103**, **2.104** and **2.105** with a flexible *sp*²-benzoxylmethyl (BOM) group at the 4-position of the dihydropyran are attractive candidates for DOS when coupled together with the *sp*³ richness of the spiroketals. Spiroketal **2.104** containing an alkynyl functional group was obtained in 41% yield due to the reduced nucleophilicity of the intermediate propargylic alcohol and competing oxidation of the alkynyl alcohol by DDQ. Generally, the BOM-containing spiroketals are isolated in slightly diminished yields as compared to the spiroketals with the 4-methyl substituent. This is probably due to the electronic destabilization of the

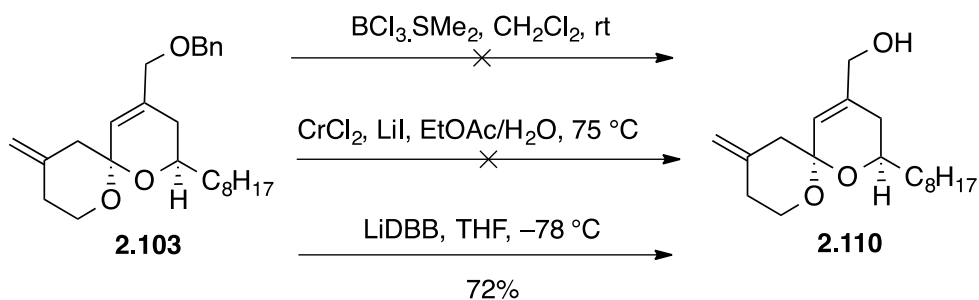
oxocarbenium intermediate conferred by the electron-withdrawing inductive effect of the BOM group.

In contrast for spiroketal **2.106**, the substitution of a conjugating phenyl group at the 4-position of the dihydropyran ring facilitates the generation of a longer-lived oxocarbenium cation, which is able to trap the longer-tethered alcohol leading to the formation of the [7.6] spiroketal. Enol silane **2.96** is also a competent nucleophile leading to the ketone-containing spiroketal **2.107**. Despite having an inductively destabilizing ketone intermediate, the mesomeric resonance of the 4-phenyl substituent seem to override that apparent deficiency resulting in productive spiroannulation to give the desired spiroketal in 66% yield. For spiroketal **2.108**, the placement of the BOM group at the 6-position of the dihydropyran seemed to have negligible detrimental consequence on the efficiency of the spirocyclization and the desired product was isolated in 65% yield. Thia/oxa-spirocycle **2.109** was also accessible from our oxidative annulation protocol. Due to the lower electronegativity of the sulfur atom, it is more susceptible to oxidation as compared to its oxygen counterparts. Spiro-annulation was completed within 15 min with only one equivalent of the oxidant, yielding 63% of the thiaspiroketal.

2.2.6 Post cyclization modifications

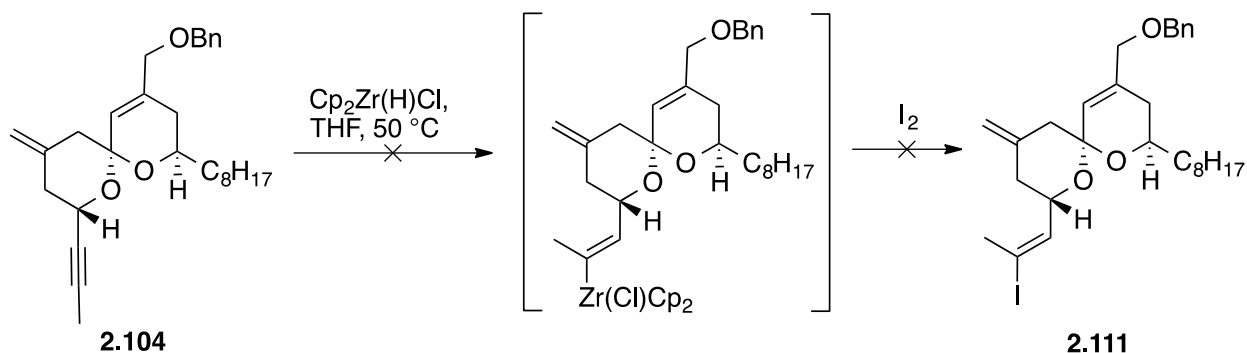
The deprotection of the Bn group in spiroketal **2.103** (scheme 2.22) was not trivial because both the endocyclic and exocyclic alkenes were vulnerable under hydrogenolysis conditions. Similarly, Lewis acid protocols employed only led to the decomposition of the spiroketal due to competitive coordination of the Lewis acids onto the oxygen atoms of the spiroketal instead of

activating the benzyl ether for cleavage. Gratifyingly, under the reductive conditions with LiDBB^[47], regioselective debenzylation was accomplished within 20 min at $-78\text{ }^{\circ}\text{C}$.



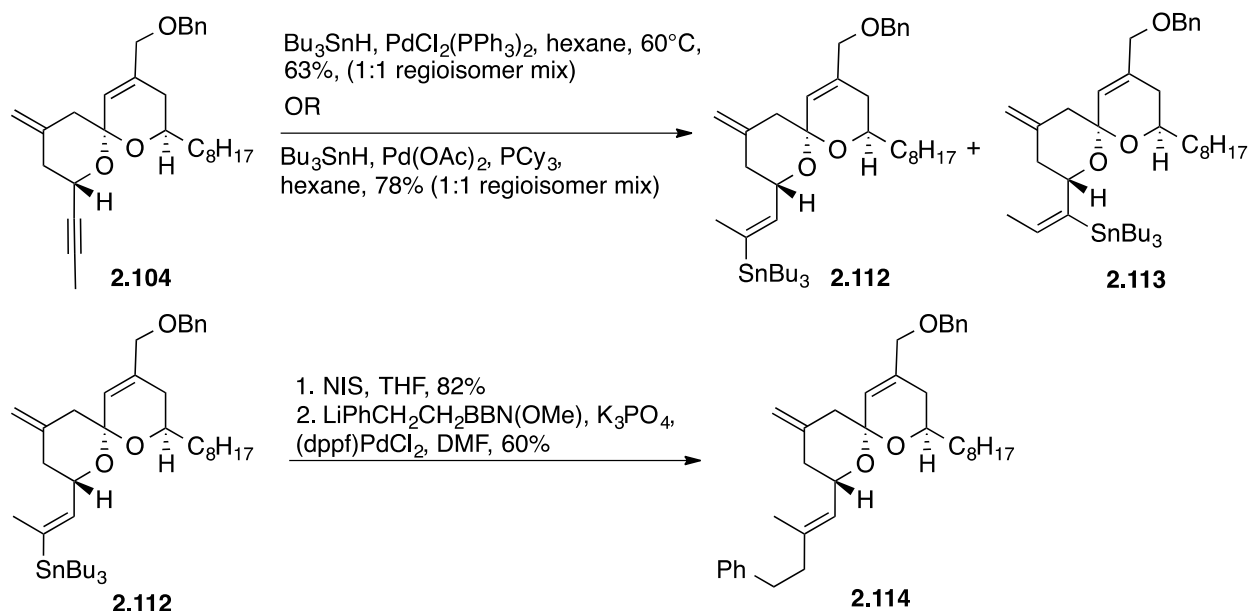
Scheme 2.22 Debenzylating conditions for spiroketals

Spiroketal **2.104** with an alkynyl moiety was well suited for post cyclization manipulation. However, an attempted one-pot hydrozirconation of the internal alkyne with Schwartz's reagent followed by sequential quenching with iodine did not afford the desired *trans*-vinyl iodide **2.111** (Scheme 2.23). The absence of chemical reactivity was probably due to the presence of the neighboring electron deficient THP ring deactivating the alkyne. The alkynyl bond is unable to effectively σ -donate into the electrophilic Zr center and form the active vinyl zirconium intermediate.



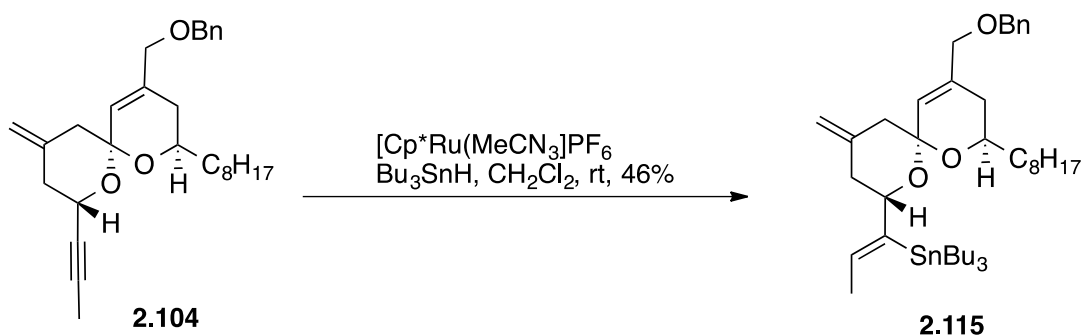
Scheme 2.23 Attempted hydrozirconation on spiroketal **2.104**

As a result, an alternative two-step palladium-catalyzed *cis*-hydrostannylation protocol followed by a tin-iodide exchange was employed (Scheme 2.24). The hydrostannylation reaction catalyzed by $\text{PdCl}_2(\text{PPh}_3)_2$ afforded a 1:1 isomeric mixture of distal alkene **2.112** and proximal alkene **2.113**, which was easily separable by column chromatography. The palladium catalyst was subsequently switched to a mixture of $\text{Pd}(\text{OAc})_2$ and PCy_3 in hope that the bulkier phosphine ligated catalyst would have better differentiation between the terminal methyl group and the internal THP ring. However, the same ratio was obtained with this new catalyst albeit with a higher yield, lower loadings of Pd and a lower temperature. The stannyl exchange with tin was completed within 30 min using NIS at 0 °C. The resultant *trans*-vinyl iodide spiroketal was deployed in an alkyl-Suzuki cross coupling^[48] with an *in-situ* generated alkyl boronate to yield the trisubstituted-alkene **2.114**.



Scheme 2.24 Post cyclization modifications of alkynyl-containing spiroketals (I)

Interestingly, when spiroketal **2.104** was subjected to hydrostannylation conditions using a ruthenium catalyst, a mixture of proximal and distal-*cis* vinyl stannyl spiroketals was obtained (Scheme 2.25). Due to scale issues, only proximal-*trans* vinyl stannyl **2.115** was isolated and characterized successfully. Nevertheless, this demonstrated that the masked alkynyl moiety within the spiroketals could be potentially transformed into at least three isomers of tri-substituted alkenes depending on the initial metal catalyst used for hydrostannylation and following through the sequence in Scheme 2.24.



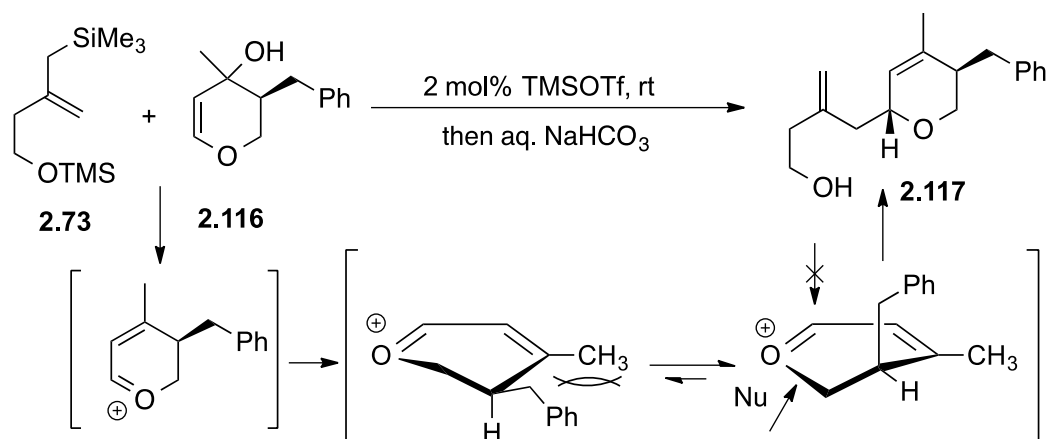
Scheme 2.25 Post cyclization modifications of alkynyl-containing spiroketals (II)

2.2.7 Stereoelectronic analysis of Ferrier-coupling and DDQ mediated C-H activation

2.2.7.1 5'-substituted pyranol

During the screening of the substrate scope for the tandem Ferrier coupling and oxidative cyclization, dihydropyranol **2.116** with a 5'-substituent tended to be sluggish, requiring more than five equivalents of DDQ and a longer reaction time to reach completion. To investigate the

rationale behind this phenomenon, intermediate Ferrier product **2.117** was synthesized independently (Scheme 2.26).



Scheme 2.26 Stereochemical analysis of Ferrier reaction

Remarkably, in the presence of 2 mol% of TMSOTf at room temperature, the 2,5-anti Ferrier adduct was obtained as a diastereomeric mixture with >20:1 α/β selectivity.

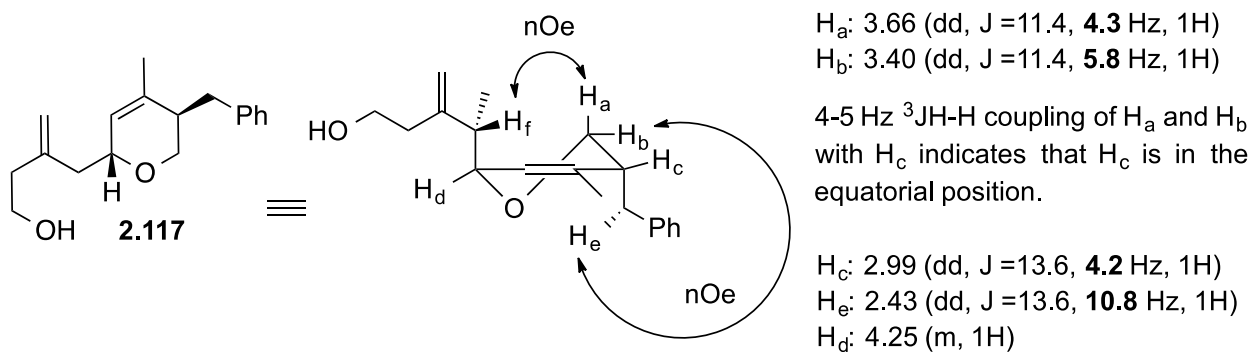


Figure 2.7 NMR determination of stereochemistry for **2.117**

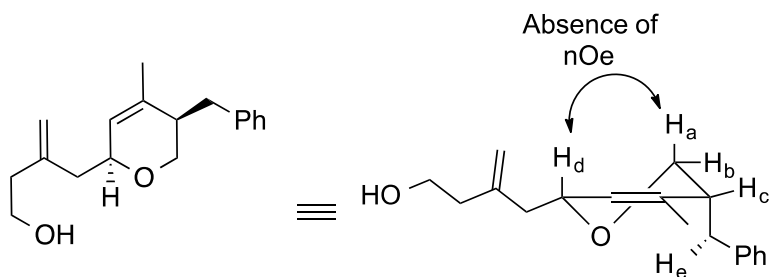


Figure 2.8 Negative control for nOe correlation

The 2, 5-*anti* stereochemistry between the incoming nucleophile and the 5-substituent has been established by 2D NOESY between H_a and H_d . Coupling constants for H_a/H_b with H_c also indicates that the benzyl substituent flips into an axial orientation in order to minimize $A^{1,2}$ strain^[49] with the adjacent methyl substituent at the 4-position (Figure 2.7). The high stereochemical fidelity of the Ferrier reaction indicated that the mechanism probably goes through an S_N1 state. The incoming nucleophile attacks on the opposite face to the benzyl substituent, undergoing a lower energy chair-like transition state instead of the top face that would result in an unfavorable twist-boat transition state (Scheme 2.26).

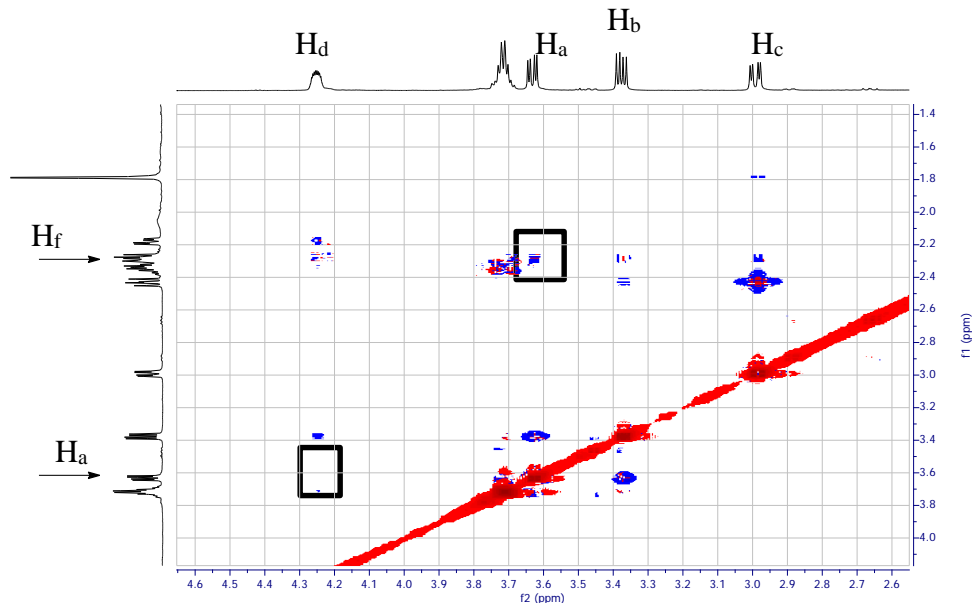


Figure 2.9 Positive and negative nOe correlation for Ferrer intermediate 2.117

The thermodynamic preferred conformer of the Ferrer product **2.118a** (Figure 2.10) places the allylic hydrogen in a pseudo-equatorial position to minimize $A^{1,2}$ strain of the benzyl substituent with the methyl substituent. However, the orbitals between the allylic hydrogen and the adjacent alkene are not in the correct spatial orientation for the oxidative cleavage event to occur. Instead, **2.118a** must undergo a ring inversion into the higher energy conformer **2.118b**. Subsequent allylic hydrogen atom abstraction by DDQ generates a single electron occupied π -orbital, which can overlap favorably with the adjacent oxygen radical cation to form the oxocarbenium intermediate **2.119a**. We hypothesize that C–H bond cleavage is the rate-determining step, which is followed up by a rapid equilibration to the more thermodynamically favorable intermediate **2.119b** and facile trapping of the tethered alcohol to yield **2.120**.

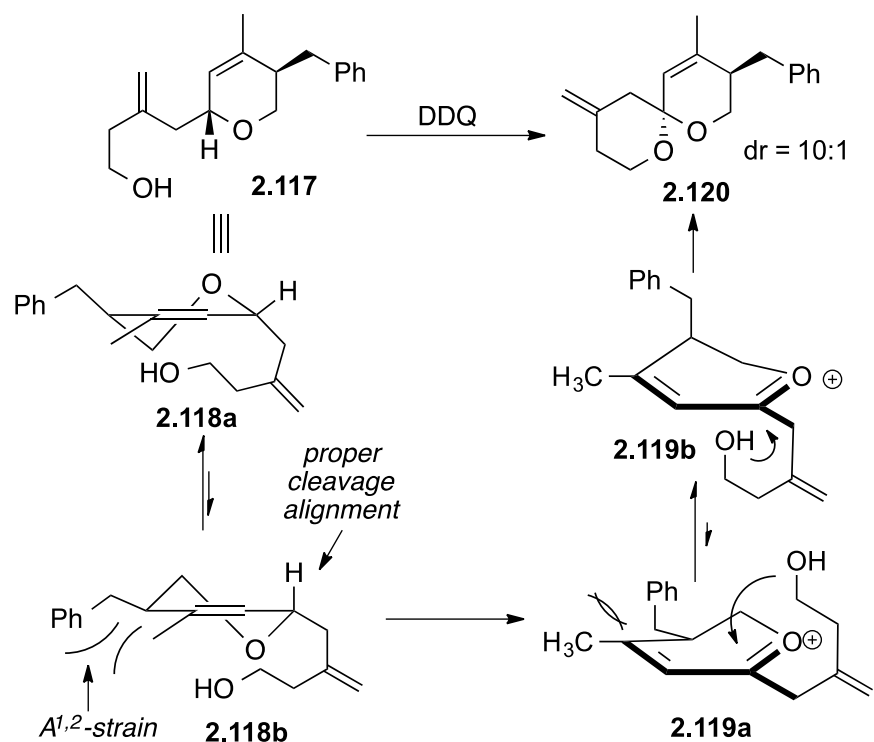


Figure 2.10 Stereochemical outcome of DDQ mediated spirocyclization

Similarly, the stereochemical orientation of **2.120** has been verified by coupling constants and NOESY spectroscopy (Figure 2.11). Both H_d and H_e have *ca* 3.7–4.0 Hz ³J_{H-H} coupling with H_a, indicating that H_a is in the equatorial position. In addition, no large coupling was observed for H_a and H_e. The nOe correlation observed for H_f and H_g confirms the 2,5-*anti* stereochemistry between the benzyl group and the trajectory of the incoming tethered alcohol, corroborating with transition state **2.119b**.

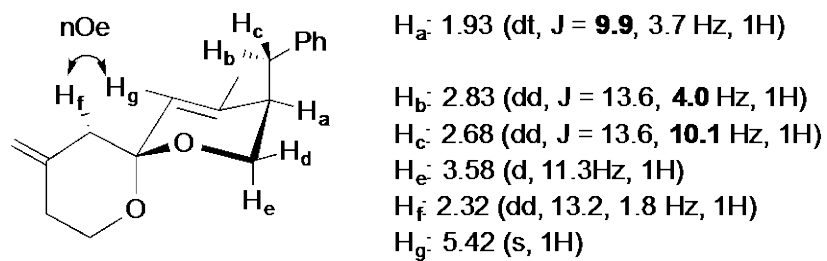


Figure 2.11 Stereochemical determination of 2.120

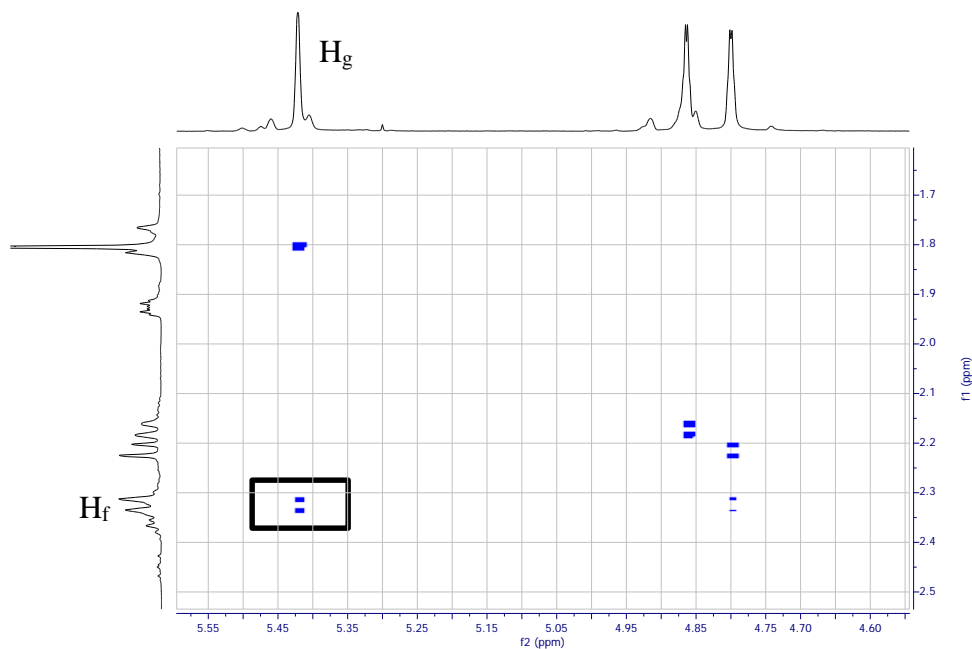


Figure 2.12 Positive nOe correlation between H_f and H_g

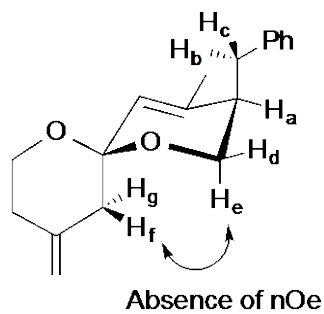


Figure 2.13 Negative nOe correlation control for alternative isomer

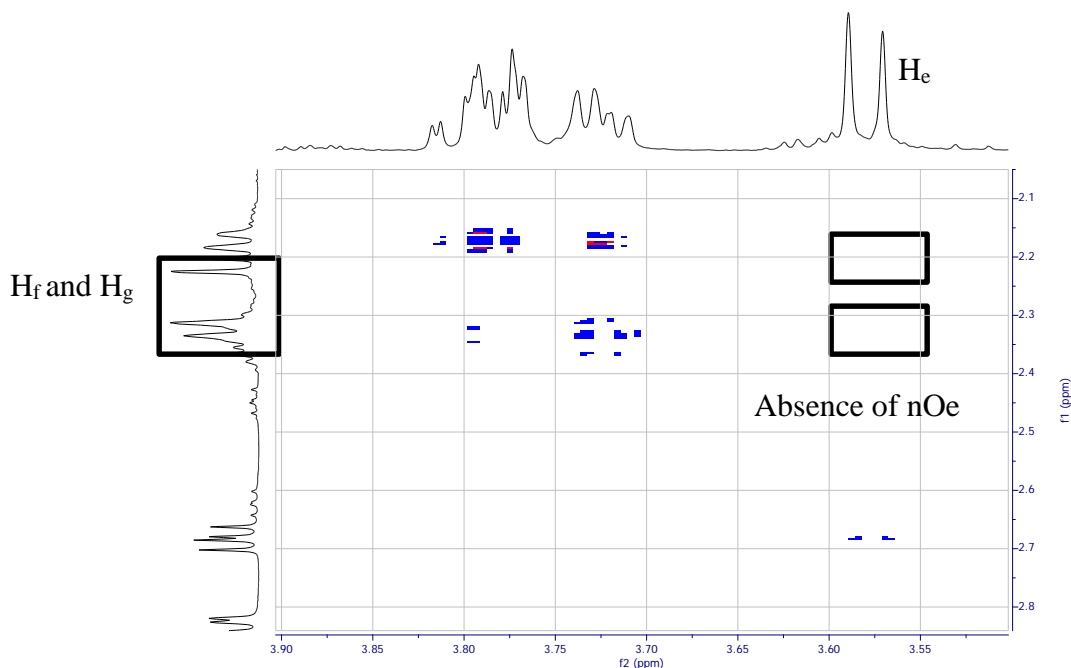


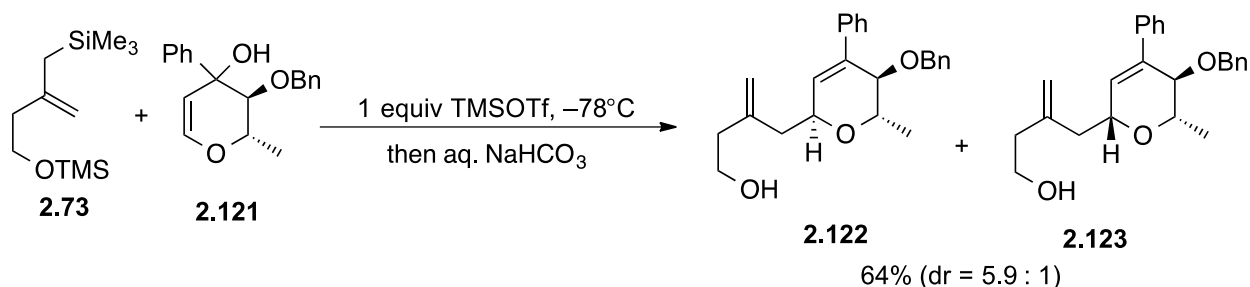
Figure 2.14 Negative control for nOe establishment

2.2.7.2 5' and 6'-disubstituted pyranol systems

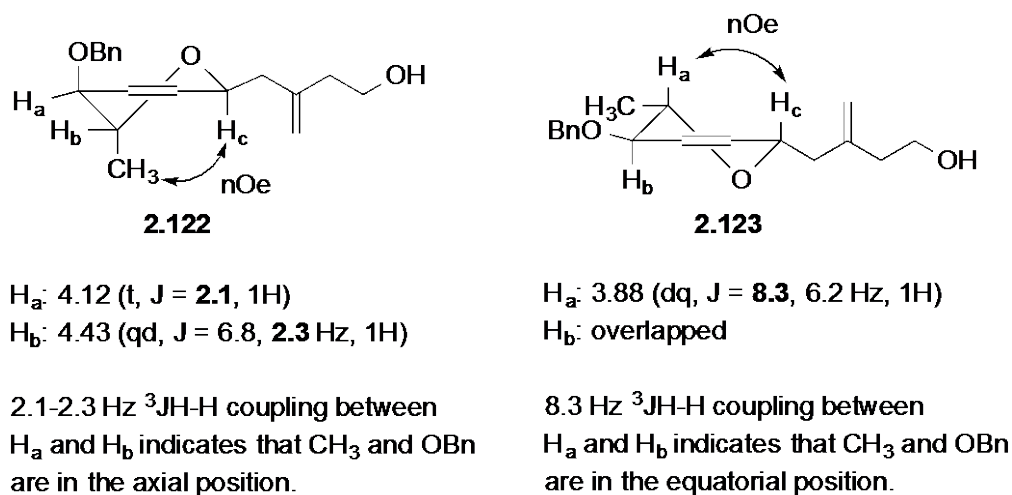
To understand how substituent effects within the elaborated dihydropyrans could affect the stereochemical outcome of the tandem Ferrier-DDQ fragment coupling reaction, dihydropyranol **2.121** with a 5'-OBn and 6'-CH₃ substituents was prepared from L-rhamnal (Scheme 2.27). The Ferrier coupling reaction was conducted using stoichiometric amount of TMSOTf at a lower temperature of -78 °C in hope of achieving higher diastereoselectivity. This also served as a control because a subsequent experiment performed using OTBS instead of OBn might be deprotected even under catalytic loadings of TMSOTf at an ambient temperature.

Under these reaction conditions (scheme 2.27), the α/β ratio was 5.9:1. After confirmation via NMR spectroscopy, the major diastereomer was determined to be dihydropyran **2.122** with the

2,6-substituents in an *anti* relationship. The minor diastereomer was determined to be dihydropyran **2.123** with the 2,6-*syn* configuration. Surprisingly, **2.122** has the 5' and 6' substituents orientated in the axial arrangement whereas in **2.123**, they occupy the equatorial position.



Scheme 2.27 Ferrier coupling of **2.121**



*phenyl substituent at the 4' position has been omitted for clarity

Figure 2.15 Stereochemical determination of Ferrier products: **2.122** and **2.123**

Analysis of the oxocarbenium ion intermediates (Figure 2.16) formed upon ionization with TMSOTf indicates that the more stable conformer **2.124b** results in the formation of the minor

diastereomer **2.123** whereas the less stable conformer **2.124a** leads to the formation of the major diastereomer **2.122**. Conformers **2.124a** and **2.124b** are postulated to be in rapid equilibrium. Although **2.124b** is the more stable oxocarbenium intermediate, interaction of the methyl group and the incoming allyl silane in the transition state results in unfavorable 1,3-*syn* pentane interactions, which substantially increased the barrier of activation in transition state **2.126**. Formation of the 2,6-diaxial Ferrier product is followed by a rapid ring inversion into the minor diastereomer **2.123** with both methyl and the tethered alcohol in the equatorial position.

Analogously, for DHP **2.122**, although the oxocarbenium intermediate **2.124a** leading to it is of higher energy due to A^{1,2} strain, the absence of a 1,3-*syn* pentane interaction between methyl and the incoming nucleophile renders transition state **2.125** as a comparatively lower activation energy barrier. Nevertheless, upon coupling the presence of the inherent A^{1,2} strain present is sufficient to trigger a ring flip into the more thermodynamically preferred configuration **2.122**.

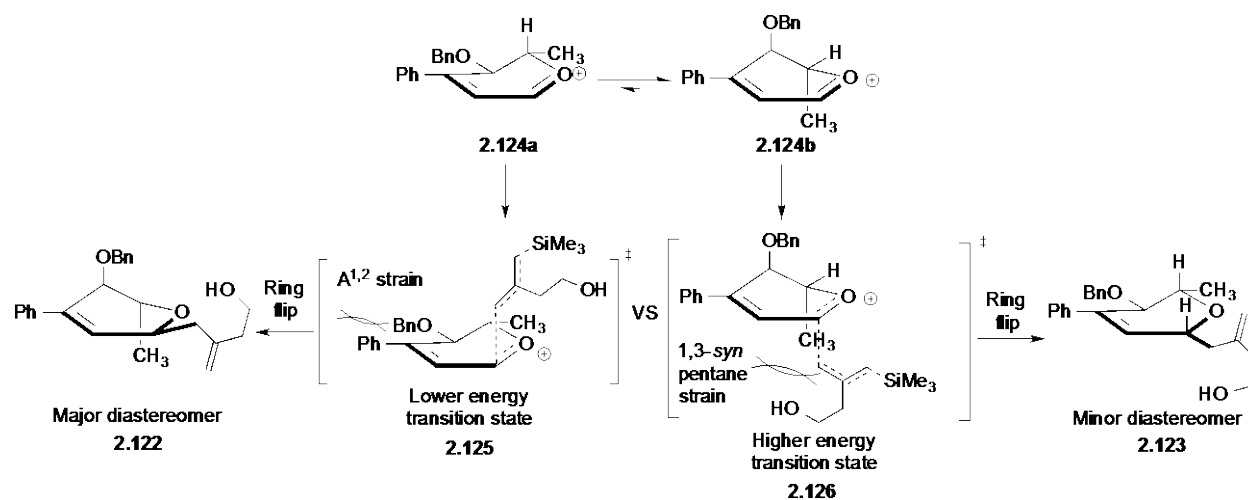
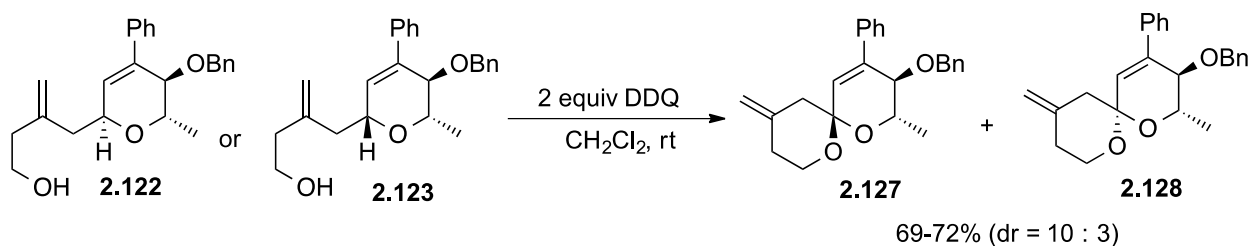


Figure 2.16 Curtin-Hammett analysis of Ferrier coupling

Unlike DHP **2.118a** (Figure 2.10) that must perform an unfavorable ring flip into DHP **2.118b** for the oxidative C–H bond cleavage, diastereomers **2.122** and **2.123** have the H atom arranged in the optimum axial orientation for facile C–H bond cleavage and formation of the oxocarbenium cation. Independent treatment of the diastereomers under oxidative cyclization resulted in a reduced reaction time (1h) and lower loadings of DDQ (2.0 equiv) used. The cyclized spiroketal products were obtained with comparable yields (69-72%) for both diastereomers. Spiroketal **2.127** and **2.128** were also consistently obtained with *ca.* dr of 10:3.



Scheme 2.28 Stereoconvergent oxidative cyclization

The structures of the spiroketals were elucidated by 2D nOe, COSY and coupling constants measurements (Figure 2.17).

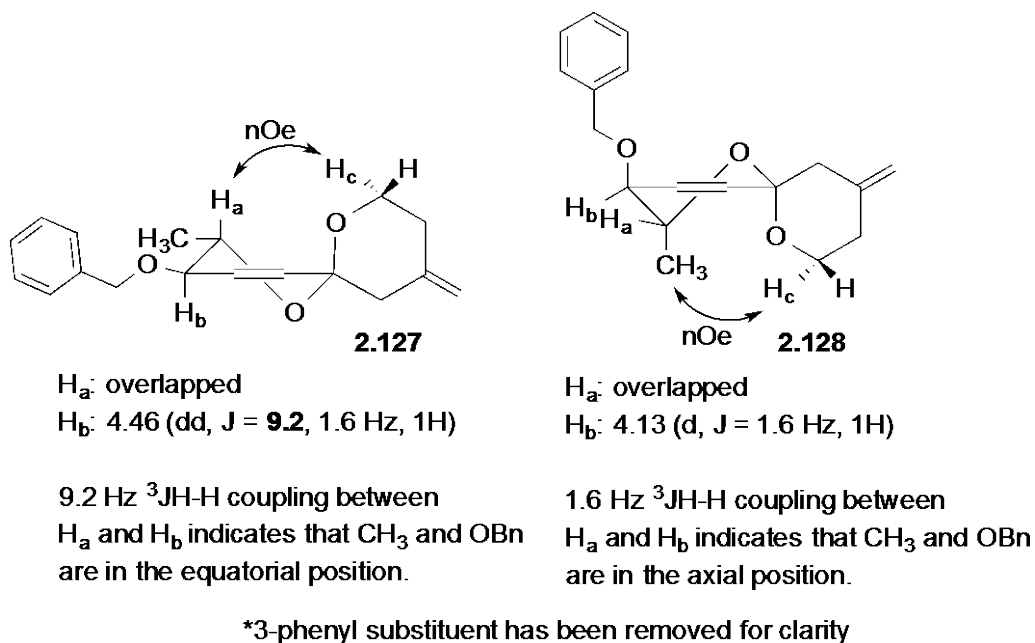


Figure 2.17 Stereochemical determination of spiroketals **2.127** and **2.128**

The consistent dr value obtained for the DDQ-mediated oxidative cyclization regardless of the diastereomer used indicates that each diastereomer goes through the common allylic oxocarbenium cation intermediate **2.129** (Figure 2.18). However, due to the inherent A^{1,2} strain between the 4-phenyl and 5-OBn substituent, **2.129** equilibrates between **2.129a** and **2.129b**.

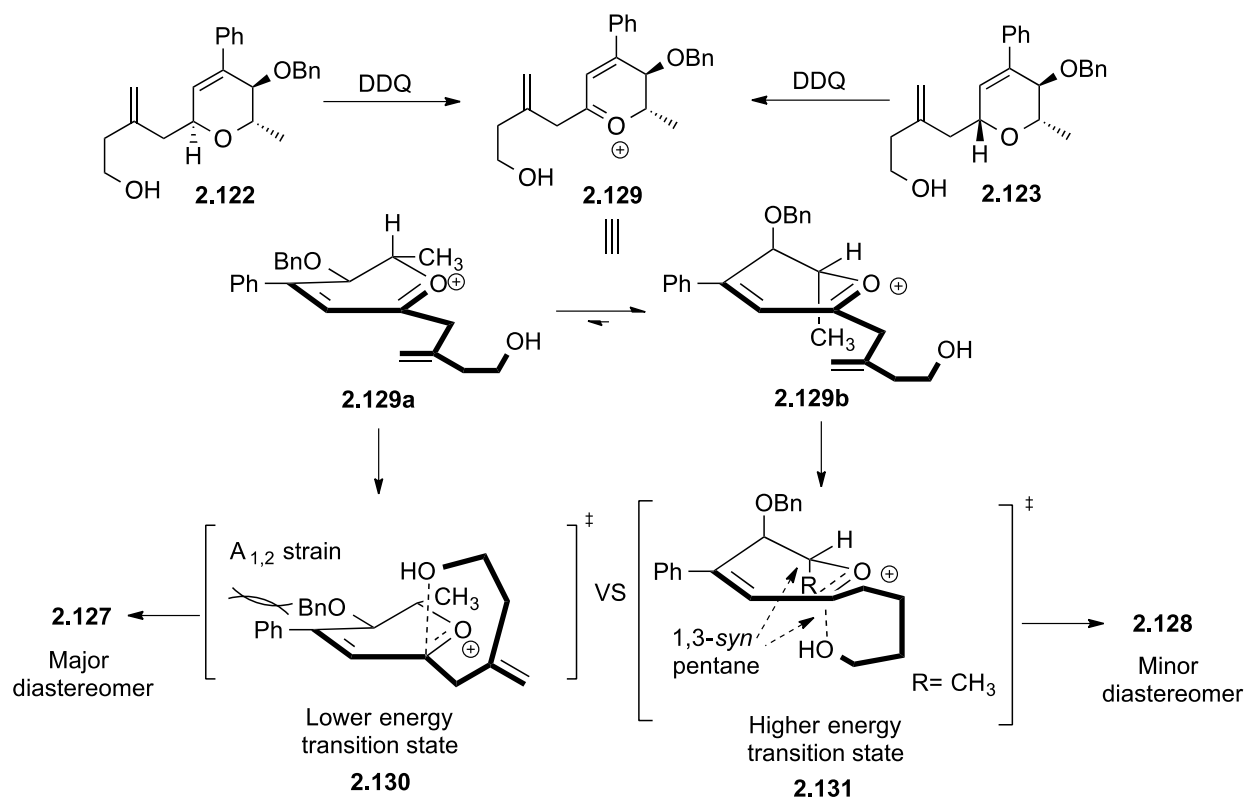
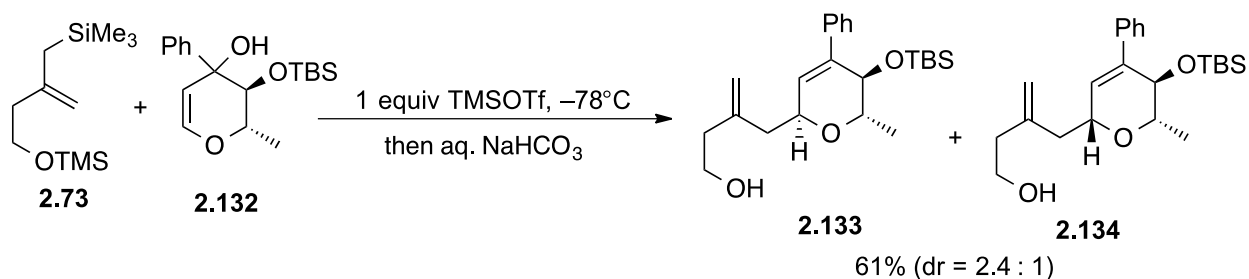


Figure 2.18 Stereochemical analysis of oxidative C-H cyclization

According to the Curtin-Hammett principle, although **2.129b** is the more favorable conformer, the transition state **2.131** leading to spiroketal **2.128** suffers from severe 1,3-*syn* pentane interaction between the methyl group and the tethered alcohol (Figure 2.18). The tethered alcohol can only approach from the bottom face to avoid an even higher energy twist-boat transition state. In contrast, although **2.129a** is the higher energy allylic oxocarbenium cation, the transition state **2.130** leading to **2.127** is of lower energy due to the tethered alcohol approaching in an *anti*-fashion with respect to the 6-methyl substituent through a chair-like transition state and avoiding any potential 1,3-*syn* pentane strain. In contrast to the Ferrier reaction where the kinetic products could undergo ring inversion to yield the more thermodynamic stable configuration, the spiroketals **2.127** and **2.128** trapped by oxidative

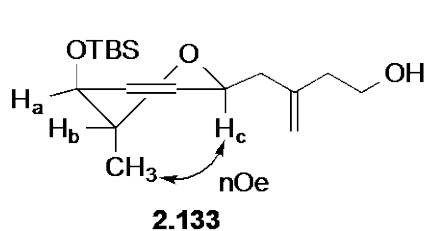
cyclization are stabilized by double anomeric effects and do not isomerize under the neutral environment of the DDQ system.



Scheme 2.29 Ferrier coupling with bulkier substituent

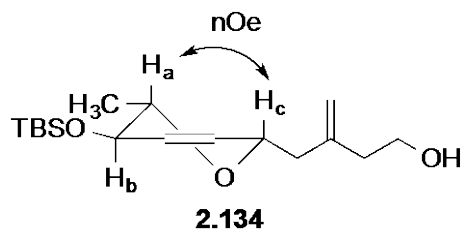
Substrate **2.132** was designed with a bulky OTBS group substituting the place of the OBn group in pyranol **2.121** (Scheme 2.29). The hypothesis was that $A^{1,2}$ strain between the 4'-phenyl group and the 5'-OTBS would be greatly enhanced and possibly exceed the rate determining 1,3-*syn* pentane strain, hence potentially inverting the diastereomeric ratio of the resultant Ferrier products and the spiroketals. Subjecting **2.132** to TMSOTf at -78°C , resulted in the formation of diastereomers **2.133** and **2.134** in 61% yield with α/β selectivity of 2.4:1.

The mixture of products obtained indicated that OTBS did not manage to lock the intermediate allylic oxocarbenium in a preferred all axial conformation cf. **2.124b** (cf. Figure 2.16) as intended. Instead equilibration with the higher energy conformer cf. **2.124a** was still occurring. Spectroscopic identification of **2.133** in the conformation shown in Figure 2.19 reveals that avoidance of 1,3-*syn* pentane strain was still the dominant determinant in ΔG^\ddagger activation for transition states.



H_a: 4.22 (dd, J = 2.6, 1.7 Hz, 1H)
 H_b: 4.10 (qd, J = 6.8, 2.6 Hz, 1H)

2.6 Hz ³JH-H coupling between H_a and H_b indicates that CH₃ and OBn are in the axial position.



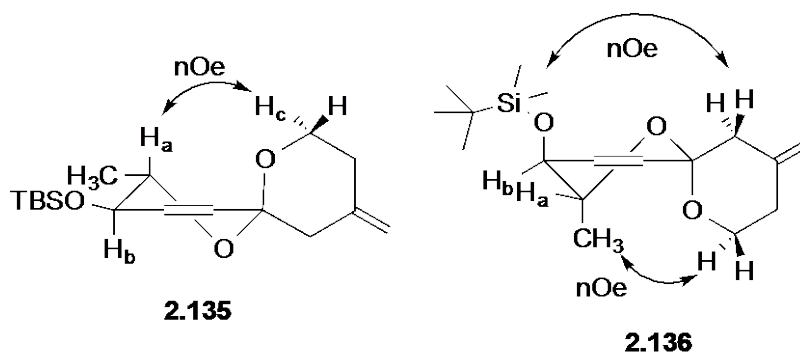
H_a: 3.63 (dq, J = 7.9, 6.2 Hz, 1H)
 H_b: 4.43 (ddd, 8.0, 2.7, 1.1 Hz, 1H)

8.0 Hz ³JH-H coupling between H_a and H_b indicates that CH₃ and OTBS are in the equatorial position.

*phenyl substituent at the 4' position has been omitted for clarity

Figure 2.19 Stereochemical determination of OTBS Ferrier products

Interestingly, subjecting THP **2.134** under the DDQ-mediated oxidative conditions, resulted in >5% of spiroketal formation. We postulated that the steric bulk of the OTBS group was impeding the approach of DDQ for H atom abstraction. Contrastingly, for the *trans*-Ferrier product **2.133**, as DDQ abstracts the H atom from the opposite face as the axial OTBS substituent, the cyclization proceeded as predicted albeit with diminished yield of 55%. The dr value of spiroketals obtained for the oxidative cyclization step was 4.6:1 (**2.135** : **2.136**). Stereochemical outcome of the spiroketalization can be rationalized in a similar manner as described for the OBn substituent in Figure 2.18. The comparable dr value obtained as the OBn substituent (10:3) indicates that both substrates go through similar transition states without much perturbation to the ΔG^\ddagger values. Based on these independent ring closure studies of **2.133** and **2.134**, a crude mixture of both diastereomers after the Ferrier reaction was subjected to oxidative DDQ chemistry in one-pot. This resulted in kinetic resolution of the diastereomers as THP **2.133** underwent spiroketalization at a much faster rate relative to THP **2.134**.



H_a: 4.02 (qd, J = **8.6**, 6.3 Hz, 1H)
 H_b: 4.39 (dd, J = **8.7**, 1.3 Hz, 1H)

8.7 Hz ³J_{H-H} coupling between H_a and H_b indicates that CH₃ and OTBS are in the equatorial position.

H_a: 4.21 (qd, J = 6.8, **2.2** Hz, 1H)
 H_b: 4.24 (d, J = **2.2** Hz, 1H)

2.2 Hz ³J_{H-H} coupling between H_a and H_b indicates that CH₃ and OTBS are in the axial position.

*3-phenyl substituent has been removed for clarity

Figure 2.20 Stereochemical determination of spiroketals 2.135 and 2.136

2.2.8 Summary

A highly convergent synthetic protocol to functionalized spiroketals has been developed. Our method utilizes a catalytic Lewis acid initiated Ferrier transposition reaction for the fragment coupling of dihydropyrans with allyl/enol silanes. This is followed by a DDQ-mediated oxidative spiroketalization. Studies on the relative geometry of the allylic hydrogen also indicate that C–H bond σ^* orbital must be in the correct *syn*-alignment with the oxygen radical cation and the adjacent alkene for constructive orbital overlap. Otherwise, there will be no effective C–H bond cleavage as the initial electron on DDQ can be reversibly transferred^[50] back to the oxygen on the glycal substrate.

Generally, the ring closure reaction for simpler substrates is stereoconvergent because the diastereoselectivity of the initial Ferrier reaction is inconsequential. Both diastereomers are oxidized to the same allylic oxocarbenium cation intermediate, which subsequently undergo a spirocyclization to yield the thermodynamically favorable spiroketals. However for more complex substrates, stereoelectronic properties of the Ferrier substrate, for example the installation of a bulky OTBS substituent at the 5'-position of the glycal ring, may impede the spatial approach of the DDQ oxidant, hence resulting in sluggish or null activity.

2.3 TELESCOPED HECK AND OXIDATIVE COUPLING

2.3.1 Design principles

The Floreancig group and others^[33, 51] have demonstrated that DDQ is a mild one-electron oxidant for the dehydrogenation of silyoxy dihydropyrans into dihydropyranones (Section 1.2). The potential of merging a transition metal-mediated cross coupling of an unsaturated glycal with an aryl electrophile followed by DDQ-mediated dehydrogenation and subsequent intramolecular oxa-Michael addition would provide an attractive streamlined entry into the family of spiroketals containing an aryl sp^2 -scaffold (Figure 2.21).

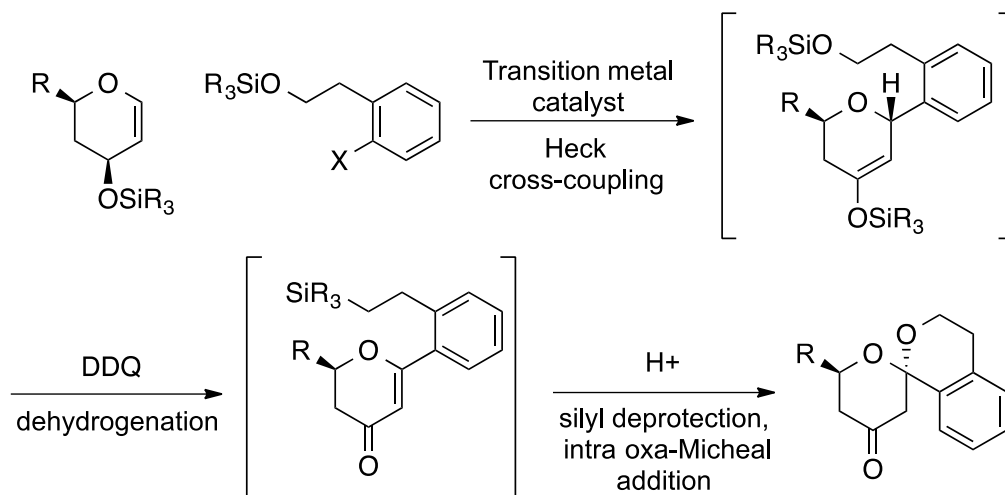


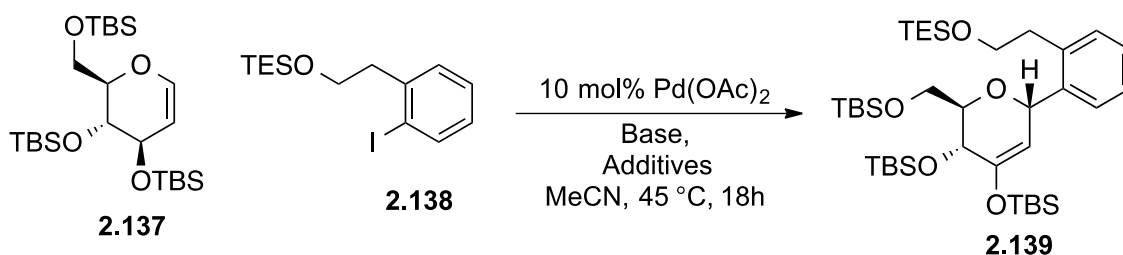
Figure 2.21 Telescoped transition metal cross-coupling with oxidative coupling

2.3.2 Reaction optimization

In the original report by Ye and co-workers^[51], boronic acids ($\text{X} = \text{B}(\text{OH})_2$) (Figure 2.21) were used as the coupling partner in an oxidative Heck type C-glycosidation with silyl-protected glycols. While boronic acids are attractive candidates due to its numerous advantageous qualities, the preparation of boronic acids usually involves an aryl halide^[52] as the starting basis and this additional transformation step is a concession step. The use of strong acid for some boronic acid preparations might also be incompatible with the tethered silyl alcohol. In addition, Ye's chemistry uses dioxygen as the terminal oxidant for the regeneration of the palladium catalyst. Seemingly benign, dioxygen is actually highly flammable and volatile. This might pose potential explosive risk during scale up operations and degrade the user-friendliness of the protocol. To this end, we have decided to focus on aryl iodides as the donor coupling partner. Silyl-protected **2.137** was selected as the unsaturated glycol for model studies due to its ease of accessibility from D-glycol.

The model reaction of **2.137** with **2.138** under Ye's conditions gave only 20% of the Heck product (Table 2). Switching the base from K_2CO_3 to Ag_2CO_3 significantly increased the yield to 68%. This marked increase in yield was attributed to the silver salt dual functions as both a base for sequestering the HI produced at the end of the Heck catalytic cycle and also facilitating the oxidative insertion of Pd(0) into the aryl iodide bond by precipitation of AgI salts. Interestingly, the omission of $Cu(OAc)_2$ as additive resulted in a detrimental effect on yield with only 20-28% of the aryl 2-deoxy-C-glycoside **2.139** isolated.

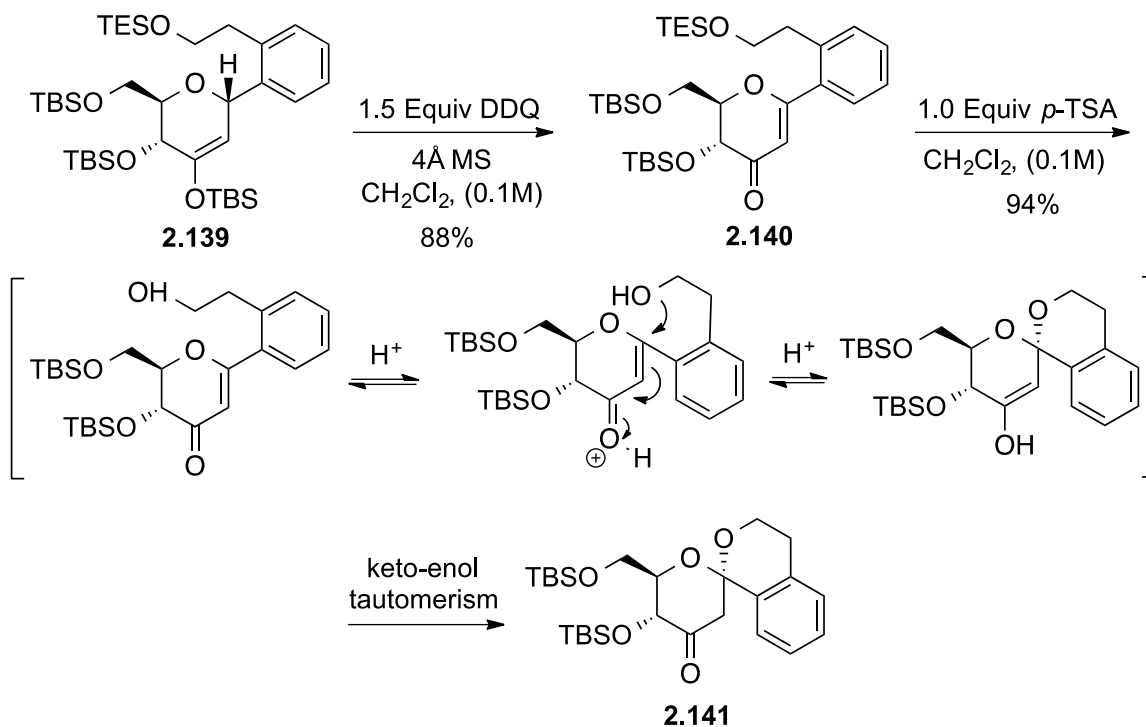
Table 2 Optimization of glycal Heck coupling



Entry	Base	Additive	Yield (%)
1.	K_2CO_3	$Cu(OAc)_2$	20%
2.	Ag_2CO_3	$Cu(OAc)_2$	68%
3.	Ag_2CO_3	none	20-28%

Upon isolation of enol ether **2.139**, the oxidative dehydrogenation to enone **2.140** occurred smoothly in the presence of DDQ at an ambient temperature to give 88% of the desired product (Scheme 2.30). Stirring with a stoichiometric amount of *p*-TSA resulted in concomitant desilylation of the tethered alcohol followed by an intramolecular oxa-Micheal to yield 94% of the desired spiroketal. Care was taken to ensure the reaction was quenched immediately with Et_3N and purified by column chromatography upon completion on TLC (~45 min). Excessive

amounts of *p*-TSA used or prolonged stirring time usually resulted in decomposition of the spiroketal **2.141** accompanied by cleavage of the OTBS appendages.



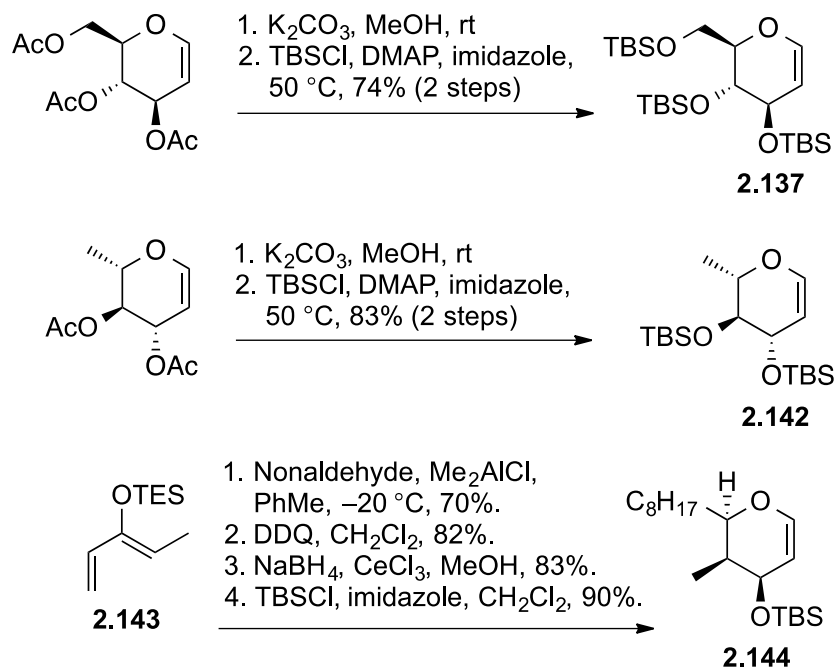
Scheme 2.30 Optimized DDQ mediated dehydrogenation and acid catalyzed oxa-Michael

Upon optimization of the individual steps for Heck coupling, dehydrogenation, and tandem desilylation with ring closure, a one-pot cyclization was attempted. Surprisingly, the DDQ-dehydrogenation reaction appeared to be extremely sluggish with less than 20% of pyranone **2.140** as estimated by TLC analysis even after 1.5 h. To this end, the reaction solvent was switched to 1,2-dichloroethane (DCE) due to its higher boiling point (84 °C) for the initial Heck coupling and also its comparable activity to dichloromethane for the subsequent dehydrogenation reaction. Using DCE as the optimum solvent, a net 55% yield was obtained for the one-pot telescoped Heck followed by DDQ-mediated cyclization reaction. Further optimization reveals

that a quick silica gel filtration after the initial Heck coupling actually improves the overall yield by (~5-7%). The extra filtration step is hypothesized to facilitate the reaction by the removal of extraneous amounts of Pd, Ag and Cu salts that might inhibit the efficacy of DDQ during the dehydrogenation step.

2.3.3 Design and preparation of silylated glycals

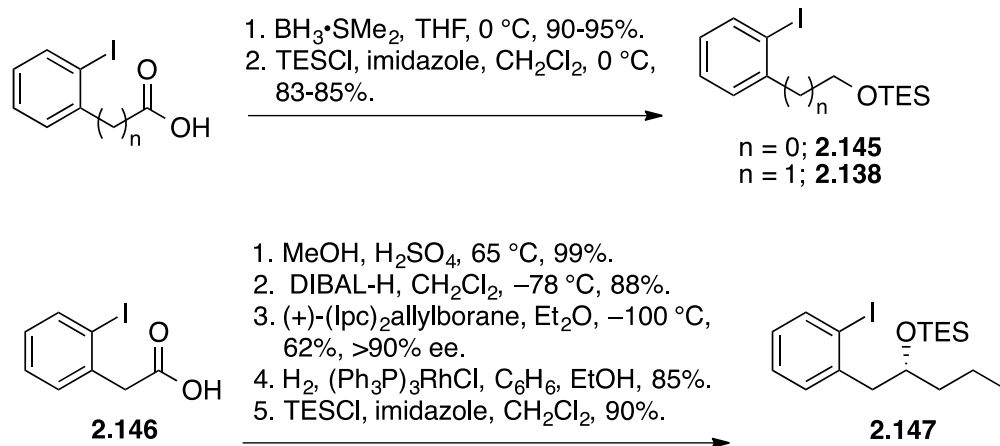
Tri-*O*-silylated-D-glycal **2.137** and di-*O*-silylated-L-rhamnol **2.142** were prepared from the corresponding commercially available sugars via a two-step deacetylation and silylation sequence. Enol ether **2.144** was prepared through an initial HDA reaction between 1,3-pentadiene **2.143** and nonaldehyde catalyzed by Me₂AlCl to give the 5'-6'-*syn* silyl enol ether containing a DHP ring. This intermediate was dehydrogenated to the pyranone, reduced via a Luche reduction^[53] to the pyranol and finally silylated to yield **2.144** (Scheme 2.31).



Scheme 2.31 Preparation of Heck glycal acceptors

2.3.4 Design and preparation of Heck aryl iodide partner

Silylated primary alcohols **2.145** and **2.138** were prepared from the corresponding 2-iodobenzoic acid and 2-iodophenylacetic acid via a two-step sequence of $BH_3 \cdot SMe_2$ -mediated acid reduction to the corresponding alcohol followed by silyl protection. TES ether **2.147** was prepared by an initial DIBAL-H reduction of methyl 2-iodobenzoate **2.146** into the aldehyde followed by an asymmetric allylation utilizing the chiral boron reagent, (+)-(Ipc)₂allylborane^[54]. The resultant allyl alcohol was reduced to the alkane using Wilkinson's catalyst and subsequently protected as the silyl ether (Scheme 2.32).



Scheme 2.32 Preparation of Heck donor partner with tethered alcohol

The size of the second ring forming within the spiroketal can be easily controlled by tapering or lengthening the tail ($n = 0, 1$) of the tethered alcohol. The triethylsilyl (TES) protecting group was chosen so that it can be selectively deprotected at a faster rate by *p*-TSA relative to other TBS functionalities. TES ether **2.147** was hypothesized to enhance the rate of the oxa-Michael ring closure due to its nucleophilicity conferred by the adjacent aliphatic alkane chain.

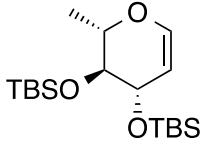
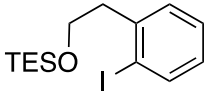
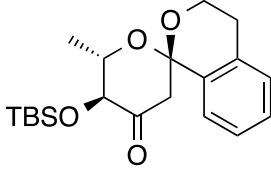
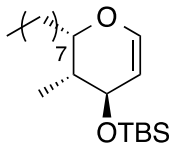
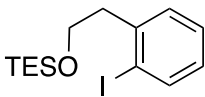
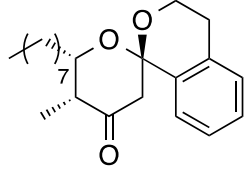
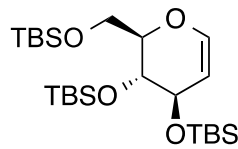
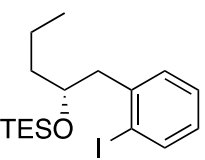
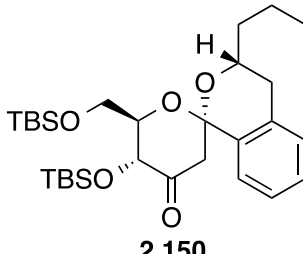
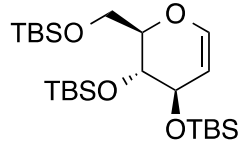
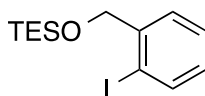
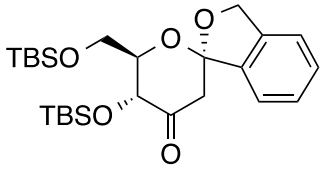
2.3.5 Substrate scope of telescoped Heck coupling with oxidative cyclization

Replacing the CH_2OTBS group at the 6'-position of the glycal with a methyl substituent did not seem to affect the net yield of the reaction (table 3, entry 1). The utilization of secondary silyl ether **2.147** gave slightly improved yield of the cyclized product **2.150** over the primary alcohol-containing iodoarenes (table 3, entry 3). Significantly, the ability to apply secondary alcohols as nucleophiles greatly expanded the plethora of complex spiroketals accessible through this methodology.

Spiroketal **2.151** possessing a [6.5]-spiroketal ring system is particularly attractive due to its close resemblance to type II diabetes lead compound, Tofogliflozin (CSG452) **2.3**. However, shortening the aliphatic alcohol tether seemed to have a detrimental effect on the yield (32%) of the spiroketal (table 3, entry 4). Analysis of the individual steps revealed that the initial Heck coupling did not proceed to completion. We hypothesize that the initial oxidative insertion of the Pd (0) catalyst into iodoarene bond encountered increased steric hindrance from the neighboring silyl-protected alcohol, hence attributing to the low coupling yield. In addition, the combined deleterious effects of the metals salts and the starting materials might have further inhibited the oxidative cyclization step. In an attempt to improve the overall yield, the Heck intermediate was purified by column chromatography before subjecting to oxidative cyclization. The best run gave a yield of 63% for the Heck coupling with the subsequent dehydrogenation and acid catalyzed ring closure giving a yield of 74%. The net yield was improved to 47%.

Notably, benzylic oxidation was not in direct competition with oxidative cyclization. We postulate that acid-mediated oxa-Micheal ring closure was faster than benzylic oxidation^[55] under our experimental conditions.

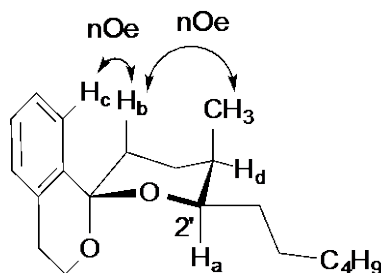
Table 3 Further examples of tandem Heck oxa-Micheal fragment coupling

Entry ^a	Dihydropyran	Iodoarene	Product	Yield (%) ^b
1	 2.142	 2.138	 2.148	58 (61)
2	 2.144	 2.138	 2.149	53 (58)
3	 2.137	 2.147	 2.150	61 (70)
4	 2.137	 2.145	 2.151	32 (47) ^c

^a Please see the Supporting Information for details regarding substrate synthesis, reaction conditions, and product characterization. ^b Yields refer to isolated, purified materials of the one-pot protocol. Parenthetical yields refer to reactions that were filtered following the Heck reaction. ^c 40% based on recovered starting material. Parenthetical yield refers to a protocol in which the product from the Heck reaction was purified by flash chromatography.

The conformation of spiroketal **2.149** (table 3, entry 2) is interesting because it has placed the 5'-methyl substituent in the axial position with the 6'-alkyl aliphatic chain in equatorial orientation so as to minimize unfavorable 2,6-*syn*-pentane strain brought about by enhanced A-values of substituents occupying the 2' and 6' position of the THP ring. Concurrently, axial placement of

the 5'-methyl substituent also alleviates any 1,2-allylic strain with the adjacent 2'-carbonyl group.



2.149

H_a: 4.21 (ddd, J = 7.9, 4.7, 2.8 Hz, 1H)

H_d: overlapped

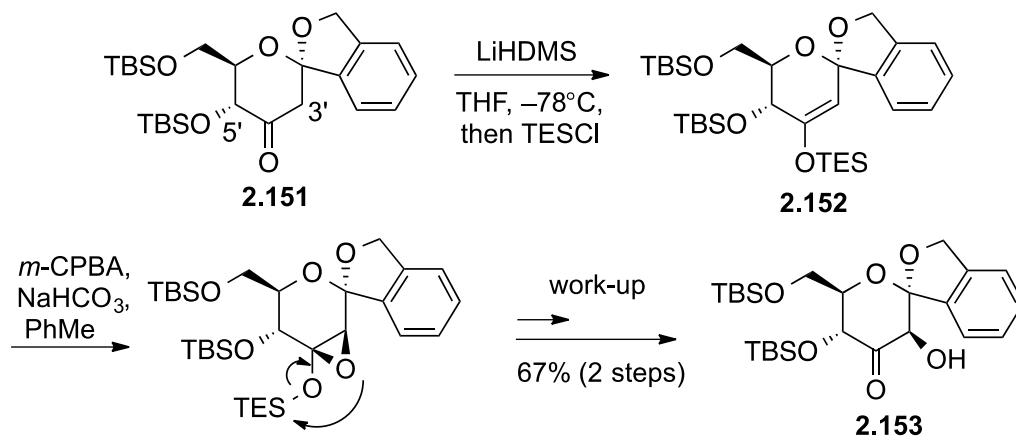
*4'-ketone has been omitted
for clarity

4.7/2.8 Hz ³JH-H coupling between
H_a and H_d indicates that CH₃
and C₆H₁₃ are in an axial-equatorial
position.

Figure 2.22 Stereochemical assignment for 2.149

2.3.6 Post cyclization modifications

Closer inspection of Tofogliflozin (CSG452) **2.3** reveals a triad of alternating stereogenic hydroxyl groups on the 3', 4' and 5'-backbone of the glycal fragment. We hypothesized that the hydroxyl group at the 3'-carbon, α to the carbonyl group can be easily introduced with a Rubottom oxidation. Provided that the newly generated hydroxyl group is in a 1,3-*syn* relationship with the 5'-OH group, the *anti*-hydroxyl group on the 4'-position can be readily installed through a stereoselective reduction.



Scheme 2.33 Rubottom oxidation of 2.166

However, conformation analysis of **2.151** indicates that it exists in the configuration where the 5' and 6'-substituents are equatorial orientated to minimize 1,3-diaxial interactions with the axial C–O bond at the 2' position. Kinetic deprotonation of **2.151** with LiHMDS followed by trapping with TESCl generates enol silane of **2.152**. Projection of **2.152** in the half-chair form (Figure 2.23) dictates that subsequent *m*-CPBA epoxidation can only proceed from the bottom face to prevent clashing with the axially orientated C–O bond on the top face. Upon work up, **2.153** was obtained as a single diastereomer in 67% overall yield over two steps. Although the 3'-hydroxyl stereogenic center formed in **2.153** is in the opposite configuration as that in Tofogliflozin **2.3**, the protocol presented provides a useful entry into possible analogs.

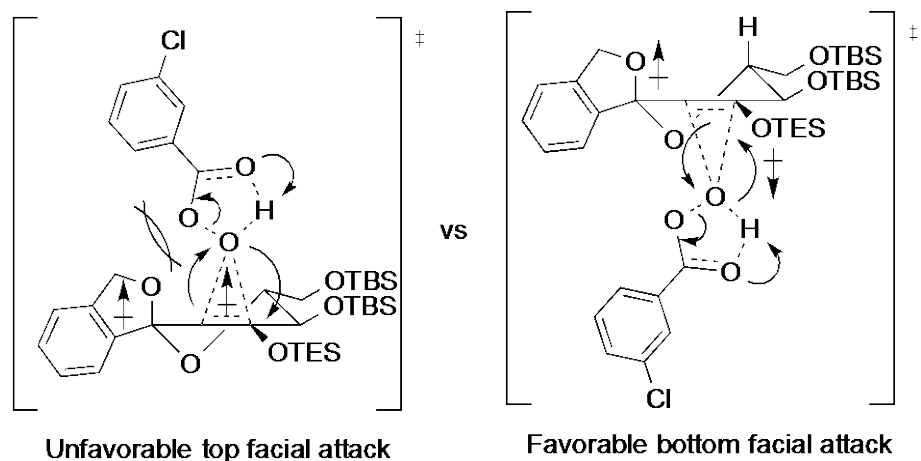


Figure 2.23 Substrate controlled stereoselective epoxidation

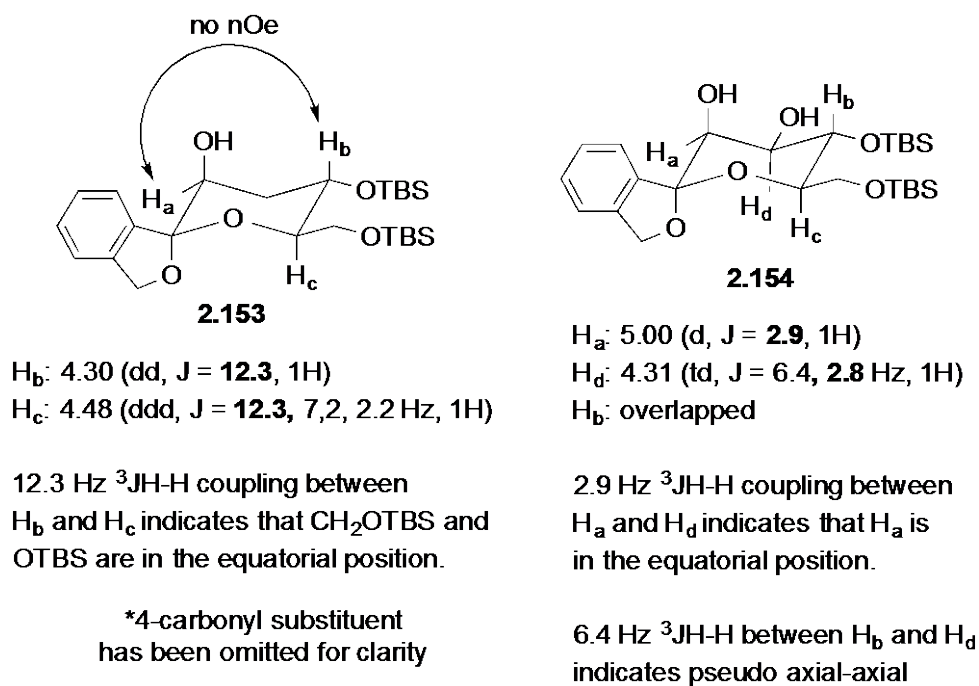


Figure 2.24 Stereochemical determination of Rubottom oxidation

The stereochemistry of the α -hydroxylated spiroketal **2.153** has been verified by 2D NMR and coupling constants analysis. In an unoptimized reaction, **2.153** was also reduced to 3',4'-OH spiroketal **2.154** for further confirmation of its structural features (Figure 2.24).

2.3.7 Stereoelectronic analysis of telescoped Heck-coupling cyclization

2.3.7.1 Heck Coupling

In order to establish a better understanding of the telescoped Heck coupling tandem oxo-Michael reaction, the key intermediates were characterized and analyzed. The tri-*O*-silylated-glycal **2.137** was chosen as the model substrate because Ye^[51] and others^[56] have shown that installation of a substituent such as a bulky TBS group at the 5' and 6'-position of the glycal ring helps to lock it in a fixed configuration, preventing conformation flexibility (Figure 2.25). In addition, the OTBS group at the 4'-position is a poor leaving group in contrast to OAc. Synergistically, these factors facilitate in the *syn* β -H elimination of the Pd- σ -adduct as palladium hydride and prevent other undesirable decomposition pathways.

In Figure 2.25, the palladium intermediate formed after oxidative addition undergoes π -complexation with the double bond on the glycal on the opposite face of the 4'-allylic OTBS group. Subsequent migratory insertion gives Pd- σ -adduct **2.155**, which can only partake in synclinal β -H elimination.

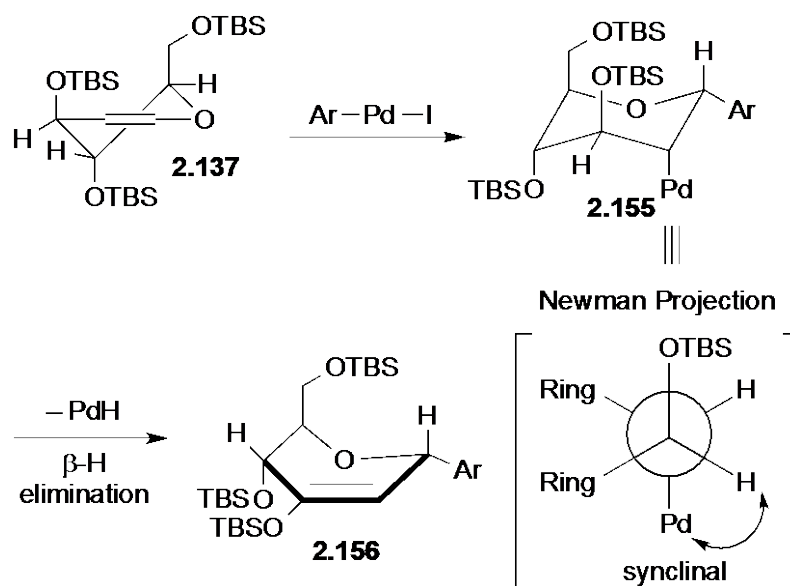
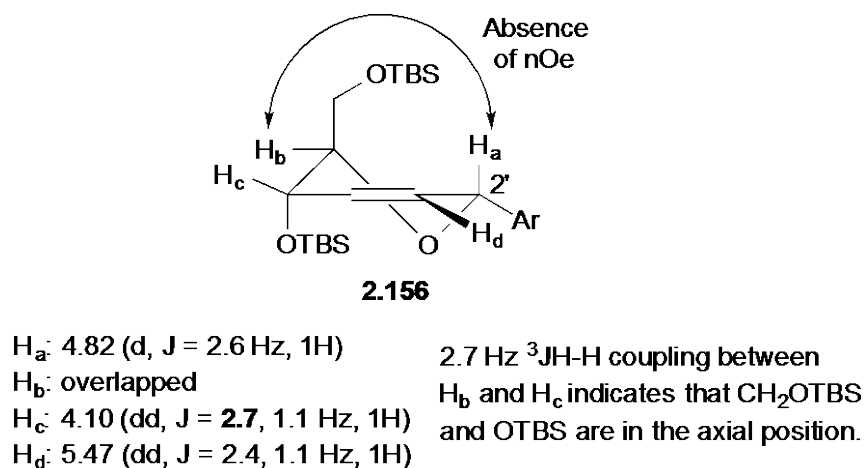


Figure 2.25 Stereochemical analysis of glycal-Heck coupling

The 2,6-*trans* stereochemical outcome of the Heck product **2.156** formed between glycal **2.137** and iodoarene **2.146** has been verified (Figure 2.26) by NMR spectroscopy.



*4-OTBS substituent has been omitted for clarity

Figure 2.26 Stereochemical analysis of Heck intermediate **2.156**

2.3.7.2 DDQ mediated dehydrogenation

The DDQ-mediated dehydrogenation (Figure 2.27) is postulated to involve an initial single electron abstraction of the electron rich TBS silyl enol ether to the allylic radical cation **2.157**. The 2'-H atom on the glycal ring being in the axial orientation is well poised for a hydrogen atom abstraction by DDQ radical to yield the oxocarbenium ion **2.158**. This is followed by isomerization into cation **2.159**, which loses TBS cation to yield 5', 6'-diaxial enone **2.160a**. Subsequently, **2.160a** undergoes ring inversion to yield the all-equatorial thermodynamic product **2.160b**.

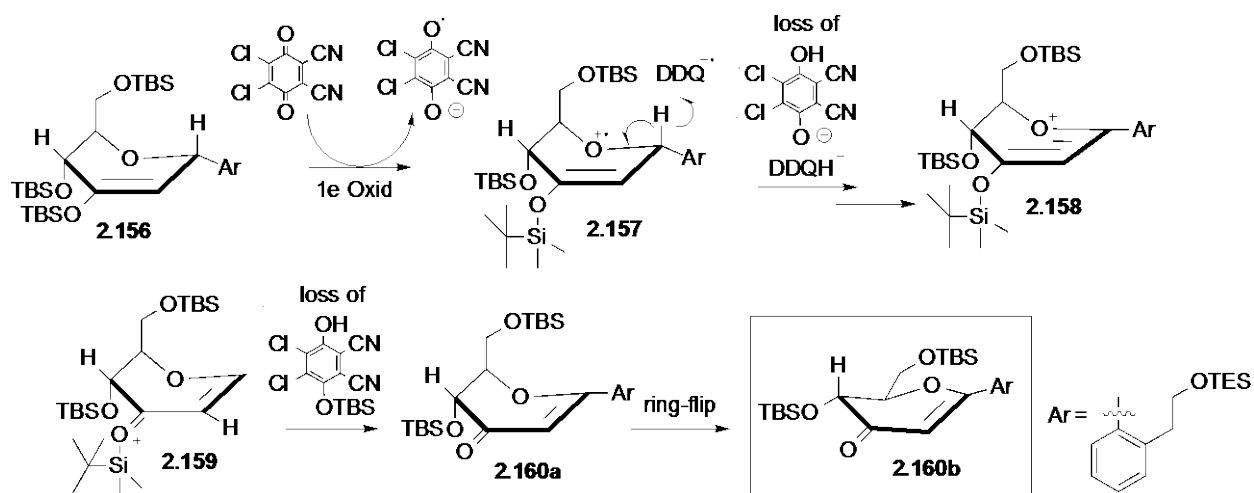
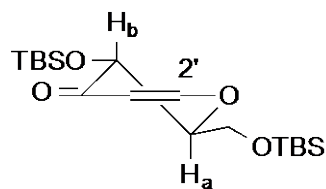


Figure 2.27 DDQ mediated dehydrogenation of glycal



2.160b

H_a: 4.36 (ddd, J = 12.0, 3.5, 2.4 Hz, 1H)

H_b: 4.49 (d, J = 12.0)

*2-Ar substituent has been omitted
for clarity

12.0 Hz ³J_{H-H} coupling between
H_a and H_b indicates that CH₂OTBS
and OTBS are in the equatorial
position.

Figure 2.28 Stereochemical correlation for 2.160b

2.3.7.3 *p*-TSA catalyzed spiroketalization

The *p*-TSA used in the reaction serves a dual role in facile deprotection of the TES group as well as rapid ionization of the carbonyl functionality within the unsaturated glycols into the allylic cation resonance forms (Figure 2.29). Similar to the Ferrier oxidative cyclization analysis, although **2.161a** is the more stabilized intermediate due to the minimization of A^{1,2} strain, the eventual built up of 1,3-diaxial strain in transition state **2.162** resulted in a larger activation barrier to overcome relative to **2.163**. Hence, **2.141** was formed as the major diastereomer. However, the absence of any minor diastereomer **2.164** indicates that transition state **2.162** must be highly unfavorable. This is coupled with the possibility that the 4'-allylic alcohol in **2.163** might also impose a lower energetic A^{1,2} strain penalty as compared to a phenyl group (cf. **2.130**, Figure 2.18), thus further favoring its equilibrium.

Nevertheless, under the acidic *p*-TSA conditions, even if a trace amount of the minor diastereomer **2.164** were to be formed, it is possible that it might equilibrate into the more

thermodynamic stable form **2.141** through a ring opening /ring closing equilibria that may be too rapid for detection on TLC.

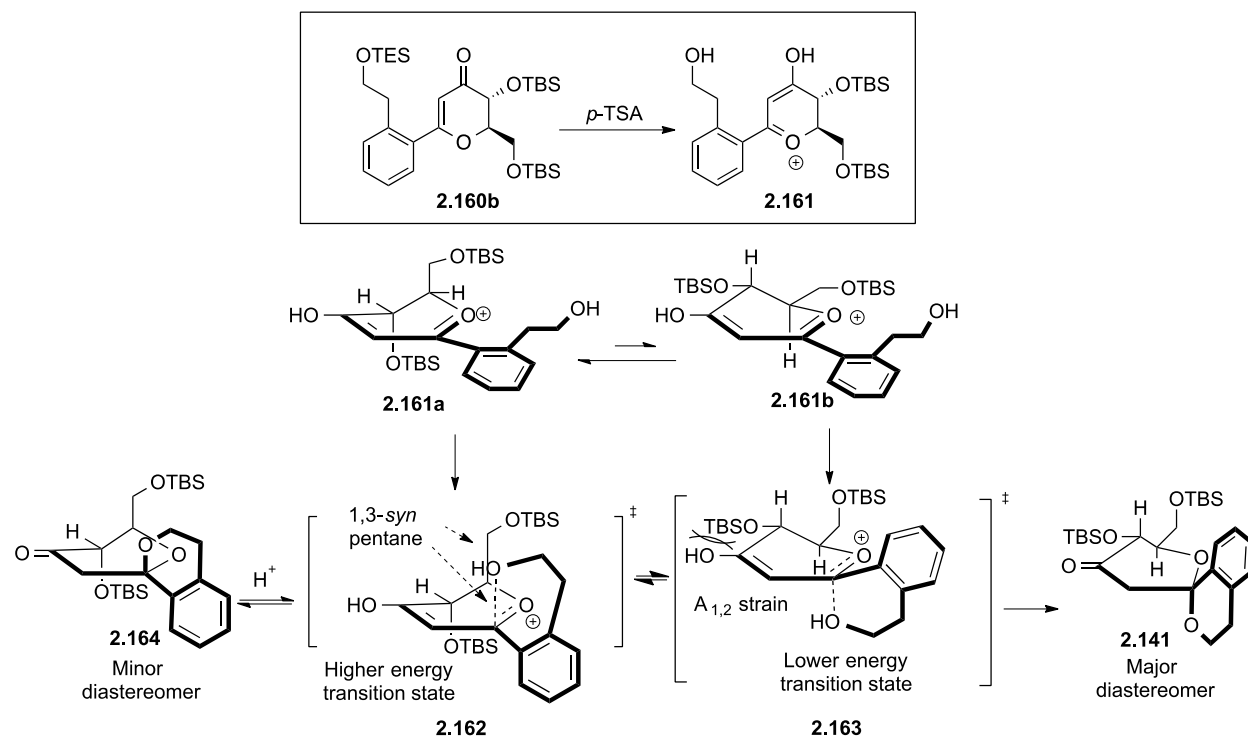


Figure 2.29 Acid catalyzed pseudo oxa-Micheal spiroketalization

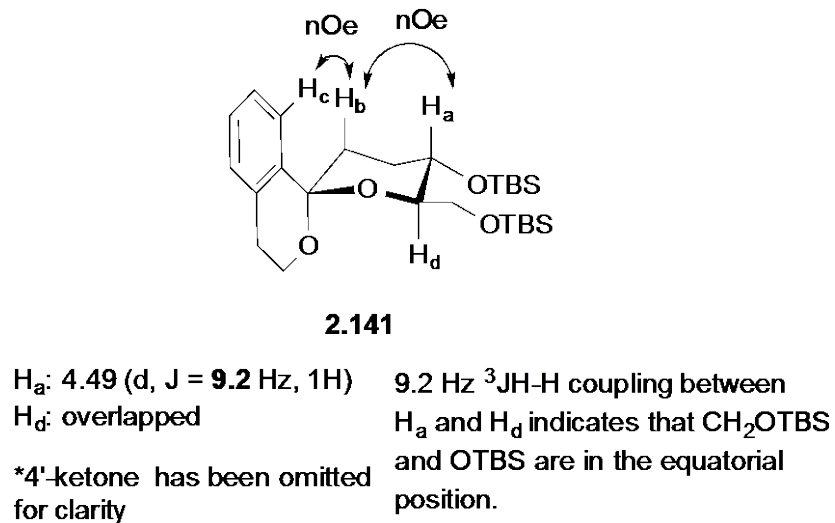


Figure 2.30 Stereochemical correlation for 2.141

2.3.8 Summary

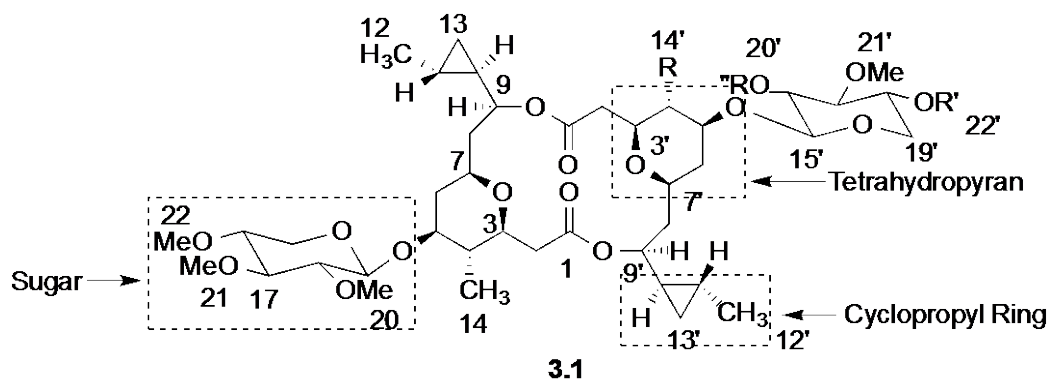
A telescoped Heck oxidative cyclization protocol to spiroketals has been developed. Unlike the tandem Ferrier-DDQ-oxidative cyclization mechanism, the role of DDQ serves to dehydrogenate the electron rich silyl enol ether into the α, β -dihydropyranone. In the presence of *p*-TSA, the pyranone readily ionizes to a transient allylic cation that is trapped by the tethered alcohol in a pseudo oxa-Michael type reaction. The stereochemical outcomes of the products are dictated solely by thermodynamics. The resultant novel spiroketals possess a planar sp^2 -aromatic backbone coupled with a 3D spiroketal scaffold; making them an attractive chemical library to target for medicinal chemistry studies.

3.0 TOTAL SYNTHESIS OF CLAVOSOLIDE A: A SHOWCASE OF OXIDATIVE OXOCARBENIUM CATION COMPATIBILITY WITH CYCLOPROPANE

3.1 INTRODUCTION

3.1.1 Isolation of clavosolides A-D from marine organism

Clavosolides A-D are metabolites isolated from the extracts of the marine sponge *Myriastragalus clavosa* off the coast of Philippines. Clavosolides A-B were reported by Faulkner and coworkers^[57] in 2001 whereas clavosolide C and D were subsequently reported by Erickson and co-workers^[58] in 2002. Previous investigation of *M. clavosa* collected in Palau afforded calvosines A-C, which are potent cytotoxins related to the calyculins^[59]. However, chemical separation of the Philippines sample did not yield any calvosines but only four interesting dimeric macrolides, which are non-cytotoxic. The structures of these trace metabolites were assigned extensively by 2-D NMR spectroscopic analyses. This family of 16-membered macrolides differs only in the substitution of the THP ring at position 14' and methylation of the glycosidic sugar core at position 20' and 22'. Due to its C₂ symmetrical architecture, clavosolide A (**3.1**) in particular has been the target of numerous synthetic groups.



clavosolide A: R= R'= R''= CH₃
 clavosolide B: R= R'= CH₃, R''= H
 clavosolide C: R= R''= CH₃, R'= H
 clavosolide D: R=H, R'= R''= CH₃

Figure 3.1 Members of the clavosolide family

3.1.2 Structural determination of clavosolide A

According to the report by Faulkner and co-workers, clavosolide A (**3.1**), $[\alpha]_D -48.5$ (*c* 1, CHCl₃), was isolated as a viscous green oil. Its molecular formula, C₄₄H₇₂O₁₆ was established from HRFABMS measurement of [M + Na]⁺ peak at *m/z* 879.470. The ¹³C NMR spectrum only contained 22 signals, which is indicative of a symmetrical dimer. The IR spectrum also revealed an ester stretch at 1730 cm⁻¹. The absence of hydroxyl bands meant that all the oxygen atoms were involved in either ester or ether linkages. Extensive 2D NMR techniques such as COSY, HMBC, ROESY as well as molecular modeling were used in peaks assignments.

The relative stereochemistry of the glycosidic bond between C₁₅ and C₅ (Figure 3.2) was determined to be a β-linkage due to the large diaxial coupling (*J* = 8-9 Hz) between the oxymethine protons based on independent study on the elucidation of clavosolide C by Erickson and co-workers^[60]. The relative stereochemistry of the cyclopropyl substituent was also

determined to be *trans* from its coupling constant of 4.4 Hz between H-10 and H-11. This was further confirmed by NOESY correlation between H₃-12 and H-10 and also between H-11 and H-9. The methylene protons of H-6 at δ 1.56 appeared as a ddd with three large *J*-values of approximately 12 Hz, thus indicating the axial orientation of neighboring H-3, H-5 and H-7 protons and placing the methyl group H₃-14 in an equatorial position.

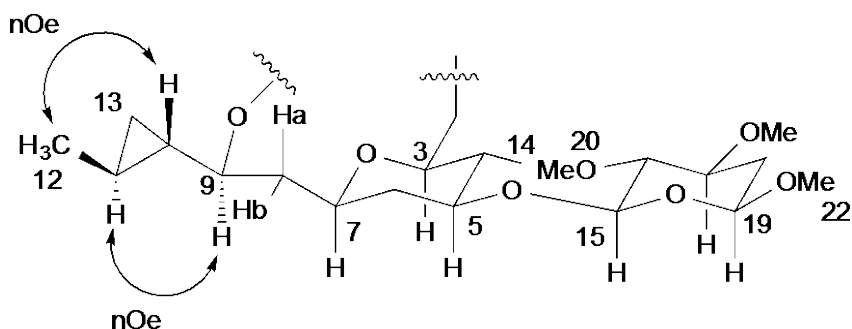


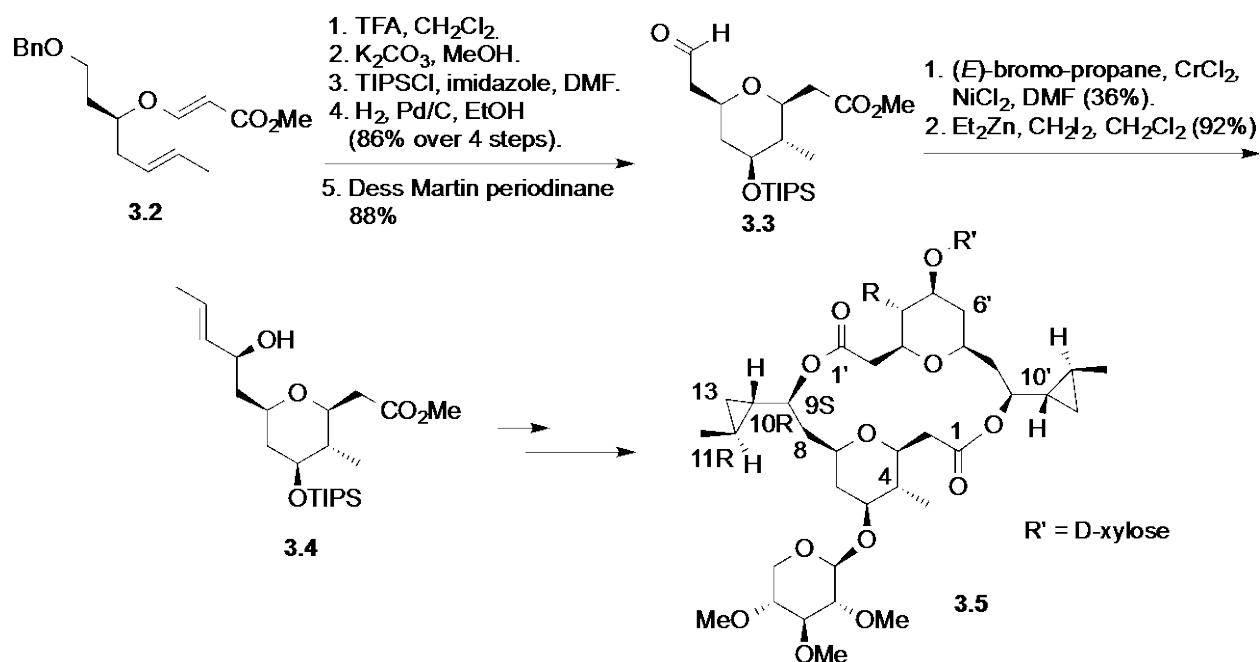
Figure 3.2 Selected spectroscopic analysis for 3.1

3.1.3 Previous syntheses of (-)-clavosolide A

The total synthesis of (-)-clavosolide A was first attempted by Willis^[61] and co-workers in 2005. Interestingly, the macrocycle cyclopropyl side-chains previously assigned 10*S*, 10'*S*, 11*S*, 11'*S* were incorrect. Following its total synthesis, it was proposed to possess the 10*R*, 10'*R*, 11*R*, 11'*R* configuration. In 2006, the proposed revised structure was confirmed by total synthesis credited to Lee and co-workers^[62]. However, Lee misinterpreted the sign of the optical rotation, misleading them to believe that they had made the enantiomer of the natural product. This error was subsequently corrected by Smith et al.^[63] as well as Willis et al.^[64], who independently synthesized the same revised structure and unambiguously established that Lee had indeed made the naturally occurring (-)-clavosolide A.

3.1.3.1 Willis's total synthesis of clavosolide A diastereomer

Willis and co-workers^[61] prepared the starting enol ether **3.2** from an asymmetric crotyl transfer reaction. Subjection of **3.2** to a Prins cyclization under acidic conditions resulted in the formation of the THP ring with three continuous stereocenters in a one-pot reaction. Further manipulation gave **3.3**, which was reacted with (*E*)-1-bromo-1-propene in a Nozaki-Hiyama-Kishi reaction to give a diastereomeric mixture of allylic alcohols. Charetté *syn*-directed cyclopropanation of the desired allylic alcohol gave intermediate **3.4**.



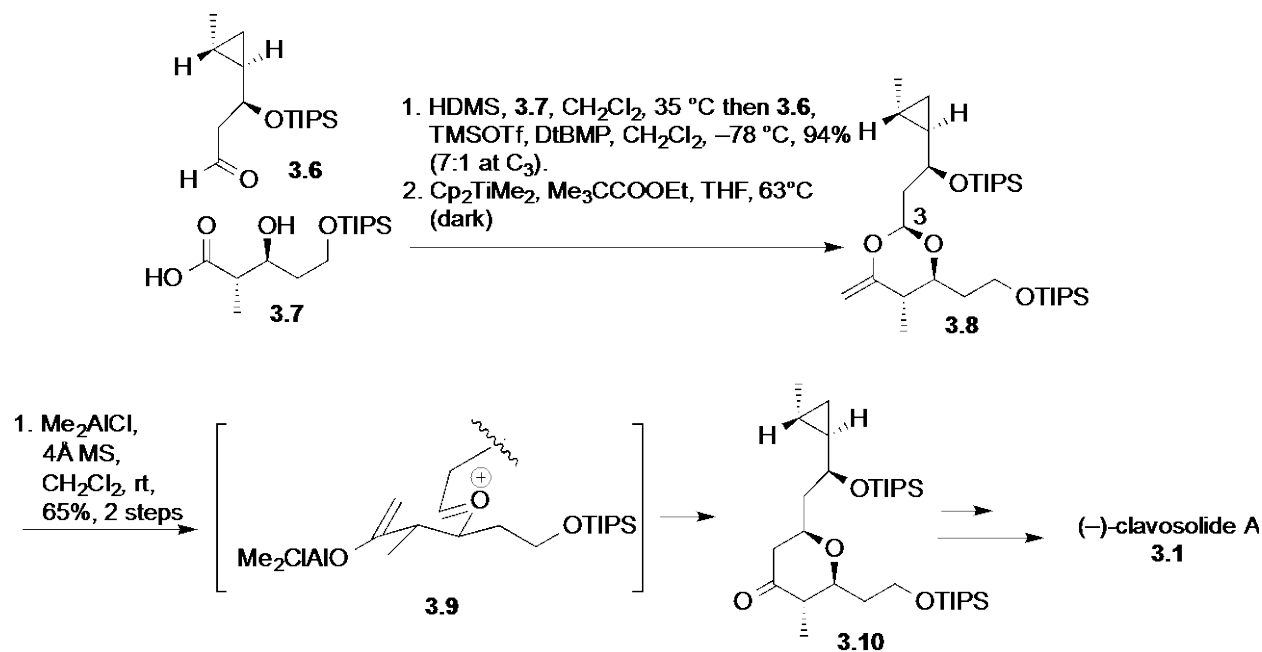
Scheme 3.1 Willis synthesis of (-)-clavosolide A diastereomer

Macrolactonization followed by Nicolaou NBS-mediated bis-glycosidation gave a mixture of [α , α], [α , β] and [β , β]. Whilst there was good correlation between the synthetic and natural product in the ¹³C NMR, the cyclopropyl protons were clearly different. Based on spectroscopic data and

molecular modeling, the Willis group concluded that they synthesized the first reported proposed structure for clavosolide A, which turned out to be the antipode **3.5** of the natural product.

3.1.3.2 Smith's total synthesis of clavosolide A

Smith and co-workers^[63] exploited a Petasis-Ferrier rearrangement tactic to construct the THP core monomer **3.10** from enol ether **3.8**, which was prepared from the condensation of cyclopropyl aldehyde **3.6** and β -hydroxyl acid **3.7**. Smith screened a variety of Lewis acids and conditions for the Petasis-Ferrier rearrangement but only obtained low yields or decomposition of the THP ring due to the inherent instability of the cyclopropyl ring.

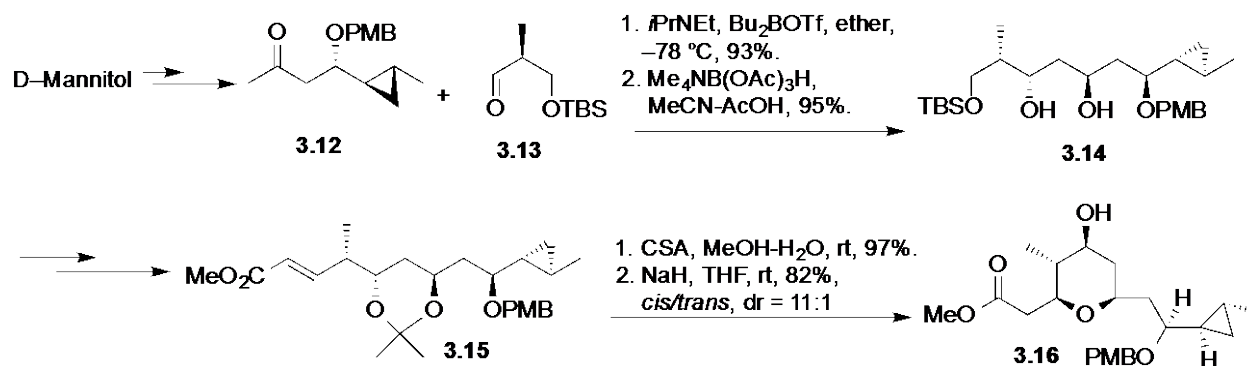


Scheme 3.2 Smith's Petasis-Ferrier rearrangement tactic

However, the optimized use of 1.1 equivalent of Me_2AlCl at room temperature for just one second, lead to 60% of the rearranged cyclized product **3.10** via intermediate **3.9**. Further functional groups manipulations followed by lactonization, dimerization and bis-glycosidation eventually lead to **3.1** in 17 steps (longest linear sequence).

3.1.3.3 Lee's total synthesis of clavosolide A

Lee's strategy^[62] for the construction of the THP ring system was through an intramolecular oxa-Micheal attack of highly functionalized intermediate **3.15**. Key intermediate **3.14** was assembled via a 1,5-*anti*-selective aldol reaction between cyclopropyl ketone **3.12** and **3.13**. Functional group manipulation followed by installation of the conjugated ester through a Horner-Wadsworth-Emmons protocol afforded (*E*)- α,β -unsaturated ester **3.15**. Acid-mediated deprotection of the acetonide followed by an intramolecular 1,5-conjugate addition under basic conditions gave the 2,6-*cis* THP intermediate **3.16** in good selectivity. Further protecting groups transformations followed by Yamaguchi's macrolactonization and Schmidt's glycosidation gave **3.1** in a total of 20 total steps.



Scheme 3.3 Lee's intramolecular oxa-Micheal cyclization strategy

3.2 DESIGN PRINCIPLE: STABILIZATION OF CYCLOPROPYL RING THROUGH CONJUGATED OXOCARBENIUM CATION

Cyclopropanes have an inherent strain energy of 27 kcal/mol, which results in a high propensity to undergo undesired ring-opening reactions not normally observed for other cycloalkanes^[65]. Facile ring opening reactions occur readily in the presence of reactive intermediates such as a carbenium ion on the adjacent carbon atom^[66]. This potentially limits the plethora of synthetic reactions that are compatible with substrates containing labile cyclopropyl functionalities. To this end, cyclopropanes are usually installed during the late stage of a sequence to avoid any unexpected ring cleavages.

Interestingly, cationic cyclopropyl ring opening reactions can be mitigated or even completely nullified with an adjacent oxocarbenium such that the usual favorable strain release of the cyclopropane is countered by the formation of a highly unstabilized carbocation that renders the thermodynamics of the entire sequence unfavorable^[67].

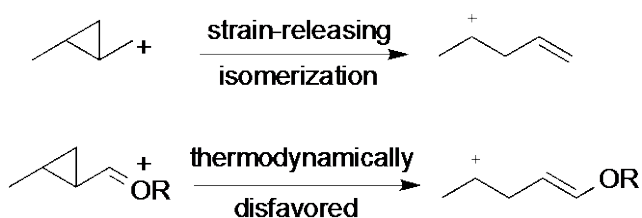


Figure 3.3 Stabilization of cationic cyclopropanes

The stability of oxocarbenium cyclopropane can be exploited through nucleophilic trapping reactions. However, classical methods of oxocarbenium generation from acetals using Lewis acids often suffer from ionization of the resultant alkoxy group and subsequent cyclopropane

cleavage. The Floreancig group has demonstrated the feasibility of generating oxocarbenium intermediates under mild, non-acidic conditions using DDQ. This formal oxidative carbon-hydrogen activation protocol has already demonstrated wide applicability in allylic, benzylic, as well as vinylic sulfides, amides and ethers systems^[8-10, 68]. Herein, this project serves to extend the scope of the methodology to include cyclopropane containing allylic ethers and apply it in the wider context of the natural product, (-)-clavosolide A.

3.2.1 Model substrate design and preparation

The cyclopropane containing allylic ethers are designed with a tethered nucleophile so that the oxidative generated transient allylic cation from DDQ can be rapidly trapped in a fast step to yield the desired cyclized product (Figure 3.4).

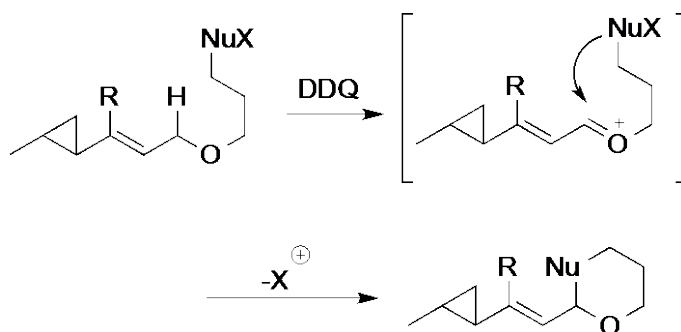
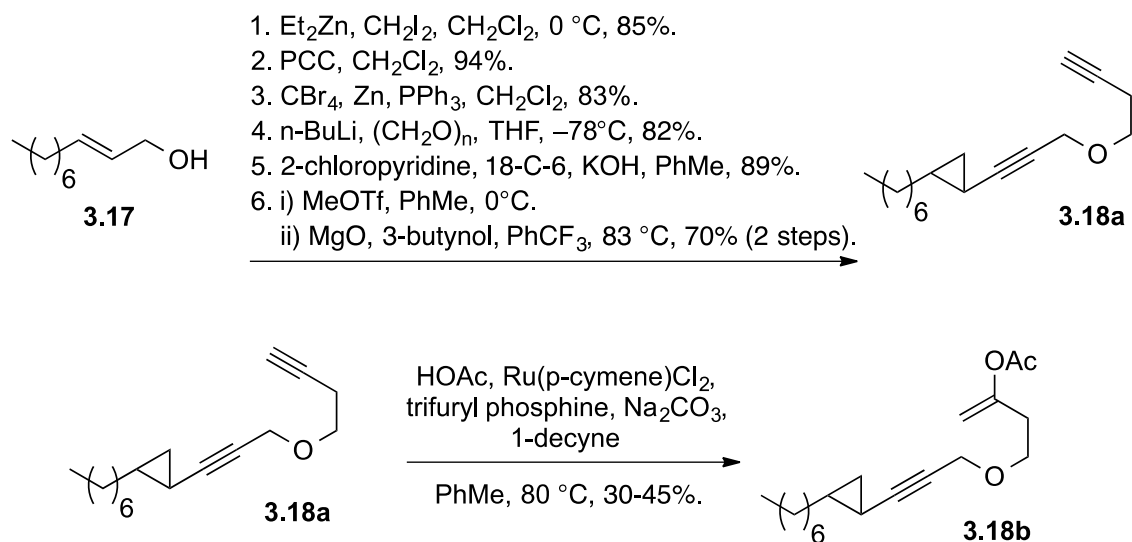


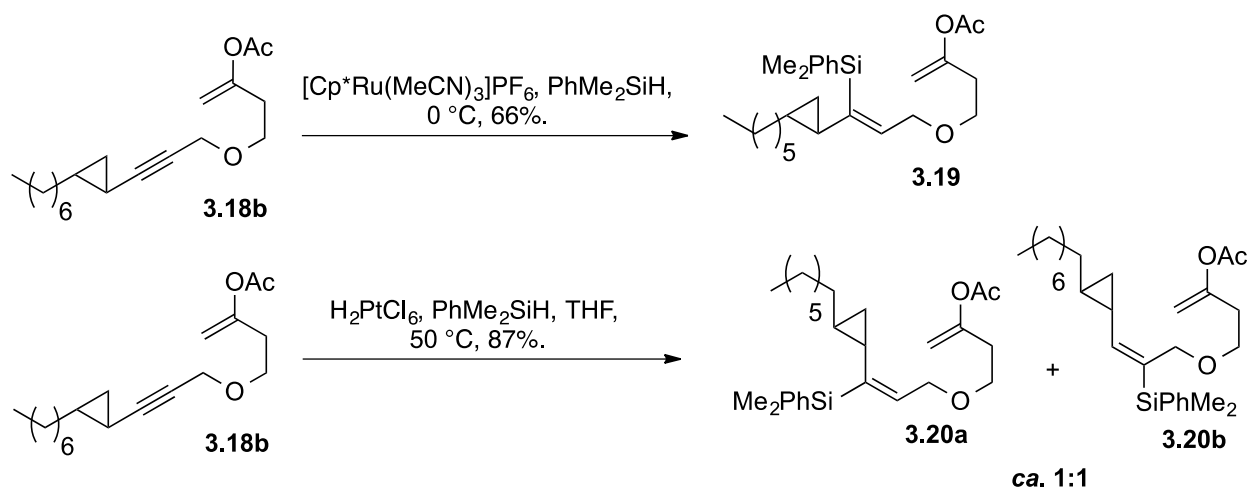
Figure 3.4 Nucleophilic addition into conjugated cyclopropyl oxocarbenium

The long chain aliphatic allylic alcohol **3.17** was carried forward to the alkynyl propargylic ether **3.18a** through a sequence of Simmons-Smith cyclopropanation, oxidation, Corey-Fuchs homologation and etherification coupling with 3-butynol through a pyridinium salt intermediate employing a variation of Dudley's protocol^[69] (Scheme 3.4).



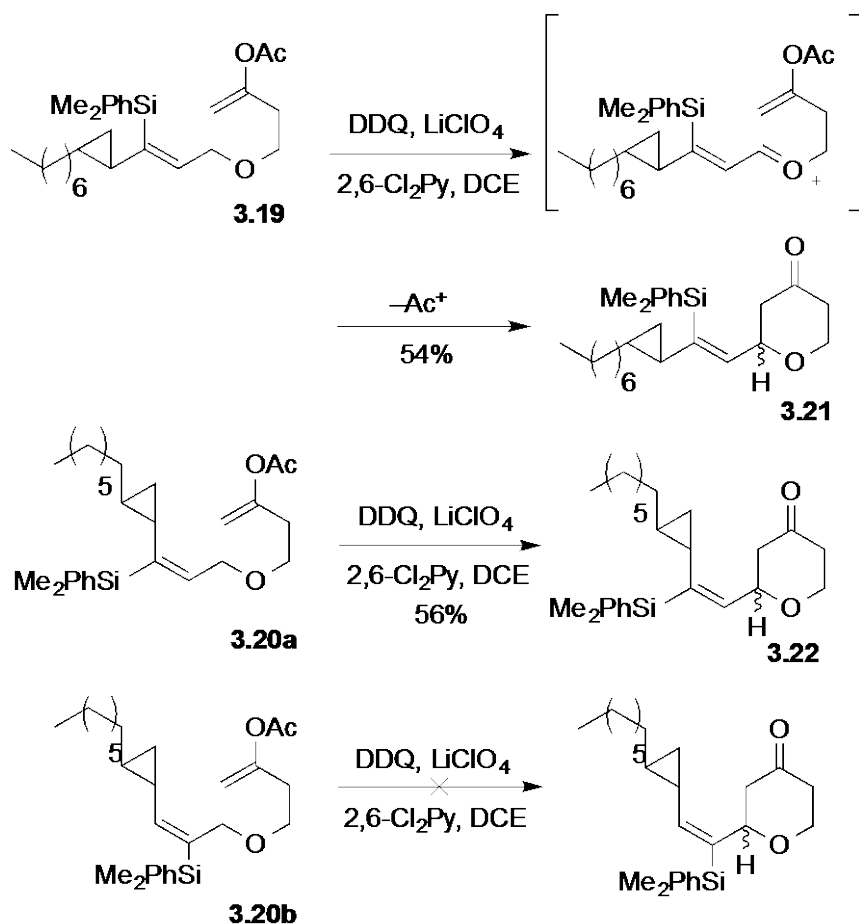
Scheme 3.4 En-route to alkynal propargylic ether 3.18

The enol acetate functionality in **3.18b** was readily installed using a ruthenium-catalyzed *cis*-Markovnikov's addition of acetic acid into alkynes following Gooßen's protocol^[70]. Enol acetate was chosen as a masked enolate nucleophile that is stable under DDQ oxidative conditions^[8, 71]. Vinyl silanes (**3.19**, **3.20a**, **3.20b**) were selected as the model substrates because they can be readily accessed with high geometric selectivity from alkynes utilizing ruthenium or platinum mediated hydrosilylation reactions^[72] (Scheme 3.5).



Scheme 3.5 Preparation of cyclopropane containing vinyl silanes

Subjecting (*Z*)-vinyl silane **3.19** and (*E*)-vinyl silane **3.20a** under our optimized DDQ oxidative conditions resulted in facile conversion into tetrahydropyrones **3.21** and **3.22** (Scheme 3.6).



Scheme 3.6 Oxidative cyclization of cyclopropane containing substrates

While oxocarbenium formation usually occurs at room temperature or even lower temperatures, heating at 45 °C was required for the oxidation to proceed. This was primarily due to the steric bulk of the vinyl silanes hindering the association with the oxidant^[68b]. In addition, due to the proximity of the silyl substituent to the alkoxy ether in **3.20b**, no cyclization was observed even at 45 °C. In addition, the cyclized tetrahydropyrones were obtained as inseparable diastereomeric mixture, indicating that the remote cyclopropane group was unable to impart any stereochemical induction on the newly formed stereogenic center. Despite the moderate yields obtained, the remainder of the mass accounting for these model substrates was attributed to nonspecific decomposition pathways not associated with cyclopropane ring opening.

3.3 RETROSYNTHETIC DISCONNECTION FOR (-)-CLAVOSOLIDE A

The encouraging results of our DDQ-mediated oxidative cyclization on the model substrates prompted us to test the feasibility of our protocol in the more complex setting of a natural product. Due to the C₂ symmetrical nature of **3.1**, an initial disconnection at the ester linkages of the molecule will yield cyclopropyl THP **3.23**. We postulate that **3.23** can be readily assembled from cyclopropyl allylic ether **3.24** generated from the union of **3.25** and **3.26** (Figure 3.5).

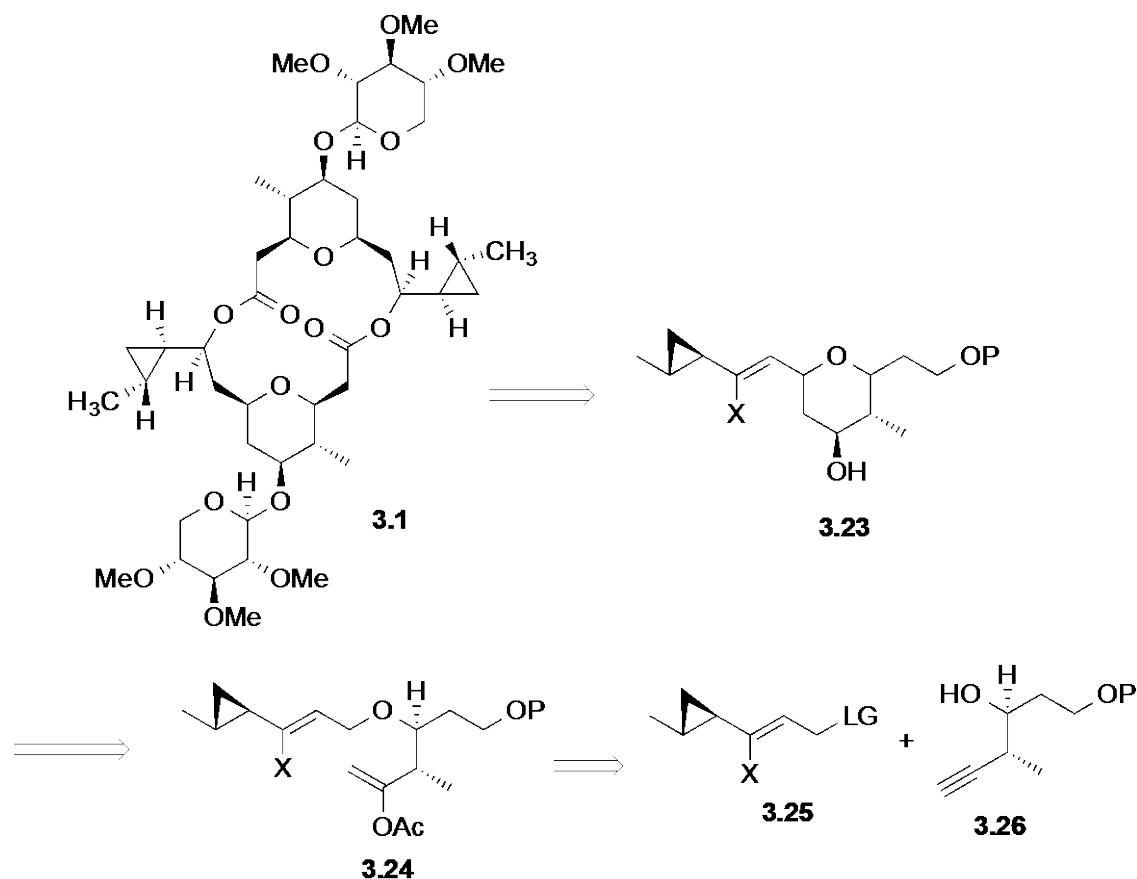


Figure 3.5 Retrosynthetic analysis of **3.1**

3.3.1 Synthesis of cyclopropyl containing subunit

The cyclopropyl-containing segment was synthesized using Feringa's CuI and (*R*)-TolBINAP-catalyzed 1,4-conjugate addition^[73] of MeMgBr into chloro enone **3.27**, prepared in one step from commercially available allyl chloride and acetyl chloride^[74]. The resultant chloro enolate **3.28** can either be directly quenched with a proton source at $-78\text{ }^{\circ}\text{C}$ to yield β -methyl chloroketone **3.29** or cyclopropane ketone **3.30** upon warming up to room temperature.

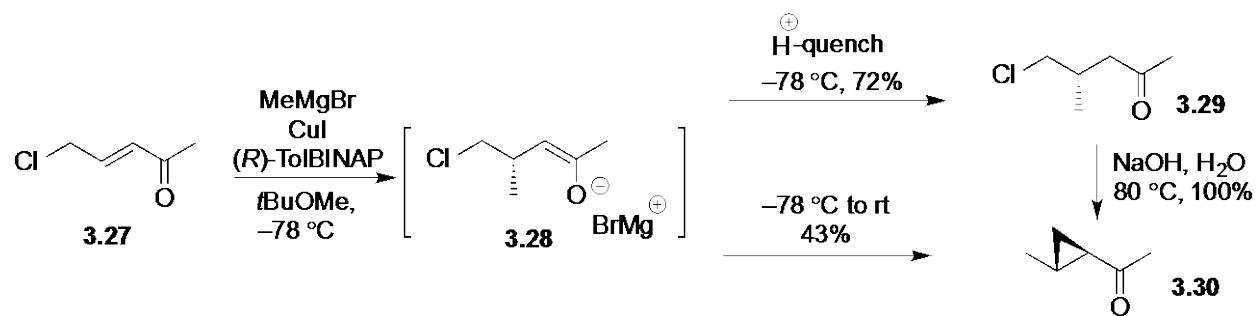


Figure 3.6 Feringa's tandem conjugate addition and cyclopropanation

Cyclopropane ketone **3.30** was formed in 43% yield upon warming up to room temperature. Unfortunately, the protocol was not reproducible and the over addition of MeMgBr into the carbonyl was a persistent side reaction. Eventually, we decided to access **3.30** via a different route and quenched enolate **3.28** at $-78\text{ }^{\circ}\text{C}$. Upon exposure of **3.29** to refluxing NaOH, the resultant carbanion displaces the γ -chloride through an intramolecular S_N2 reaction to afford **3.30** in 72% yield over 2 steps. The enantiomeric excess (% ee) calculated from the HPLC trace of intermediate **3.29** was determined to be at least >90%. This was estimated because baseline resolution of the enantiomeric peaks in the racemic control proved difficult (refer appendix B).

The *trans*-cyclopropyl ketone **3.30** was formed selectively over the *cis*-configuration due to minimization of eclipsing torsional strain in the transition state.

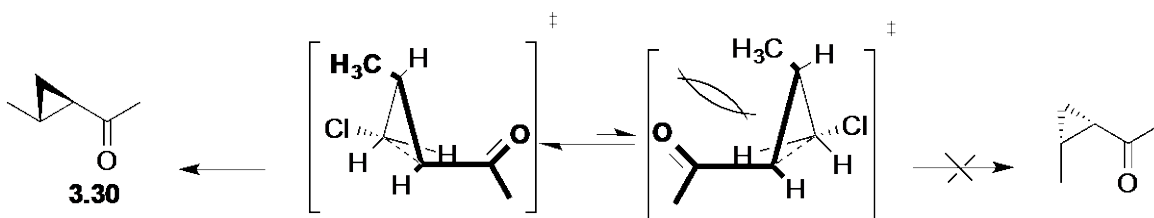
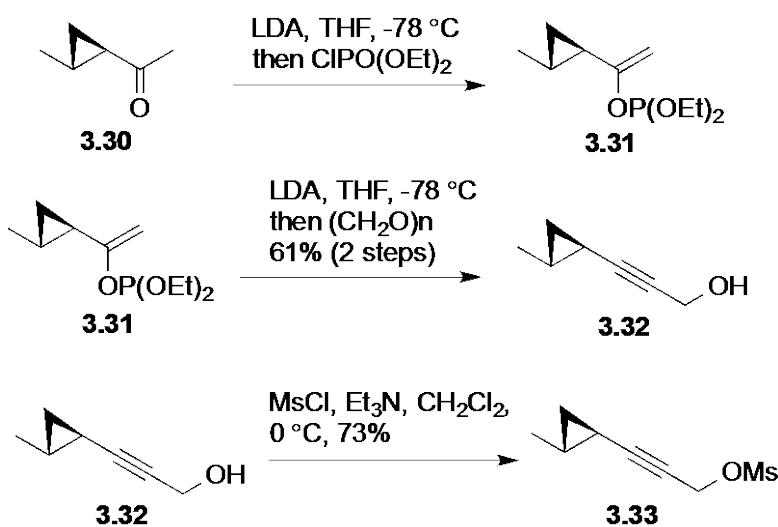


Figure 3.7 Stereochemical analysis of intramolecular S_N2 reaction

Cyclopropyl ketone **3.30** was subsequently converted into the propargyl alcohol using Negishi's protocol^[75]. Quenching of the enolate with diethyl phosphoryl chloride afforded the enol phosphate **3.31** (Scheme 3.7). Treatment of **3.31** with 2 equivalent of LDA led to β -elimination of the phosphate group to give the terminal alkyne, which was deprotonated by another equivalent of LDA to give the acetylenic anion. Subsequent quenching with paraformaldehyde affords the propargylic alcohol **3.32**.

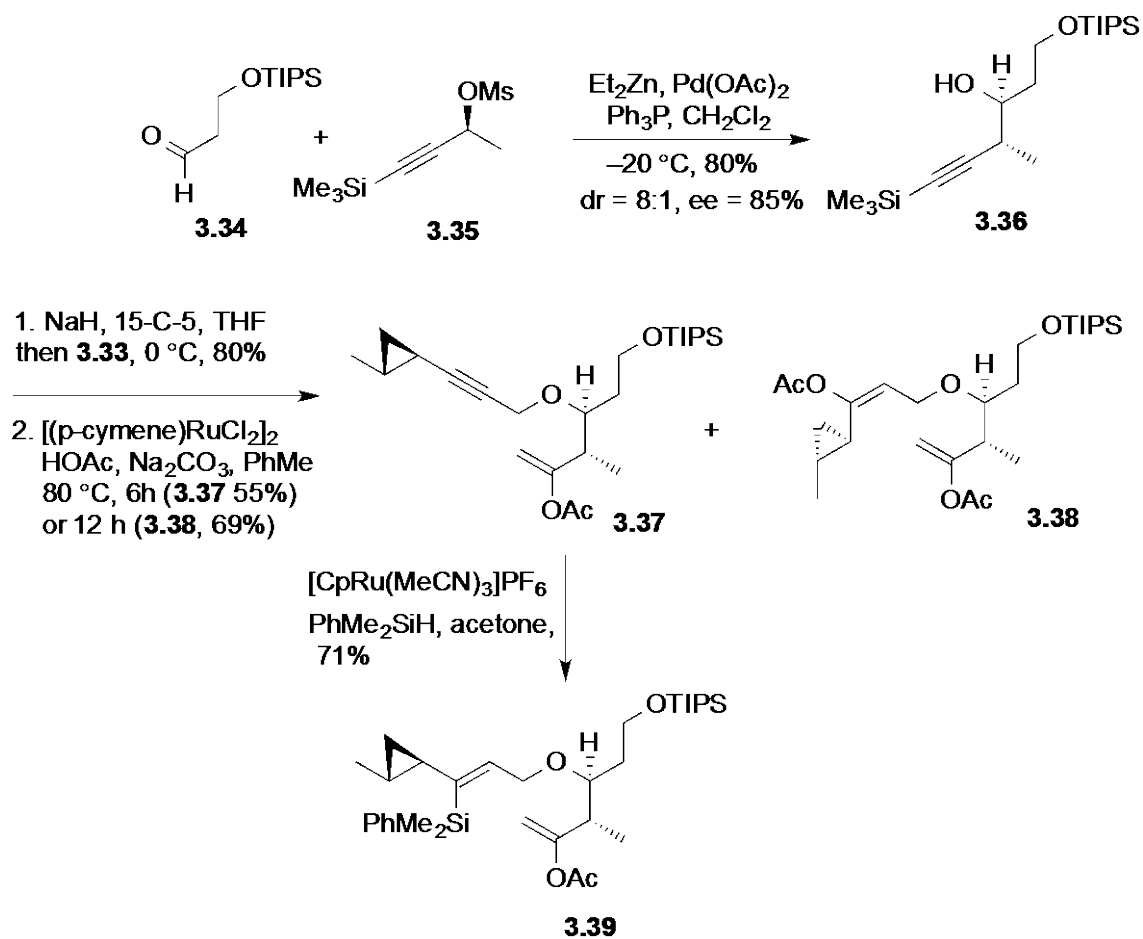


Scheme 3.7 Cyclopropane subunit homologation

Conversion of the hydroxyl group into an appropriate leaving group proved challenging due to the incompatibility of cyclopropyl group with harsh halogenating reagents and elevated heating. Alcohol **3.32** was eventually mesylated under standard conditions to yield **3.33**, which should be used quickly due to its high propensity for degradation and ionization.

3.3.2 Synthesis of cyclization substrates

The other half of the fragment **3.26** required for the formation of the cyclization substrate allylic ether was synthesized under Marshall's conditions^[76], which coupled aldehyde **3.34** with mesylate **3.35** that was conveniently prepared from Noyori reduction^[44a] of the corresponding alkynyl ketone (Scheme 3.8). Good diastereo and enantioselectivity were obtained using this protocol. Subsequent union of the cyclopropyl mesylate **3.33** with **3.36** using a modified Williamson etherification^[77] afforded the desired ether with concomitant desilylation of the terminal TMS group.



Scheme 3.8 Fragment coupling and enol acetates formation

Under the optimized ruthenium catalyzed enol acetate conditions, we observed the formation of the mono enol acetate **3.37** (55%) as well as the dienol acetate **3.38** (27%) in 6 h. Upon exposure to higher catalyst loadings and longer reaction time, **3.38** was obtained in a net yield of 69%. Subjection of **3.37** under Trost's conditions^[78] afforded vinyl silane **3.39**, which has a useful silyl handle for post cyclization manipulation^[68b].

Interestingly for **3.38**, where a second equivalent of HOAc has inserted into the internal alkyne, it adds into the triple bond in a strictly *cis*-manner with excellent regioselectivity. The

stereochemical outcome has been corroborated through NMR analysis of **3.37** and nOe correlation of a subsequent intermediate. As Gooßen's protocol usually exhibits a high selectivity for the terminal alkyne, we postulated that the cyclopropane group might be playing some activating role.

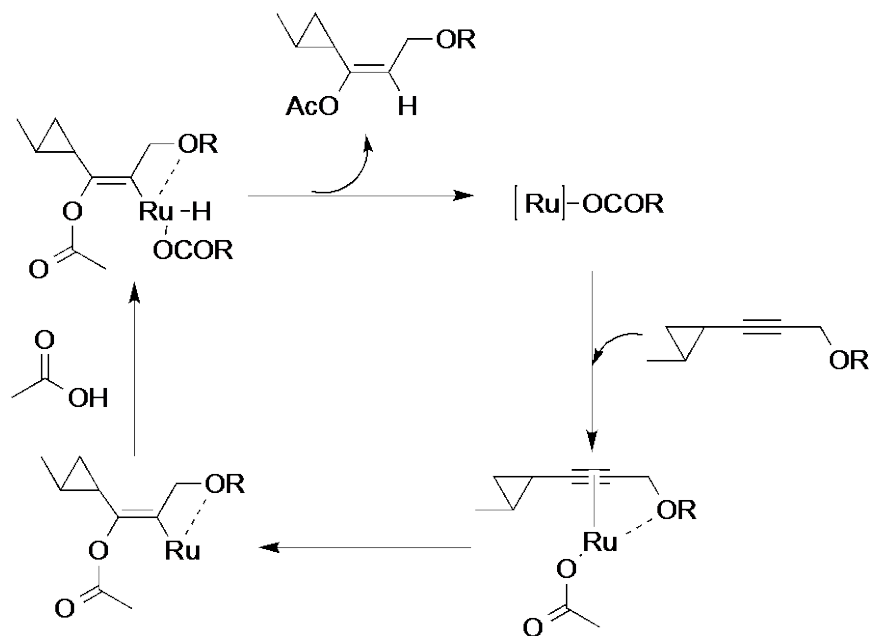
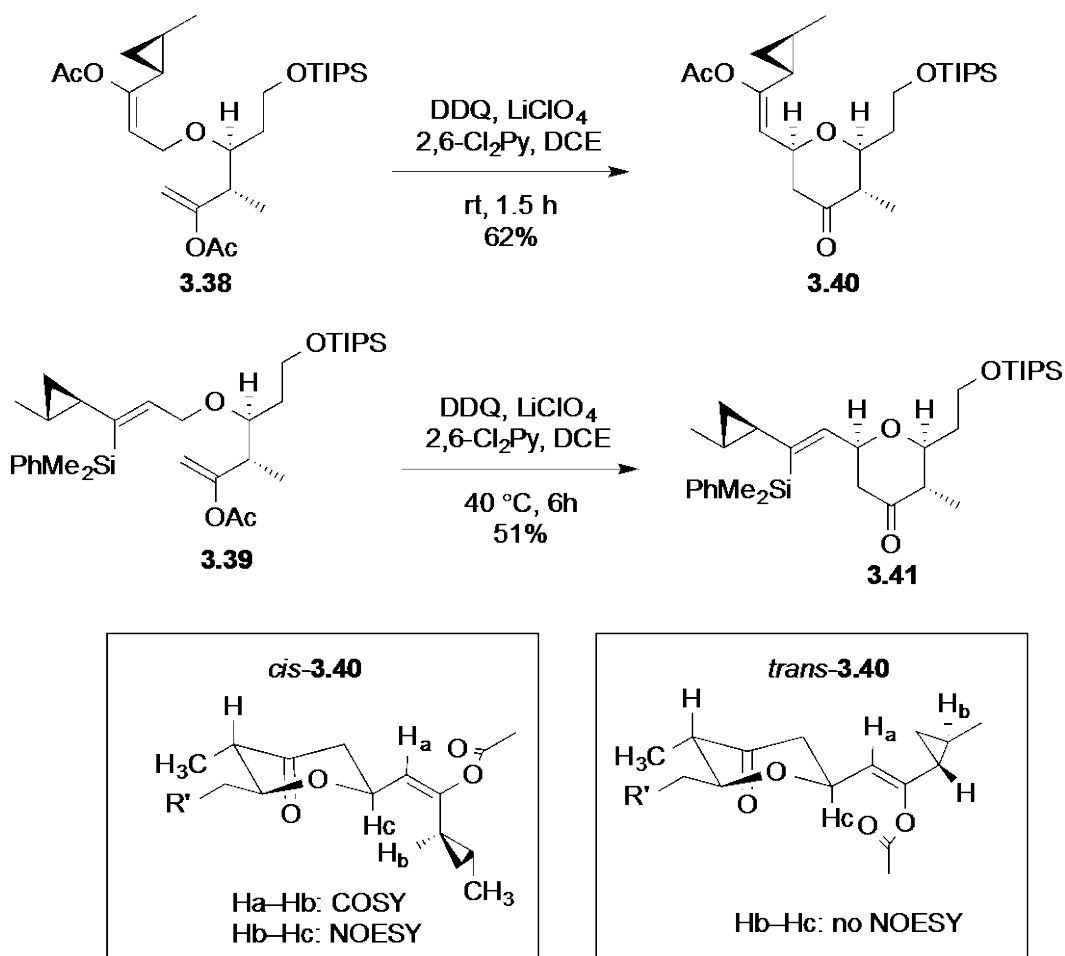


Figure 3.8 Proposed directing group effect by cyclopropane

A putative mechanism (Figure 3.8) for the directing effect involves ruthenium coordination with the alkyne triple bond followed by the acetate migratory inserting into the hindered end of the internal alkyne with the ruthenium catalyst and its bulky phosphine ligand migrating to the less hindered end. In addition, the adjacent oxygen of the ether may possess subtle bonding interactions with the electrophilic Ru center, thus further enhancing the regioselectivity of the acetic acid addition.

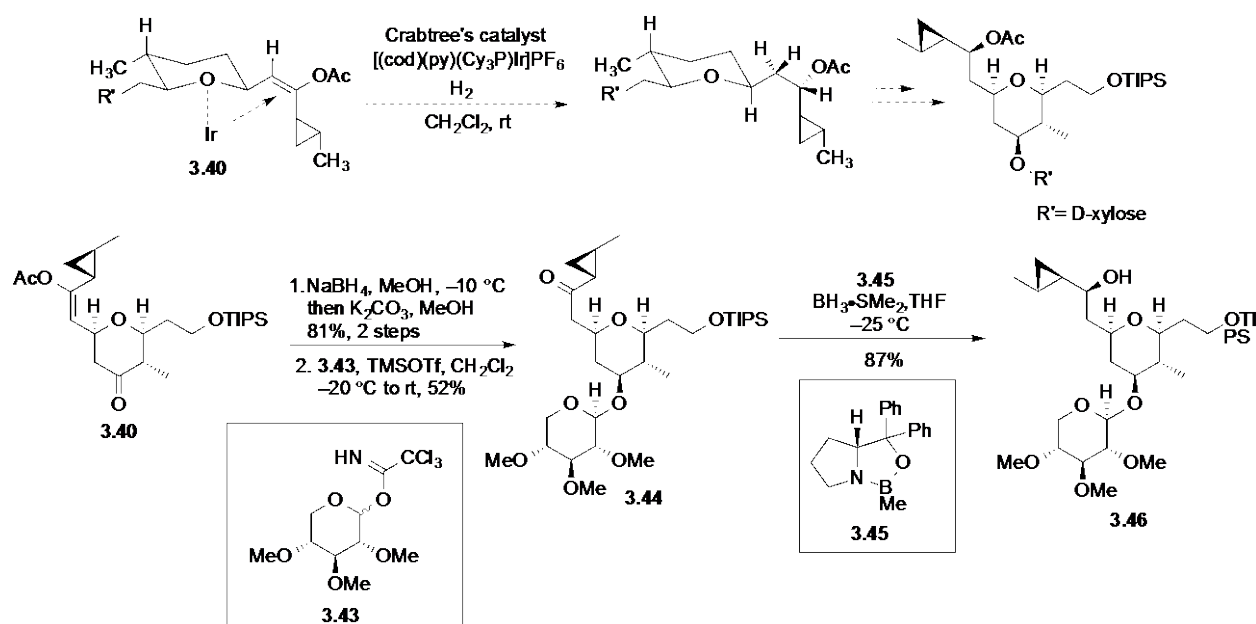
3.3.3 Oxidative cyclization and completion of the synthesis



Scheme 3.9 DDQ mediated oxidative cyclization

Under the optimized conditions of the DDQ-mediated oxidative C–H activation, cyclopropyl containing dienol acetate **3.38** underwent smooth ring closure at rt to yield a single stereoisomer of the cyclized product **3.40** in 62% yield within 1.5 h. In contrast, vinyl silane **3.39** was relatively inert to our oxidative method and required prolonged heating at 40 °C to give a comparatively lower yield of 51% (Scheme 3.9). No further optimization was attempted for **3.39** due to superiority of **3.38** in terms of ease of reaction, atom economy, and accessibility of

starting materials. The serendipitous observation that enol acetates are excellent stabilizing groups for oxidative oxocarbenium formation is significant as it offers an additional alternative for the formation of functionalized alkenyl THP rings that are very versatile for further structural diversification. In addition, 2D COSY and NOESY spectroscopic analysis of **3.40** also unambiguously confirmed the *cis*-regiochemistry of the acetic acid addition for intermediate **3.38** as previously predicted.



Scheme 3.10 Glycosidation and reduction of cyclopropyl ketone

Cyclopropane-containing vinyl acetate **3.40** was first subjected to Crabtree's hydrogenation^[79] under substrate control (Scheme 3.10). The iridium catalyst was known to coordinate to the oxygen atom of the THP ring, aiding in facial selective hydrogenation of vinyl silanes as previously demonstrated^[68b]. However, in the presence of a conjugated cyclopropyl subunit, **3.40** rapidly decomposed with concomitant cyclopropyl ring cleavage. This is not unusual due to the

isosteric resemblance of cyclopropane to alkenes that can undergo double bond isomerization under Crabtree's hydrogenation conditions^[80].

An alternative approach (Scheme 3.10) was taken where the 4'-ketone was reduced by sodium borohydride to give the equatorial alcohol. Subsequently, the vinyl acetate was hydrolyzed under basic conditions into the cyclopropyl enol, which readily tautomerized into the ketone form. Schmidt's TMSOTf-catalyzed glycosidation^[81] with trichloroacetimidate **3.43** was utilized to tether D-xylose, which gave a *ca.* 1:1 of the desired glycoside together with the other α -anomer. The sugar moiety was installed at this stage^[82] because the glycosyl group can potentially function as a hydroxyl-protecting group and because a glycosidation after macrodiolide formation can result in a complex mixture of three anomeric stereoisomers due to the low selectivity of the glycosidation reaction.

The substrate-controlled reduction of cyclopropyl ketone **3.44** on a similar compound^[83] has been performed with good stereocontrol. Disappointingly, the reduction of **2.44** with LAH and $\text{Zn}(\text{BH}_4)_2$ gave no product at low temperatures and a mixture of diastereomeric alcohols upon warming up to ambient temperature. To this end, reagent-controlled CBS reduction^[45] on **3.44** was attempted and turned out to be the reagent of choice, giving the desired (*S*)-carbinol **3.46** in excellent yield and good diastereoselectivity. The high stereoselectivity of the CBS reduction was due to the stereoelectronic effects of the cyclopropyl group^[84] behaving as both a stereo-differentiating bulky group and also an electron-donating group that directs coordination of the anti lone pair on the carbonyl to the catalytic reactive boron center on the catalyst (Figure 3.9).

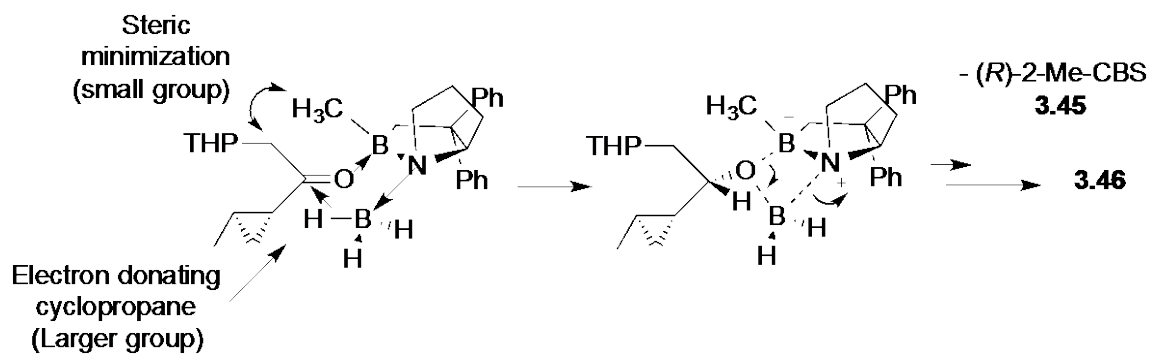
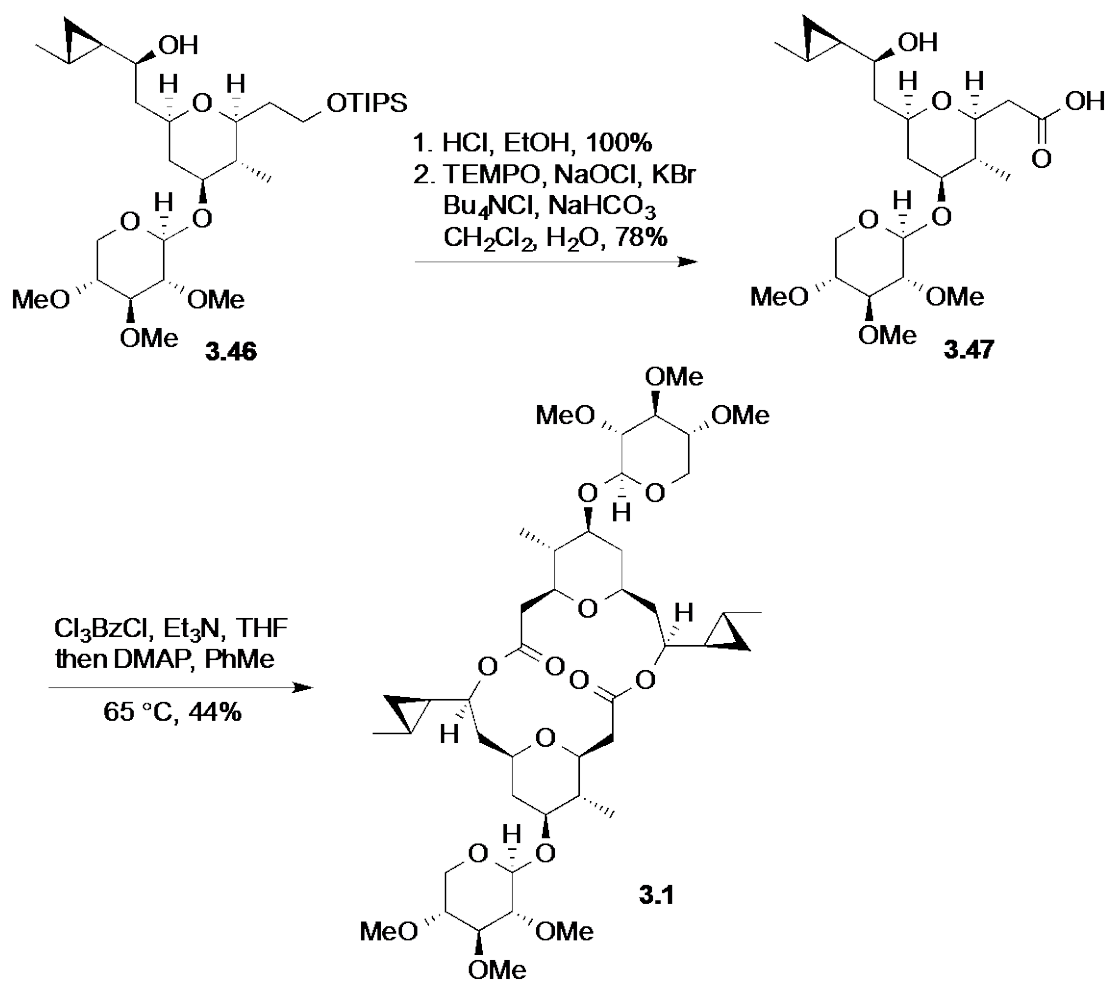


Figure 3.9 Stereochemical model for CBS reduction

Careful triisopropyl silyl (TIPS) deprotection using 1% HCl in EtOH gave the primary alcohol, which was subjected to selective TEMPO oxidation^[85] into carboxylic acid **3.47**. Subsequent macrolactonization under Yamaguchi's esterification conditions^[86] gave the (–)-clavosolide A **3.1** in 44%. The total synthesis of **3.1** has been accomplished in a total of 20 steps with 14 steps being the longest linear sequence.



Scheme 3.11 End game for (-)-clavoslide A

3.3.4 Summary

The proof of concept that cyclopropanes are compatible with oxocarbenium formation has been demonstrated through the synthesis of cyclopropane-substituted THP rings. The mild reaction conditions and functional group tolerance of the DDQ mediated C–H activation protocol has been applied in a convergent synthesis of the natural product, (-)-clavoslide A. Significant transformations in the synthesis include an early stage Feringa asymmetric cyclopropanation and an oxidation of the acetoxy-substituted allylic ether into a highly functionalized stable

oxocarbenium ion. The ability to introduce the cyclopropyl moiety at an early stage of the synthetic route that survives through a carbocation forming reaction showcases the viability of oxidative C–H bond functionalization as a valuable strategy in the toolkit of synthetic chemists for complex molecule synthesis.

APPENDIX A

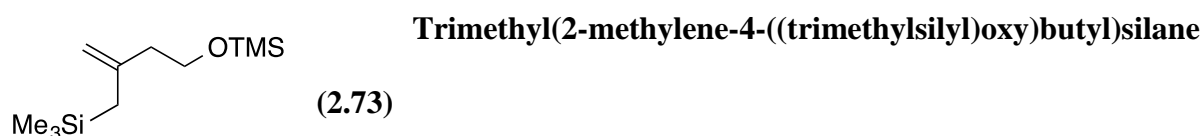
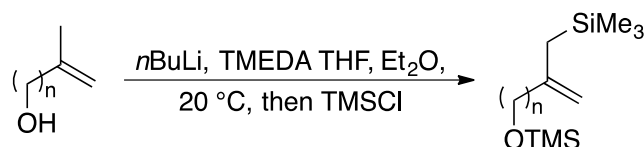
[N+1] APPROACHES TO THE SYNTHESIS OF DIVERSE SPIROACETALS THROUGH OXIDATIVE CATION FORMATION

General Information

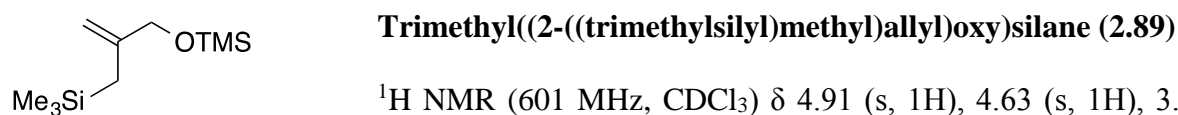
Proton (^1H NMR) and carbon (^{13}C NMR) nuclear magnetic resonance spectra were recorded on a Bruker Avance 300 spectrometer at 300 MHz and 75 MHz, a Bruker Avance 400 spectrometer at 400 MHz and 100 MHz, a Bruker Avance 500 spectrometer at 500 MHz and 125 MHz. The chemical shifts are reported in parts per million (ppm) on the delta (δ) scale. The solvent peak was used as a reference value, for ^1H NMR: $\text{CDCl}_3 = 7.27$ ppm, $\text{C}_6\text{D}_6 = 7.16$ ppm, for ^{13}C NMR: $\text{CDCl}_3 = 77.23$, $\text{C}_6\text{D}_6 = 128.4$ ppm. Data are reported as follows: (s = singlet; d = doublet; t = triplet; q = quartet; sept = septet; dd = doublet of doublets; ddd = doublet of doublet of doublets; dddd = doublet of doublet of doublet of doublet; td = triplet of doublets; dtd = doublet of triplet of doublets; br = broad). High-resolution mass spectra were recorded on a Thermo Scientific Q-Exactive spectrometer. Infrared (IR) spectra were collected on a Mattson Cygnus 100 spectrometer. Samples for IR were prepared as a thin film on a NaCl plate by dissolving the compound in CH_2Cl_2 and then evaporating the CH_2Cl_2 . Tetrahydrofuran and diethyl ether were distilled from sodium and benzophenone. Methylene chloride was distilled under N_2 from CaH_2 .

Analytical TLC was performed on E. Merck pre-coated (25 mm) silica gel 60F-254 plates. Visualization was done under UV (254 nm). Flash chromatography was done using ICN SiliTech 32-63 60 Å silica gel. Reagent grade ethyl acetate, diethyl ether, toluene and hexanes (commercial mixture) were purchased from EM Science and used as is for chromatography.

Lithiation route to simple allylsilanes



^1H NMR (500 MHz, CDCl_3) δ 4.59 (s, 1H), 4.56 (s, 1H), 3.68 (t, $J = 7.4$ Hz, 2H), 2.20 (t, $J = 7.4$ Hz, 2H), 1.53 (s, 2H), 0.12 (s, 9H), 0.02 (s, 9H); ^{13}C NMR (126 MHz, CDCl_3) δ 144.8, 108.7, 62.1, 41.7, 27.7, -0.1 , -1.1 . These data are consistent with literature values.¹

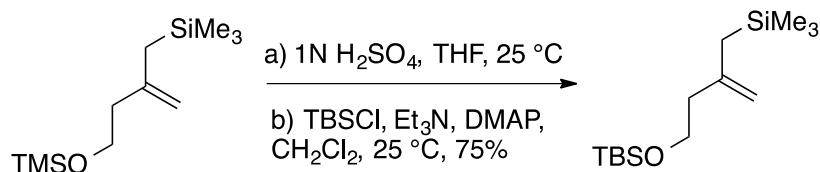


^1H NMR (601 MHz, CDCl_3) δ 4.91 (s, 1H), 4.63 (s, 1H), 3.95 (s, 2H), 1.49 (s, 2H), 0.13 (s, 9H), 0.02 (s, 9H); ^{13}C NMR (151 MHz, CDCl_3) δ 146.2, 106.8, 66.7, 23.0, -0.2 , -1.1 ; IR (thin film) 2957, 1647, 1416, 1251, 1160, 1123, 1086, 882, 842, 749 693 cm^{-1} .

¹. These data are consistent with literature values.²

¹ F. Alonso, M. Rodriguez-Fernandez, D. Sanchez, M. Yus, *Synthesis* **2010**, 3013-3020.

² B. M. Trost, P. Renaut, *J. Am. Chem. Soc.* **1982**, *104*, 6668-6672.

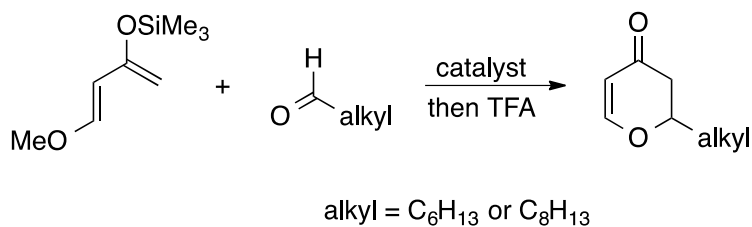



3-((trimethylsilyl)methyl)but-3-en-1-ol

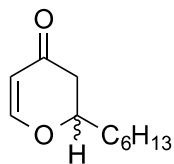
$^1\text{H NMR}$ (601 MHz, CDCl_3) δ 4.69 (s, $J = 1.9$ Hz, 1H), 4.67 (s, 1H), 3.71 (q, $J = 6.1$ Hz, 2H), 2.24 (td, $J = 6.2, 0.9$ Hz, 2H), 1.55 (d, $J = 0.9$ Hz, 2H), 0.04 (s, 9H). These data are consistent with literature values³.


tert-butyl dimethyl((3-((trimethylsilyl)methyl)but-3-en-1-yl)oxy)silane (2.72)

$^1\text{H NMR}$ (601 MHz, CDCl_3) δ 4.59 (s, 1H), 4.55 (s, 1H), 3.71 (t, $J = 7.2$ Hz, 2H), 2.19 (t, $J = 6.8$ Hz, 2H), 1.54 (s, 2H), 0.90 (s, 9H), 0.06 (s, 6H), 0.02 (s, 9H). $^{13}\text{C NMR}$ (151 MHz, CDCl_3) δ 144.8, 108.6, 62.7, 41.8, 27.5, 26.2, 18.6, -1.2, -5.0. IR (thin film) 2955, 2859, 1634, 1472, 1417, 1388, 1252, 1157, 1098, 931, 837, 775 cm^{-1} ; HRMS (ES+) calcd for $\text{C}_{14}\text{H}_{33}\text{OSi}_2$ $[\text{M}+\text{H}]^+$: 273.2070, found: 273.2060.



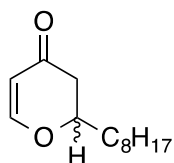
³ Ahmed-Schofield, R.; Mariano, P. S. *The Journal of Organic Chemistry* **1985**, 50, (26), 5667-5677.



(±)-2-hexyl-2,3-dihydro-4H-pyran-4-one

$^1\text{H NMR}$ (601 MHz, CDCl_3) δ 7.38 (d, $J = 6.0$ Hz, 1H), 5.42 (dd, $J = 6.0, 1.1$ Hz, 1H), 4.45 – 4.39 (m, 1H), 2.54 (dd, $J = 16.7, 13.5$ Hz, 1H), 2.45 (ddd, $J = 16.7,$

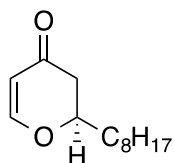
3.7, 1.2 Hz, 1H), 1.87 – 1.81 (m, 1H), 1.71 – 1.65 (m, 1H), 1.51 – 1.26 (m, 8H), 0.92 (t, $J = 6.8$ Hz, 3H). These data are consistent with literature values⁴.



(±)-2-Octyl-2,3-dihydro-4H-pyran-4-one (2.82a)

To a solution of Danishefsky's diene (1.15g, 6.65 mmol, 1.0 equiv) and nonanal (1.82g, 12.8 mmol, 1.93 equiv) in Et_2O (25 mL) at -20 °C was added $\text{BF}_3 \cdot \text{OEt}_2$

(840 μL , 6.78 mmol, 1.02 equiv) dropwise over 30 min. The mixture was stirred for 1h, then was warmed to 0 °C and carefully quenched with 10 mL of NaHCO_3 . The resultant organic layer was extracted with Et_2O (2 x 15 mL). The combined organic layers were washed with brine (20 mL) and concentrated in vacuo. Flash column chromatography as above afforded the racemic pyranone (1.05 g, 75%) as a yellow viscous oil. All spectral data other than optical rotation matched those of the enantiomerically enriched material.



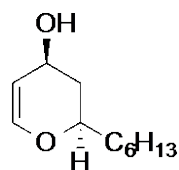
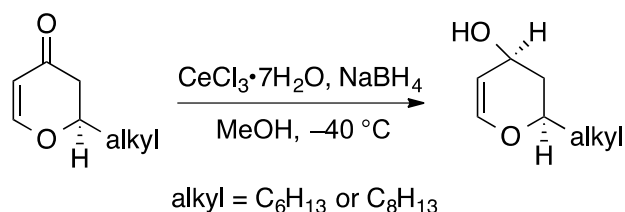
(R)-2-Octyl-2,3-dihydro-4H-pyran-4-one (2.82b)

To a rapidly stirring mixture of nonanal (495 μL , 2.87 mmol, 1 equiv), 4 Å molecular sieves (60 wt%) and (1*S*, 2*R*)-Jacobsen's catalyst (71 mg, 0.14 mmol,

0.05 equiv) under N_2 at 0 °C was added Danishefsky's diene (620 μL , 3.20 mmol, 1.1 equiv).

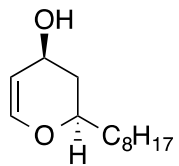
⁴ Zulauf, A.; Mellah, M.; Guillot, R.; Schulz, E. *Eur. J. Org. Chem.* **2008**, (12), 2118-2129.

The mixture was gradually warmed to rt and stirred for 16 h. The reaction was diluted with CH₂Cl₂ (5 mL) and cooled to 0 °C. One drop of TFA acid was added and the reaction was stirred for 15 min. The mixture was filtered through a short plug of celite, rinsed with CH₂Cl₂ (5 mL), and concentrated in vacuo. Flash column chromatography purification (20% EtOAc in hexanes) afforded the desired product (430 mg, 71%) as a viscous yellow oil. ¹H NMR (601 MHz, CDCl₃) δ 7.35 (d, *J* = 6.0 Hz, 1H), 5.39 (d, *J* = 6.0 Hz, 1H), 4.40 (ddd, *J* = 12.7, 8.6, 4.7 Hz, 1H), 2.51 (dd, *J* = 16.7, 13.5 Hz, 1H), 2.43 (dd, *J* = 16.7, 3.7 Hz, 1H), 1.86 – 1.77 (m, 1H), 1.65 (ddd, *J* = 14.8, 10.6, 5.4 Hz, 1H), 1.50 – 1.43 (m, 1H), 1.43 – 1.36 (m, 1H), 1.35 – 1.22 (m, 10H), 0.89 (t, *J* = 6.8 Hz, 3H); ¹³C NMR (151 MHz, CDCl₃) δ 193.0, 163.5, 107.2, 79.8, 42.1, 34.6, 32.0, 29.6, 29.5, 29.4, 25.0, 22.9, 14.3; IR (thin film) 2928, 2856, 1680, 1597, 1465, 1406, 1273, 1225, 1038, cm⁻¹; [α]_D²⁰ +100.4 (c 1.06, CHCl₃); HRMS (ASAP) calcd for C₁₃H₂₃O₂ [M+H]⁺: 211.1698, found: 211.1697.



(2R,4S)-2-hexyl-3,4-dihydro-2H-pyran-4-ol

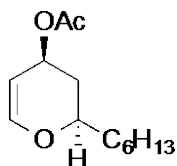
¹H NMR (601 MHz, CDCl₃) δ 6.37 (dd, *J* = 6.2, 1.3 Hz, 1H), 4.73 (dt, *J* = 6.2, 1.9 Hz, 1H), 4.44 (t, *J* = 7.6 Hz, 1H), 3.93 – 3.89 (m, 1H), 2.16 (ddt, *J* = 13.1, 6.6, 1.9 Hz, 1H), 1.60 – 1.57 (m, 1H), 1.55 – 1.49 (m, 1H), 1.37 – 1.25 (m, 9H), 0.88 (t, *J* = 6.7 Hz, 3H). ¹³C NMR (151 MHz, CDCl₃) δ 145.6, 105.5, 75.2, 63.6, 38.4, 35.3, 32.0, 29.4, 25.3, 22.8, 14.3; IR (thin film) 3340, 2928, 2859, 1643, 1465, 1234, 1108, 1036, 739 cm⁻¹; HRMS (ES⁺) calcd for C₁₁H₁₉O₂ [M-H]⁺: 183.1385, found: 183.1375.



(2S,4R)-2-Octyl-3,4-dihydro-2H-pyran-4-ol (2.79)

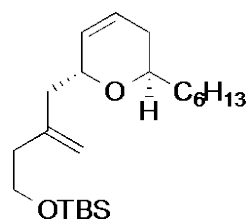
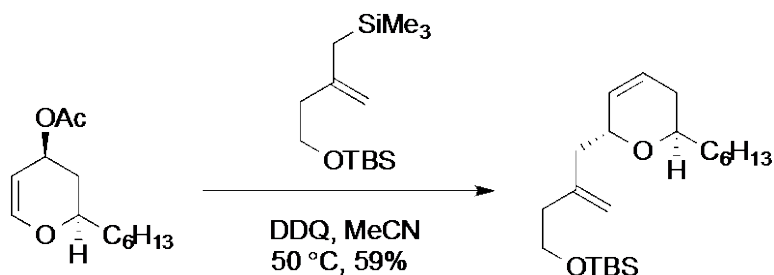
To the pyranone **2.82b** (2.81g, 13.3 mmol) in MeOH (130 mL) was added CeCl₃•7H₂O (5.96g, 16 mmol, 1.2 equiv). The reaction was stirred for 10 min at rt then was cooled to –40 °C. NaBH₄ (606 mg, 16 mmol, 1.2 equiv) was added in one portion under nitrogen and the mixture was stirred for 1h. The mixture was warmed to 0 °C, then was carefully quenched with a 1:1 mixture of brine/water (50 mL). The mixture was extracted with CH₂Cl₂ (3 x 25 mL). The combined organic layers were washed with brine (50 mL) and concentrated in vacuo. Flash column chromatography purification (30% EtOAc in hexanes) afforded the desired product as a colorless oil (2.32 g, 82%). ¹H NMR (500 MHz, CDCl₃) δ 6.36 (d, *J* = 6.2 Hz, 1H), 4.72 (d, *J* = 6.2 Hz, 1H), 4.43 (t, *J* = 8.1 Hz, 1H), 3.90 (dt, *J* = 12.0, 6.2 Hz, 1H), 2.15 (dd, *J* = 13.1, 6.6 Hz, 1H), 1.69 – 1.61 (m, 1H), 1.58 (dd, *J* = 12.1, 2.7 Hz, 1H), 1.56 –

1.46 (m, 2H), 1.32 – 1.23 (m, 12H), 0.87 (t, $J = 6.7$ Hz, 3H); ^{13}C NMR (126 MHz, CDCl_3) δ 145.6, 105.6, 75.3, 63.7, 38.5, 35.4, 32.2, 29.8, 29.8, 29.5, 25.4, 23.0, 14.4; $[\alpha]_{\text{D}}^{20} +5.8$ (c 0.65, CHCl_3); IR (thin film) 3338, 3062, 2926, 2856, 1643, 1465, 1379, 1234, 1110, 1032, 920, 875. 739 cm^{-1} ; HRMS (ASAP) calcd for $\text{C}_{14}\text{H}_{25}\text{O}$ $[\text{M}-\text{OH}]^+$: 209.1905, found: 209.1897.



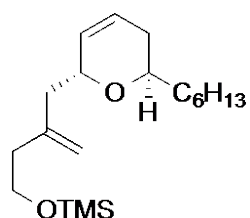
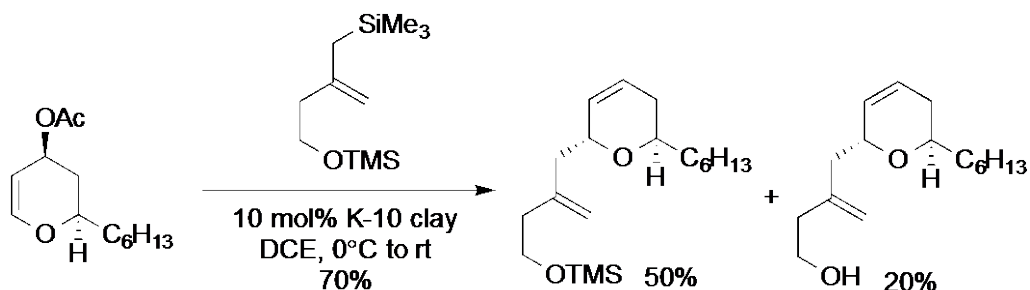
(2*R*,4*S*)-2-hexyl-3,4-dihydro-2H-pyran-4-yl acetate (2.71)

To a solution of the pyranol (717mg, 3.89 mmol) in CH_2Cl_2 (8 mL) under N_2 at rt was added DMAP (50mg, 0.389 mmol, 0.1 equiv) and Et_3N (1.2 mL, 0.817 mmol, 2.1 equiv). The mixture was later cooled to $0\text{ }^\circ\text{C}$ and Ac_2O (700 μL , 3.20 mmol, 1.1 equiv) was added drop-wise. After 1.5 h, the mixture was quenched at $0\text{ }^\circ\text{C}$ with MeOH (2 mL), washed with NaHCO_3 (5 mL x 2), brine (5 mL) and dried over MgSO_4 . Flash column chromatography purification with basified silica gel (2% EtOAc in hexanes) afforded the product (506 mg, 57%) as a colorless oil. ^1H NMR (400 MHz, CDCl_3) δ 6.44 (dd, $J = 6.3, 1.3$ Hz, 1H), 5.41 – 5.36 (m, 1H), 4.71 (dt, $J = 6.2, 2.0$ Hz, 1H), 3.96 (dddd, $J = 10.8, 7.4, 5.2, 2.1$ Hz, 1H), 2.23 (ddt, $J = 13.3, 6.7, 1.9$ Hz, 1H), 2.05 (s, 3H), 1.78 – 1.61 (m, 2H), 1.59 – 1.49 (m, 2H), 1.36 – 1.21 (m, 4H), 0.88 (t, $J = 6.7$ Hz, 3H). ^{13}C NMR (101 MHz, CDCl_3) δ 171.2, 147.0, 101.0, 74.8, 66.1, 35.0, 33.6, 32.0, 29.4, 25.3, 22.8, 21.5, 14.3; IR (thin film) 2931, 2859, 1741, 1645, 1466, 1372, 1236, 1110, 1025, 741 cm^{-1} ; HRMS (ESIP) calcd for $\text{C}_{13}\text{H}_{23}\text{O}_3$ $[\text{M}+\text{H}]^+$: 227.1642, found: 227.1646.



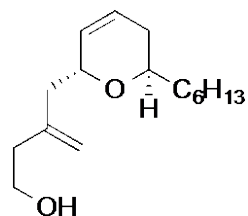
***tert*-butyl(4-((2*R*,6*R*)-6-hexyl-5,6-dihydro-2*H*-pyran-2-yl)butoxy)dimethylsilane (2.74)**

To a solution of the pyranyl acetate **2.71** (45 mg, 0.20 mmol) and OTBS allyl silane **2.72** (82 mg, 0.30 mmol, 1.5 equiv) in MeCN (1 mL) under N₂ was added DDQ (23 mg, 0.10 mmol, 0.5 equiv). The mixture was allowed to stir at 50 °C for 18h. Upon cooling down to rt, the reaction was quenched with Et₃N (100 μL) and concentrated. Flash column chromatography purification (2% EtOAc in hexanes) afforded the product as a colorless oil (43 mg, 59%). ¹H NMR (601 MHz, CDCl₃) δ 5.80 (dtd, *J* = 7.6, 5.0, 2.3 Hz, 1H), 5.72 – 5.68 (m, 1H), 4.86 (s, 1H), 4.84 (s, 1H), 4.35 – 4.31 (m, 1H), 3.76 – 3.69 (m, 2H), 3.65 (tt, *J* = 7.9, 3.9 Hz, 1H), 2.39 (dd, *J* = 14.1, 8.5 Hz, 1H), 2.31 (td, *J* = 7.0, 1.1 Hz, 2H), 2.21 (dd, *J* = 13.9, 5.5 Hz, 1H), 1.46 – 1.39 (m, 2H), 1.33 – 1.24 (m, 8H), 0.89 – 0.87 (m, 12H), 0.05 (s, 6H). IR (thin film) 2928, 2857, 1645, 1469, 1390, 1254, 1094, 937, 889, 836, 776 cm⁻¹; HRMS (ESI) calcd for C₂₂H₄₃O₂Si [M+H]⁺: 367.3028, found: 367.3038.



((3-(((2R,6R)-6-hexyl-5,6-dihydro-2H-pyran-2-yl)methyl)but-3-en-1-yl)oxy)trimethylsilane (2.75)

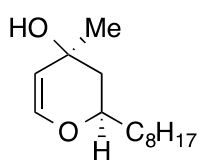
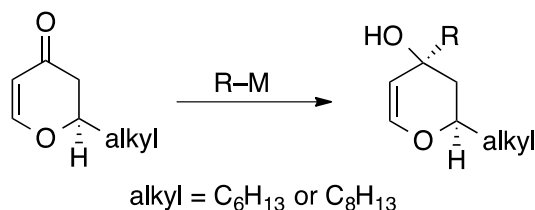
A solution of pyranyl acetate **2.71** (30 mg, 0.13 mmol) and allyl silane **2.73** (37 mg, 0.16 mmol, 1.2 equiv) in DCE (500 μ L) under N₂ was cooled to 0 °C. K-10 clay (3 mg, 10 wt%) was added and the mixture was allowed to warm up to rt over 1h. The mixture was then filtered and concentrated. Flash column chromatography purification (2% to 20% EtOAc in hexanes) afforded **2.75** (9 mg, 20%) and **2.76** (17 mg, 50%) as colorless oils. ¹H NMR (400 MHz, CDCl₃) δ 5.83 (dtd, J = 7.5, 4.9, 2.3 Hz, 1H), 5.73 (dtd, J = 10.2, 2.7, 1.4 Hz, 1H), 4.87 (s, 1H), 4.85 (s, 1H), 4.35 (ddd, J = 7.4, 5.5, 2.7 Hz, 1H), 3.73 (td, J = 7.3, 1.1 Hz, 2H), 3.71 – 3.64 (m, 1H), 2.42 (ddd, J = 14.1, 8.5, 1.0 Hz, 1H), 2.35 (t, J = 7.2 Hz, 2H), 2.23 (ddd, J = 14.1, 5.6, 1.1 Hz, 1H), 2.06 – 2.03 (m, 1H), 2.00 (ddt, J = 5.1, 3.7, 1.4 Hz, 1H), 1.52 – 1.25 (m, 10H), 0.91 (t, J = 6.5 Hz, 3H), 0.14 (s, 9H). ¹³C NMR (101 MHz, CDCl₃) δ 143.6, 129.7, 124.5, 113.5, 71.3, 67.8, 61.9, 41.3, 39.3, 35.8, 32.1, 31.0, 29.6, 25.9, 22.9, 14.3, -0.2; IR (thin film) 2956, 2929, 2858, 1644, 1433, 1391, 1250, 1092, 886, 841, 747 cm^{-1} ; HRMS (ESI) calcd for C₁₉H₃₇O₂Si [M+H]⁺: 325.2557, found: 325.2561.



3-(((2*R*,6*R*)-6-hexyl-5,6-dihydro-2*H*-pyran-2-yl)methyl)but-3-en-1-ol

(2.76)

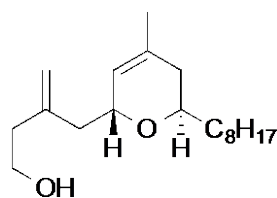
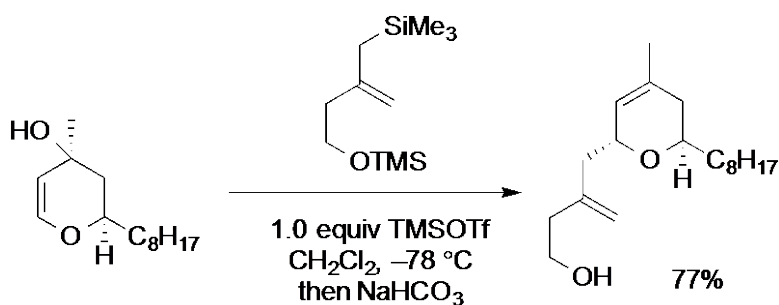
^1H NMR (500 MHz, CDCl_3) δ 5.82 (ddt, $J = 10.1, 5.0, 2.3$ Hz, 1H), 5.69 (ddd, $J = 10.3, 4.1, 2.3$ Hz, 1H), 4.98 (s, 1H), 4.96 (s, 1H), 4.38 – 4.33 (m, 1H), 3.75 (t, $J = 6.1$ Hz, 2H), 3.67 (tt, $J = 8.4, 4.0$ Hz, 1H), 2.44 – 2.39 (m, 1H), 2.36 (t, $J = 6.1$ Hz, 2H), 2.21 (dd, $J = 14.3, 5.0$ Hz, 1H), 2.05 – 1.98 (m, 1H), 1.94 – 1.87 (m, 1H), 1.44 – 1.39 (m, 2H), 1.32 – 1.24 (m, 8H), 0.88 (t, $J = 6.6$ Hz, 3H). ^{13}C NMR (126 MHz, CDCl_3) δ 143.3, 129.5, 124.6, 114.9, 71.2, 68.0, 61.0, 40.9, 39.2, 35.6, 32.0, 30.8, 29.6, 25.8, 22.8, 14.3; IR (thin film) 3411, 2927, 2855, 1734, 1645, 1465, 1377, 1183, 1088, 1047, 890, 715 cm^{-1} ; HRMS (ESI) calcd for $\text{C}_{16}\text{H}_{29}\text{O}_2$ $[\text{M}+\text{H}]^+$: 253.2162, found: 253.2165.



(2*R*,4*S*)-4-Methyl-2-octyl-3,4-dihydro-2*H*-pyran-4-ol (2.77)

To the pyranone **2.82b** (300 mg, 1.43 mmol, 1.0 equiv) in THF (10 mL) at -78 °C was added MeLi (1.6 M, 1.05 mL, 1.64 mmol, 1.15 equiv) dropwise over 10 min. The mixture was stirred for 1h then was quenched with NH_4Cl (2 mL). The mixture was extracted with EtOAc (2 x 5 mL). The combined organic layers were washed with brine (10 mL) and concentrated in vacuo. Flash column chromatography purification (30% EtOAc in hexanes) afforded the desired product as a colorless oil (269 mg, 83%, 10:1 mixture of

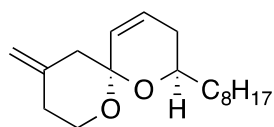
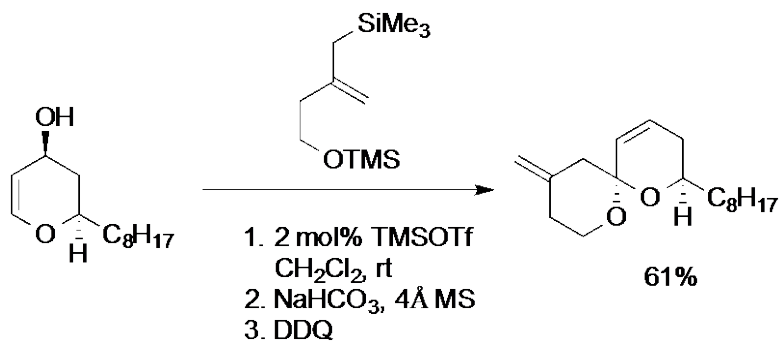
diastereomers). This compound is unstable and should not be stored for prolonged periods. Major diastereomer: ^1H NMR (500 MHz, CDCl_3) δ 6.28 (d, $J = 6.2$ Hz, 1H), 4.69 (dd, $J = 6.2$, 2.0 Hz, 1H), 3.86 – 3.77 (m, 1H), 1.89 (dt, $J = 13.3$, 2.1 Hz, 1H), 1.81 – 1.71 (m, 2H), 1.67 – 1.59 (m, 1H), 1.54 – 1.37 (m, 2H), 1.35 (s, 3H), 1.31 – 1.22 (m, 10H), 0.86 (t, $J = 6.7$ Hz, 3H); ^{13}C NMR (126 MHz, CDCl_3) δ 144.2, 109.5, 75.5, 67.1, 44.6, 35.5, 32.1, 30.5, 29.8, 29.8, 29.5, 25.5, 22.9, 14.4; $[\alpha]_{\text{D}}^{20} +6.6$ (c 2.20, CHCl_3); IR (thin film) 2926, 2855, 1673, 1637, 1465, 1396, 1236, 1138, 960 cm^{-1} ; HRMS (ASAP) calcd for $\text{C}_{14}\text{H}_{25}\text{O}$ $[\text{M}-\text{OH}]^+$: 209.1905, found: 209.1897.



3-(((2*R*,6*R*)-4-methyl-6-octyl-5,6-dihydro-2*H*-pyran-2-yl)methyl)but-3-en-1-ol (2.78)

A solution of racemic pyranyl acetate **2.77** (20 mg, 0.09 mmol) and allyl silane **2.73** (41 mg, 0.18 mmol, 2.0 equiv) in CH_2Cl_2 (1 mL) under N_2 was cooled to $-78\text{ }^\circ\text{C}$. TMSOTf (16 μL , 0.09 mmol, 1.0 equiv) was added and the mixture was allowed to stir for 1h at this temperature. NaHCO_3 (100 μL , 0.10 mmol) was added and the mixture was allowed to warm up to rt. The mixture was then concentrated. Flash column chromatography purification (5% to 25% EtOAc in hexanes) afforded the product (20 mg, 77%) as a colorless oil. ^1H NMR (500 MHz, CDCl_3) δ 5.38 (d, $J = 1.0$ Hz, 1H), 4.96 (s, 1H), 4.94 (s, 1H), 4.32 (s, 1H), 3.73 (t, $J = 6.1$ Hz, 2H), 3.69 – 3.62 (m, 1H), 2.36 – 2.33 (m, 2H), 2.16 (dd, $J = 14.3$, 4.7 Hz, 1H), 2.01 (s, 1H), 1.87 – 1.81 (m, 2H), 1.69 (s, 3H), 1.59 – 1.49 (m, 1H), 1.46 – 1.36 (m, 2H), 1.34 – 1.20 (m, 12H), 0.87 (t, $J = 6.9$ Hz, 3H). ^{13}C NMR (126 MHz, CDCl_3) δ 143.5, 132.2, 123.0, 114.7, 71.3,

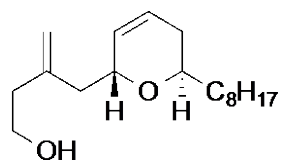
68.1, 61.0, 41.1, 39.3, 35.7, 35.5, 32.1, 29.9, 29.8, 29.5, 25.9, 23.4, 22.9, 14.3; IR (thin film) 3400, 2927, 2855, 1644, 1439, 1380, 1130, 1109, 1046, 889 cm^{-1} ; HRMS (ESIP) calcd for $\text{C}_{19}\text{H}_{35}\text{O}_2$ $[\text{M}+\text{H}]^+$: 295.2632, found: 295.2623.



(2*R*,6*S*)-10-Methylene-2-octyl-1,7-dioxaspiro[5.5]undec-4-ene (2.81)

To a solution of tetrahydropyranol **2.79** (10 mg, 0.04 mmol, 1 equiv) and allylsilane **2.73** (12 mg, 0.05 mmol, 1.5 equiv) in CH_2Cl_2 (550 μL) under nitrogen was added TMSOTf (2 mol%, 8 μL , 0.8 μmol , 0.1M) dropwise at rt. Upon stirring for 45 min, the reaction was quenched by adding of a saturated aqueous solution of NaHCO_3 (5 μL , 5 μmol). After stirring for 30 min, 4 ÅMS (10 mg was added and stirred for another 30 min. DDQ (36 mg, 0.16 mmol) was added portion-wise. The oxidation step proceeded for 2 h and was quenched by Et_3N upon complete consumption of starting material. The crude mixture was concentrated and purified by flash chromatography (5% EtOAc in hexane) to give the desired product (6.8 mg, 61%) as a colorless oil. ^1H NMR (500 MHz, CDCl_3) δ 5.98 – 5.92 (m, 1H), 5.67 (dd, $J = 10.0$, 2.0 Hz, 1H), 4.81 (s, 1H), 4.77 (s, 1H), 3.86 – 3.79 (m, 2H), 3.72 (dd, $J = 10.7$, 5.9 Hz, 1H), 2.35 – 2.30 (m, 3H), 2.17 (d, $J = 13.6$ Hz, 1H), 1.92 (dt, $J = 5.2$, 3.9 Hz, 2H), 1.61 – 1.52 (m, 1H), 1.50 – 1.42 (m, 2H), 1.32 – 1.23 (m, 11H), 0.88 (t, $J = 6.8$ Hz, 3H); ^{13}C NMR (126 MHz, CDCl_3)

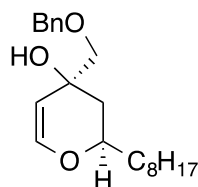
δ 141.5, 129.8, 128.9, 110.4, 95.5, 67.7, 61.5, 44.5, 35.8, 34.2, 32.2, 31.0, 29.9, 29.9, 29.6, 26.0, 23.0, 14.4; HRMS (ASAP) calcd for C₁₈H₃₁O₂ [M+H]⁺: 279.2324, found: 279.2331; IR (thin film) 2927, 2855, 1658, 1463, 1396, 1370, 1238, 1176, 1115, 1069, 1049, 1017, 989, 886 cm⁻¹.



3-(((2*R*,6*R*)-6-octyl-5,6-dihydro-2*H*-pyran-2-yl)methyl)but-3-en-1-ol

(2.80)

Formed as a single diastereomer: ¹H NMR (400 MHz, CDCl₃) δ 5.81 (dtd, *J* = 7.5, 4.9, 2.3 Hz, 1H), 5.71 – 5.66 (m, 1H), 4.97 (s, 1H), 4.95 (s, 1H), 4.37 – 4.31 (m, 1H), 3.74 (t, *J* = 6.1 Hz, 2H), 3.66 (tt, *J* = 8.3, 4.0 Hz, 1H), 2.41 (dd, *J* = 14.3, 9.3 Hz, 1H), 2.35 (t, *J* = 6.2 Hz, 2H), 2.20 (dd, *J* = 14.3, 5.0 Hz, 1H), 2.01 (dt, *J* = 17.4, 4.5 Hz, 1H), 1.94 – 1.85 (m, 1H), 1.58 – 1.49 (m, 1H), 1.29 – 1.21 (m, 10H), 0.87 (t, *J* = 6.5 Hz, 3H); ¹³C NMR (101 MHz, CDCl₃) δ 143.3, 129.4, 124.6, 114.9, 71.1, 67.9, 61.0, 40.9, 39.2, 35.6, 32.1, 30.8, 29.9, 29.8, 29.5, 25.8, 22.9, 14.3; IR (thin film, neat) 3392, 2927, 2855, 1645, 1466, 1434, 1377, 1184, 1087, 1048, 890, 713 cm⁻¹; HRMS (ESIP) calcd for C₁₈H₃₃O₂ [M+H]⁺: 281.2475, found: 281.2475.

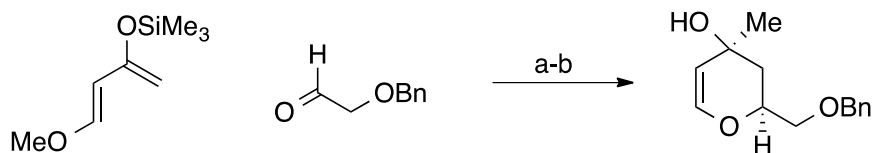


(2*R*,4*S*)-4-((Benzyloxy)methyl)-2-octyl-3,4-dihydro-2*H*-pyran-4-ol (2.84)

To Bu₃SnCH₂OBn⁵ (244 mg, 0.594 mmol, 1.25 equiv) in THF (1 mL) at -78 °C was added *n*-BuLi (1.6M, 360 μ L, 0.571 mmol, 1.2 equiv) dropwise over 5 min and the mixture was stirred for 15 min. A solution of the pyranone (100 mg, 0.475 mmol, 1.0

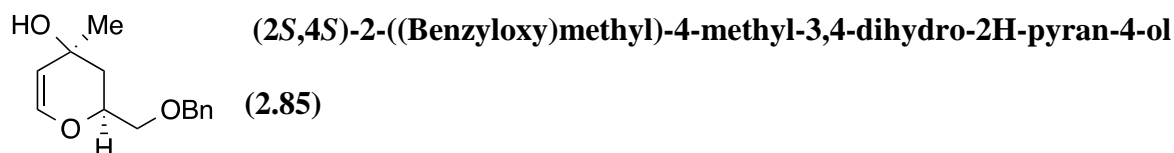
⁵ Still, W. C. *J. Am. Chem. Soc.* **1978**, *100*, 1481

equiv) in THF (500 μ L) was added by cannulation. The reaction was stirred at -78 $^{\circ}$ C for 1h, then was quenched with water (1 mL) and warmed to rt. The mixture was extracted with Et₂O (2 x 5 mL). The combined organic layers were washed with brine (10 mL) and concentrated in vacuo. Flash column chromatography purification (30% EtOAc in hexanes) afforded the product (198 mg, 91%) as a colorless oil. Formed as a 6.7:1 mixture of diastereomers. Major diastereomer: ¹H NMR (601 MHz, CDCl₃) δ 7.39 – 7.28 (m, 5H), 6.40 (d, *J* = 6.3 Hz, 1H), 4.66 – 4.63 (m, 1H), 4.59 (ABq, 2H, $\Delta\delta_{AB}$ = 0.08, *J*_{AB} = 12.0 Hz), 3.49 (d, *J* = 9.3 Hz, 1H), 3.38 (d, *J* = 9.5 Hz, 1H), 2.12 (dt, *J* = 13.6, 2.1 Hz, 1H), 1.70 (m, 1H), 1.66 – 1.60 (m, 1H), 1.52 – 1.46 (m, 1H), 1.45 – 1.37 (m, 1H), 1.34 – 1.25 (m, 12H), 0.89 (t, *J* = 6.9 Hz, 3H); ¹³C NMR (151 MHz, CDCl₃) δ 146.3, 138.2, 128.7, 128.1, 127.9, 104.3, 76.5, 74.8, 73.6, 68.4, 38.5, 35.3, 32.1, 29.8, 29.7, 29.5, 25.4, 22.9, 14.3; $[\alpha]_D^{20}$ +40.8 (c 1.02, CHCl₃); IR (thin film) 3437, 2926, 2856, 1644, 1455, 1239, 1097 cm^{-1} ; HRMS (ASAP) calcd for C₂₁H₃₁O₂[M–OH]⁺: 315.2324, found: 315.2352.



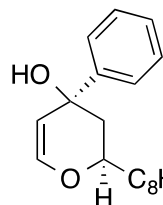
Reagents and conditions

a) BF₃·OEt₂, Et₂O, -20 $^{\circ}$ C, then TFA, 62%. b) MeLi, THF, -78 $^{\circ}$ C, 78%.



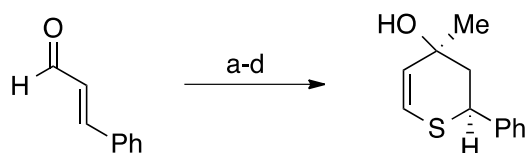
Formed as a 17:1 mixture of diastereomers. Major diastereomer: ¹H NMR (500 MHz, CDCl₃) δ 7.30 – 7.25 (m, 4H), 7.25 – 7.20 (m, 1H), 6.27 (d, *J* = 6.2 Hz, 1H), 4.68 (dd, *J* = 6.2, 1.6 Hz, 1H), 4.55 – 4.52 (m, 3H), 4.07 (ddt, *J* = 9.5, 5.5, 3.6 Hz, 1H), 3.55 (qd, *J* =

10.4, 4.8 Hz, 2H), 1.91 (ddd, $J = 13.5, 3.4, 1.6$ Hz, 1H), 1.85 (dd, $J = 13.5, 10.0$ Hz, 1H), 1.30 (s, 3H); ^{13}C NMR (126 MHz, CDCl_3) δ 143.7, 138.0, 128.7, 128.0, 109.4, 107.4, 74.1, 73.8, 72.6, 65.9, 40.8, 30.3; IR (thin film) 3424, 2924, 1644, 1595, 1454, 1367, 1236, 1099, 1073, 1046, 920, 748, 699 cm^{-1} ; HRMS (ASAP) calcd for $\text{C}_{14}\text{H}_{17}\text{O}_3$ $[\text{M}-\text{H}]^+$: 233.1178, found: 233.1179.



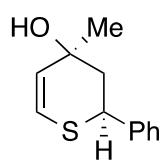
(2*R*)-2-Octyl-4-phenyl-3,4-dihydro-2H-pyran-4-ol (2.86)

^1H NMR (601 MHz, CDCl_3) δ 7.61 – 7.58 (m, 2H), 7.38 – 7.35 (m, 2H), 7.30 – 7.27 (m, 1H), 6.61 (d, $J = 6.2$ Hz, 1H), 4.84 (dd, $J = 6.2, 2.1$ Hz, 1H), 3.72 – 3.67 (m, 1H), 2.18 – 2.06 (m, 2H), 1.62 – 1.55 (m, 1H), 1.46 – 1.34 (m, 2H), 1.29 – 1.20 (m, 11H), 0.86 (t, $J = 7.1$ Hz, 3H); ^{13}C NMR (151 MHz, CDCl_3) δ 147.6, 145.6, 128.4, 127.7, 126.6, 106.4, 74.1, 71.4, 45.2, 35.2, 32.0, 29.8, 29.7, 29.4, 25.3, 22.9, 14.3; IR (thin film) 3367, 2926, 2855, 1644, 1448, 1239, 1034, 759, 701 cm^{-1} ; HRMS (ASAP) calcd for $\text{C}_{19}\text{H}_{27}\text{O}$ $[\text{M}-\text{OH}]^+$: 271.2062, found: 271.2056.



Reagents and conditions

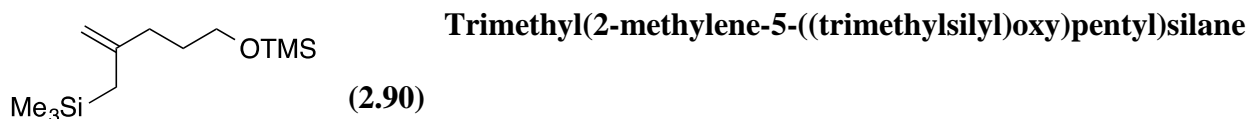
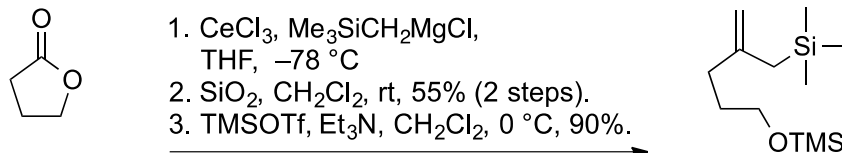
a) LiCCSiMe_3 , THF, -78°C . b) MnO_2 , CH_2Cl_2 , 78%, two steps. c) $\text{NaSH}\cdot 9\text{H}_2\text{O}$, 2-methoxyethanol, 60°C , 35%. d) MeLi , THF, -78°C , 60%.



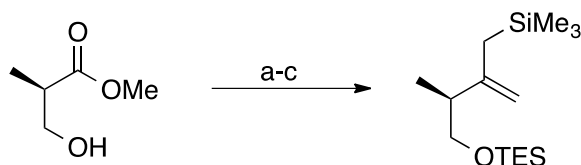
(2*R*,4*R*)-4-Methyl-2-phenyl-3,4-dihydro-2H-thiopyran-4-ol (2.88)

This compound was formed as a 6:1 mixture of diastereomers. It is unstable and should not be stored for prolonged periods. Major diastereomer: ^1H NMR (500 MHz, CDCl_3) δ 7.36 – 7.25 (m, 4H), 7.25 – 7.20 (m, 1H), 6.06 (d, $J = 10.2$ Hz, 1H), 5.69 (dd, J

= 10.2, 1.2 Hz, 1H), 4.32 (dd, $J = 12.5, 2.6$ Hz, 1H), 2.33 (m, 1H), 2.23 (ddd, $J = 13.1, 2.6, 1.2$ Hz, 1H), 1.36 (s, 3H); ^{13}C NMR (126 MHz, CDCl_3) δ 140.7, 129.2, 128.2, 128.2, 127.9, 121.4, 70.3, 45.9, 44.5, 29.5; HRMS (ASAP) calcd for $\text{C}_{12}\text{H}_{13}\text{S}$ $[\text{M}-\text{OH}]^+$: 189.0738, found: 189.0730; IR (thin film) 3368, 3028, 2969, 2927, 1666, 1603, 1494, 1452, 1371, 1115, 699 cm^{-1} .

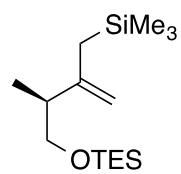


^1H NMR (601 MHz, CDCl_3) δ 4.59 (s, 1H), 4.52 (s, 1H), 3.58 (dd, $J = 8.3, 5.0$ Hz, 2H), 2.00 – 1.97 (m, 2H), 1.67 (dt, $J = 15.4, 6.7$ Hz, 2H), 1.53 (s, 2H), 0.11 (s, 9H), 0.02 (s, 9H); ^{13}C NMR (151 MHz, CDCl_3) δ 147.5, 107.1, 62.6, 34.6, 31.1, 27.2, -0.2 , -1.1 ; IR (thin film) 2955, 1634, 1417, 1250, 1157, 1099, 981, 960, 841, 748, 693, 657 cm^{-1} ; HRMS (ASAP) calcd for $\text{C}_{12}\text{H}_{29}\text{OSi}_2$ $[\text{M}+\text{H}]^+$: 245.1757, found: 245.1761.



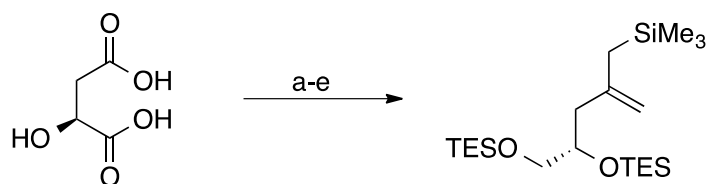
Reagents and conditions

a) TESCl, imidazole, CH_2Cl_2 , 84%. b) $\text{Me}_3\text{SiCH}_2\text{MgCl}$, CeCl_3 , THF, -78 °C. c) SiO_2 , CH_2Cl_2 , 85%, two steps.



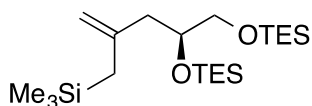
(S)-Triethyl((2-methyl-3-((trimethylsilyl)methyl)but-3-en-1-yl)oxy)silane
(2.91)

^1H NMR (601 MHz, CDCl_3) δ 4.60 (s, 1H), 4.58 (s, 1H), 3.66 (dd, $J = 9.8, 5.0$ Hz, 1H), 3.31 (dd, $J = 9.7, 8.4$ Hz, 1H), 2.10 (m, 1H), 1.05 (d, $J = 6.8$ Hz, 3H), 0.96 (t, $J = 8.0$ Hz, 9H), 0.60 (q, $J = 7.9$ Hz, 6H), 0.02 (s, 9H); ^{13}C NMR (126 MHz, CDCl_3) δ 150.2, 106.4, 67.9, 43.8, 27.4, 16.9, 7.0, 4.7, -1.1 ; $[\alpha]_{\text{D}}^{20} -16.2$ (c 0.9, CHCl_3). IR (thin film) 2956, 2912, 2878, 1632, 1460, 1416, 1248, 1080, 1014, 855, 743 cm^{-1} ; HRMS (ASAP) calcd for $\text{C}_{14}\text{H}_{31}\text{OSi}_2$ $[\text{M}-\text{CH}_3]^+$: 271.1913, found: 271.1909.



Reagents and conditions

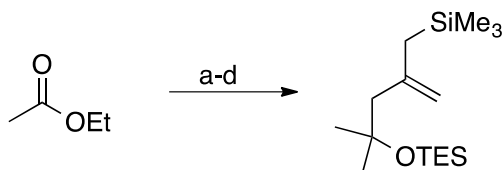
a) SOCl_2 , EtOH, reflux, 90%. b) $\text{BH}_3 \cdot \text{SMe}_2$, NaBH_4 , THF, 0 $^\circ\text{C}$, 75%.
c) TESCl, imidazole, CH_2Cl_2 , 78%. d) $\text{Me}_3\text{SiCH}_2\text{MgCl}$, CeCl_3 , THF, -78 $^\circ\text{C}$. e) SiO_2 , CH_2Cl_2 , 79%, two steps.



(S)-3,3,8,8-Tetraethyl-5-(2-((trimethylsilyl)methyl)allyl)-
4,7-dioxa-3,8-disiladecane (2.92)

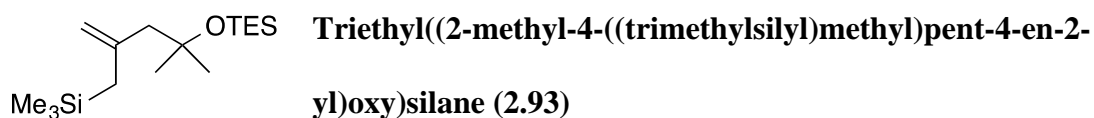
^1H NMR (601 MHz, CDCl_3) δ 4.64 (s, 1H), 4.57 (s, 1H), 3.80 (dq, $J = 7.0, 5.6$ Hz, 1H), 3.50 (dd, $J = 10.0, 5.7$ Hz, 1H), 3.45 (dd, $J = 10.0, 5.8$ Hz, 1H), 2.25 (ddd, $J = 13.7, 5.2, 1.0$ Hz, 1H), 2.00 (dd, $J = 13.7, 7.1$ Hz, 1H), 1.54 (s, 2H), 0.99 – 0.91 (m, 18H), 0.62 – 0.57 (m, 12H), 0.02 (s, 9H); ^{13}C NMR (151 MHz, CDCl_3) δ 144.5, 110.1, 72.6, 67.2, 43.6, 27.3, 7.0, 5.3, 4.6, -1.2 ; $[\alpha]_{\text{D}}^{20} +0.9$ (c 0.76, CHCl_3); IR (thin film) 2955, 2912, 2878, 1633, 1459, 1415, 1247, 1113, 1077,

1006, 856, 742 cm^{-1} ; HRMS (ASAP) calcd for $\text{C}_{21}\text{H}_{49}\text{O}_2\text{Si}_3$ $[\text{M}+\text{H}]^+$: 417.3040, found: 417.3058.

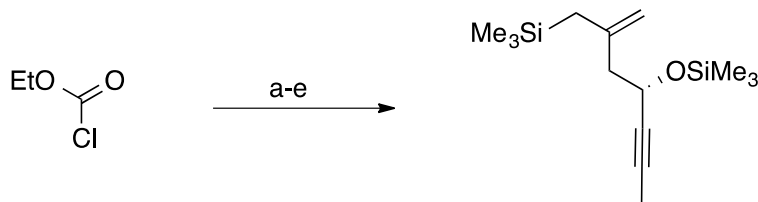


Reagents and conditions

a) LiHMDS, THF, -78°C , then acetone. b) TESOTf, 2,6-lutidine, 0°C , CH_2Cl_2 48% (two steps). c) $\text{Me}_3\text{SiCH}_2\text{MgCl}$, CeCl_3 , THF, -78°C . d) SiO_2 , CH_2Cl_2 , 83%, two steps.

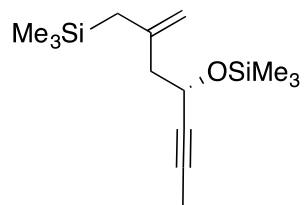


^1H NMR (601 MHz, CDCl_3) δ 4.61 (s, 1H), 4.56 (s, 1H), 2.10 (s, 2H), 1.54 (s, 2H), 1.22 (s, 6H), 0.99 – 0.91 (m, 9H), 0.62 – 0.54 (m, 6H), 0.01 (s, 9H); ^{13}C NMR (151 MHz, CDCl_3) δ 145.4, 111.0, 74.3, 53.0, 30.4, 28.2, 7.3, 7.0, -1.2 ; IR (thin film) 2956, 2912, 2878, 1629, 1460, 1416, 1380, 1364, 1247, 1150, 1043, 1007, 851, 742 cm^{-1} ; HRMS (ASAP) calcd for $\text{C}_{14}\text{H}_{31}\text{OSi}_2$ $[\text{M}-\text{CH}_2\text{CH}_3]^+$: 271.1913, found: 271.1927.



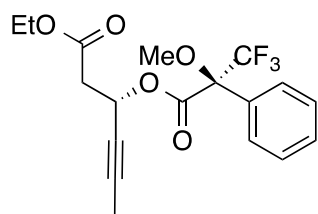
Reagents and conditions

a) *n*-BuLi, propyne, THF, -78°C , 95%. b) LDA, EtOAc, THF, -78°C , 91%. c) $\text{CIRu}[(S,S)\text{-TsDPEN}](p\text{-cymene})$, Et_3N , HCO_2H , 72%, $>90\%$ ee. d) $\text{Me}_3\text{SiCH}_2\text{MgCl}$, CeCl_3 , THF, -78°C , then SiO_2 , CH_2Cl_2 , 52%. e) TMSOTf, collidine, CH_2Cl_2 , 0°C , 88%.

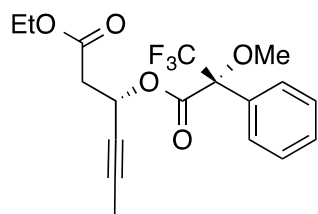


(S)-Trimethyl(2-methylene-4-((trimethylsilyl)oxy)hept-5-yn-1-yl)silane (2.94)

^1H NMR (500 MHz, CDCl_3) δ 4.66 (s, 1H), 4.60 (s, 1H), 4.39 (dd, $J = 6.8, 2.0$ Hz, 1H), 2.32 – 2.22 (m, 2H), 1.80 (s, 3H), 1.55 (s, 2H), 0.13 (s, 9H), 0.00 (s, 9H); ^{13}C NMR (126 MHz, CDCl_3) δ 143.7, 110.3, 81.1, 80.7, 62.8, 47.8, 27.6, 3.9, 0.5, -1.1. $[\alpha]_{\text{D}}^{20} -34.1$ (c 0.83, CHCl_3); IR (thin film, neat) 2956, 2921, 1634, 1419, 1343, 1250, 1158, 1083, 945, 844, 754, 693 cm^{-1} ; HRMS (ASAP) calcd for $\text{C}_{14}\text{H}_{29}\text{OSi}_2$ $[\text{M}+\text{H}]^+$: 269.1757, found: 269.1769.



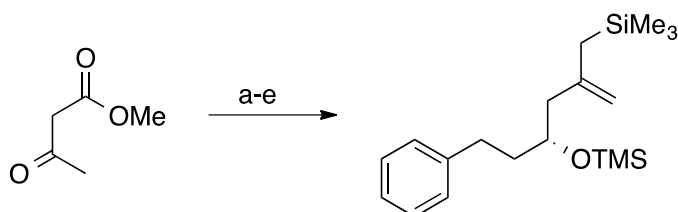
^1H NMR (500 MHz, CDCl_3) δ 7.54 (m, 2H), 7.41 – 7.36 (m, 3H), 5.93 (m, 1H), 4.11 – 4.00 (m, 2H), 3.58 (s, 3H), 2.85 (dd, $J = 16.4, 9.2$ Hz, 1H), 2.76 (dd, $J = 16.4, 4.7$ Hz, 1H), 1.86 (d, $J = 2.1$ Hz, 3H), 1.18 (t, $J = 7.2$ Hz, 3H); ^{13}C NMR (126 MHz, CDCl_3) δ 168.9, 165.6, 132.6, 129.9, 128.6, 127.8, 123.52 (q, $^1J_{\text{C-F}} = 288.5$ Hz, CF_3), 84.7 (q, $^2J_{\text{C-F}} = 28.0$ Hz), 84.2, 74.7, 62.9, 61.3, 55.8, 40.3, 14.3, 3.9. The dr of this (S)-Mosher ester⁶ was found to be > 95:5 by both ^1H and ^{19}F NMR analysis. [$\delta -71.73$ (major) and $\delta -71.86$ (minor), in CDCl_3].



^1H NMR (400 MHz, CDCl_3) δ 7.54 – 7.50 (m, 2H), 7.42 – 7.37 (m, 3H), 5.89 (ddq, $J = 8.8, 4.3, 2.1$ Hz, 1H), 4.18 – 4.09 (m, 2H), 3.54 (s, 3H), 2.91 (dd, $J = 16.6, 9.5$ Hz, 1H), 2.79 (dd, $J = 16.6, 4.4$ Hz, 1H), 1.82 (d, $J = 2.1$ Hz, 3H), 1.23 (t, $J = 7.2$ Hz, 3H). ^{13}C NMR (101 MHz, CDCl_3) δ 169.2, 165.7,

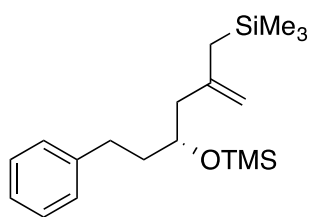
⁶ Dale, J. A.; Mosher, H. S. *J. Am. Chem. Soc.* **1973**, 95, 512.

132.4, 129.9, 128.6, 127.8, 123.4 (q, $^1J_{C-F} = 288.6$ Hz, CF_3), 85.0 (dd, $^2J_{C-F} = 55.3, 27.6$ Hz), 84.1, 74.4, 63.1, 61.4, 55.9, 40.1, 14.4, 3.8. The dr of this (*R*)-Mosher ester was found to be > 95:5 by both 1H and ^{19}F NMR analysis. [$\delta -71.73$ (minor) and $\delta -71.85$ (major), in $CDCl_3$].



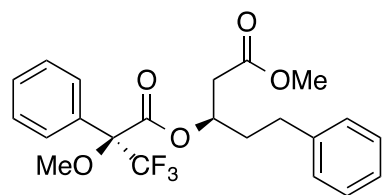
Reagents and conditions

a) *n*-BuLi, THF, then BnBr, 0 °C, 85%. b) (*R*)-Me-CBS catalyst, $BH_3 \cdot SMe_2$, THF, rt, 65%, 74% ee. c) $Me_3SiCH_2MgCl, CeCl_3$, THF, -78 °C. d) SiO_2, CH_2Cl_2 , 83%, two steps. e) TMSOTf, 2,6-lutidine, CH_2Cl_2 , 0 °C, 90%.

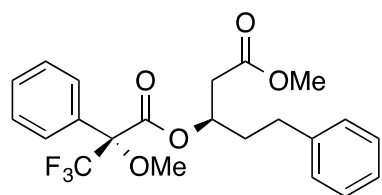


**(*R*)-Trimethyl(2-methylene-6-phenyl-4-
((trimethylsilyloxy)hexyl)silane (2.95)**

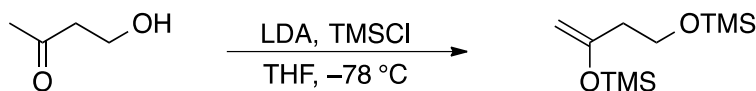
1H NMR (500 MHz, $CDCl_3$): δ 7.29 – 7.26 (m, 2H), 7.20 – 7.16 (m, 3H), 4.63 (s, 1H), 4.57 (s, 1H), 3.84 (m, 1H), 2.76 (ddd, $J = 13.3, 11.3, 5.4$ Hz, 1H), 2.57 (ddd, $J = 13.4, 11.1, 5.4$ Hz, 1H), 2.18 (dd, $J = 13.5, 6.2$ Hz, 1H), 2.12 (dd, $J = 13.6, 6.6$ Hz, 1H), 1.84 (m, 1H), 1.74 – 1.66 (m, 1H), 1.52 (s, 2H), 0.13 (s, 9H), 0.03 (s, 9H); ^{13}C NMR (151 MHz, $CDCl_3$) δ 144.5, 142.8, 128.7, 128.6, 126.0, 110.3, 71.6, 47.0, 39.2, 32.5, 27.5, 0.8, -1.0; IR (thin film) 3067, 3028, 2954, 1632, 1496, 1454, 1368, 1250, 1155, 1091, 1063, 986, 841, 748, 698 cm^{-1} ; $[\alpha]_D^{20} +3.8$ (c 0.42, $CHCl_3$); HRMS (ASAP) calcd for $C_{18}H_{31}SiO_2 [M-CH_3]^+$: 319.1913, found: 319.1924. Mosher ester analysis (see below) show the compound to have an ee of 74%.

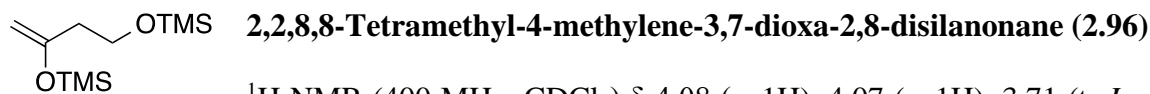


Major diastereomer: ^1H NMR (500 MHz, CDCl_3) δ 7.49 (dd, $J = 6.2, 3.2$ Hz, 2H), 7.35 – 7.33 (m, 3H), 7.21 (dd, $J = 15.2, 7.8$ Hz, 3H), 7.14 (d, $J = 7.5$ Hz, 1H), 7.07 (d, $J = 7.5$ Hz, 1H), 5.45 (dq, $J = 7.3, 5.1$ Hz, 1H), 3.52 (s, 3H), 3.47 (s, 3H), 2.66 – 2.52 (m, 4H), 2.06 – 1.87 (m, 2H); ^{13}C NMR (126 MHz, CDCl_3) δ 170.4, 166.2, 140.9, 132.4, 129.9, 128.9, 128.7, 128.6, 127.8, 126.6, 123.6 (q, $J_{\text{C-F}} = 289.2$ Hz), 84.9, 73.3, 55.7, 52.1, 38.7, 35.9, 31.7; ^{19}F NMR (CDCl_3) δ -71.24 (minor) and δ -71.36 (major). The dr of this (*S*)-Mosher ester was found to be 1.0:0.15 by both ^1H and ^{19}F NMR analyses.



Major diastereomer: ^1H NMR (400 MHz, CDCl_3) δ 7.56 – 7.44 (m, 2H), 7.39 – 7.29 (m, 2H), 7.24 – 7.15 (m, 3H), 7.15 – 7.10 (m, 1H), 7.01 – 6.98 (m, 2H), 5.45 (tt, $J = 6.7, 5.1$ Hz, 1H), 3.59 (s, 3H), 3.49 (s, 3H), 2.68 (dd, $J = 16.0, 7.9$ Hz, 1H), 2.57 (dd, $J = 15.9, 4.9$ Hz, 1H), 2.45 (dt, $J = 7.8, 6.2$ Hz, 2H), 1.94 – 1.87 (m, 2H); ^{13}C NMR (126 MHz, CDCl_3) δ 170.6, 166.3, 140.9, 132.6, 130.0, 128.8, 128.7, 128.5, 127.7, 126.5, 123.5 (q, $J_{\text{C-F}} = 289.3$ Hz), 84.9, 73.2, 55.8, 52.2, 38.9, 35.8, 31.3; ^{19}F NMR (CDCl_3) δ -71.23 (major) and δ -71.36 (minor). The dr of this (*R*)-Mosher ester was found to be 1.0:0.15 by both ^1H and ^{19}F NMR analysis.

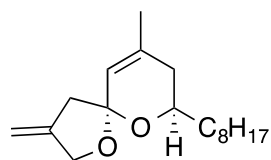




$^1\text{H NMR}$ (400 MHz, CDCl_3) δ 4.08 (s, 1H), 4.07 (s, 1H), 3.71 (t, $J = 7.1$ Hz, 2H), 2.26 (t, $J = 7.1$ Hz, 2H), 0.20 (s, 9H), 0.11 (s, 9H). These data are consistent with literature values.⁷

General protocol for Ferrier reaction-based [n+1] annulations

To a solution of the tetrahydropyranol (1 equiv) and allylsilane (1.5 equiv) in CH_2Cl_2 (~0.15 M) under nitrogen was added TMSOTf (2-5 mol%, 0.1 M solution in CH_2Cl_2 stored over NaHCO_3) dropwise at rt. Upon stirring for 45 min, the reaction was quenched by adding of a saturated aqueous solution of NaHCO_3 (1.2 equiv). After stirring for 30 min, 4Å MS (150 wt%) was added and stirred for another 30 min. DDQ (5.0-8.0 equiv) was added portion-wise. The reaction was monitored by TLC and quenched by Et_3N upon complete consumption of starting material. After concentration under vacuum, the reaction was purified by flash column chromatography to give the desired product.



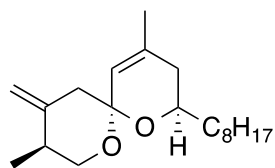
(7R)-9-Methyl-3-methylene-7-octyl-1,6-dioxaspiro[4.5]dec-9-ene

(2.97)

The general cyclization procedure was followed with **2.89** (29 mg, 0.13 mmol), **2.77** (20 mg, 0.09 mmol), TMSOTf (2 mol%, 20 μL , 1.8 μmol), NaHCO_3 (sat) (30 μL ,

⁷ Martin, V. A.; Murray, D. H.; Pratt, N. E.; Zhao, Y. B.; Albizati, K. F. *J. Am. Chem. Soc.* **1990**, *112*, 6965.

0.03 mmol), 4Å MS (45 mg), dichloromethane (0.9 mL), and DDQ (120 mg, 0.53 mmol). The oxidation proceeded at 0 °C for 5 h. The crude mixture was purified by flash chromatography (10% EtOAc in hexane) to give the desired product (17 mg, 68%) as a colorless oil. ¹H NMR (400 MHz, CDCl₃) δ 5.41 (s, 1H), 4.99 (s, 1H), 4.92 (s, 1H), 4.38 (ABq, 2H, Δδ_{AB} = 0.008, J_{AB} = 2.0 Hz), 3.89 (ddd, J = 11.5, 8.1, 4.1 Hz, 1H), 2.57 (ABq, 2H, Δδ_{AB} = 0.01, J_{AB} = 2.4 Hz), 1.93 – 1.76 (m, 2H), 1.74 (s, 3H), 1.58 – 1.49 (m, 1H), 1.49 – 1.39 (m, 2H), 1.35 – 1.24 (m, 11H), 0.88 (t, J = 6.5 Hz, 3H); ¹³C NMR (101 MHz, CDCl₃) δ 147.6, 138.9, 121.8, 104.6, 104.2, 69.6, 68.6, 44.7, 35.7, 35.5, 32.1, 29.8, 29.7, 29.5, 25.8, 23.0, 22.9, 14.3.); IR (thin film) 2926, 2856, 1673, 1459, 1379, 1323, 1225, 1459, 1102, 1025, 1001, 968, 880, 861 cm⁻¹; HRMS (ASAP) calcd for C₁₈H₃₁O₂ [M+H]⁺: 279.2324, found: 279.2319.

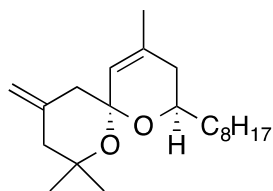


(2R,6S,9S)-4,9-Dimethyl-10-methylene-2-octyl-1,7-

dioxaspiro[5.5]undec-4-ene (2.98)

The general cyclization procedure was followed with **2.91** (42 mg, 0.15 mmol), **2.77** (30 mg, 0.13 mmol), TMSOTf (5 mol%, 70 μL, 7.0 μmol), NaHCO₃ (sat) (140 μL, 0.14 mmol), 4Å MS (210 mg), dichloromethane (1.5 mL), and DDQ (60 mg, 0.26 mmol). The oxidation proceeded at rt for 1.5 h. The crude mixture was purified by flash chromatography (10% EtOAc in hexane) to give the desired product (25 mg, 61%) as a colorless oil. ¹H NMR (601 MHz, CDCl₃) δ 5.38 (s, 1H), 4.79 (s, 1H), 4.75 (s, 1H), 3.80 (ddt, J = 11.7, 8.2, 3.9 Hz, 1H), 3.57 (dd, J = 10.4, 5.5 Hz, 1H), 3.37 (t, J = 10.9 Hz, 1H), 2.33 (ABq, 2H, Δδ_{AB} = 0.04, J_{AB} = 13.2 Hz), 1.86 (dd, J = 17.2, 11.0 Hz, 1H), 1.78 (dd, J = 17.2, 3.6 Hz, 1H), 1.58 – 1.51 (m, 1H), 1.48 – 1.40 (m, 2H), 1.32 – 1.22 (m, 11H), 0.98 (d, J = 6.6 Hz, 3H), 0.87 (t, J = 6.9 Hz, 3H); ¹³C NMR (151 MHz, CDCl₃) δ 146.2, 137.5, 124.0, 107.7, 96.2, 67.7, 67.6, 45.4, 36.0, 36.0,

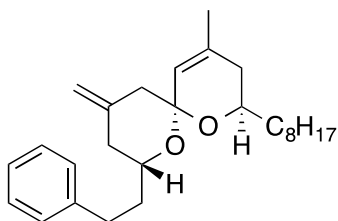
35.7, 32.2, 29.9, 29.9, 29.6, 26.0, 23.1, 23.0, 14.4, 12.9; $[\alpha]_D^{20} +28.6$ (c 2.97, CHCl_3); IR (thin film) 3085, 2927, 2856, 1682, 1654, 1458, 1380, 1248, 1220, 1174, 1042, 1010, 887, 621 cm^{-1} ; HRMS (ASAP) calcd for $\text{C}_{20}\text{H}_{35}\text{O}_2$ $[\text{M}+\text{H}]^+$: 307.2637, found: 307.2622.



(2*R*,6*R*)-4,8,8-Trimethyl-10-methylene-2-octyl-1,7-

dioxaspiro[5.5]undec-4-ene (2.99)

The general cyclization procedure was followed with **2.77** (30 mg, 0.13 mmol), **2.93** (52 mg, 0.17 mmol), TMSOTf (7.5 mol%, 70 μL , 7.0 μmol), NaHCO_3 (sat) (140 μL , 0.14 mmol), 4 \AA MS (210 mg), dichloromethane (2.0 mL), and DDQ (90 mg, 0.40 mmol). The oxidation proceeded at 0 $^\circ\text{C}$ for 1.5 h. The crude mixture was purified by flash chromatography (5% EtOAc in hexane) to give the desired product (19 mg, 44%) as a colorless oil. ^1H NMR (601 MHz, CDCl_3) δ 5.32 (s, 1H), 4.88 (s, 1H), 4.82 (s, 1H), 3.90 (ddt, $J = 9.2, 7.6, 5.3$ Hz, 1H), 2.34 – 2.24 (m, 3H), 2.16 (d, $J = 13.2$ Hz, 1H), 1.83 – 1.79 (m, 2H), 1.70 (s, 3H), 1.31 – 1.23 (m, 20H), 0.88 (t, $J = 7.0$ Hz, 3H); ^{13}C NMR (151 MHz, CDCl_3) δ 140.5, 136.5, 125.6, 111.1, 96.9, 74.3, 67.9, 45.6, 44.1, 35.6, 35.3, 32.1, 31.9, 30.0, 29.7, 29.5, 27.7, 25.6, 23.2, 22.9, 14.3; IR (thin film) 2926, 2855, 1466, 1379, 1223, 1155, 1024, 1007, 984 cm^{-1} ; HRMS (EI) calcd for $\text{C}_{21}\text{H}_{37}\text{O}_2$ $[\text{M}+\text{H}]^+$: 321.2788, found: 321.2793.

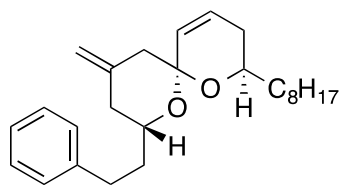


(2*R*,6*S*,8*R*)-4-Methyl-10-methylene-2-octyl-8-phenethyl-1,7-

dioxaspiro[5.5]undec-4-ene (2.100)

The general cyclization procedure was followed with **2.95** (53 mg, 0.16 mmol), **2.77** (30 mg, 0.13 mmol), TMSOTf (2 mol%, 30 μL , 2.7 μmol), NaHCO_3 (sat) (50 μL , 0.05 mmol), 4 \AA MS (75 mg), dichloromethane (1.3 mL), and DDQ (150 mg, 0.66 mmol). The oxidation proceeded for 2 h. The crude mixture was purified by

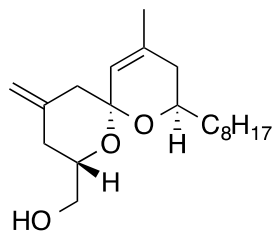
flash chromatography (5% EtOAc in hexane) to give the desired product (39 mg, 74%) as a 6:1 mixture of diastereomers resulting from the use of an allylsilane with an ee of 74%. Rigorous separation of diastereomers provided pure product (26 mg, 49%) as a colorless oil. ^1H NMR (601 MHz, CDCl_3) δ 7.29 (dd, $J = 8.8, 6.2$ Hz, 2H), 7.24 – 7.18 (m, 3H), 5.45 (s, 1H), 4.81 (s, 1H), 4.79 (s, 1H), 3.83 (m, 2H), 2.86 (ddd, $J = 14.0, 10.4, 5.6$ Hz, 1H), 2.65 (ddd, $J = 14.0, 10.2, 6.1$ Hz, 1H), 2.31 (s, 2H), 2.28 (dd, $J = 13.2, 2.4$ Hz, 1H), 2.02 (dd, $J = 13.5, 11.3$ Hz, 1H), 1.95 – 1.87 (m, 2H), 1.84 (dd, $J = 17.8, 4.3$ Hz, 2H), 1.76 (s, 3H), 1.34 – 1.27 (m, 14H), 0.90 (t, $J = 6.8$ Hz, 3H); ^{13}C NMR (151 MHz, CDCl_3) δ 142.4, 142.0, 137.2, 128.5, 128.5, 125.9, 124.4, 110.1, 96.0, 70.2, 67.8, 44.3, 40.1, 37.7, 35.9, 35.6, 32.3, 32.1, 30.0, 29.8, 29.6, 26.0, 23.1, 22.9, 14.3; $[\alpha]_{\text{D}}^{20} +3.4$ (c 1.41, CHCl_3); IR (thin film) 2927, 2855, 1656, 1455, 1379, 1237, 1112, 994, 887, 699 cm^{-1} ; HRMS (ASAP) calcd for $\text{C}_{27}\text{H}_{41}\text{O}_2$ $[\text{M}+\text{H}]^+$: 397.3107, found: 397.3089.



(2*R*,6*R*,8*R*)-10-methylene-2-octyl-8-phenethyl-1,7-dioxaspiro[5.5]undec-4-ene (2.101)

The general cyclization procedure was followed with **2.95** (57 mg, 0.17 mmol), **2.79** (30 mg, 0.14 mmol), TMSOTf (2 mol%, 30 μL , 2.8 μmol), NaHCO_3 (sat) (50 μL , 0.05 mmol), 4Å MS (75 mg), dichloromethane (1.4 mL), and DDQ (160 mg, 0.70 mmol). The oxidation proceeded for 2.5 h. The crude mixture was purified by flash chromatography (5% EtOAc in hexane) to give the desired product (21 mg, 39%) as a colorless oil. ^1H NMR (400 MHz, CDCl_3) δ 7.29 – 7.24 (m, 3H), 7.22 – 7.16 (m, 2H), 5.96 (ddd, $J = 9.9, 5.3, 2.4$ Hz, 1H), 5.69 (dt, $J = 9.9, 2.1$ Hz, 1H), 4.79 (d, $J = 8.3$ Hz, 1H), 3.87 – 3.77 (m, 1H), 2.85 (ddd, $J = 13.9, 10.4, 5.6$ Hz, 1H), 2.63 (ddd, $J = 14.0, 10.1, 6.2$ Hz, 1H), 2.31 (s, 2H), 2.26 (dd, $J = 13.2, 2.5$ Hz, 1H), 2.05 – 1.85 (m, 3H), 1.84 – 1.74 (m, 2H), 1.28 – 1.25 (m, 14H), 0.87 (t, $J = 6.6$ Hz, 3H). ^{13}C

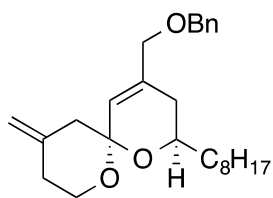
NMR (101 MHz, CDCl₃) δ 142.4, 141.7, 130.2, 128.7, 128.5, 128.5, 125.9, 110.3, 95.6, 70.1, 67.6, 44.0, 40.1, 37.8, 35.7, 32.3, 32.1, 30.9, 30.0, 29.8, 29.6, 25.9, 22.9, 14.3. $[\alpha]_D^{20} +9.7$ (c 0.64, CHCl₃); IR (thin film, neat) 2926, 2855, 1656, 1455, 1240, 1088, 1000, 887, 700 cm⁻¹. HRMS (EI) calcd for C₂₆H₃₈O₂ [M+H]⁺: 383.2950, found: 383.2952.



((2R,6R,8R)-10-Methyl-4-methylene-8-octyl-1,7-

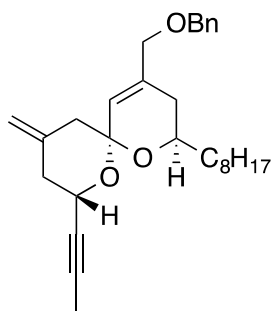
dioxaspiro[5.5]undec-10-en-2-yl)methanol (2.102)

The general cyclization procedure was followed with **2.77** (30 mg, 0.13 mmol), **2.92** (83 mg, 0.20 mmol), TMSOTf (5 mol%, 70 μ L, 7.0 μ mol), NaHCO₃ (sat) (140 μ L, 0.14 mmol), 4Å MS (210 mg), dichloromethane (1.9 mL), and DDQ (150 mg, 0.66 mmol). The oxidation proceeded for 2 h. The crude mixture was purified by flash chromatography (25% EtOAc in hexane) to give the desired product (25 mg, 58%) as a colorless oil. ¹H NMR (601 MHz, CDCl₃) δ 5.39 (s, 1H), 4.83 (s, 1H), 4.80 (s, 1H), 3.87 (ddd, *J* = 13.9, 6.4, 3.3 Hz, 1H), 3.80 (ddt, *J* = 11.7, 8.1, 3.9 Hz, 1H), 3.66 (dd, *J* = 11.6, 3.1 Hz, 1H), 3.56 (dd, *J* = 11.5, 6.3 Hz, 1H), 2.28 (s, 2H), 2.17 – 2.09 (m, 2H), 1.91 – 1.78 (m, 2H), 1.73 (s, 3H), 1.31 – 1.24 (m, 14H), 0.87 (t, *J* = 6.9 Hz, 3H); ¹³C NMR (151 MHz, CDCl₃) δ 141.0, 137.6, 123.9, 110.9, 96.1, 71.2, 67.8, 66.1, 44.3, 35.8, 35.6, 35.4, 32.1, 29.8, 29.8, 29.5, 25.9, 23.0, 22.9, 14.3; $[\alpha]_D^{20} +3.8$ (c 1.2, CHCl₃); IR (thin film) 3468, 2926, 2855, 1681, 1657, 1457, 1379, 1236, 1164, 1097, 1042, 992, 936, 887, 856 cm⁻¹; HRMS (EI) calcd for C₂₀H₃₅O₃ [M+H]⁺: 323.2581, found: 323.2590.



(2*R*,6*S*)-4-((Benzyloxy)methyl)-10-methylene-2-octyl-1,7-dioxaspiro[5.5]undec-4-ene (2.103)

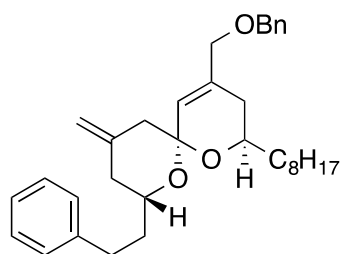
The general cyclization procedure was followed with **2.73** (28 mg, 0.12 mmol), **2.84** (20 mg, 0.06 mmol), TMSOTf (1 mol%, 6 μ L, 0.6 μ mol), NaHCO₃ (sat) (10 μ L, 0.01 mmol), 4Å MS (15 mg), dichloromethane (600 μ L), and DDQ (102 mg, 0.45 mmol). The oxidation proceeded for 2 h. The crude mixture was purified by flash chromatography (5% EtOAc in hexane) to give the desired product (15 mg, 61%) as a colorless oil. ¹H NMR (500 MHz, CDCl₃) δ 7.36 – 7.31 (m, 4H), 7.30 – 7.26 (m, 1H), 5.70 (s, 1H), 4.81 (s, 1H), 4.77 (s, 1H), 4.49 (s, 2H), 3.95 (s, 2H), 3.88 – 3.80 (m, 2H), 3.72 (ddd, J = 10.6, 5.9, 1.7 Hz, 1H), 2.41 – 2.28 (m, 3H), 2.18 (ddd, J = 13.3, 3.9, 2.0 Hz, 1H), 1.98 – 1.87 (m, 2H), 1.37 – 1.18 (m, 14H), 0.88 (t, J = 6.7 Hz, 3H); ¹³C NMR (126 MHz, CDCl₃) δ 141.4, 138.4, 137.8, 128.6, 127.9, 127.8, 125.6, 110.4, 95.6, 77.4, 73.0, 72.3, 67.8, 61.5, 44.5, 35.6, 34.2, 32.1, 31.7, 29.8, 29.8, 29.5, 25.9, 22.9; IR (thin film) 2985, 2934, 2857, 1736, 1370, 1332, 1271, 1151, 1036 cm⁻¹; HRMS (EI) calcd for C₂₆H₃₉O₃ [M+H]⁺: 399.2894, found: 399.2907.



(2*R*,6*R*,8*S*)-4-((benzyloxy)methyl)-10-methylene-2-octyl-8-(prop-1-yn-1-yl)-1,7-dioxaspiro[5.5]undec-4-ene (2.104)

The general cyclization procedure was followed with **2.94** (41 mg, 0.15 mmol), **2.84** (48 mg, 0.15 mmol), TMSOTf (5 mol%, 75 μ L, 7.5 μ mol), NaHCO₃ (sat) (150 μ L, 0.15 mmol), 4Å MS (220 mg), dichloromethane (2.5 mL) and DDQ (102 mg, 0.45 mmol). The reaction was stirred at rt for 2 h and then quenched by Et₃N. The crude mixture was purified by flash chromatography (5% EtOAc in hexane) to give the desired product (26 mg, 41%) as a colorless oil. ¹H NMR (500 MHz, CDCl₃) δ 7.37 – 7.30 (m, 4H), 7.30 – 7.27 (m, 1H), 5.70 (s, 1H), 4.84 (d, J = 1.9 Hz, 1H), 4.80 (d, J = 1.9

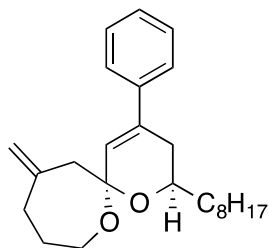
Hz, 1H), 4.50 (t, $J = 2.5$ Hz, 1H), 4.48 (s, 2H), 3.94 (s, 2H), 3.89 (tt, $J = 9.3, 4.8$ Hz, 1H), 2.47 – 2.32 (m, 3H), 2.29 – 2.23 (m, 1H), 1.92 (dd, $J = 8.1, 3.1$ Hz, 2H), 1.85 (d, $J = 2.1$ Hz, 3H), 1.61 – 1.52 (m, 1H), 1.50 – 1.41 (m, 2H), 1.34 – 1.23 (m, 11H), 0.88 (t, $J = 6.7$ Hz, 3H). ^{13}C NMR (126 MHz, CDCl_3) δ 140.2, 138.4, 137.9, 128.6, 127.8, 127.8, 125.3, 111.4, 96.0, 81.1, 78.7, 73.0, 72.4, 67.9, 61.7, 43.8, 40.9, 35.5, 32.1, 31.6, 29.8, 29.5, 25.8, 22.9, 14.3, 4.0. $[\alpha]_{\text{D}}^{20}$ -24.5 (c 1.2, CHCl_3); IR (thin film, neat) 2926, 2855, 1723, 1657, 1454, 1356, 1260, 1165, 1113, 1036, 985, 738, 698 cm^{-1} . HRMS (APCI) calcd for $\text{C}_{29}\text{H}_{41}\text{O}_3$ $[\text{M}+\text{H}]^+$: 437.3056, found: 437.3045.



(2*R*,6*S*,8*R*)-4-((Benzyloxy)methyl)-10-methylene-2-octyl-8-phenethyl-1,7-dioxaspiro[5.5]undec-4-ene (2.105)

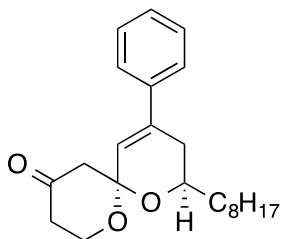
The general cyclization procedure was followed with **2.95** (36 mg, 0.11 mmol), **2.84** (30 mg, 0.09 mmol), TMSOTf (2 mol%, 20 μL , 1.8 μmol), NaHCO_3 (sat) (30 μL , 0.03 mmol), 4Å MS (45 mg), dichloromethane (0.9 mL) and DDQ (154 mg, 0.68 mmol). The oxidation proceeded for 2 h. The crude mixture was purified by flash chromatography (10% EtOAc in hexane) to give the desired product (23 mg, 51%) as a colorless oil. ^1H NMR (400 MHz, CDCl_3) δ 7.40 – 7.36 (m, 4H), 7.35 – 7.27 (m, 3H), 7.25 – 7.18 (m, 3H), 5.73 (s, 1H), 4.83 (s, 1H), 4.81 (s, 1H), 4.54 (ABq, 2H, $\Delta\delta_{\text{AB}} = 0.01$, $J = 2.0$ Hz), 4.00 (s, 2H), 3.93 – 3.80 (m, 2H), 2.87 (ddd, $J = 13.9, 10.3, 5.7$ Hz, 1H), 2.66 (ddd, $J = 13.9, 10.0, 6.2$ Hz, 1H), 2.35 (s, 2H), 2.30 (dd, $J = 13.4, 2.5$ Hz, 1H), 2.09 – 1.76 (m, 5H), 1.53 – 1.41 (m, 2H), 1.36 – 1.26 (m, 12H), 0.91 (t, $J = 6.3$ Hz, 3H); ^{13}C NMR (126 MHz, CDCl_3) δ 142.4, 141.7, 138.4, 137.5, 128.6, 128.5, 128.0, 127.9, 126.2, 125.9, 110.3, 95.8, 73.2, 72.4, 70.2, 67.8, 44.2, 40.1, 37.8, 35.6, 32.3, 32.1, 31.8, 30.0, 29.9, 29.8, 29.6, 26.0, 22.9, 14.3; $[\alpha]_{\text{D}}^{20}$ -2.3 (c

1.67, CHCl₃); IR (thin film) 2927, 2855, 1746, 1456, 1253, 1176, 1111, 1068, 1017, 888 cm⁻¹; HRMS (ASAP) calcd for C₃₄H₄₇O₃ [M+H]⁺: 503.3525, found: 503.3527.



(2*R*,6*S*)-11-Methylene-2-octyl-4-phenyl-1,7-dioxaspiro[5.6]dodec-4-ene (2.106)

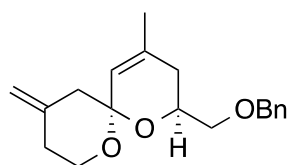
The general cyclization procedure was followed with **2.86** (30 mg, 0.10 mmol), **2.90** (33 mg, 0.14 mmol), TMSOTf (3 mol%, 30 μL, 2.7 μmol), NaHCO₃ (sat) (45 μL, 0.05 mmol), 4Å MS (68 mg), dichloromethane (1.0 mL), and DDQ (24 mg, 0.10 mmol). The oxidation proceeded at 0 °C for 1 h. The crude mixture was purified by flash chromatography (5% EtOAc in hexane) to give the desired product (23 mg, 59%) as a colorless oil. ¹H NMR (500 MHz, CDCl₃) δ 7.43 – 7.40 (m, 2H), 7.35 – 7.31 (m, 2H), 7.29 – 7.24 (m, 1H), 6.24 (s, 1H), 4.94 (s, 1H), 4.82 (s, 1H), 4.06 – 4.00 (m, 2H), 3.69 (ddd, *J* = 12.8, 4.1, 2.7 Hz, 1H), 2.61 (ABq, 2H, Δδ_{AB} = 0.09, *J*_{AB} = 14.3 Hz), 2.48 (dt, *J* = 13.4, 3.8 Hz, 2H), 2.31 (dd, *J* = 7.2, 1.6 Hz, 2H), 1.78 – 1.71 (m, 2H), 1.70 – 1.62 (m, 2H), 1.38 – 1.23 (m, 12H), 0.89 (t, *J* = 6.5 Hz, 3H). ¹³C NMR (126 MHz, CDCl₃) δ 144.4, 140.4, 136.3, 128.6, 127.8, 125.5, 124.7, 114.4, 97.6, 68.1, 62.1, 47.0, 37.8, 35.7, 33.4, 32.1, 30.6, 29.9, 29.8, 29.6, 25.9, 22.9, 14.3. IR (thin film, neat) 2927, 2855, 1720, 1449, 1097, 1040, 698 cm⁻¹; HRMS (ESI) calcd for C₂₅H₃₇O₂ [M+H]⁺: 369.27881, found: 369.27921.



(6*S*,8*R*)-8-Octyl-10-phenyl-1,7-dioxaspiro[5.5]undec-10-en-4-one (2.107)

The general cyclization procedure was followed with **2.96** (50 mg, 0.22 mmol), **2.86** (50 mg, 0.17 mmol), TMSOTf (2 mol%, 35 μL, 3.5 μmol), NaHCO₃ (sat) (70 μL, 0.07 mmol), 4Å MS (100 mg), dichloromethane (1.7 mL) and DDQ (58

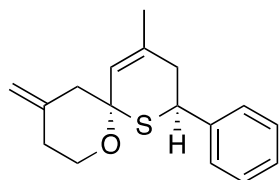
mg, 0.26 mmol). The oxidation proceeded at rt for 1.5 h. The crude mixture was purified by flash chromatography (15% EtOAc in hexane) to give the desired product (41 mg, 66%) as a white solid (mp = 97.5 – 99.5 °C). ¹H NMR (400 MHz, CDCl₃) δ 7.41 (m, 2H), 7.38 – 7.34 (m, 1H), 7.34 – 7.29 (m, 2H), 6.04 (s, 1H), 4.14 (td, *J* = 11.6, 3.1 Hz, 1H), 4.05 (ddd, *J* = 11.1, 7.9, 1.3 Hz, 1H), 3.95 (m, 1H), 2.70 – 2.60 (m, 2H), 2.52 (dd, *J* = 14.2, 1.9 Hz, 1H), 2.42 – 2.33 (m, 3H), 1.71 – 1.59 (m, 1H), 1.56 – 1.46 (m, 1H), 1.31 – 1.25 (m, 12H), 0.88 (t, *J* = 6.7 Hz, 3H); ¹³C NMR (101 MHz, CDCl₃) δ 205.4, 139.7, 139.5, 128.7, 128.5, 125.51, 123.2, 98.8, 68.7, 59.7, 52.1, 41.3, 35.5, 32.7, 32.1, 29.8, 29.8, 29.5, 25.9, 22.9, 14.3; mp: 97.5–99.5 °C; IR (thin film) 2925, 2850, 1716, 1467, 1314, 1247, 1158, 1059, 1011, 954, 873 cm⁻¹; HRMS (EI) calcd for C₂₃H₃₃O₃ [M+H]⁺: 357.2424, found: 357.2434;



(2*S*,6*S*)-2-((Benzyloxy)methyl)-4-methyl-10-methylene-1,7-dioxaspiro[5.5]undec-4-ene (2.108)

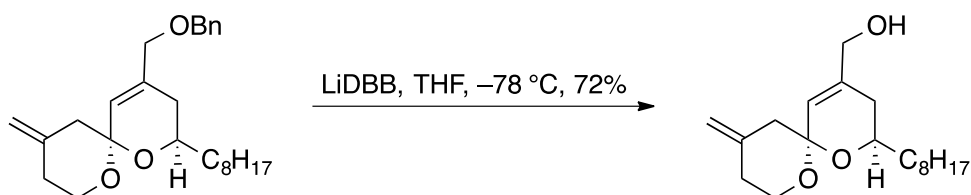
The general cyclization procedure was followed with **2.73** (64 mg, 0.28 mmol), **2.85** (50 mg, 0.21 mmol), TMSOTf (3 mol%, 65 μL, 6.4 μmol), NaHCO₃ (sat) (15 μL, 0.013 mmol), 4Å MS (25 mg), dichloromethane (2.2 mL), and DDQ (195 mg, 0.85 mmol). The oxidation proceeded for 2 h. The crude mixture was purified by flash chromatography (10% EtOAc in hexane) to give the desired product (42 mg, 65%) as a colorless oil. ¹H NMR (500 MHz, CDCl₃) δ 7.37 – 7.32 (m, 4H), 7.29 – 7.27 (m, 1H), 5.44 (s, 1H), 4.84 (s, 1H), 4.79 (s, 1H), 4.63 (s, 2H), 4.16 – 4.10 (m, 1H), 3.88 (ddd, *J* = 12.3, 10.7, 3.0 Hz, 1H), 3.72 (ddd, *J* = 10.7, 5.9, 1.6 Hz, 1H), 3.57 (m, 2H), 2.39 – 2.30 (m, 3H), 2.20 – 2.15 (m, 1H), 2.05 – 1.98 (m, 1H), 1.82 (dd, *J* = 17.2, 3.6 Hz, 1H), 1.74 (s, 3H); ¹³C NMR (101 MHz, CDCl₃) δ 141.7, 138.8, 136.8, 128.5, 127.7, 127.6, 123.9, 110.3, 95.8, 73.5, 72.6, 67.6, 61.5, 44.5, 34.1, 32.0, 23.0; IR (thin

film) 3070, 3030, 2915, 1680, 1658, 1452, 1379, 1254, 1233, 1173, 1123, 1100, 1017, 987, 889, 855, 737, 698 cm^{-1} ; HRMS (ASAP) calcd for $\text{C}_{19}\text{H}_{25}\text{O}_3$ $[\text{M}+\text{H}]^+$: 301.1804, found: 301.1792.

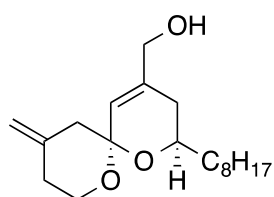


(6*S*,8*S*)-10-methyl-4-methylene-8-phenyl-1-oxa-7-thiaspiro[5.5]undec-10-ene (2.109)

The general cyclization procedure was followed with **2.73** (51 mg, 0.23 mmol), **2.88** (40 mg, 0.19 mmol), TMSOTf (2 mol%, 40 μL , 4.0 μmol), NaHCO_3 (sat) (80 μL , 0.08 mmol), 4 \AA MS (120 mg), dichloromethane (2.0 mL), and DDQ (44 mg, 0.19 mmol). The oxidation proceeded at rt for 15 min. The crude mixture was purified by flash chromatography (5% EtOAc in hexane) to give the desired product (33 mg, 63%) as a pale yellow oil. ^1H NMR (601 MHz, CDCl_3) δ 7.38 (broad app d, 2H), 7.34 (broad app t, 2H), 7.29 – 7.26 (m, 1H), 5.65 (s, 1H), 4.84 (s, 1H), 4.81 (s, 1H), 4.23 (td, $J = 11.8, 3.1$ Hz, 1H), 4.15 (dd, $J = 12.2, 3.8$ Hz, 1H), 3.87 (dd, $J = 11.1, 6.0$ Hz, 1H), 2.62 – 2.52 (m, 3H), 2.45 (dd, $J = 17.7, 3.7$ Hz, 1H), 2.36 (td, $J = 12.9, 5.8$ Hz, 1H), 2.20 (dd, $J = 13.6, 2.7$ Hz, 1H), 1.86 (s, 3H); ^{13}C NMR (151 MHz, CDCl_3) δ 141.5, 140.9, 139.4, 128.8, 127.8, 127.6, 126.2, 111.0, 85.0, 62.8, 47.3, 41.4, 39.6, 34.4, 24.7; IR (thin film) 3027, 2948, 2913, 2881, 1656, 1494, 1452, 1376, 1252, 1044, 1009, 980, 1009, 980, 897, 809, 787, 766, 744, 698, 638 cm^{-1} ; HRMS (ASAP) calcd for $\text{C}_{17}\text{H}_{21}\text{OS}$ $[\text{M}+\text{H}]^+$: 273.1313, found: 273.1322.



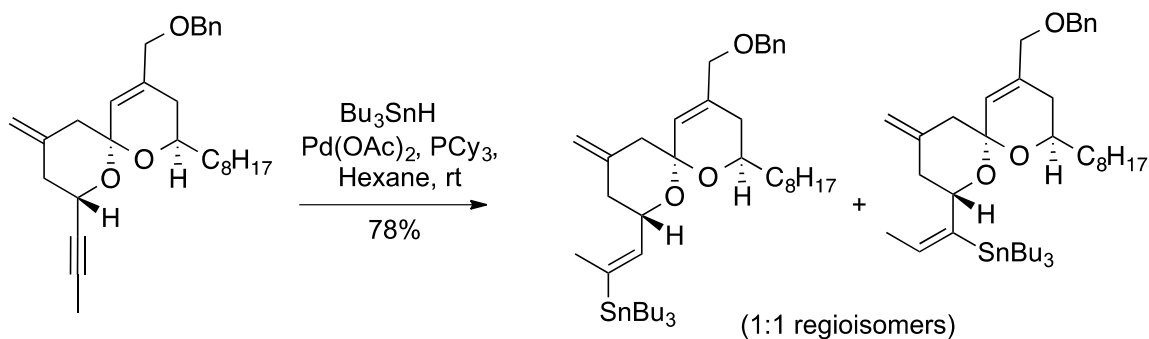
Preparation of an LiDBB (0.4M) solution: A 25 mL 2-neck RBF was charged with 4,4'-di-*tert*-butylbiphenyl (DBB) (374 mg, 1.36 mmol) and THF (3.4 mL). To the stirring solution was added (0.5 mg) of 1,10-phenanthroline. The mixture was cooled to 0 °C, then *n*-BuLi was added until a red coloration persisted. Active lithium wire (113 mg, 16.3 mmol) was prepared by filing away the surface lithium oxide layer under oil followed by rinsing with pentane, and drying with a paper towel. The active wire was quickly added into the solution under Ar. The mixture was stirred at 0 °C for 3 h to obtain a solution of LiDBB (~0.4M).



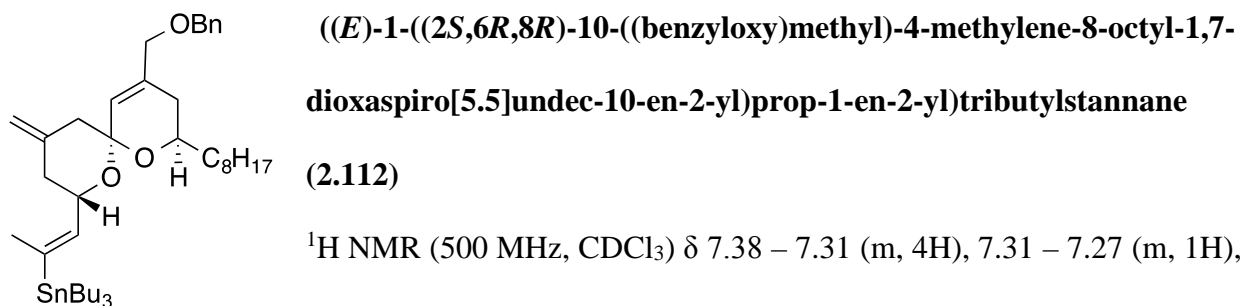
((2*R*,6*S*)-10-Methylene-2-octyl-1,7-dioxaspiro[5.5]undec-4-en-4-yl)methanol (2.110)

Spiroketal **2.103** (14 mg, 0.04 mmol) was dissolved in THF (600 μ L). The reaction mixture was cooled to -78 °C and the LiDBB (0.4M) solution was added dropwise until the green color persisted for >5 min. The mixture was quenched with (500 μ L) of NH_4Cl , then the organic layer extracted with EtOAc (2 x 5 mL) and dried with Na_2SO_4 . The crude mixture was purified by flash chromatography (35% EtOAc in hexane) to give the desired product (7.8 mg, 72%) as a colorless oil. ^1H NMR (601 MHz, CDCl_3) δ 5.66 (s, 1H), 4.81 (s, 1H), 4.77 (s, 1H), 4.07 (ABq, 2H, $\Delta\delta_{\text{AB}} = 0.03$, $J_{\text{AB}} = 14.0$ Hz), 3.86 – 3.78 (m, 2H), 3.72 (dd, $J = 10.8, 5.8$ Hz, 1H), 2.33 – 2.38 (m, 1H), 2.33 (ABq, 2H, $\Delta\delta_{\text{AB}} = 0.05$, $J_{\text{AB}} = 13.5$ Hz), 2.18 (d, $J = 13.6$ Hz, 1H), 1.94 (dd, $J = 17.1, 3.8$ Hz, 1H), 1.88 (dd, $J = 17.3, 10.5$ Hz, 1H), 1.64 – 1.56 (m, 1H), 1.52 – 1.44 (m, 3H), 1.34 – 1.21 (m, 12H), 0.88 (t, $J = 6.9$ Hz, 3H); ^{13}C NMR (126 MHz, CDCl_3) δ 141.4, 140.7, 123.8, 110.6, 95.7, 67.9, 66.0, 61.6, 44.6, 35.7, 34.2, 32.2, 31.4, 29.9, 29.9, 30.0, 26.0, 23.0, 14.4; IR (thin film, neat) 3380, 2926, 2855, 1688, 1659, 1462, 1370, 1333,

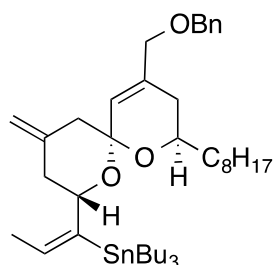
1254, 1235, 1177, 1107, 1068, 1016, 986, 887, 856 cm^{-1} ; HRMS (ASAP) calcd for $\text{C}_{19}\text{H}_{34}\text{O}_3$
 $[\text{M}+\text{H}]^+$: 309.2430, found: 309.2423.



Procedure for Pd-catalyzed hydrostannylation: To an oven dried vial fitted with a rubber septum was charged $\text{Pd}(\text{OAc})_2$ (1 mg, 4 μmol), tricyclohexylphosphine (2.5 mg, 9 μmol) and hexane (130 μL). The orange suspension was heated to 50 $^\circ\text{C}$ for 5 min to give a clear orange solution and subsequently cooled to rt. Alkyne spiroketal **2.104** (9 mg, 0.02 mmol) dissolved in (70 μL) of hexane was added dropwise followed dropwise addition of tributyltin hydride (25 μL , 0.08 mmol) over 5 min. The reaction was stirred at rt for 2 h and filtered through celite and concentrated. The crude mixture was purified by flash chromatography (10% ether in pentane) to give the distal *cis*-vinyl stannane **2.112** (5.8 mg) and proximal *cis*-vinyl stannane **2.113** (5.7 mg) regioisomers with a combined yield of (11.5 mg, 78%).

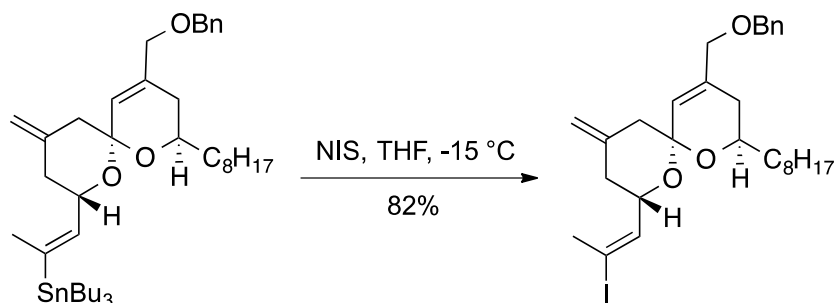


5.71 (t, $J = 1.6$ Hz, 1H), 5.57 (dq, $J = 7.9, 1.8$ Hz, 1H), 4.85 (s, 1H), 4.74 (ddd, $J = 11.1, 7.8, 2.9$ Hz, 1H), 4.48 (ABq, 2H, $\Delta\delta_{AB} = 0.02$, $J_{AB} = 11.9$ Hz), 3.95 (ABq, 2H, $\Delta\delta_{AB} = 0.02$, $J_{AB} = 12.6$ Hz), 3.90 – 3.84 (m, 1H), 2.42 – 2.27 (m, 3H), 2.19 (ddd, $J = 13.4, 2.9, 1.4$ Hz, 1H), 2.10 – 2.05 (m, 1H), 1.95 – 1.91 (m, 3H), 1.90 (d, $J = 1.8$ Hz, 3H), 1.58 – 1.41 (m, 12H), 1.37 – 1.21 (m, 20H), 0.92 – 0.84 (m, 12H). ^{13}C NMR (101 MHz, CDCl_3) δ 142.0, 141.6, 140.9, 138.4, 137.6, 128.6, 127.9, 127.8, 126.0, 110.3, 96.1, 73.2, 72.4, 68.0, 66.9, 44.0, 40.0, 35.8, 32.1, 31.8, 30.0, 29.8, 29.5, 29.4, 27.6, 26.2, 22.9, 19.9, 14.3, 13.9, 9.3; $[\alpha]_{\text{D}}^{20}$ -12.4 (c 0.3, CHCl_3); IR (thin film, neat) 2956, 2925, 2854, 1738, 1656, 1456, 1377, 1261, 1168, 1095, 1039, 989, 885, 802, 735, 697 cm^{-1} ; HRMS (APCI) calcd for $\text{C}_{41}\text{H}_{69}\text{O}_3\text{Sn}$ $[\text{M}+\text{H}]^+$: 729.4269, found: 729.4288.

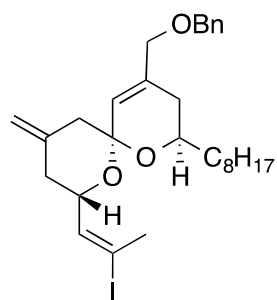


((E)-1-((2S,6R,8R)-10-((benzyloxy)methyl)-4-methylene-8-octyl-1,7-dioxaspiro[5.5]undec-10-en-2-yl)prop-1-en-1-yl)tributylstannane
(2.113)

^1H NMR (500 MHz, CDCl_3) δ 7.30 – 7.25 (m, 4H), 7.24 – 7.20 (m, 1H), 5.52 (m, 1H), 4.75 (s, 1H), 4.72 (s, 1H), 4.70 (dt, $J = 12.2, 2.5$ Hz, 1H), 4.41 (ABq, 2H, $\Delta\delta_{AB} = 0.02$, $J_{AB} = 11.9$ Hz), 3.87 (s, 2H), 3.75 (qd, $J = 7.5, 3.8$ Hz, 1H), 2.23 (s, 2H), 2.19 – 2.10 (m, 1H), 1.84 (d, $J = 7.1$ Hz, 3H), 1.67 – 1.58 (m, 3H), 1.45 – 1.32 (m, 6H), 1.27 – 1.16 (m, 26H), 0.86 – 0.74 (m, 12H). ^{13}C NMR (151 MHz, CDCl_3) δ 149.0, 141.7, 138.5, 137.0, 132.7, 128.6, 127.8, 126.4, 110.3, 96.0, 73.0, 72.3, 71.9, 67.7, 44.0, 39.2, 35.6, 32.1, 31.9, 30.0, 29.8, 29.5, 27.8, 26.2, 22.9, 15.9, 14.3, 14.0, 10.9; $[\alpha]_{\text{D}}^{20}$ +1.6 (c 0.3, CHCl_3); IR (thin film, neat) 2955, 2925, 2854, 1656, 1456, 1376, 1260, 1095, 1026, 987, 886, 802, 697 cm^{-1} . HRMS (APCI) calcd for $\text{C}_{41}\text{H}_{69}\text{O}_3\text{Sn}$ $[\text{M}+\text{H}]^+$: 729.4269, found: 729.4297.



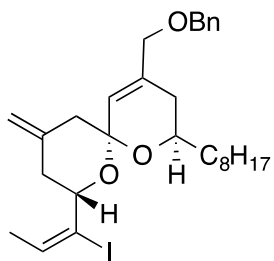
General procedure for tin-iodide exchange: To an oven dried vial charged with distal vinyl stannane **2.112** (5 mg, 7 μmol) was added THF (500 μL) followed by cooling to -15°C . N-iodosuccinimide (NIS) (2.5 mg, 0.01 mmol) dissolved in (100 μL) of THF was added drop-wise over 5 min. The reaction was stirred at -15°C for 10 min followed by warming up to rt and stirring for an additional 30 min. Upon completion of reaction, the mixture was quenched with a sat. solution of $\text{Na}_2\text{S}_2\text{O}_3$ (100 μL) and sat. NaHCO_3 (100 μL), extracted with (3 x 5mL) of EtOAc and the combined organic layer dried with Na_2SO_4 . The crude mixture was purified by flash chromatography (10% ether in pentane) to give the desired distal vinyl iodide (3.2 mg, 82%).



(2R,6R,8S)-4-((benzyloxy)methyl)-8-((E)-2-iodoprop-1-en-1-yl)-10-methylene-2-octyl-1,7-dioxaspiro[5.5]undec-4-ene

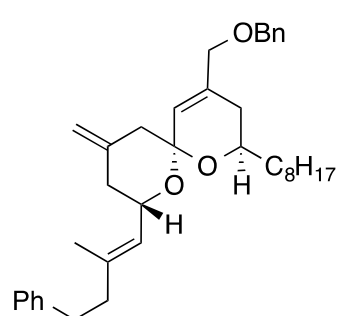
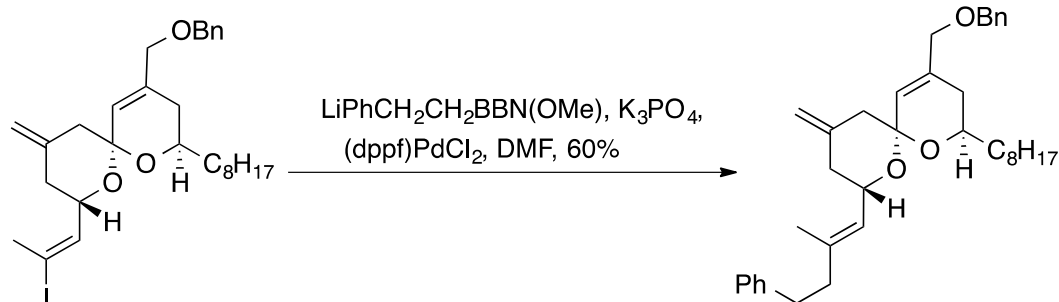
^1H NMR (601 MHz, CDCl_3) δ 7.37 – 7.31 (m, 4H), 7.31 – 7.27 (m, 1H), 6.22 (dq, $J = 8.7, 1.5$ Hz, 1H), 5.67 (s, 1H), 4.84 (s, 1H), 4.81 (s, 1H), 4.52 – 4.49 (m, 1H), 4.49 (ABq, 2H, $\Delta\delta_{\text{AB}} = 0.01$, $J_{\text{AB}} = 11.9$ Hz), 3.94 (s, 2H), 3.85 – 3.80 (m, 1H), 2.46 (d, $J = 1.5$ Hz, 3H), 2.33 – 2.29 (m, 2H), 2.23 (dd, $J = 3.0, 1.2$ Hz, 1H), 2.21 (dd, $J = 2.9, 1.2$ Hz, 1H), 1.94 – 1.91 (m, 2H), 1.37 – 1.23 (m, 14H), 0.88 (t, $J = 7.0$ Hz, 3H). ^{13}C NMR (151 MHz, CDCl_3) δ 141.6, 140.4, 138.4, 138.0, 128.6, 127.9, 127.9, 125.3, 111.2, 99.0, 96.2, 73.0, 72.5, 68.6, 68.3, 43.9, 39.4, 35.7, 32.1, 31.7, 29.9, 29.8, 29.5, 28.6, 26.3,

22.9, 14.3. $[\alpha]_D^{20}$ -24.40 (c 0.4, CHCl₃); IR (thin film, neat) 2925, 2854, 1736, 1656, 1456, 1378, 1260, 1168, 1120, 1045, 986, 888, 803, 735, 698 cm⁻¹. HRMS (APCI) calcd for C₂₉H₄₂O₃I [M+H]⁺: 565.2179, found: 565.2200.



(2*R*,6*R*,8*S*)-4-((benzyloxy)methyl)-8-((*E*)-1-iodoprop-1-en-1-yl)-10-methylene-2-octyl-1,7-dioxaspiro[5.5]undec-4-ene. The iodination procedure was followed with **2.113** (5 mg, 7 μmol), NIS (2.5 mg, 0.01 mmol), THF (600 μL). The crude mixture was purified by flash

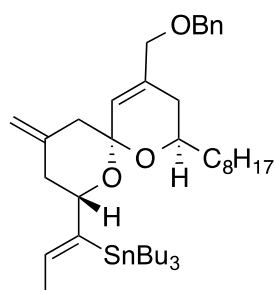
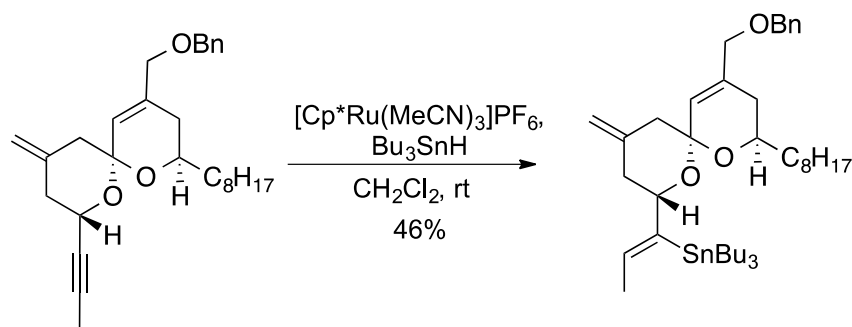
chromatography (10 % ether in pentane) to give the desired product (3.4 mg, 88%). ¹H NMR (601 MHz, CDCl₃) δ 7.36 – 7.33 (m, 4H), 7.30 – 7.27 (m, 1H), 6.41 (q, *J* = 7.1 Hz, 1H), 5.70 (s, 1H), 4.85 (s, 1H), 4.82 (s, 1H), 4.49 (ABq, 2H, Δδ_{AB} = 0.01, *J*_{AB} = 11.9 Hz), 4.08 (dd, *J* = 11.2, 2.9 Hz, 1H), 3.94 (s, broad, 2H), 3.86 – 3.81 (m, 1H), 2.41 – 2.35 (m, 1H), 2.33 (dd, *J* = 3.6, 1.9 Hz, 1H), 2.30 – 2.27 (m, 1H), 2.10 (ddd, *J* = 13.4, 2.9, 1.5 Hz, 1H), 1.93 – 1.90 (m, 2H), 1.76 (d, *J* = 7.2 Hz, 3H), 1.29 – 1.22 (m, 14H), 0.89 – 0.87 (m, 3H). ¹³C NMR (151 MHz, CDCl₃) δ 140.2, 138.3, 138.1, 137.5, 128.6, 128.0, 127.9, 125.7, 111.3, 107.2, 96.3, 73.0, 72.4, 68.6, 68.3, 43.9, 40.3, 35.8, 32.1, 31.7, 30.5, 29.9, 29.8, 29.5, 26.3, 22.9, 14.3. $[\alpha]_D^{20}$ -5.9 (c 0.3, CHCl₃); IR (thin film, neat) 2925, 2854, 1737, 1456, 1377, 1259, 1165, 1022, 985, 888, 800, 734, 697 cm⁻¹. HRMS (ESIP) calcd for C₂₉H₄₂O₃I [M+H]⁺: 565.2173, found: 565.21769.



(2*R*,6*R*,8*S*)-4-((benzyloxy)methyl)-8-((*E*)-2-methyl-4-phenylbut-1-en-1-yl)-10-methylene-2-octyl-1,7-dioxaspiro[5.5]undec-4-ene
(2.114)

Suzuki coupling: To a solution of (2-iodoethyl) benzene (4 μ L, 0.02 mmol) in diethyl ether (400 μ L) at -78 $^{\circ}$ C was added *t*-BuLi (1.7 M, 35 μ L, 0.05 mmol). After 5 min, 9-BBN-OMe (65 μ L, 0.065 mmol) was added dropwise followed by THF (400 μ L). The mixture was allowed to warm up to rt over 1.5 h. A solution of $\text{K}_3\text{PO}_4 \cdot \text{H}_2\text{O}$ (3M, 22 μ L, 0.06 mmol) was added followed by the spiroketal vinyl iodide (4.5 mg, 8 μ mol), dissolved in DMF (400 μ L). $\text{PdCl}_2(\text{dppf})$ (3 mg, 3.68 μ mol) was added in one portion and the mixture was allowed to stir at rt for 18 h. The mixture was quenched with NH_4Cl (100 μ L), then the organic layer was extracted with EtOAc (2 x 5 mL) and dried with Na_2SO_4 . The crude mixture was purified by flash chromatography (5% EtOAc in hexane) to give the desired product (2.7 mg, 60%) as a colorless oil. ^1H NMR (601 MHz, CDCl_3) δ 7.36 – 7.31 (m, 4H), 7.28 (dd, $J = 7.2, 5.5$ Hz, 3H), 7.17 (dd, $J = 11.5, 7.4$ Hz, 3H), 5.69 (s, 1H), 5.23 (d, $J = 8.6$ Hz, 1H), 4.82 (s, 1H), 4.79 (s, 1H), 4.56 (ddd, $J = 11.4, 8.6, 2.8$ Hz, 1H), 4.48 (ABq, 2H, $\Delta\delta_{\text{AB}} = 0.02$, $J_{\text{AB}} = 11.9$ Hz), 3.94 (ABq, 2H, $\Delta\delta_{\text{AB}} = 0.01$, $J_{\text{AB}} = 13.3$ Hz), 3.90 – 3.85 (m, 1H), 2.79 – 2.68 (m, 2H), 2.30 (m, 3H), 2.15 (dd, $J = 13.5, 2.7$ Hz, 1H), 2.04 (t, $J = 12.6$ Hz, 2H), 1.93 (d, $J = 6.6$ Hz, 2H), 1.73 (s, 3H), 1.33 – 1.24 (m, 14H), 0.88 (t, $J = 6.9$ Hz, 3H); ^{13}C NMR (151 MHz,

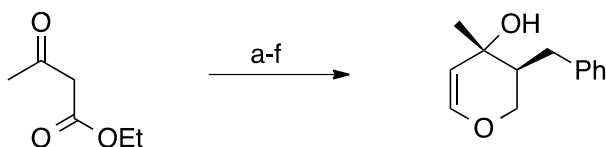
CDCl₃) δ 142.4, 141.5, 138.8, 138.4, 137.5, 128.6, 128.5, 127.9, 127.8, 126.0, 126.0, 125.9, 110.4, 95.9, 73.2, 72.4, 68.1, 67.9, 44.0, 41.7, 40.1, 35.8, 34.5, 32.1, 31.8, 30.0, 29.9, 29.8, 29.5, 26.3, 22.9, 17.1, 14.3; $[\alpha]_D^{20}$ -7.0 (c 0.3, CHCl₃); IR (thin film, neat) 2925, 2854, 1739, 1657, 1455, 1380, 1261, 1153, 1096, 1041, 987, 884, 802, 744, 698 cm⁻¹; HRMS (ESIP) calcd for C₃₇H₅₁O₃ [M+H]⁺: 543.3833, found: 543.3842.



((Z)-1-((2S,6R,8R)-10-((benzyloxy)methyl)-4-methylene-8-octyl-1,7-dioxaspiro[5.5]undec-10-en-2-yl)prop-1-en-1-yl)tributylstannane
(2.115)

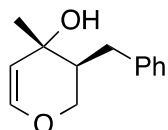
To an oven dried vial charged with alkyne spiroketal **2.104** (6.6 mg, 0.02 mmol) was added CH₂Cl₂ (500 μ L) followed by [Cp*Ru(MeCN)₃]PF₆ (1 mg, 2 μ mol) under Ar. Tributyltin hydride (5 μ L, 0.02 mmol) was added dropwise over 2 min. The reaction was stirred at rt for 1 h and filtered through celite and concentrated. The crude mixture was purified by flash chromatography (10% ether in pentane) to give the product (5.3 mg, 55%) as a colorless oil. ¹H NMR (400 MHz, CDCl₃) δ 7.37 – 7.34 (m, 3H), 7.33 (m, 2H), 6.26 (q, *J* = 6.5 Hz, 1H), 5.62 (s, 1H), 4.80 (s, 1H), 4.78 (s, 1H), 4.47 (ABq, 2H, $\Delta\delta_{AB}$ = 0.01, *J*_{AB} = 12.0 Hz), 4.27 (dd, *J* = 11.5, 2.8 Hz, 1H), 3.93 (s, broad, 1H), 3.85 – 3.77 (m, 1H), 2.28 (s, broad, 2H), 2.13 (dd, *J* = 13.3, 3.0

Hz, 1H), 2.00 (t, $J = 12.2$ Hz, 1H), 1.92 – 1.86 (m, 2H), 1.72 (d, $J = 6.4$ Hz, 3H), 1.53 – 1.41 (m, 6H), 1.36 – 1.24 (m, 26H), 0.90 – 0.84 (m, 12H). ^{13}C NMR (126 MHz, CDCl_3) δ 147.3, 141.9, 138.5, 136.8, 134.7, 128.6, 127.9, 127.8, 126.6, 110.2, 95.8, 78.5, 73.0, 71.9, 67.4, 43.8, 41.7, 35.6, 32.2, 31.9, 29.9, 29.8, 29.6, 29.4, 27.6, 26.0, 22.9, 19.3, 14.3, 14.0, 11.7. $[\alpha]_{\text{D}}^{20}$ -11.9 (c 0.3, CHCl_3); IR (thin film, neat) 2955, 2925, 2854, 1723, 1456, 1376, 1261, 1149, 1112, 1072, 1032, 988, 887, 734, 696 cm^{-1} . HRMS (ESIP) calcd for $\text{C}_{41}\text{H}_{69}\text{O}_3\text{Sn}$ $[\text{M}+\text{H}]^+$: 729.4263, found: 729.4280.



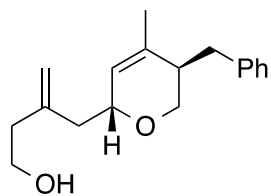
Reagents and conditions

a) KO^tBu , BnBr , THF, 70 $^\circ\text{C}$, 75%. b) Ethylene glycol, CSA, PhMe , 110 $^\circ\text{C}$, 83%. c) LiAlH_4 , Et_2O , 0 $^\circ\text{C}$, 88%. d) Oxalic acid, SiO_2 , CH_2Cl_2 , 85%. e) $(\text{EtO})_3\text{CH}$, SnCl_4 , CH_2Cl_2 , -40 $^\circ\text{C}$, 43%. f) MeLi , THF, -78 $^\circ\text{C}$, 82%.



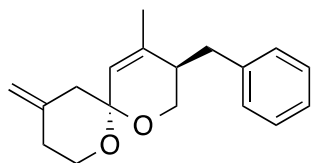
(3R,4R)-3-Benzyl-4-methyl-3,4-dihydro-2H-pyran-4-ol (2.116)

^1H NMR (500 MHz, CDCl_3) δ 7.34 – 7.28 (m, 3H), 7.24 – 7.16 (m, 2H), 6.37 (d, $J = 6.0$ Hz, 1H), 4.82 (d, $J = 6.0$ Hz, 1H), 3.85 (dt, $J = 10.9, 3.6$ Hz, 1H), 3.64 (appt, $J = 11.2$ Hz, 1H), 3.04 (dd, $J = 14.2, 3.6$ Hz, 1H), 2.40 (dd, $J = 14.3, 11.0$ Hz, 1H), 1.97 (tt, $J = 11.2, 3.6$ Hz, 1H), 1.40 (s, 3H); ^{13}C NMR (126 MHz, CDCl_3) δ 145.6, 140.4, 129.3, 128.8, 126.5, 109.0, 66.1, 65.6, 45.8, 31.9, 27.8. IR (thin film) 3434, 2925, 1733, 1642, 1495, 1455, 1379, 1243, 1136, 1064, 965, 742, 700 cm^{-1} ; HRMS (ASAP) calcd for $\text{C}_{13}\text{H}_{15}\text{O}$ $[\text{M}-\text{OH}]^+$: 187.1123, found: 187.1124.



3-(((2*R*,5*R*)-5-benzyl-4-methyl-5,6-dihydro-2*H*-pyran-2-yl)methyl)but-3-en-1-ol (2.117)

^1H NMR (601 MHz, CDCl_3) δ 7.33 – 7.27 (m, 2H), 7.23 – 7.16 (m, 3H), 5.43 (s, 1H), 4.98 (s, 2H), 4.30 – 4.25 (m, 1H), 3.77 – 3.70 (m, 2H), 3.66 (dd, $J = 11.4, 4.3$ Hz, 1H), 3.40 (dd, $J = 11.4, 5.8$ Hz, 1H), 3.02 (dd, $J = 13.6, 4.2$ Hz, 1H), , 2.46 (dd, $J = 13.6, 10.8$ Hz, 1H), 2.36 (dt, $J = 9.7, 6.3$ Hz, 2H), 2.31 (dd, $J = 14.3, 9.2$ Hz, 2H), 2.20 (dd, $J = 14.4, 4.8$ Hz, 1H), 1.81 (s, 3H). ^{13}C NMR (151 MHz, CDCl_3) δ 143.4, 140.3, 136.1, 129.2, 128.6, 126.3, 124.7, 114.8, 73.0, 65.4, 60.7, 41.1, 40.5, 39.7, 36.6, 21.5. IR (thin film, neat) 3411, 2929, 1645, 1495, 1454, 1380, 1126, 1047, 895, 700 cm^{-1} ; HRMS (ASAP) calcd for $\text{C}_{18}\text{H}_{25}\text{O}_2$ $[\text{M}+\text{H}]^+$: 273.1855, found: 273.1856.



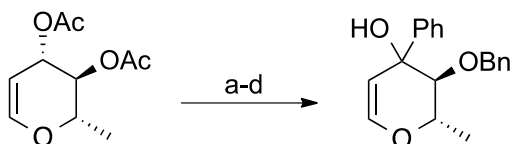
(3*S*,6*R*)-3-Benzyl-4-methyl-10-methylene-1,7-dioxaspiro[5.5]undec-4-ene (2.120)

The general cyclization procedure was followed with **2.73** (44 mg, 0.19 mmol), **2.116** (30 mg, 0.15 mmol), TMSOTf (2 mol%, 30 μL , 3.0 μmol), NaHCO_3 (sat) (60 μL , 0.06 mmol), 4Å MS (90 mg), dichloromethane (0.9 mL), and DDQ (200 mg, 0.88 mmol). The oxidation proceeded at rt for 2 h. The crude mixture was purified by flash chromatography (25% EtOAc in hexane) to give the desired product (24 mg, 61%) as a 10:1 mixture of diastereomers. Major diastereomer: ^1H NMR (500 MHz, CDCl_3) δ 7.33 – 7.28 (m, 2H), 7.26 – 7.22 (m, 3H), 5.45 (s, 1H), 4.89 (s, 1H), 4.82 (s, 1H), 3.81 (m, 2H), 3.76 (m, 1H), 3.60 (d, $J = 11.3$ Hz, 1H), 2.86 (dd, $J = 13.6, 4.0$ Hz, 1H), 2.71 (dd, $J = 13.6, 10.1$ Hz, 1H), 2.38 – 2.32 (m, 2H), 2.24 (m, 1H), 2.22 – 2.17 (m, 1H), 1.95 (dt, $J = 10.0, 3.6$ Hz, 1H), 1.83 (s, 3H); ^{13}C NMR (101 MHz, CDCl_3) δ 141.8, 140.8, 140.3, 129.6, 128.6, 126.3, 124.7, 110.7, 95.1, 61.6, 61.1, 44.6, 41.3,

36.8, 34.1, 22.0; IR (thin film) 3026, 2927, 1657, 1495, 1454, 1379, 1252, 1172, 1120, 1070, 1051, 1015, 986, 872, 740, 700 cm^{-1} ; HRMS (ASAP) calcd for $\text{C}_{18}\text{H}_{23}\text{O}_2$ $[\text{M}+\text{H}]^+$: 271.1698, found: 271.1689.

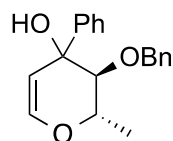
General protocol for Ferrier reaction of 5', 6'-disubstitued pyranol

To a oven dried flask charged with the tertiary pyranol (1 equiv) and allyl silane (1.35 equiv) was added CH_2Cl_2 (~0.10 M) followed by cooling to -78°C . Neat TMSOTf (1.2 equiv) was added the reaction was stirred at that temperature for 1h. The reaction was quenched at that temperature with a saturated aqueous solution of NaHCO_3 (1.2 equiv) and allowed to warm up to rt. After concentration under vacuum, the reaction was purified by flash column chromatography to give the desired product.



Reagents and conditions

a) K_2CO_3 , MeOH, rt, 95%. b) PDC, AcOH, EtOAc, rt, 62%.
c) BnBr, Ag_2O , CH_2Cl_2 , 78%. d) PhLi, THF, -78°C , 72%.

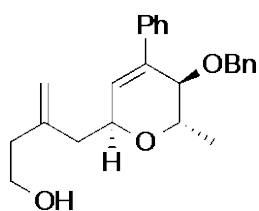


(2*S*,3*S*)-3-(benzyloxy)-2-methyl-4-phenyl-3,4-dihydro-2*H*-pyran-4-ol (2.121)

Formed as a (~1:1) mixture of diastereomers: ^1H NMR (500 MHz, CDCl_3) δ 7.54 (d, $J = 7.4$ Hz, 2H), 7.44 (d, $J = 7.8$ Hz, 2H), 7.35 – 7.25 (m, 14H), 6.95 (dd, $J = 6.5, 2.9$ Hz, 2H), 6.45 (d, $J = 5.9$ Hz, 1H), 6.43 (d, $J = 6.1$ Hz, 1H), 4.91 (d, $J = 11.6$ Hz, 1H), 4.78 (d, $J = 5.9$ Hz, 1H), 4.69 (d, $J = 11.6$ Hz, 1H), 4.63 (d, $J = 6.1$ Hz, 1H), 4.12 (dq, $J = 10.2, 6.3$ Hz, 1H), 4.07

– 4.05 (m, 1H), 3.84 (d, $J = 10.6$ Hz, 1H), 3.80 (dq, $J = 10.1, 6.4$ Hz, 1H), 3.60 (d, $J = 10.0$ Hz, 1H), 3.53 (d, $J = 10.1$ Hz, 1H), 1.29 (d, $J = 6.3$ Hz, 3H), 1.16 (d, $J = 6.4$ Hz, 3H); ^{13}C NMR (126 MHz, CDCl_3) δ 146.1, 146.0, 144.1, 142.8, 138.3, 137.1, 128.6, 128.6, 128.5, 128.5, 128.3, 127.9, 127.8, 127.7, 127.4, 106.7, 106.2, 85.2, 83.9, 76.7, 75.3, 75.1, 72.9, 71.5, 71.0, 18.0, 17.8; $[\alpha]_{\text{D}}^{20}$ -111.2 (c 2.5, CHCl_3); IR (thin film, neat) 3462, 3061, 3030, 2974, 2932, 1648, 1494, 1450, 1239, 1099, 1030, 984, 700, 623 cm^{-1} ; HRMS (ESIP) calcd for $\text{C}_{19}\text{H}_{19}\text{O}_2$ $[\text{M}-\text{OH}]^+$: 271.1380, found: 271.1376.

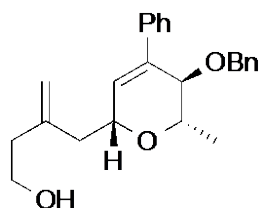
Ferrier coupling (5'-OBn pyranol): The general Ferrier reaction procedure for 5'-OBn pyranol was followed with pyranol **2.121** (32 mg, 0.11 mmol), silane **2.73** (36 mg, 0.15 mmol), TMSOTf (25 μL , 0.12 mmol), NaHCO_3 (sat) (130 μL , 0.14 mmol). The crude mixture was purified by flash chromatography (15% EtOAc in hexane) to give a mixture of **2.122** and **2.123** (26 mg, 64%) in 5.9:1 dr ratio.



3-(((2S,5R,6S)-5-(benzyloxy)-6-methyl-4-phenyl-5,6-dihydro-2H-pyran-2-yl)methyl)but-3-en-1-ol (2.122)

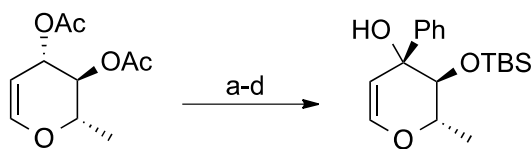
Major diastereomer: ^1H NMR (500 MHz, CDCl_3) δ 7.43 – 7.40 (m, 2H), 7.36 – 7.31 (m, 2H), 7.31 – 7.27 (m, 1H), 7.27 – 7.24 (m, 3H), 7.16 (dd, $J = 7.4, 2.0$ Hz, 2H), 6.20 (d, $J = 2.1$ Hz, 1H), 5.06 (s, 1H), 5.04 (s, 1H), 4.49 (ddt, $J = 7.7, 5.5, 2.0$ Hz, 1H), 4.55 (ABq, 2H, $\Delta\delta_{\text{AB}} = 0.023$, $J_{\text{AB}} = 11.4$ Hz), 4.43 (qd, $J = 6.8, 2.3$ Hz, 1H), 4.12 (t, $J = 2.1$ Hz, 1H), 3.82 – 3.74 (m, 2H), 2.53 – 2.44 (m, 2H), 2.42 (t, $J = 6.2$ Hz, 2H), 1.30 (d, $J = 6.8$ Hz, 3H); ^{13}C NMR (126 MHz, CDCl_3) δ 142.9, 139.5, 138.4, 134.0, 130.1, 128.6, 128.5, 128.3, 127.8, 127.8, 126.2, 115.1, 74.7, 70.7, 70.2, 68.4, 60.7, 41.1, 39.8, 16.6; $[\alpha]_{\text{D}}^{20}$ -64.6 (c 2.1, CHCl_3); IR (thin

film, neat) 3435, 3030, 2931, 1644, 1496, 1453, 1377, 1152, 1064, 897, 763, 698 cm^{-1} ; HRMS (ESIP) calcd for $\text{C}_{24}\text{H}_{29}\text{O}_3$ $[\text{M}+\text{H}]^+$: 365.2111, found: 365.2099.



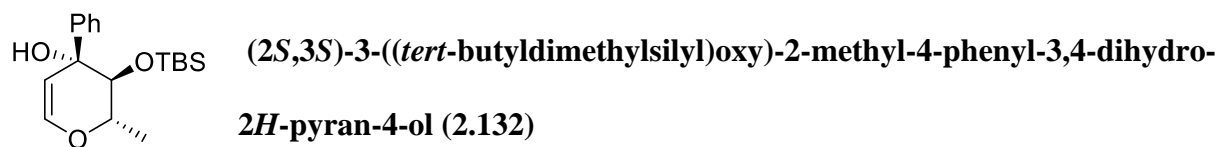
3-(((2R,5R,6S)-5-(benzyloxy)-6-methyl-4-phenyl-5,6-dihydro-2H-pyran-2-yl)methyl)but-3-en-1-ol (2.123)

Minor diastereomer: ^1H NMR (500 MHz, CDCl_3) δ 7.44 – 7.41 (m, 2H), 7.38 – 7.33 (m, 2H), 7.33 – 7.30 (m, 1H), 7.19 – 7.17 (m, 3H), 6.86 (dd, $J = 6.4, 3.0$ Hz, 2H), 5.99 (t, $J = 1.4$ Hz, 1H), 5.01 (d, $J = 3.3$ Hz, 2H), 4.44 (td, $J = 6.4, 3.3$ Hz, 1H), 4.41 – 4.39 (m, 1H), 4.28 (ABq, 2H, $\Delta\delta_{\text{AB}} = 0.03$, $J_{\text{AB}} = 10.4$ Hz), 3.88 (dq, $J = 8.3, 6.2$ Hz, 1H), 3.81 – 3.71 (m, 2H), 2.45 – 2.32 (m, 4H), 1.44 (d, $J = 6.2$ Hz, 3H); ^{13}C NMR (126 MHz, CDCl_3) δ 142.8, 139.4, 139.2, 138.1, 130.6, 128.5, 128.4, 128.1, 127.8, 127.6, 127.3, 115.3, 77.9, 74.3, 73.2, 70.8, 60.7, 41.8, 40.1, 19.3; $[\alpha]_{\text{D}}^{20} -13.5$ (c 0.3, CHCl_3); IR (thin film, neat) 3431, 2963, 2927, 1729, 1645, 1495, 1446, 1261, 1091, 801, 699 cm^{-1} ; HRMS (ESIP) calcd for $\text{C}_{24}\text{H}_{29}\text{O}_3$ $[\text{M}+\text{H}]^+$: 365.2111, found: 365.2101.



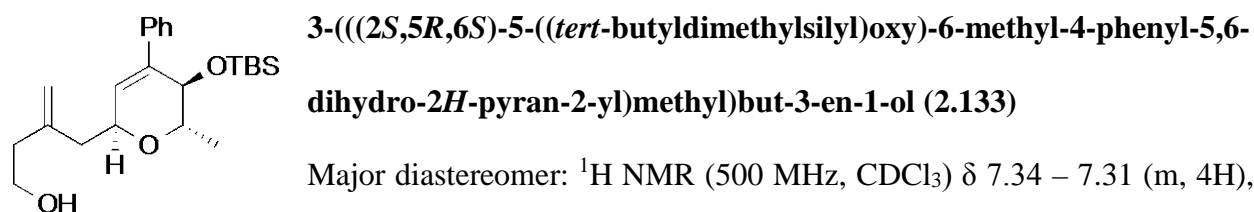
Reagents and conditions

- a) K_2CO_3 , MeOH, rt, 95%. b) PDC, AcOH, EtOAc, rt, 62%.
c) TBSCl, imidazole, CH_2Cl_2 , 74 %. d) PhLi, THF, -78 °C, 65%.



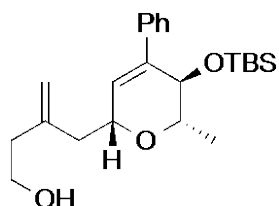
Formed as a single diastereomers: ^1H NMR (601 MHz, CDCl_3) δ 6.51 (d, $J = 6.0$ Hz, 1H), 4.73 (d, $J = 6.1$ Hz, 1H), 3.87 – 3.82 (m, 2H), 1.24 (d, $J = 5.7$ Hz, 3H), 0.78 (s, 9H), 0.22 (s, 3H), 0.09 (s, 3H); ^{13}C NMR (151 MHz, CDCl_3) δ 144.0, 142.7, 128.8, 127.4, 127.3, 106.1, 78.0, 75.5, 74.1, 26.2, 18.3, 18.2, -3.3, -4.4; $[\alpha]_{\text{D}}^{20}$ -142.8 (c 1.8, CHCl_3); IR (thin film, neat) 3469, 2931, 2858, 1650, 1449, 1388, 1256, 1037, 917, 838, 702. 620 cm^{-1} ; HRMS (ESIP) calcd for $\text{C}_{18}\text{H}_{27}\text{O}_2$ Si [M–OH] $^+$: 303.1775, found: 303.1772.

Ferrier coupling (5'-OTBS pyranol): The general Ferrier reaction procedure for 5'-OTBS pyranol was followed with pyranol **2.132** (44 mg, 0.14 mmol), silane **2.73** (43 mg, 0.19 mmol), TMSOTf (30 μL , 0.15 mmol), NaHCO_3 (sat) (160 μL , 0.18 mmol). The crude mixture was purified by flash chromatography (15% EtOAc in hexane) to give a mixture of **2.133** and **2.134** (33 mg, 61%) in 2.4:1 dr ratio.



Major diastereomer: ^1H NMR (500 MHz, CDCl_3) δ 7.34 – 7.31 (m, 4H), 7.28 – 7.25 (m, 1H), 5.89 (d, $J = 2.2$ Hz, 1H), 5.04 (s, 1H), 5.01 (s, 1H), 4.44 (ddt, $J = 7.3, 5.3, 2.0$ Hz, 1H), 4.22 (dd, $J = 2.6, 1.7$ Hz, 1H), 4.10 (q, $J = 6.8, 2.6$ Hz, 1H), 3.82 – 3.72 (m, 2H), 2.51 – 2.45 (m, 3H), 2.44 – 2.37 (m, 1H), 1.28 (d, $J = 6.8$ Hz, 3H), 0.76 (s, 9H), -0.06 (s, 3H), -0.25 (s, 3H). ^{13}C NMR (126 MHz, CDCl_3) δ 143.4, 140.4, 137.2, 128.5, 128.4, 127.6, 127.1,

115.1, 73.8, 69.9, 68.6, 60.7, 40.7, 39.9, 25.9, 18.3, 16.5, -4.1, -4.3; $[\alpha]_D^{20}$ -62.8 (c 1.4, CHCl₃); IR (thin film, neat) 3400, 2930, 2857, 1645, 1472, 1446, 1361, 1255, 1093, 836, 776, 698 cm⁻¹; HRMS (ESIP) calcd for C₂₃H₃₇O₃Si [M+H]⁺: 389.2507, found: 389.2496.



3-(((2R,5R,6S)-5-((tert-butyldimethylsilyl)oxy)-6-methyl-4-phenyl-5,6-dihydro-2H-pyran-2-yl)methyl)but-3-en-1-ol (2.134)

Minor diastereomer: ¹H NMR (400 MHz, CDCl₃) δ 7.34 – 7.22 (m, 6H), 5.77 (m, 1H), 4.99 (m, 1H), 4.43 (ddd, J = 8.0, 2.7, 1.1 Hz, 1H), 4.41 – 4.36 (m, 1H), 3.81 – 3.69 (m, 2H), 3.63 (dq, J = 7.9, 6.2 Hz, 1H), 2.42 – 2.33 (m, 2H), 2.32 – 2.29 (m, 2H), 1.39 (d, J = 6.2 Hz, 3H), 0.67 (s, 9H), -0.15 (s, 3H), -0.47 (s, 3H); ¹³C NMR (101 MHz, CDCl₃) δ 142.83, 141.42, 140.10, 129.51, 128.30, 127.90, 127.40, 115.25, 76.39, 74.04, 72.48, 60.68, 41.77, 40.11, 26.01, 19.56, 18.41, -3.81, -3.91; $[\alpha]_D^{20}$ -20.5 (c 0.9, CHCl₃); IR (thin film, neat) 3411, 2930, 2857, 1472, 1361, 1255, 1094, 879, 835, 775, 699 697 cm⁻¹; HRMS (ESIP) calcd for C₂₃H₃₇O₃Si [M+H]⁺: 389.2507, found: 389.2494.

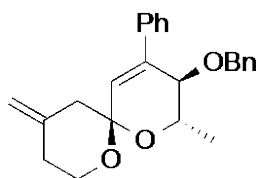
General protocol for DDQ mediated oxidative cyclization reaction

To a solution of the 5', 6'-disubstitued Ferrier intermediates in CH₂Cl₂ (~0.10 M) under nitrogen was added DDQ (1–1.5 equiv) in one portion at rt. The reaction was monitored by TLC and quenched by Et₃N upon complete consumption of starting material. After concentration under vacuum, the reaction was purified by flash column chromatography to give the desired product.

DDQ annulation (5'-OBn pyranol):

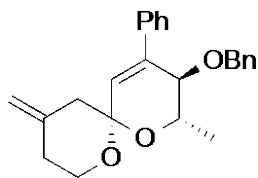
The general cyclization procedure was followed with alcohol **2.122** (11 mg, 0.03 mmol), DDQ (7 mg, 0.03 mmol) in (300 μ L) of CH_2Cl_2 . The crude mixture was purified by flash chromatography (5% EtOAc in hexane) to give a mixture of **2.127** and **2.128** (8 mg, 72%) in 10:3 dr ratio.

The general cyclization procedure was followed with alcohol **2.123** (10 mg, 0.03 mmol), DDQ (7mg, 0.03 mmol) in (300 μ L) of CH_2Cl_2 . The crude mixture was purified by flash chromatography 15% EtOAc in hexane) to give a mixture of spiroketals **2.127** and **2.128** (7 mg, 69%) in 10:3 dr ratio.



(2*S*,3*R*,6*R*)-3-(benzyloxy)-2-methyl-10-methylene-4-phenyl-1,7-dioxaspiro[5.5]undec-4-ene (**2.127**)

Major diastereomer: ^1H NMR (601 MHz, CDCl_3) δ 7.47 (dd, $J = 7.0, 1.6$ Hz, 2H), 7.38 – 7.31 (m, 4H), 7.16 (dd, $J = 4.8, 1.9$ Hz, 2H), 6.82 (dd, $J = 6.5, 2.8$ Hz, 2H), 5.98 (s, 1H), 4.87 (s, 1H), 4.81 (s, 1H), 4.45 (dd, $J = 9.2, 1.6$ Hz, 1H), 4.33 – 4.27 (m, 1H), 4.30 (d, $J = 10.6$ Hz, 1H), 4.18 (d, $J = 10.5$ Hz, 1H), 3.88 – 3.80 (m, 2H), 2.45 – 2.36 (m, 3H), 2.23 (dd, $J = 13.7, 2.6$ Hz, 1H), 1.44 (d, $J = 6.3$ Hz, 3H); ^{13}C NMR (151 MHz, CDCl_3) δ 142.6, 140.7, 138.3, 138.1, 129.9, 128.5, 128.4, 128.0, 127.7, 127.3, 111.1, 95.6, 77.3, 69.1, 65.5, 62.0, 44.5, 34.0, 18.7; $[\alpha]_{\text{D}}^{20}$ -92.1 (c 1.5, CHCl_3); IR (thin film, neat) 3031, 2931, 1657, 1496, 1454, 1384, 1336, 1253, 1175, 1100, 1069, 1049, 1017, 990, 887, 763, 698 cm^{-1} ; HRMS (ESIP) calcd for $\text{C}_{24}\text{H}_{27}\text{O}_3$ $[\text{M}+\text{H}]^+$: 363.1955, found: 363.1942.

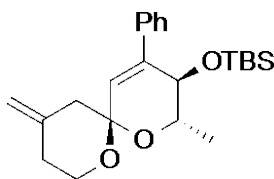


(2*S*,3*R*,6*S*)-3-(benzyloxy)-2-methyl-10-methylene-4-phenyl-1,7-dioxaspiro[5.5]undec-4-ene (2.128)

Minor diastereomer: ^1H NMR (601 MHz, CDCl_3) δ 7.49 – 7.47 (m, 2H), 7.35 – 7.30 (m, 3H), 7.30 – 7.25 (m, 3H), 7.21 (dd, $J = 7.6, 1.6$ Hz, 2H), 6.21 (s, 1H), 4.91 (s, 1H), 4.84 (s, 1H), 4.56 (s, 2H), 4.57 (dd, $J = 7.2, 1.8$ Hz, 2H), 4.13 (d, $J = 1.7$ Hz, 1H), 4.07 – 4.02 (m, 1H), 3.80 (ddd, $J = 10.8, 6.1, 1.6$ Hz, 1H), 2.49 – 2.37 (m, 3H), 2.27 – 2.23 (m, 1H), 1.37 (d, $J = 7.0$ Hz, 3H); ^{13}C NMR (151 MHz, CDCl_3) δ 141.3, 138.9, 138.3, 135.3, 128.9, 128.7, 128.5, 128.3, 128.2, 127.9, 126.3, 110.9, 95.2, 74.3, 71.5, 70.1, 61.7, 45.1, 34.1, 19.4; $[\alpha]_{\text{D}}^{20}$ -32.3 (c 0.8, CHCl_3); IR (thin film, neat) 3063, 3030, 2931, 2879, 1656, 1496, 1454, 1376, 1318, 1177, 1153, 1070, 1052, 1021, 985, 888, 742, 697 cm^{-1} ; HRMS (ESIP) calcd for $\text{C}_{24}\text{H}_{27}\text{O}_3$ $[\text{M}+\text{H}]^+$: 363.1955, found: 363.1942.

DDQ annulation (5'-OTBS pyranol):

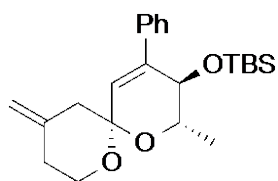
The general cyclization procedure was followed with alcohol **2.133** (9 mg, 0.02 mmol), DDQ (5 mg, 0.02 mmol) in (500 μL) of CH_2Cl_2 . The crude mixture was purified by flash chromatography (5% EtOAc in hexane) to give a mixture of spiroketals **2.135** and **2.136** (4 mg, 55%) in 10:3 dr ratio.



***tert*-butyl dimethyl(((2*S*,3*R*,6*R*)-2-methyl-10-methylene-4-phenyl-1,7-dioxaspiro[5.5]undec-4-en-3-yl)oxy)silane (2.135)**

Major diastereomer: ^1H NMR (601 MHz, CDCl_3) δ 7.32 – 7.25 (m, 5H), 5.70 (d, $J = 1.4$ Hz, 1H), 4.85 (m, 1H), 4.80 (m, 1H), 4.38 (dd, $J = 8.7, 1.5$ Hz, 1H), 4.01 (dq, $J = 8.7, 6.3$ Hz, 1H), 3.86 – 3.80 (m, 2H), 2.40 – 2.34 (m, 4H), 2.21 (dt, $J = 13.6, 2.2$ Hz, 1H), 1.38

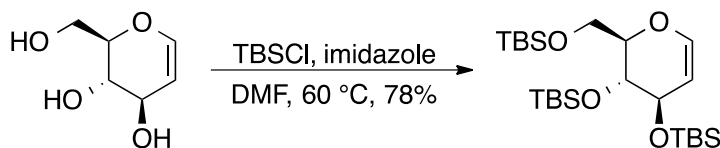
(d, $J = 6.2$ Hz, 3H), 0.66 (s, 9H), -0.14 (s, 3H), -0.46 (s, 3H); ^{13}C NMR (151 MHz, CDCl_3) δ 145.0, 140.9, 139.5, 128.4, 128.2, 128.1, 127.7, 110.9, 95.4, 72.5, 69.1, 61.9, 44.5, 34.0, 26.0, 19.1, 18.4, -3.8, -3.9; $[\alpha]_{\text{D}}^{20}$ -57.0 (c 1.9, CHCl_3); IR (thin film, neat) 2929, 2854, 1255, 1145, 1174, 1096, 1069, 1046, 989, 886, 863, 837, 779, 700 cm^{-1} ; HRMS (ESIP) calcd for $\text{C}_{23}\text{H}_{35}\text{O}_3\text{Si}$ $[\text{M}+\text{H}]^+$: 387.2350, found: 387.2336.

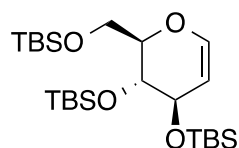


***tert*-butyldimethyl(((2*S*,3*R*,6*S*)-2-methyl-10-methylene-4-phenyl-1,7-dioxaspiro[5.5]undec-4-en-3-yl)oxy)silane (2.136)**

Minor diastereomer: ^1H NMR (601 MHz, CDCl_3) δ 7.43 – 7.40 (m, 2H), 7.36 – 7.32 (m, 2H), 7.31 – 7.27 (m, 1H), 5.94 (s, 1H), 4.89 (d, $J = 2.0$ Hz, 1H), 4.80 (d, $J = 1.9$ Hz, 1H), 4.24 (d, $J = 2.2$ Hz, 1H), 4.21 (qd, $J = 6.9, 2.2$ Hz, 1H), 4.04 (ddd, $J = 12.4, 10.8, 3.0$ Hz, 1H), 3.78 (ddd, $J = 10.7, 6.0, 1.5$ Hz, 1H), 2.45 (dd, $J = 13.3, 1.4$ Hz, 1H), 2.41 – 2.35 (m, 3H), 2.23 (ddt, $J = 13.4, 2.9, 1.5$ Hz, 1H), 1.31 (d, $J = 6.9$ Hz, 3H), 0.80 (s, 9H), -0.01 (s, 3H), -0.20 (s, 3H); ^{13}C NMR (151 MHz, CDCl_3) δ 141.5, 128.5, 128.0, 127.5, 126.9, 95.1, 74.8, 69.4, 61.6, 34.2, 25.9, 19.1, -4.2, -4.3; $[\alpha]_{\text{D}}^{20}$ -44.5 (c 0.3, CHCl_3); IR (thin film, neat) 2929, 2856, 1657, 1462, 1361, 1255, 1176, 1155, 1103, 1071, 1022, 984, 837, 775, 697 cm^{-1} ; HRMS (ESIP) calcd for $\text{C}_{23}\text{H}_{35}\text{O}_3\text{Si}$ $[\text{M}+\text{H}]^+$: 387.2350, found: 387.2338.

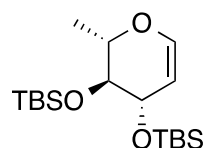
Dihydropyran preparation





(((2*R*,3*R*,4*R*)-2-(((*tert*-Butyldimethylsilyl)oxy)methyl)-3,4-dihydro-2H-pyran-3,4-diyl)bis(oxy))bis(*tert*-butyldimethylsilane) (2.137)

^1H NMR (601 MHz, CDCl_3) δ 6.32 (d, $J = 6.3$ Hz, 1H), 4.69 (ddd, $J = 5.9, 4.5, 1.2$ Hz, 1H), 3.99 (dtd, $J = 5.1, 3.7, 1.4$ Hz, 1H), 3.93 (dd, $J = 11.3, 7.4$ Hz, 1H), 3.89 (t, $J = 3.8$ Hz, 1H), 3.79 (td, $J = 3.7, 1.2$ Hz, 1H), 3.76 (dd, $J = 11.3, 3.6$ Hz, 1H), 0.90 (s, 9H), 0.89 (s, 9H), 0.89 (s, 9H), 0.10 (s, 6H), 0.08 (s, 3H), 0.08 (s, 3H), 0.06 (s, 3H), 0.05 (s, 3H); ^{13}C NMR (151 MHz, CDCl_3) δ 143.3, 101.7, 80.4, 70.5, 67.0, 62.1, 26.3, 26.2, 26.2, 18.8, 18.4, 18.3, -3.9, -4.0, -4.1, -4.4, -4.9, -4.9. These data are consistent with literature values.⁸

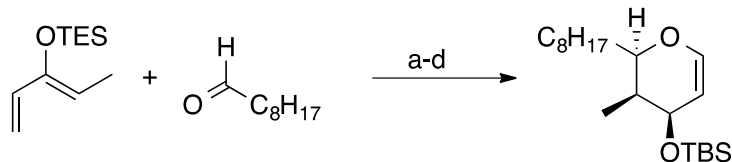


(((2*S*,3*S*,4*R*)-2-methyl-3,4-dihydro-2H-pyran-3,4-diyl)bis(oxy))bis(*tert*-butyldimethylsilane) (2.142)

^1H NMR (500 MHz, CDCl_3) δ 6.28 (d, $J = 6.2$ Hz, 1H), 4.66 (dd, $J = 6.2, 3.2$ Hz, 1H), 4.07 (t, $J = 4.0$ Hz, 1H), 3.94 (p, $J = 6.7$ Hz, 1H), 3.57 (dd, $J = 6.4, 4.9$ Hz, 1H), 1.32 (d, $J = 6.7$ Hz, 3H), 0.90 (s, 18H), 0.11 (s, 3H), 0.10 (s, 3H), 0.10 (s, 3H), 0.09 (s, 3H); ^{13}C NMR (101 MHz, CDCl_3) δ 143.3, 103.1, 75.4, 74.9, 69.5, 26.2, 26.2, 18.4, 18.3, 17.4, -3.5, -3.7, -4.0, -4.0; $[\alpha]_{\text{D}}^{20} +49.2$ (c 1.20, CHCl_3); IR (thin film) 2956, 2931, 2888, 2858, 1651, 1472, 1390, 1361, 1251, 1116, 1074, 1047, 939, 838, 777 cm^{-1} ; HRMS (ASAP) calcd for $\text{C}_{18}\text{H}_{37}\text{O}_3\text{Si}_2$ $[\text{M}-\text{H}]^-$: 357.2281, found: 357.2283. These data are consistent with literature values.⁹

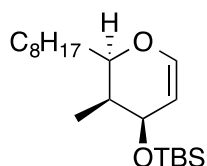
⁸ Shuto, S.; Yahiro, Y.; Ichikawa, S.; Matsuda, A. *J. Org. Chem.* **2000**, *65*, 5547.

⁹ Paquette, L. A.; Oplinger, J. A. *Tetrahedron* **1989**, *45*, 107.



Reagents and conditions

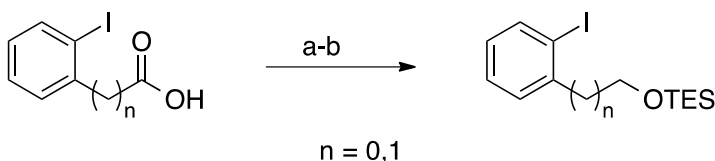
a) Me_2AlCl , PhMe, -20°C , 70%. b) DDQ, CH_2Cl_2 , 82%. c) NaBH_4 , CeCl_3 , MeOH, 83%. d) TBSCl, imidazole, CH_2Cl_2 , 90%.



***tert*-Butyldimethyl(((2*S*,3*R*,4*R*)-3-methyl-2-octyl-3,4-dihydro-2*H*-pyran-4-yl)oxy)silane (2.144)**

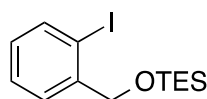
^1H NMR (601 MHz, CDCl_3) δ 6.24 (d, $J = 4.7$ Hz, 1H), 4.50 (m, 2H), 3.88 – 3.85 (m, 1H), 1.86 (dd, $J = 14.1, 7.2$ Hz, 1H), 1.75 – 1.69 (m, 1H), 1.45 – 1.38 (m, 1H), 1.33 – 1.24 (m, 12H), 0.92 (m, 3H), 0.90 (s, $J = 2.4$ Hz, 9H), 0.87 (d, $J = 2.8$ Hz, 3H), 0.07 (s, 3H), 0.06 (s, 3H); ^{13}C NMR (151 MHz, CDCl_3) δ 143.9, 104.8, 78.7, 36.6, 32.2, 29.9, 29.8, 29.6, 29.5, 26.2, 26.0, 23.0, 18.5, 14.4, 7.2, 7.1, 6.7, -4.4 , -4.5 ; IR (thin film) 3066, 2928, 2857, 1644, 1464, 1390, 1360, 1255, 1230, 1119, 1084, 1006, 893, 776, 726, 673 cm^{-1} ; HRMS (ASAP) calcd for $\text{C}_{20}\text{H}_{39}\text{O}_2\text{Si}$ $[\text{M}-\text{H}]^+$: 339.2719, found: 339.2703.

Aryl iodide synthesis



Reagents and conditions

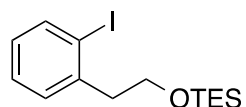
a) $\text{BH}_3 \cdot \text{SMe}_2$, THF, 0°C , 90-95%. b) TESCl, imidazole, CH_2Cl_2 , 0°C , 83-85%.



Triethyl((2-iodobenzyl)oxy)silane (2.145)

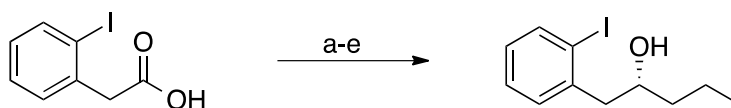
^1H NMR (601 MHz, CDCl_3) δ 7.77 (dd, $J = 7.8, 1.2$ Hz, 1H), 7.53 (dd, $J = 7.7, 1.6$ Hz, 1H), 7.36 (td, $J = 7.5, 1.2$ Hz, 1H), 6.96 (td, $J = 7.6, 1.6$ Hz, 1H), 4.64 (s, 2H), 1.00

(t, $J = 8.0$ Hz, 9H), 0.69 (q, $J = 8.0$ Hz, 6H); ^{13}C NMR (151 MHz, CDCl_3) δ 143.2, 138.9, 128.8, 128.5, 127.7, 96.2, 69.4, 7.1, 4.8; IR (thin film) 2955, 2910, 2876, 1459, 1413, 1375, 1239, 1203, 1092, 1117, 1012, 804, 745 cm^{-1} ; HRMS (ASAP) calcd for $\text{C}_{13}\text{H}_{20}\text{OSiI}$ $[\text{M}-\text{H}]^+$: 347.0328, found: 347.0327.



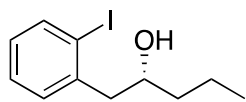
Triethyl(2-iodophenoxy)silane (2.138)

^1H NMR (601 MHz, CDCl_3) δ 7.81 (d, $J = 7.9$ Hz, 1H), 7.27 (s, $J = 1.7$ Hz, 2H), 6.90 (ddd, $J = 7.9, 5.6, 3.5$ Hz, 1H), 3.80 (dd, $J = 9.1, 5.4$ Hz, 2H), 3.04 – 2.96 (m, 2H), 0.94 (t, $J = 8.0$ Hz, 9H), 0.59 (q, $J = 7.9$ Hz, 6H); ^{13}C NMR (151 MHz, CDCl_3) δ 141.9, 139.7, 130.9, 128.5, 128.4, 101.0, 62.7, 44.4, 7.1, 4.7; IR (thin film) 2954, 2910, 2875, 1466, 1436, 1414, 1238, 1096, 1009, 913, 846, 745 cm^{-1} ; HRMS (ASAP) calcd for $\text{C}_{14}\text{H}_{24}\text{OSiI}$ $[\text{M}+\text{H}]^+$: 363.0641, found: 363.0636.



Reagents and conditions

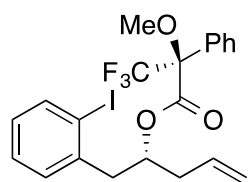
a) MeOH , H_2SO_4 , 65 $^\circ\text{C}$, 99%. b) DIBAL-H, CH_2Cl_2 , -78 $^\circ\text{C}$, 88%. c) (+)-(Ipc) $_2$ allylborane, Et_2O , -100 $^\circ\text{C}$, 62%, >90% ee. d) H_2 , $(\text{Ph}_3\text{P})_3\text{RhCl}$, C_6H_6 , EtOH , 85%. e) TESCl, imidazole, CH_2Cl_2 , 90%.



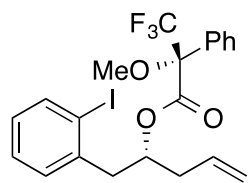
(R)-Triethyl(1-(2-iodophenyl)pentan-2-yl)oxy)silane (2.147)

^1H NMR (601 MHz, CDCl_3) δ 7.82 (dd, $J = 7.9, 1.2$ Hz, 1H), 7.28 – 7.23 (m, 2H), 6.91 (ddd, $J = 7.9, 6.9, 2.1$ Hz, 1H), 4.03 – 3.98 (m, 1H), 2.94 (dd, $J = 13.4, 4.8$ Hz, 1H), 2.80 (dd, $J = 13.4, 8.2$ Hz, 1H), 1.55 – 1.47 (m, 3H), 1.45 – 1.40 (m, 1H), 0.97 – 0.91 (m, 9H), 0.91 – 0.83 (m, 3H), 0.50 – 0.38 (m, 6H); ^{13}C NMR (101 MHz, CDCl_3) δ 142.5, 139.5, 132.2, 128.2, 128.1, 101.1, 71.7, 48.4, 40.3, 18.8, 14.6, 7.1, 5.1; $[\alpha]_D^{20}$ -26.2 (c 0.86, CHCl_3); IR (thin film) 2956, 2875, 1465, 1377, 1238, 1071, 1011, 929, 741 cm^{-1} ; HRMS (ASAP) calcd for

$C_{11}H_{12}I [M-OH]^+$: 270.9984, found: 270.9980. The ee of this material was determined to be approximately 85% by Mosher ester analysis (see below).



1H NMR (400 MHz, $CDCl_3$) δ 7.78 (dd, $J = 7.9, 1.2$ Hz, 1H), 7.42 – 7.34 (m, 3H), 7.34 – 7.27 (m, 2H), 7.13 – 7.06 (m, 1H), 7.04 (dd, $J = 7.6, 1.8$ Hz, 1H), 6.87 (td, $J = 7.6, 1.8$ Hz, 1H), 5.85 (ddt, $J = 17.3, 10.4, 7.0$ Hz, 1H), 5.52 (dq, $J = 7.3, 6.0$ Hz, 1H), 5.21 – 5.15 (m, 2H), 3.44 (s, 3H), 3.04 (s, 1H), 3.02 (d, $J = 2.1$ Hz, 1H), 2.53 (ddd, $J = 6.6, 2.7, 1.3$ Hz, 2H); ^{13}C NMR (101 MHz, $CDCl_3$) δ 166.3, 139.9, 139.8, 133.1, 132.5, 131.3, 129.7, 128.9, 128.6, 128.6, 127.6, 119.3, 101.1, 75.9, 55.8, 44.4, 38.7; ^{19}F NMR ($CDCl_3$) δ -71.22 (minor), δ -71.37 (major). The dr of this (*S*)-Mosher ester was determined to be >14:1 by both 1H and ^{19}F NMR.



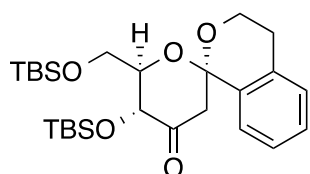
1H NMR (400 MHz, $CDCl_3$) δ 7.78 (d, $J = 7.9$ Hz, 1H), 7.35 – 7.24 (m, 1H), 7.23 – 7.18 (m, 4H), 7.14 (d, $J = 7.3$ Hz, 1H), 7.10 (dd, $J = 7.6, 1.9$ Hz, 1H), 6.87 (td, $J = 7.6, 1.9$ Hz, 1H), 5.75 – 5.63 (m, 1H), 5.43 (dq, $J = 8.0, 5.7$ Hz, 1H), 5.06 – 5.02 (m, 2H), 3.32 (s, 3H), 3.02 (d, $J = 1.4$ Hz, 1H), 3.00 (d, $J = 3.9$ Hz, 1H), 2.43 (t, $J = 6.5$ Hz, 2H); ^{13}C NMR (101 MHz, $CDCl_3$) δ 166.4, 140.1, 132.6, 132.5, 131.5, 129.7, 129.0, 128.7, 128.6, 127.7, 119.3, 101.1, 76.1, 55.6, 44.3, 38.6; ^{19}F NMR ($CDCl_3$) δ -71.22 (major), -71.37 (minor). The dr of this (*R*)-Mosher ester was determined to be 12.5:1 by both 1H and ^{19}F NMR analysis.

General protocol Heck reaction-based [n+1] annulations

One-pot procedure: The glycal derivative (1 equiv) and aryl iodide (1.5-2.0 equiv) were dissolved in 1,2-dichloroethane (nitrogen-purged) to give a (~0.10 M) solution. $Pd(OAc)_2$ (10-20

mol%), Cu(OAc)₂ (1.5- 2.0 equiv) and Ag₂CO₃ (1.0-1.5 equiv) were added sequentially under an argon atmosphere. The reaction was stirred at 40 °C for 18h, then was cooled to rt and DDQ (5.0-8.0 equiv) was added directly portion-wise every 15 min until complete conversion of the TBS-enol silane into the enone as monitored by TLC. TsOH•H₂O (1.0-1.5 equiv) was added and stirred for ~45 min. The mixture was filtered through a plug of Celite, then was concentrated under vacuum and purified by flash column chromatography to give the desired product.

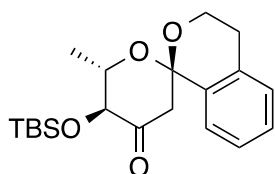
Two-pot protocol: The crude mixture from the Heck coupling was filtered through a plug of silica gel and rinsed with a minimal volume of 1,2-dichloroethane (DCE). DDQ (3.0-5.0 equiv) was added portion-wise every 15 min until complete conversion of the enolsilane into the enone as monitored by TLC. Acid-catalyzed spiroketalization, work-up, and purification proceeded as above.



(1*R*,5'*R*,6'*R*)-5'-((*tert*-Butyldimethylsilyl)oxy)-6'-(((*tert*-butyldimethylsilyl)oxy)methyl)-5',6'-dihydrospiro[isochromane-1,2'-pyran]-4'(3'*H*)-one (2.141)

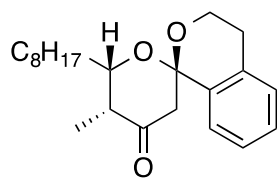
The general cyclization procedure was followed with **2.137** (50 mg, 0.10 mmol), **2.138** (73 mg, 0.20 mmol), Pd(OAc)₂ (20 mol%, 4.5 mg, 0.02 mmol), Cu(OAc)₂ (37 mg, 0.21 mmol), Ag₂CO₃ (30 mg, 0.11 mmol), dichloroethane (1.5 mL). After filtration, DDQ (116 mg, 0.51 mmol) and TsOH•H₂O (23 mg, 0.12 mmol) was added. The resultant mixture was stirred at rt for 40 min, then was quenched by Et₃N. The crude mixture was purified by flash chromatography (5% EtOAc in hexane) to give the desired product (31 mg, 62%) as a white solid (mp = 89 – 90 °C). ¹H NMR (400 MHz, CDCl₃) δ 7.39 – 7.35 (m, 1H), 7.28 – 7.23 (m, 2H), 7.13 (dd, *J* = 6.4, 2.4 Hz, 1H), 4.50 (dd, *J* = 9.1, 1.1 Hz, 1H), 3.99 – 3.86 (m, 5H), 3.09 (dd, *J* = 13.7, 1.2 Hz, 1H), 3.10 – 3.02 (m, 1H), 2.61 (d, *J* = 13.5 Hz, 1H), 2.57

(dq, $J = 3.8, 1.9$ Hz, 1H), 0.94 (s, 9H), 0.89 (s, 9H), 0.22 (s, 3H), 0.07 (s, 3H), 0.02 (s, 3H), -0.01 (s, 3H); ^{13}C NMR (101 MHz, CDCl_3) δ 205.5, 135.6, 134.3, 128.8, 128.4, 127.0, 126.6, 100.1, 74.2, 62.3, 58.9, 51.6, 28.5, 26.1, 26.1, 18.7, 18.6, -4.0, -4.8, -5.1, -5.4; mp: 89.0 – 90.0 °C; $[\alpha]_{\text{D}}^{20} +5.5$ (c 2.08, CHCl_3); IR (thin film) 2929, 2856, 1738, 1471, 1312, 1253, 1133, 1105, 837, 780, 683 cm^{-1} ; HRMS (EI) calcd for $\text{C}_{26}\text{H}_{45}\text{O}_5\text{Si}_2$ $[\text{M}+\text{H}]^+$: 493.2806, found: 493.2823.



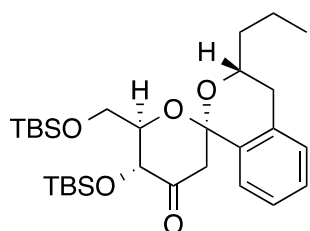
(1R,5'S,6'S)-5'-((*tert*-Butyldimethylsilyloxy)-6'-methyl-5',6'-dihydrospiro[isochromane-1,2'-pyran]-4'(3'H)-one (2.148)

The general cyclization procedure was followed with **2.138** (148 mg, 0.41 mmol), **2.142** (75 mg, 0.21 mmol), $\text{Pd}(\text{OAc})_2$ (20 mol%, 9.5 mg, 0.042 mmol), $\text{Cu}(\text{OAc})_2$ (74 mg, 0.41 mmol), Ag_2CO_3 (68 mg, 0.25 mmol), and dichloroethane (3.0 mL). After filtration, DDQ (140 mg, 0.61 mmol) and $\text{TsOH}\cdot\text{H}_2\text{O}$ (51 mg, 0.27 mmol) was added. The resultant mixture was stirred at rt for 40 min, then was quenched by Et_3N . The crude mixture was purified by flash chromatography (5% EtOAc in hexane) to give the desired product (45 mg, 61%) as a white solid (mp = 81.0 – 83.5 °C). ^1H NMR (400 MHz, CDCl_3) δ 7.46 – 7.38 (m, 1H), 7.31 – 7.23 (m, 2H), 7.17 – 7.10 (m, 1H), 4.14 – 3.89 (m, 4H), 3.15 (dd, $J = 13.8, 1.1$ Hz, 1H), 3.08 (ddd, $J = 16.0, 10.7, 5.8$ Hz, 1H), 2.64 (d, $J = 13.7$ Hz, 1H), 2.59 (ddd, $J = 16.5, 2.7, 1.3$ Hz, 1H), 1.43 (d, $J = 5.9$ Hz, 3H), 0.95 (s, 9H), 0.21 (s, 3H), 0.08 (s, 3H); ^{13}C NMR (101 MHz, CDCl_3) δ 204.3, 135.5, 134.3, 129.1, 128.6, 127.0, 126.6, 99.8, 80.6, 72.23, 58.9, 51.7, 28.4, 26.0, 19.5, 18.8, -3.9, -5.3; mp: 81.0 – 83.5 °C; $[\alpha]_{\text{D}}^{20} -57.1$ (c 3.48, CHCl_3); IR (thin film) 2931, 2857, 1739, 1463, 1377, 1312, 1251, 1136, 834, 781, 680 cm^{-1} ; HRMS (EI) calcd for $\text{C}_{20}\text{H}_{31}\text{O}_4\text{Si}$ $[\text{M}+\text{H}]^+$: 363.1992, found: 363.1996.



(1*S*,5'*R*,6'*S*)-5'-Methyl-6'-octyl-5',6'-dihydrospiro[isochromane-1,2'-pyran]-4'(3'*H*)-one (2.149)

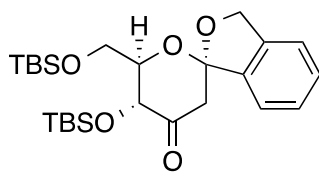
The general cyclization procedure was followed with **2.138** (85 mg, 0.24 mmol), **2.144** (40 mg, 0.12 mmol), Pd(OAc)₂ (10 mol%, 6 mg, 0.024 mmol), Cu(OAc)₂ (43 mg, 0.24 mmol), Ag₂CO₃ (47 mg, 0.17 mmol), and dichloroethane (1.8 mL). After filtration, DDQ (80 mg, 0.35 mmol) and TsOH•H₂O (25 mg, 0.13 mmol) was added. The resultant mixture was stirred at rt for 30 min, then was quenched by Et₃N. The crude mixture was purified by flash chromatography (5% EtOAc in hexane) to give the desired product (25 mg, 58%) as a colorless oil. ¹H NMR (601 MHz, CDCl₃) δ 7.38 – 7.34 (m, 1H), 7.30 – 7.24 (m, 2H), 7.13 (dd, *J* = 7.8, 4.9 Hz, 1H), 4.21 (ddd, *J* = 7.9, 4.8, 2.7 Hz, 1H), 4.01 – 3.96 (m, 1H), 3.90 (dd, *J* = 11.1, 6.0 Hz, 1H), 3.17 (d, *J* = 14.7 Hz, 1H), 3.11 – 3.05 (m, 1H), 2.58 (dd, *J* = 16.4, 2.6 Hz, 1H), 2.45 (d, *J* = 14.6 Hz, 2H), 1.32 – 1.21 (m, 17H), 0.87 (t, *J* = 6.9 Hz, 3H); ¹³C NMR (101 MHz, CDCl₃) δ 210.8, 136.6, 134.4, 129.0, 128.4, 127.0, 126.8, 99.5, 71.7, 58.8, 48.6, 32.0, 31.7, 29.8, 29.7, 29.5, 28.6, 26.1, 22.8, 14.3, 10.9; IR (thin film) 2926, 2855, 1722, 1456, 1318, 1111, 1081, 1039, 1016, 972, 755 cm⁻¹; HRMS (ESI) calcd for C₂₂H₃₃O₃ [M+H]⁺: 345.2424, found: 345.2435.



(1*R*,3*R*,5'*R*,6'*R*)-5'-((*tert*-Butyldimethylsilyl)oxy)-6'-(((*tert*-butyldimethylsilyl)oxy)methyl)-3-propyl-5',6'-dihydrospiro[isochromane-1,2'-pyran]-4'(3'*H*)-one (2.150)

The general cyclization procedure was followed with **2.137** (68 mg, 0.17 mmol), **2.147** (38 mg, 0.08 mmol), Pd(OAc)₂ (15 mol%, 2.5 mg, 11 μmol), Cu(OAc)₂ (40 mg, 0.22 mmol), Ag₂CO₃ (31 mg, 0.11 mmol), and dichloroethane (0.85 mL). After filtration, DDQ (75 mg, 0.33 mmol) and TsOH•H₂O (31 mg, 0.17 mmol) were added. The resultant mixture was stirred at rt for 30 min, then was quenched by Et₃N. The crude mixture was purified

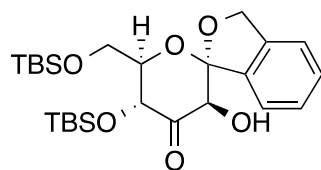
by flash chromatography (5% EtOAc in hexane) to give the desired product (30 mg, 70%) as a colorless oil. ^1H NMR (400 MHz, CDCl_3) δ 7.39 – 7.34 (m, 1H), 7.26 – 7.21 (m, 2H), 7.13 – 7.08 (m, 1H), 4.46 (dd, $J = 9.0, 1.1$ Hz, 1H), 3.97 – 3.82 (m, 4H), 3.06 (dd, $J = 13.7, 1.2$ Hz, 1H), 2.74 – 2.56 (m, 4H), 1.71 – 1.24 (m, 4H), 0.96 – 0.87 (m, 21H), 0.21 (s, 3H), 0.07 (s, 3H), 0.01 (s, 3H), -0.03 (s, 3H); ^{13}C NMR (101 MHz, CDCl_3) δ 205.3, 135.7, 134.7, 128.7, 128.3, 126.9, 126.5, 100.7, 74.3, 68.6, 62.5, 51.9, 37.7, 34.5, 26.1, 19.0, 18.7, 18.6, 14.3, -3.9 , -4.8 , -5.1 , -5.3 ; $[\alpha]_{\text{D}}^{20} +67.2$ (c 0.9, CHCl_3); IR (thin film) 2930, 2857, 1739, 1463, 1409, 1309, 1253, 1124, 1025, 990, 837, 780, 673 cm^{-1} ; HRMS (ASAP) calcd for $\text{C}_{29}\text{H}_{51}\text{O}_5\text{Si}_2$ $[\text{M}+\text{H}]^+$: 535.3275, found: 535.3286.



(1*R*,5'*R*,6'*R*)-5'-((*tert*-Butyldimethylsilyl)oxy)-6'-(((*tert*-butyldimethylsilyl)oxy)methyl)-5',6'-dihydro-3H-spiro[isobenzofuran-1,2'-pyran]-4'(3'H)-one (2.151)

The general cyclization procedure was followed with **2.145** (50 mg, 0.14 mmol), **2.137** (35 mg, 0.07 mmol), $\text{Pd}(\text{OAc})_2$ (20 mol%, 3.5 mg, 0.014 mmol), $\text{Cu}(\text{OAc})_2$ (26 mg, 0.14 mmol), Ag_2CO_3 (30 mg, 0.11 mmol), and dichloroethane (1.0 mL). After flash column chromatography, the enolsilane was dissolved in dichloroethane (1.0 mL), followed by addition of DDQ (49 mg, 0.22 mmol) and $\text{TsOH}\cdot\text{H}_2\text{O}$ (21 mg, 0.11 mmol). The resultant mixture was stirred at rt for 40 min, then was quenched by Et_3N . The crude mixture was purified by flash chromatography (5% EtOAc in hexane) to give the desired product (16 mg, 47%) as a colorless oil. ^1H NMR (601 MHz, CDCl_3) δ 7.43 – 7.38 (m, 1H), 7.38 – 7.35 (m, 2H), 7.31 – 7.27 (m, 1H), 5.10 (ABq, 2H, $\Delta\delta_{\text{AB}} = 0.07$, $J_{\text{AB}} = 12.6$ Hz), 4.55 (d, $J = 9.4$ Hz, 1H), 4.07 (dt, $J = 9.5, 2.2$ Hz, 1H), 3.98 (dd, $J = 11.6, 3.0$ Hz, 1H), 3.85 (dd, $J = 11.6, 1.7$ Hz, 1H), 3.18 (d, $J = 13.5$ Hz, 1H), 2.71 (d, $J = 13.5$ Hz, 1H), 0.96 (s, $J = 3.3$ Hz, 9H), 0.90 (s, $J = 3.6$ Hz, 9H), 0.23 (s, 3H), 0.10 (s, 3H), 0.04 (s, 3H), -0.02 (s, 3H); ^{13}C NMR (151 MHz, CDCl_3) δ 205.0, 139.7, 139.6, 129.6,

128.0, 122.3, 121.5, 110.9, 78.0, 74.2, 72.2, 62.4, 50.2, 26.2, 26.2, 18.8, 18.7, -3.9, -4.6, -5.0, -5.3. IR (thin film) 2954, 2930, 2886, 2857, 1471, 1738, 1471, 1363, 1308, 1254, 1130, 999, 964, 879, 779, 674 cm^{-1} ; $[\alpha]_{\text{D}}^{20} +62.5$ (c 1.50, CHCl_3); HRMS (ASAP) calcd for $\text{C}_{20}\text{H}_{43}\text{O}_5\text{Si}_2$ $[\text{M}+\text{H}]^+$: 479.2649, found: 479.2671.

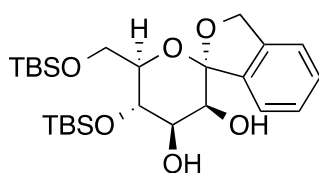


3'-Hydroxy-5',6'-dihydro-3H-spiro[isobenzofuran-1,2'-pyran]-4'(3'H)-one (2.153)

Enol silane formation: A 10 mL flask was charged with THF (150 μL) and was cooled to -78°C . LiHMDS (1.0M, 85 μL , 0.08 mmol) was added to the solution followed by TESCO (15 μL , 0.08 mmol). Spirocyclic ketone **2.151** (0.05 mmol, 26 mg) in THF (100 μL) was added drop-wise over 5 min. The resultant mixture was stirred at -78°C for 40 min, then was quenched with NH_4Cl (200 μL) and warmed to rt. The crude enol silane spiroketal was used directly in the next step without further purification.

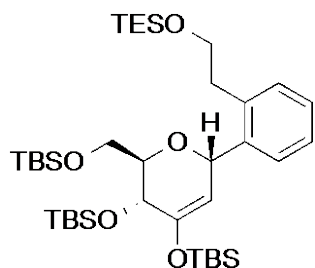
Epoxidation procedure: To a suspension of *m*-CPBA (16.5 mg, 0.07 mmol) and NaHCO_3 (10.5 mg, 0.12 mmol) in toluene (600 μL) and water (120 μL) at 0°C was added the crude enol silane in toluene (100 μL) dropwise over 5 min. The mixture was allowed to stir for 1h at 0°C , then was warmed to rt and stirred for 30 min. NaHSO_3 (50 mg) in water (200 μL) was subsequently added. The mixture was stirred for 30 min, then was extracted with EtOAc (2 x 5mL). The organic layers were combined, washed with satd. NaHCO_3 (5 mL), and brine (5 mL), then was concentrated. The oil was dissolved in a solvent mixture of THF, H_2O , and MeOH (1.4 mL) in a 5:1:1 ratio and stirred overnight. The crude mixture was purified by flash chromatography (20% EtOAc in hexane) to give the desired product (18 mg, 67%) as a colorless oil over 2 steps. ^1H NMR (601 MHz, CDCl_3) δ 7.48 – 7.47 (m, 2H), 7.46 (s, 1H), 7.44 (s, 1H), 7.38 – 7.33 (m, 1H),

5.66 (s, 1H), 4.62 (ABq, 2H, $\Delta\delta_{AB} = 0.03$, $J_{AB} = 12.9$ Hz), 4.48 (ddd, $J = 12.3, 7.2, 2.2$ Hz, 1H), 4.30 (d, $J = 12.3$ Hz, 1H), 4.20 (dd, $J = 11.4, 2.3$ Hz, 1H), 4.00 (dd, $J = 11.4, 7.2$ Hz, 1H), 3.24 (s, 1H), 0.93 (s, 9H), 0.92 (s, 9H), 0.27 (s, $J = 4.0$ Hz, 3H), 0.12 (d, $J = 1.8$ Hz, 9H); ^{13}C NMR (151 MHz, CDCl_3) δ 193.4, 172.6, 140.3, 132.9, 131.7, 131.0, 129.5, 128.3, 104.1, 84.1, 70.4, 64.0, 63.5, 26.1, 26.1, 18.8, 18.7, -3.6, -5.2, -5.2, -5.4; $[\alpha]_{\text{D}}^{20} +116.3$ (c 1.1, CHCl_3); IR (thin film, neat) 2929, 2857, 1736, 1684, 1604, 1463, 1369, 1253, 1151, 1005, 837, 780 cm^{-1} ; HRMS (ESI) calcd for $\text{C}_{25}\text{H}_{41}\text{O}_5\text{Si}_2$ $[\text{M}-\text{OH}]^+$: 477.2487, found: 477.2509.



(1*S*,3'*S*,4'*R*,5'*S*,6'*R*)-5'-((*tert*-butyldimethylsilyl)oxy)-6'-(((*tert*-butyldimethylsilyl)oxy)methyl)-3',4',5',6'-tetrahydro-3*H*-spiro[isobenzofuran-1,2'-pyran]-3',4'-diol (2.154)

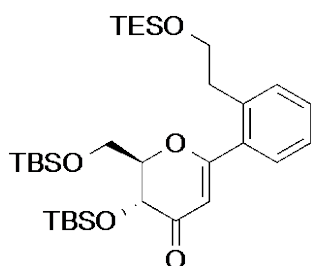
To a solution of **2.153** (1 mg, 2.7 μmol) in MeOH (100 μL) at -10 $^\circ\text{C}$ was added NaBH_4 (1 mg, 0.03 mmol). The resultant mixture was allowed to stir at that temperature for 25 min, then was quenched by water. The crude mixture was purified by flash chromatography (20% EtOAc in hexane) to give the desired product (0.3 mg, 22%). ^1H NMR (601 MHz, CDCl_3) δ 5.00 (d, $J = 2.9$ Hz, 1H), 4.58 (dd, $J = 12.3, 6.0$ Hz, 1H), 4.52 (dd, $J = 12.2, 8.3$ Hz, 1H), 4.31 (td, $J = 6.4, 2.8$ Hz, 1H), 4.15 – 4.04 (m, 2H), 3.83 (dd, $J = 10.8, 6.9$ Hz, 1H), 3.76 (dd, $J = 8.7, 6.4$ Hz, 1H), 0.93 (s, 8H), 0.91 (s, $J = 6.4$ Hz, 10H), 0.20 (s, 2H), 0.15 (s, 2H), 0.09 (s, 3H), 0.09 (s, 2H).



(((2*R*,3*R*,6*S*)-2-(((*tert*-butyldimethylsilyl)oxy)methyl)-6-(2-(2-(triethylsilyl)oxy)ethyl)phenyl)-3,6-dihydro-2*H*-pyran-3,4-diyl)bis(oxy))bis(*tert*-butyldimethylsilyl silane) (2.156)

The general cyclization procedure was followed with **2.137** (25 mg, 0.05 mmol), **2.138** (37 mg, 0.10 mmol), $\text{Pd}(\text{OAc})_2$ (20 mol%, 2 mg, 0.01 mmol), $\text{Cu}(\text{OAc})_2$ (19

mg, 0.10 mmol), Ag₂CO₃ (17 mg, 0.06 mmol), dichloroethane (700 μL). The resultant mixture was stirred at 45 °C for 18h, filtered through a plug of celite and concentrated. The crude mixture was purified by flash chromatography (2% EtOAc in hexane) to give the desired product (33 mg, 89%) as a colorless oil. Formed as a single diastereomer: ¹H NMR (601 MHz, CDCl₃) δ 7.56 – 7.53 (m, 1H), 7.21 – 7.19 (m, 2H), 7.19 – 7.16 (m, 1H), 5.47 (dd, *J* = 2.7, 1.3 Hz, 1H), 4.82 (d, *J* = 2.6 Hz, 1H), 4.10 (dd, *J* = 2.8, 1.3 Hz, 1H), 3.87 – 3.70 (m, 5H), 3.04 (ddd, *J* = 13.4, 8.8, 6.6 Hz, 1H), 2.94 – 2.89 (m, 1H), 0.95 (s, 9H), 0.93 (s, 3H), 0.92 (s, 9H), 0.90 – 0.88 (m, 15H), 0.57 (q, *J* = 8.0 Hz, 6H), 0.18 (s, 3H), 0.16 (s, 3H), 0.14 (s, 3H), 0.12 (s, 3H), 0.06 – 0.05 (m, 6H); ¹³C NMR (151 MHz, CDCl₃) δ 148.9, 139.8, 137.1, 130.5, 129.3, 128.0, 126.7, 106.3, 79.4, 69.8, 67.1, 64.5, 62.4, 36.3, 26.2, 26.1, 18.6, 18.4, 18.3, 7.0, 4.6, -3.7, -3.9, -4.3, -5.2; [α]_D²⁰ +14.1 (c 0.8, CHCl₃); IR (thin film, neat) 2955, 2858, 1668, 1471, 1388, 1361, 1330, 1256, 1200, 1089, 1007, 933, 837, 778, 672 cm⁻¹; HRMS (ESIP) calcd for C₃₈H₇₅O₅ Si₄ [M+H]⁺: 723.4681, found: 723.4678



(2*R*,3*R*)-3-((*tert*-butyldimethylsilyl)oxy)-2-(((*tert*-butyldimethylsilyl)oxy)methyl)-6-(2-(2-((triethylsilyl)oxy)ethyl)phenyl)-2,3-dihydro-4*H*-pyran-4-one (2.160b)

To a solution of **2.156** (188 mg, 0.26 mmol) in CH₂Cl₂ (3.5 mL) was added 4Å MS (188mg, 100 wt%) and the mixture was allowed to stir at rt for 15 min. DDQ (180 mg, 0.78 mmol) was then added portion wise every 15 min. The resultant yellow suspension was allowed to stir at rt for 1.5h, then was quenched by Et₃N. The crude mixture was purified by flash chromatography (15% EtOAc in hexane) to give the desired product (138 mg, 88%) as a colorless oil. ¹H NMR

(601 MHz, CDCl₃) δ 7.37 – 7.33 (m, 2H), 7.30 (dd, $J = 7.7, 1.3$ Hz, 1H), 7.23 (td, $J = 7.5, 1.3$ Hz, 1H), 5.52 (s, 1H), 4.49 (d, $J = 12.0$ Hz, 1H), 4.36 (ddd, $J = 12.1, 3.6, 2.3$ Hz, 1H), 4.07 (dd, $J = 11.7, 2.4$ Hz, 1H), 4.04 (dd, $J = 11.7, 3.6$ Hz, 1H), 3.77 (t, $J = 6.9$ Hz, 2H), 3.08 (dt, $J = 13.6, 6.8$ Hz, 1H), 2.89 (dt, $J = 13.7, 6.9$ Hz, 1H), 0.94 (s, $J = 2.9$ Hz, 9H), 0.89 – 0.86 (m, 18H), 0.52 (q, $J = 7.9$ Hz, 7H), 0.27 (s, 3H), 0.14 (d, $J = 3.2$ Hz, 3H), 0.04 (d, $J = 3.6$ Hz, 3H), 0.03 (s, 3H); ¹³C NMR (101 MHz, CDCl₃) δ 194.2, 173.3, 138.1, 134.0, 131.4, 130.5, 129.3, 126.5, 104.6, 84.3, 69.4, 63.7, 61.9, 37.2, 26.1, 26.1, 18.8, 18.6, 6.9, 4.5, -3.7, -5.0, -5.1, -5.4; $[\alpha]_D^{20} +123.0$ (c 3.0, CHCl₃); IR (thin film, neat) 2954, 2930, 2880, 2858, 1688, 1603, 1463, 1365, 1253, 1151, 1107, 1007, 974, 837, 780, 745, 673 cm⁻¹; HRMS (ESIP) calcd for C₃₂H₅₉O₅Si₃ [M+H]⁺: 607.3665, found: 607.3651.

APPENDIX B

TOTAL SYNTHESIS OF CLAVOSOLIDE A: A SHOWCASE OF OXIDATIVE OXOCARBENIUM CATION COMPATIBILITY WITH CYCLOPROPANE

General Information

Proton (^1H NMR) and carbon (^{13}C NMR) nuclear magnetic resonance spectra were recorded on a Bruker Avance 300 spectrometer at 300 MHz and 75 MHz, a Bruker Avance 400 spectrometer at 400 MHz and 100 MHz, a Bruker Avance 500 spectrometer at 500 MHz, a Bruker Avance 600 spectrometer at 600 MHz if specified. The chemical shifts are reported in parts per million (ppm) on the delta (δ) scale. The solvent peak was used as a reference value, for ^1H NMR: $\text{CDCl}_3 = 7.26$ ppm, $\text{DMSO} = 2.50$, for ^{13}C NMR: $\text{CDCl}_3 = 77.23$, $\text{DMSO} = 39.52$. Data are reported as follows: (s = singlet; d = doublet; t = triplet; q = quartet; sept = septet; dd = doublet of doublets; ddd = doublet of doublet of doublets; dddd = doublet of doublet of doublet of doublet; td = triplet of doublets; dtd = doublet of triplet of doublets; br = broad). High resolution and low resolution mass spectra were recorded on a VG 7070 spectrometer. Infrared (IR) spectra were collected on a Mattson Cygnus 100 spectrometer. Samples for IR were prepared as a thin film on a NaCl plate by dissolving the compound in CH_2Cl_2 and then evaporating the CH_2Cl_2 . Tetrahydrofuran and diethyl ether were distilled from sodium and benzophenone. Methylene chloride and *t*BuOMe

were distilled from CaH_2 under a N_2 atmosphere prior to use. CuI was purchased from Avacado Chemical research Ltd. (*R*)-TolBINAP was purchased from Strem chemical Inc. Grignard reagent (MeMgBr) was purchased from Sigma-Aldrich. Analytical TLC was performed on E. Merck pre-coated (25 mm) silica gel 60F-254 plates. Visualization was done under UV (254 nm). Flash chromatography was done using ICN SiliTech 32-63 60 Å silica gel. Reagent grade ethyl acetate, diethyl ether, toluene and hexanes (commercial mixture) were purchased from EM Science and used as is for chromatography. All reactions were performed using oven or flame-dried glassware under N_2 with magnetic stirring unless otherwise noted.

General procedure for enol acetate preparation

A mixture of Na_2CO_3 (15% mol equiv.), $[(p\text{-cymene})\text{RuCl}_2]_2$ (0.04 equiv), tri(2-furyl)phosphine (0.08 equiv), acetic acid (2.0 equiv), and 1-decyne (2.0 equiv) in toluene was heated to 80 °C and stirred for 1 h. Another portion of acetic acid (2.0 equiv.) and the alkyne substrate (1.0 equiv.) were dissolved in toluene and added to the mixture (~0.15 M final substrate concentration). The reaction was stirred at 80 °C for 8 h. Then the crude mixture was concentrated on a rotary evaporator and purified by flash column chromatography to give the desired enol acetate product.

General procedure for $[\text{Cp}^*\text{Ru}(\text{MeCN})_3]\text{PF}_6$ catalyzed alkyne hydrosilylation

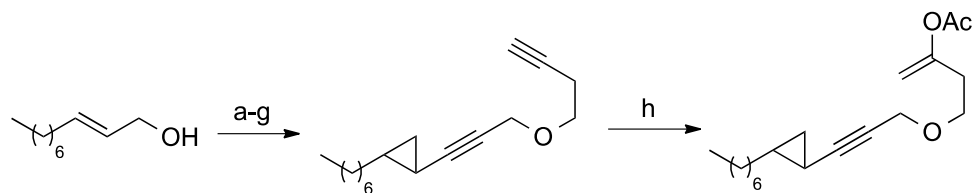
Alkyne (1 eq) and silane (1.2 eq) were dissolved in acetone to give a ~0.5 M solution. $[\text{Cp}^*\text{Ru}(\text{MeCN})_3]\text{PF}_6$ (0.02 eq) was added to the mixture at 0 °C. The reaction was monitored by TLC at 0 °C and, upon starting material consumption, was concentrated and purified by flash chromatography to give the (*Z*)-vinylsilane.

General procedure for $\text{H}_2\text{PtCl}_6 \cdot 6\text{H}_2\text{O}$ catalyzed alkyne hydrosilylation

To a stirred solution of alkyne (1 eq) in THF was added the silane (1.1 eq) and a 0.001 M solution of $\text{H}_2\text{PtCl}_6 \cdot 6\text{H}_2\text{O}$ (0.001 eq) in THF (~0.53 M final substrate concentration). The mixture was heated at 50 °C for 5 h unless specified, cooled and filtered through Celite with Et₂O. The solvent was removed under vacuum and purified by flash chromatography to give the (*E*)-vinylsilane.

General procedure for DDQ cyclization reactions

The substrate (1 equiv), 2,6-dichloropyridine (2 equiv) and 4 Å molecular sieves (200 wt%) were dissolved in anhydrous 1,2-dichloroethane (~0.1 M). The mixture was stirred at room temperature for 15 min, followed by the addition of LiClO_4 (0.2 equiv). After 5 min, DDQ (4 equiv) was added. The reaction was monitored by TLC at rt or 45 °C unless otherwise specified and, upon starting material consumption, was quenched with 5% aqueous NaHCO_3 . The mixture was extracted with CH_2Cl_2 (3x), and the combined organic layers were dried over NaHCO_3 . The filtrate was concentrated in vacuo and purified by flash column chromatography to give the desired product.



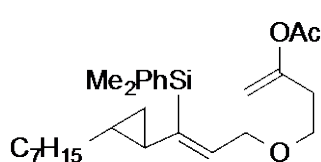
Reagents and conditions

a) Et_2Zn , CH_2I_2 , CH_2Cl_2 , 0 °C to rt, 85%. b) PCC, CH_2Cl_2 , 94%. c) CBr_4 , Zn, PPh_3 , CH_2Cl_2 , 83%. d) $n\text{-BuLi}$, $(\text{CH}_2\text{O})_n$, THF, -78 °C to rt, 82%. e) KOH, 2-chloropyridine, 18-C-6, PhMe, reflux, 89%. f) MeOTf, PhMe, 0 °C. g) MgO, 3-butyn-1-ol, PhCF_3 , 83 °C, 70% (2 steps). h) HOAc, $\text{Ru}(p\text{-cymene})\text{Cl}_2$, Fur_3P , Na_2CO_3 , 1-decyne, PhMe, 80 °C, 41%.

1-(3-(but-3-yn-1-yloxy)prop-1-yn-1-yl)-2-heptylcyclopropane (3.18a)
 C_7H_{15} ^1H NMR (400 MHz, CDCl_3) δ 4.14 (d, $J = 2.0$ Hz, 2H), 3.62 (t, $J = 7.0$ Hz, 2H), 2.49 (td, $J = 7.0, 2.7$ Hz, 2H), 1.99 (t, $J = 2.7$ Hz, 1H), 1.46 – 1.35 (m, 2H), 1.35 – 1.20 (m, 10H), 1.05 (ddt, $J = 15.1, 12.8, 5.6$ Hz, 1H), 0.96 (dtd, $J = 10.5, 4.5, 2.0$ Hz, 1H), 0.88 (t, $J = 6.9$ Hz, 3H), 0.84 – 0.79 (m, 1H), 0.55 (ddd, $J = 8.4, 5.9, 4.3$ Hz, 1H); ^{13}C NMR (101 MHz, CDCl_3) δ 90.5, 81.4, 71.2, 69.5, 67.8, 59.1, 33.8, 32.1, 29.5, 29.5, 29.3, 22.9, 22.8, 19.9, 15.6, 14.3, 6.7; IR (thin film, neat) 2926, 2855, 2226, 1710, 1459, 1256, 1130 cm^{-1} .

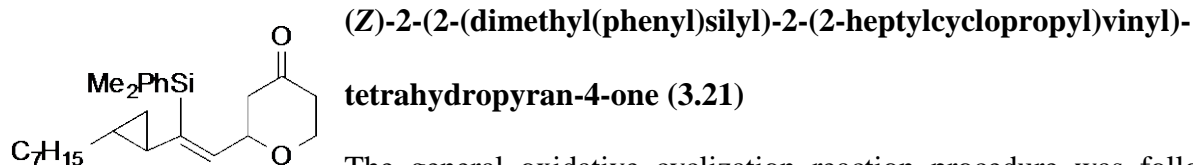
4-((3-(2-heptylcyclopropyl)prop-2-yn-1-yl)oxy)but-1-en-2-yl acetate (3.18b)
 C_7H_{15} The general enol acetate preparation procedure was followed with Na_2CO_3 (8 mg, 0.07 mmol, 0.12 equiv.), $[(p\text{-cymene})\text{RuCl}_2]_2$ (11 mg, 0.019 mmol, 0.04 equiv.), tri(2-furyl)phosphine (9 mg, 0.037 mmol, 0.08 equiv.), acetic acid (106 μL , 1.86 mmol, 4 equiv.), 1-decyne (59 μL , 0.23 mmol, 0.7 equiv) and (108 mg, 0.44 mmol, 1 equiv.) of ether. The reaction was stirred for 2.5 h and purified by flash column chromatography (8% EtOAc in hexane) to give a colorless oil (41 mg, 30%). ^1H NMR (300 MHz, CDCl_3) δ 4.87 – 4.76 (m, 2H),

4.10 (d, $J = 2.0$ Hz, 2H), 3.60 (t, $J = 6.6$ Hz, 2H), 2.52 (td, $J = 6.5, 0.6$ Hz, 2H), 2.14 (s, 3H), 1.46 – 1.33 (m, 2H), 1.33 – 1.23 (m, 7H), 1.17 (dd, $J = 13.8, 6.7$ Hz, 2H), 1.12 – 1.00 (m, 1H), 0.99 – 0.91 (m, 1H), 0.88 (t, $J = 6.7$ Hz, 3H), 0.84 – 0.77 (m, 2H), 0.55 (ddd, $J = 8.4, 5.8, 4.2$ Hz, 1H); ^{13}C NMR (101 MHz, CDCl_3) δ 169.4, 153.5, 103.2, 90.4, 71.4, 66.6, 59.0, 33.9, 33.8, 32.1, 29.5, 29.5, 29.3, 22.9, 22.8, 21.3, 15.6, 14.3, 6.7; IR (thin film neat) 2925, 2854, 1758, 1666, 1368, 1214, 1184, 1100, 1020 cm^{-1} ; HRMS (ESI) calcd for $\text{C}_{19}\text{H}_{31}\text{O}_3$ $[\text{M}+\text{H}]^+$: 307.2273, found: 307.2281.

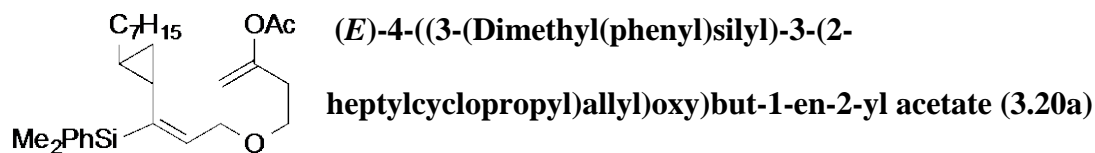


(Z)-4-(3-(Dimethyl(phenyl)silyl)-3-(2-heptylcyclopropyl)allyloxy)but-1-en-2-yl acetate (3.19)

The general *trans*-hydrosilylation reaction procedure was followed with enol acetate ether **3.18b** (60 mg, 0.2 mmol, 1.0 equiv.), $[\text{Cp}^*\text{Ru}(\text{MeCN})_3]\text{PF}_6$ (2 mg, 0.004 mmol, 0.02 equiv.) and dimethylphenylsilane (32 μL , 0.21 mmol, 1.05 equiv.) in 0.5 mL of acetone. Purification by flash column chromatography (5% EtOAc in hexane) afforded (86.2 mg, 66%) of the desired product as a colorless oil. ^1H NMR (400 MHz, CDCl_3) δ 7.53 – 7.50 (m, 2H), 7.36 – 7.32 (m, 3H), 5.97 (td, $J = 6.6, 1.4$ Hz, 1H), 4.75 (d, $J = 1.5$ Hz, 1H), 4.71 (d, $J = 1.5$ Hz, 1H), 3.80 (dd, $J = 6.6, 0.9$ Hz, 2H), 3.26 (t, $J = 6.7$ Hz, 2H), 2.36 (t, $J = 6.5$ Hz, 1H), 2.11 (s, 3H), 1.47 – 1.38 (m, 1H), 1.37 – 1.21 (m, 10H), 1.18 – 1.12 (m, 1H), 1.11 – 1.01 (m, 1H), 0.88 (t, $J = 6.9$ Hz, 3H), 0.81 – 0.71 (m, 1H), 0.70 – 0.64 (m, 1H), 0.45 – 0.41 (m, 6H), 0.41 – 0.35 (m, 1H); ^{13}C NMR (101 MHz, CDCl_3) δ 169.3, 153.6, 143.1, 139.4, 136.3, 133.9, 129.1, 128.0, 103.0, 70.1, 67.1, 34.5, 34.0, 32.1, 29.7, 29.5, 25.4, 22.9, 21.7, 21.3, 14.3, 13.6, -0.8, -0.8; IR (thin film neat) 2957, 2924, 2854, 1759, 1667, 1428, 1368, 1250, 1214, 1185, 1109, 1020, 834, 816, 772, 732 cm^{-1} ; HRMS (ESI) calcd for $\text{C}_{25}\text{H}_{42}\text{O}_3\text{Si}$ $[\text{M}+\text{Na}]^+$: 465.2801, found: 465.2794.

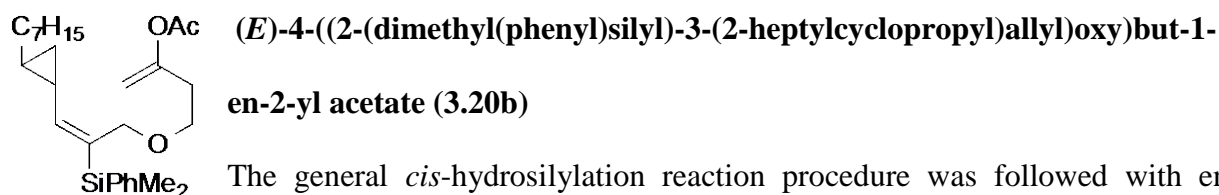


The general oxidative cyclization reaction procedure was followed with **4** (21 mg, 0.047 mmol), 2,6-dichloropyridine (14 mg, 0.094 mmol), 4 Å molecular sieves (42 mg), 1,2 dichloroethane (0.7 mL), LiClO₄ (1.5 mg, 0.014 mmol), and DDQ (32 mg, 0.14 mmol). The reaction was stirred at 45 °C for 8 h, then was quenched with 5% aqueous NaHCO₃. The crude mixture was extracted with CH₂Cl₂, concentrated, and purified by flash chromatography (5%-15% EtOAc in hexane) to give the desired product (11 mg, 54%). ¹H NMR (400 MHz, CDCl₃) δ 7.54 – 7.48 (m, 2H), 7.35 (dd, *J* = 5.5, 1.7 Hz, 3H), 5.80 (ddd, *J* = 8.8, 3.5, 1.4 Hz, 1H), 4.12 – 4.03 (m, *J* = 11.5, 7.3, 1.0 Hz, 1H), 3.99 – 3.91 (m, 1H), 3.17 – 3.07 (m, 1H), 2.53 – 2.40 (m, 1H), 2.30 – 2.20 (m, 1H), 2.18 – 2.05 (m, 1H), 1.35 – 1.17 (m, 13H), 1.15 – 1.00 (m, 1H), 0.94 – 0.79 (m, 4H), 0.74 – 0.64 (m, 1H), 0.46 – 0.45 (m, 3H), 0.43 – 0.42 (m, 3H); ¹³C NMR (101 MHz, CDCl₃) δ 206.5, 145.7, 139.0, 137.3, 137.2, 133.9, 129.4, 128.2, 76.7, 66.1, 48.3, 48.2, 42.1, 34.4, 34.4, 32.1, 29.9, 29.5, 25.3, 25.2, 22.9, 22.4, 21.9, 14.3, 14.1, 13.7, -0.7, -0.7, -0.9; IR (thin film neat) 2955, 2923, 2853, 1721, 1462, 1427, 1374, 1249, 1154, 1111, 1080, 832 cm⁻¹; HRMS (EI) calcd for C₂₅H₃₇O₂Si [M-H]⁺: 397.2563, found: 397.2549.



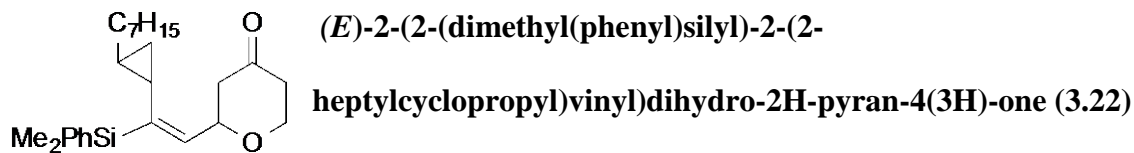
The general *cis*-hydrosilylation reaction procedure was followed with enol acetate ether **3.18b** (31 mg, 0.11 mmol, 1.0 equiv.), H₂PtCl₆•6H₂O (0.06 mg, 0.001 mmol, 0.001 equiv.) and dimethylphenylsilane (20 μL, 0.12 mmol, 1.1 equiv.) in 0.5 mL of THF. Purification by flash column chromatography (5% Et₂O in hexane) afforded (19 mg, 42%) of the

desired product as a colorless oil. ^1H NMR (300 MHz, CDCl_3) δ 7.50 – 7.46 (m, 2H), 7.34 – 7.30 (m, 3H), 5.96 (td, $J = 5.5, 1.7$ Hz, 1H), 4.81 (t, $J = 1.8$ Hz, 2H), 4.28 (ddd, $J = 5.3, 1.7, 1.0$ Hz, 2H), 3.59 (t, $J = 6.6$ Hz, 2H), 2.54 (t, $J = 6.6$ Hz, 2H), 2.13 (s, 3H), 1.33 – 1.15 (m, 12H), 1.12 – 0.95 (m, 2H), 0.70 – 0.59 (m, 1H), 0.46 – 0.37 (m, 1H), 0.35 (s, 6H); ^{13}C NMR (101 MHz, CDCl_3) δ 169.4, 153.7, 142.8, 140.8, 139.3, 134.0, 129.0, 127.9, 103.1, 69.0, 67.7, 34.7, 34.2, 32.1, 29.7, 29.5, 29.4, 22.9, 21.3, 20.6, 19.9, 14.3, 13.7, –1.7, –1.7; IR (thin film, neat) 2955, 2924, 2854, 1722, 1674, 1462, 1372, 1250, 1181, 1120, 815 cm^{-1} ; HRMS (ESI) calcd for $\text{C}_{27}\text{H}_{42}\text{NaO}_3\text{Si}$ $[\text{M}+\text{Na}]^+$: 465.2801, found: 465.2794.



The general *cis*-hydrosilylation reaction procedure was followed with enol acetate ether **3.18b** (31 mg, 0.11 mmol, 1.0 equiv.), $\text{H}_2\text{PtCl}_6 \cdot 6\text{H}_2\text{O}$ (0.06 mg, 0.001 mmol, 0.001 equiv.) and dimethylphenylsilane (20 μL , 0.12 mmol, 1.1 equiv.) in 0.5 mL of THF. Purification by flash column chromatography (5% Et_2O in hexane) afforded (19 mg, 44%) of the desired product as a colorless oil. ^1H NMR (400 MHz, CDCl_3) δ 7.52 – 7.49 (m, 2H), 7.32 (dd, $J = 4.2, 2.3$ Hz, 2H), 5.19 (d, $J = 9.9$ Hz, 1H), 4.73 (dd, $J = 11.8, 1.5$ Hz, 2H), 4.21 (qd, $J = 11.3, 1.2, 1.0$ Hz, 2H), 3.42 (t, $J = 6.8$ Hz, 2H), 2.40 (dd, $J = 7.1, 6.4$ Hz, 2H), 2.12 (s, 3H), 1.42 (qd, $J = 8.5, 4.5$, 1H), 1.36 (d, $J = 2.8$ Hz, 2H), 1.25 (s, broad, 10H), 0.88 (t, $J = 6.8$, 3H), 0.83 (s, 1H), 0.80 – 0.69 (m, 1H), 0.63 – 0.57 (m, 1H), 0.57 – 0.52 (m, 1H), 0.34 (s, 6H); ^{13}C NMR (101 MHz, CDCl_3) δ 169.3, 153.8, 149.0, 139.4, 134.3, 133.2, 128.8, 127.7, 103.0, 69.9, 67.3, 33.9, 32.1, 29.9, 29.6, 22.9, 22.2, 21.3, 19.6, 15.5, 14.3, –2.2 ; IR (thin film, neat) 2953, 2920, 2852, 1720,

1663, 1460, 1378, 12542, 1185, 815 cm^{-1} ; HRMS (ESI) calcd for $\text{C}_{27}\text{H}_{42}\text{NaO}_3\text{Si}$ $[\text{M}+\text{Na}]^+$: 465.2801, found: 465.2832.



The general cyclization reaction procedure was followed with **3.20a** (10 mg, 0.023 mmol), 2,6-dichloropyridine (21 mg, 0.14 mmol), 4 Å molecular sieves (21 mg), 1,2-dichloroethane (0.5 mL), LiClO_4 (0.7 mg, 0.007 mmol), and DDQ (16 mg, 0.069 mmol). The reaction was stirred at 45 °C for 4 h, then was quenched with 5% aqueous NaHCO_3 . The crude mixture was extracted with CH_2Cl_2 , concentrated, and purified by flash chromatography (5%-15% EtOAc in hexane) to give the desired product as a 3.6:1 mixture of diastereomers (5.1 mg, 56%). Major diastereomer: ^1H NMR (400 MHz, CDCl_3) δ 7.48 – 7.43 (m, 2H), 7.37 – 7.30 (m, 3H), 5.87 (dt, $J = 7.2, 1.3$ Hz, 1H), 4.80 – 4.72 (m, 1H), 4.37 – 4.31 (m, 1H), 3.75 (tt, $J = 11.9, 2.7$ Hz, 1H), 2.64 (ddd, $J = 13.8, 12.6, 7.4$ Hz, 1H), 2.54 – 2.31 (m, 3H), 1.25 (s, br, 12H), 0.92 – 0.84 (m, 5H), 0.68 – 0.60 (m, 1H), 0.51 (dt, $J = 8.3, 4.9$ Hz, 1H), 0.36 (s, br, 6H). For the mixture of inseparable diastereomers: ^{13}C NMR (126 MHz, CDCl_3) δ 206.83, 206.78, 144.4, 144.2, 141.7, 141.6, 138.7, 134.0, 133.9, 129.4, 129.2, 128.2, 128.0, 75.6, 75.4, 66.9, 66.1, 48.0, 47.8, 42.5, 34.63, 34.58, 32.1, 29.6, 29.5, 29.4, 29.3, 22.88, 22.9, 20.8, 20.5, 20.2, 20.0, 14.34, 14.29, 14.1, 13.8, -0.7, -0.8, -1.68, -1.72; IR (thin film neat) 2956, 2924, 2854, 1759, 1666, 1612, 1462, 1428, 1368, 1246, 1213, 1184, 1109, 1019, 815, 833 cm^{-1} ; HRMS (ESI) calcd for $\text{C}_{25}\text{H}_{39}\text{O}_2\text{Si}$ $[\text{M}+\text{H}]^+$: 399.2735, found: 399.2735.



To a stirred solution of acetyl chloride (6.9 mL, 100 mmol) and allyl chloride (16.3 mL, 200 mmol) in CH₂Cl₂ was added AlCl₃ (16 g, 120 mmol, 1.2 equiv.) in portions over 20 min. The mixture was stirred for 2 h at 0 °C and for 1 h at rt. The reaction was quenched by pouring the mixture onto crushed ice (100 g). The organic layer was separated, dried with Na₂SO₄, and filtered. Triethylamine (21 mL, 150 mmol, 1.5 equiv.) was added, then the mixture was refluxed for 2 h, cooled to rt and washed successively with HCl (2 x 100 mL), NaHCO₃ (2 x 100 mL), H₂O (1 x 200 mL) and brine (1 x 200 mL). The combined organic extracts were dried with Na₂SO₄ and concentrated. Purification by flash chromatography (10:90 EtOAc: hexane) yielded the desired product (4.03 g, 34%). ¹H NMR (500 MHz, CDCl₃) δ 6.79 (dt, *J* = 15.7, 6.1 Hz, 1H), 6.31 (d, *J* = 15.7 Hz, 1H), 4.19 (dd, *J* = 6.1, 1.4 Hz, 2H), 2.30 (s, 3H); ¹³C NMR (126 MHz, CDCl₃) δ 197.8, 140.4, 132.5, 42.9, 27.6. IR (thin film, neat) 1701, 1680, 1636, 1424, 1362, 1254, 977 cm⁻¹. *These data are consistent with literature values.*¹⁰



The catalyst was prepared by stirring CuI (76 mg, 0.40 mmol,) and (*R*)-TolBINAP (407 mg, 0.60 mmol) in anhydrous *t*BuOMe (320 mL) for 1 h to give a clear yellow solution. The mixture was cooled to -78 °C and MeMgBr (2.7 M solution in Et₂O, 17 mL, 46 mmol) was added. After stirring for 10 min, a solution of **3.27** (4.74 g, 40 mmol) in anhydrous CH₂Cl₂ (320 mL) was added over 2 h with a syringe pump. The mixture was stirred for 4 h (including addition time) at -78 °C. The reaction was quenched at -78 °C with EtOH (16 mL, 0.4 mL/mmol substrate), followed by a 1 M aq. NH₄Cl-solution (80 mL, 2 mL/mmol substrate), and was allowed to warm

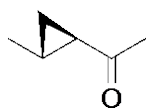
¹⁰ Kulinkovich, O. G.; Tischenko, I. G.; Sorokin, V. L. *Synthesis* **1985**, 1058.

to room temperature. A 1 M aq. NH_4Cl -solution (200 mL, 5 mL/mmol substrate) and Et_2O (100 mL, 2.5 mL/mmol substrate) were added and the layers were separated. After extraction with Et_2O (2 x 200 mL, 5 mL/mmol substrate), the combined organic extracts were dried and carefully concentrated to a yellow oil. Purification by flash chromatography (10:90 EtOAc: hexane) yielded the desired product (3.9 g, 72%). ^1H NMR (500 MHz, CDCl_3) δ 3.56 (dd, $J = 10.8, 4.8$ Hz, 1H), 3.47 (dd, $J = 10.8, 5.4$ Hz, 1H), 2.69 (dd, $J = 17.1, 5.8$ Hz, 1H), 2.43 (td, $J = 11.9, 5.5$ Hz, 1H), 2.35 (dd, $J = 17.1, 7.1$ Hz, 1H), 2.16 (s, 3H), 1.03 (d, $J = 6.7$ Hz, 3H); ^{13}C NMR (126 MHz, CDCl_3) δ 207.5, 50.6, 47.2, 31.1, 30.6, 17.9. $[\alpha]_{\text{D}}^{20} +4.7$ (c 0.95, CHCl_3); IR (thin film, neat) 2962, 1714, 1459, 1440, 1408, 1366, 1299, 1159 cm^{-1} .



Figure 3.10 HPLC traces for conjugate addition product of 3.29: Enantioenriched sample (pink) and racemic mixture (black)

Ee was determined to be >90% by chiral HPLC analysis using a Phenomenex Lux 5μ Cellulose-3 column (250 x 4.60 mm) with isopropanol/Hexane (0.5/95.5, v/v); 25 °C over 30 min; 0.7mL/min; retention times (min): 10.2 min (*S*-addition product), 10.5 min (*R*-addition product).



1-((1R,2R)-2-Methylcyclopropyl)ethanone (3.30)¹¹

To a solution of NaOH (3.54 g, 0.088 mmol) in of H₂O (4.4 mL) was added the chloro ketone **3.29** (7.9 g, 59 mmol) over 20 min with a 10 mL syringe. The reaction mixture was stirred for 1 h (including addition time) at 80 °C. H₂O (8.7 mL) was added slowly to the reaction mixture over a 20 min period, and the mixture heated under reflux for an additional hour. Upon cooling to rt, the reaction mixture was extracted with Et₂O (2 x 15 mL). The aqueous layer of the extraction was saturated with K₂CO₃ and extracted with additional Et₂O (15 mL). The combined organic layers were dried over Na₂SO₄ and concentrated at 0 °C under reduced pressure (168 mm Hg) to yield the desired compound (5.55 g, 96%). ¹H NMR (400 MHz, CDCl₃) δ 2.22 (s, 3H), 1.67 (ddd app dt, *J* = 8.1, 4.2, 4.2 Hz, 1H), 1.46-1.36 (m, 1H), 1.23 (ddd, *J* = 8.5, 4.5, 3.8 Hz, 1H), 1.11 (d, *J* = 6.0 Hz, 3H), 0.72 (ddd, *J* = 7.9, 6.5, 3.7 Hz, 1H); ¹³C NMR (101 MHz, CDCl₃) δ 208.7, 30.6, 30.5, 20.3, 19.6, 18.3. IR (thin film neat) 2923, 1706, 1601, 1451, 1195, 1114, 808 cm⁻¹; [α]_D²⁰ -125.7 (*c* 0.82, CHCl₃).



3-((1R,2R)-2-Methylcyclopropyl)prop-2-yn-1-ol (3.32)

To a solution of LDA prepared at 0 °C from diisopropylamine (2.98 mL, 21.2 mmol) and *n*-butyllithium in hexane (1.56M, 13.6 mL, 21.2 mmol) in dry THF (40 mL) at -78 °C was added **3.30** (1.98 g, 20.2 mmol) in THF (25 mL). The solution was stirred for 1 h, then diethyl chlorophosphate (3.51 mL, 24.2 mmol) was added. The mixture was allowed to warm to rt slowly over 2-3 h, then was added dropwise over 45 min to a solution of LDA in THF (46.5 mmol) prepared at 0 °C as described above. The reaction was allowed to stir at 0 °C for 30

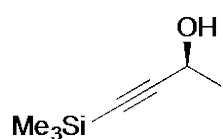
¹¹ Cannon, G. W.; Ellis, R. C.; Leal, J. R., *Organic Synth.* **1963**, *4*, 597.

min, producing a brown-black color and a precipitate. HMPA (13 mL, 71 mmol) was added and the mixture was warmed to 5 °C. Paraformaldehyde (1.87 g, 61 mmol, 3.0 equiv.) was added and the mixture was refluxed for 1 h. The reaction was quenched with saturated NH₄Cl (100 mL) and EtOAc (100 mL). After extraction with EtOAc (2x 75 mL), the combined yellow-orange organic extracts were dried and concentrated. Purification by flash chromatography (15% EtOAc in hexane) yielded the desired product (1.36 g, 61%). ¹H NMR (500 MHz, CDCl₃) δ 4.22 (s, 2H), 1.51 (s, br, 1H), 1.11 – 1.04 (m, 4H), 0.93 (dddd, *J* = 8.6, 4.9, 2.0, 2.0 Hz, 1H), 0.85 – 0.81 (m, 1H), 0.54 (ddd, *J* = 7.0, 4.4, 4.4 Hz, 1H); ¹³C NMR (126 MHz, CDCl₃) δ 89.7, 74.1, 51.7, 18.5, 17.0, 16.7, 7.7; [α]_D²⁰ –117.8 (*c* 0.93, CHCl₃); IR (thin film, neat) 3333, 3055, 2955, 2929, 2868, 2227, 1444, 1377, 1308, 1068, 1013, 965, 908, 848, 775 cm⁻¹; HRMS (EI) calcd for C₇H₁₀O [M]⁺: 110.0732, found: 110.0699 cm⁻¹.



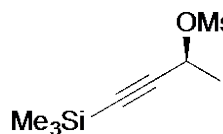
3-((1*R*,2*R*)-2-Methylcyclopropyl)prop-2-ynyl methanesulfonate (3.33)

To the cyclopropyl homopropargylic alcohol (50 mg, 0.45 mmol) in CH₂Cl₂ (1 mL) at 0 °C followed by Et₃N (130 μL, 0.91 mmol) and of methanesulfonyl chloride (45 μL, 0.55 mmol). The reaction was stirred for 1 h then was quenched with sat. aq. NaHCO₃ solution. The mixture was allowed to warm to room temperature, then was concentrated in vacuo and diluted with H₂O (5 mL) and Et₂O (10 mL). The organic layer was separated, dried (MgSO₄), filtered and concentrated to yield the desired product (63 mg, 73%), which was used without further purification. *Characterization was not performed on this intermediate due to its instability and volatility.*



(S)-4-Trimethylsilyl-3-butyn-2-ol

To 4-(trimethylsilyl)-3-butyn-2-one (3.12 g, 22.2 mmol) in CH₂Cl₂ (65 mL) was added (*S,S*)-Noyori-TsDPEN catalyst (280 mg, 0.445 mmol) in CH₂Cl₂ (3 mL) and NEt₃ (9.4 mL, 68 mmol). The mixture was cooled to 10 °C and formic acid (6 mL, 155 mmol) was added dropwise over 2 h. The reaction was stirred at rt overnight. CH₂Cl₂ was partially removed under reduced pressure. The mixture was diluted with 80 mL of pentane, and K₂CO₃ (13g) and MgSO₄ (8g) were added. The slurry was stirred vigorously for 2 h at rt, then was filtered through a plug of silica gel and concentrated under reduced pressure to yield the desired product (3.04 g, 96%). ¹H NMR (300 MHz, CDCl₃) δ 4.52 (dt, *J* = 13.0, 6.6 Hz, 1H), 1.79 (d, *J* = 5.2 Hz, 1H), 1.45 (d, *J* = 6.6 Hz, 3H), 0.17 (s, 9H). [α]_D²⁰ -23.8 (*c* 0.93, CHCl₃). The dr of the (*R*)-Mosher ester of this material was found to be > 95:5 by ¹⁹F NMR analysis. [δ -72.02 (major) and δ -71.66 (minor), in CDCl₃]. *These data are consistent with literature values.*¹²

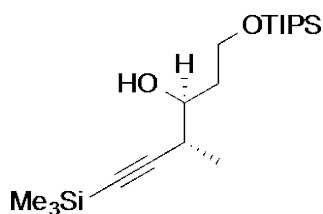


(S)-3-Butyn-2-yl Mesylate (3.35)

To (*S*)-4-trimethylsilyl-3-butyn-2-ol (1.84 g, 12.9 mmol) in CH₂Cl₂ (155 mL) at -78 °C was added Et₃N (3.7 mL, 26.1 mmol) and methanesulfonyl chloride (1.6 mL, 19.8 mmol). The solution was stirred at -78 °C for 1 h then was quenched with sat. aq. NaHCO₃ solution. The mixture was allowed to warm to room temperature, concentrated in vacuo and then diluted with H₂O (100 mL) and Et₂O (50 mL). The organic layer was separated, dried over MgSO₄, filtered and concentrated to the desired product (2.65 g, 93%), which was used without further purification. ¹H NMR (400 MHz, CDCl₃) δ 5.24 (q, *J* = 6.7 Hz, 1H), 3.10 (s, 3H), 1.61 (d, *J* = 6.7 Hz, 3H), 0.19 – 0.15 (m, 9H). ¹³C NMR (126 MHz, CDCl₃) δ 101.4, 93.8, 68.7, 39.3,

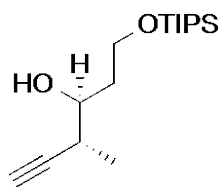
¹² Marshall, J. A.; Chobanian, H. R.; Yanik, M. M. *Org. Lett.* **2001**, *3*, 3369.

22.6, -0.3. $[\alpha]_D^{20} -109.3$ (c 1.18, CHCl_3); lit $[\alpha]_D^{20} -113.5$ (c 1.18, CHCl_3); er > 90:10 based on optical rotation. *These data are consistent with literature values.*¹²



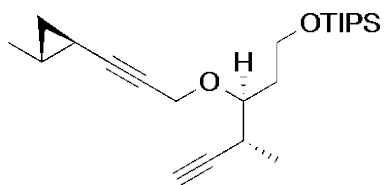
(3*S*,4*R*)-4-Methyl-1-(triisopropylsilyloxy)-6-(trimethylsilyl)hex-5-yn-3-ol (3.36)

To a solution of $\text{Pd}(\text{OAc})_2$ (107 mg, 0.48 mmol) in THF (67 mL) at -78 °C was added PPh_3 (125 mg, 0.48 mmol). Mesylate **3.35** (3.48 g, 11.4 mmol) and aldehyde **3.34** (2.20 g, 9.52 mmol) were added, followed by Et_2Zn (1M in hexane, 28.6 mL, 28.6 mmol, added dropwise over 15 min). The resulting yellow solution was immediately warmed to -20 °C and stirred for 16 h. The reaction was quenched by pouring into a rapidly stirring solution of sat. aq. NH_4Cl (50 mL). After 15 min the phases were separated and the aqueous layer was extracted with (2 x 50 mL) Et_2O . The combined organic layers were washed with brine, dried over MgSO_4 , filtered, and concentrated. Purification by flash chromatography (10% EtOAc in hexane) provided the desired product (3.08 g, 82%) as an inseparable 8:1 mixture with the *syn*-diastereomer. ^1H NMR (400 MHz, CDCl_3) δ 4.01 – 3.87 (m, 2H), 3.78 (dt, $J = 7.5, 3.5$ Hz, 1H), 3.14 (s, 1H), 2.62 (qd, $J = 7.0, 4.3$ Hz, 1H), 1.86 – 1.69 (m, 2H), 1.21 (d, $J = 7.1$ Hz, 3H), 1.06 (dd, $J = 6.4, 3.7$ Hz, 21H), 0.15 (d, $J = 3.5$ Hz, 9H). ^{13}C NMR (101 MHz, CDCl_3) δ 108.5, 86.8, 73.7, 62.7, 36.2, 34.0, 18.2, 16.5, 12.0, 0.4. $[\alpha]_D^{20} +6.6$ (c 1.11, CHCl_3); IR (thin film, neat) 3502, 2944, 2893, 2867, 2165, 1463, 1385, 1249, 1100, 1012, 994, 921, 843, 759 cm^{-1} ; HRMS (ASAP+) calcd for $\text{C}_{19}\text{H}_{39}\text{OSi}_2$ $[\text{M}-\text{OH}]^+$: 339.2539, found: 339.2546.



(3*S*,4*R*)-4-Methyl-1-((triisopropylsilyloxy)hex-5-yn-3-ol

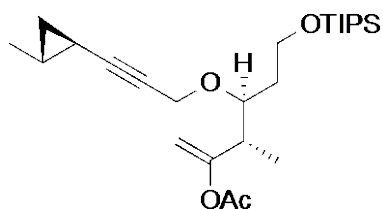
For analytical purpose of determining e.r., (20 mg, 0.056 mmol, 1.0 equiv.) of **3.36** was dissolved in 0.5 mL of MeOH and (24 mg, 0.056 mmol, 1.0 equiv) of K_2CO_3 was added at rt. After 1.5 h, the reaction was quenched with 1 mL of sat. NH_4Cl and extracted with (3 x 5 mL) of Et_2O . The combined extracts were washed with H_2O (2 x 5 mL) and dried over $MgSO_4$. Purification by flash column chromatography (10% Et_2O in hexane) to yield a clear oil (12 mg, 75%) of the major desilylated *anti*-homopropargylic alcohol. 1H NMR (500 MHz, $CDCl_3$) δ 4.03 (ddd, $J = 9.4, 5.4, 1.5$ Hz, 1H), 3.95-3.90 (m, 1H), 3.86 (s, $J = 2.3$ Hz, 1H), 3.74 – 3.69 (m, 1H), 2.56 – 2.49 (m, 1H), 2.06 (dd, $J = 2.4, 1.7$ Hz, 1H), 1.95 (ddd, $J = 6.5, 3.3, 1.7$ Hz, 1H), 1.92 (ddd, $J = 6.5, 3.3, 1.7$ Hz, 1H), 1.79 (dddd, $J = 10.9, 9.3, 4.2, 1.6$ Hz, 1H), 1.23 (d, $J = 7.0$ Hz, 3H), 1.06-1.00 (m, 21 H). The ee of this material was found to be 87% by ^{19}F NMR analysis. [$\delta -71.49$ (minor) and $\delta -71.60$ (major), in $CDCl_3$] of the (*R*)-Mosher ester.



Triisopropyl((3*S*,4*R*)-4-methyl-3-(3-((1*R*,2*R*)-2-methylcyclopropyl)prop-2-ynyloxy)hex-5-ynyloxy)silane

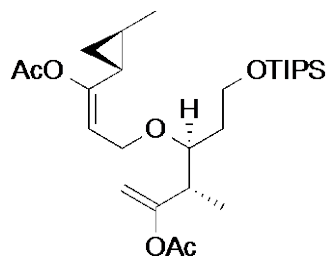
To the homopropargylic alcohol **3.36** (660 mg, 1.84 mmol) and mesylate **3.35** (289 mg, 1.54 mmol) in THF (4 mL) at 0 °C was added 15-crown-5 (425 μ L, 2.15 mmol). The reaction stirred for 15 min, then NaH (85 mg, 2.1 mmol) was added portion wise (17 mg/5 mins). The reaction was warmed to rt and stirred overnight. The reaction was quenched with brine (3 mL) and extracted with Et_2O (3 x 5mL). The combined organic extracts were dried and the solvent was concentrated in vacuo. Purification by flash chromatography (5% EtOAc in hexane) provided the desired product (414 mg, 63%). 1H NMR (400 MHz, $CDCl_3$) δ 4.18 (d, $J = 2.0$ Hz, 2H), 3.81

(dd, $J = 7.1, 5.5$ Hz, 2H), 3.68 (dt, $J = 8.3, 4.2$ Hz, 1H), 2.80 (dtd, $J = 6.9, 4.4, 1.4$ Hz, 1H), 2.06 (d, $J = 2.5$ Hz, 1H), 1.93 – 1.83 (m, 1H), 1.81 – 1.71 (m, 1H), 1.21 (d, $J = 7.0$ Hz, 3H), 1.09 – 1.04 (m, 25H), 0.95 – 0.87 (m, 1H), 0.85 – 0.77 (m, 1H), 0.54 – 0.48 (m, 1H); ^{13}C NMR (101 MHz, CDCl_3) δ 89.5, 86.2, 78.2, 72.2, 69.9, 60.3, 58.3, 34.6, 29.5, 18.5, 18.2, 16.8, 16.6, 16.0, 12.2, 7.8; $[\alpha]_{\text{D}}^{20} -37.2$ (c 0.90, CHCl_3); IR (thin film, neat) 3311, 2943, 2866, 2239, 1462, 1379, 1250, 1100, 1060, 882, 847 cm^{-1} ; HRMS (ESI) calcd for $\text{C}_{23}\text{H}_{40}\text{O}_2\text{Si}$ $[\text{M}+\text{H}]^+$: 377.2876, found: 377.2881.



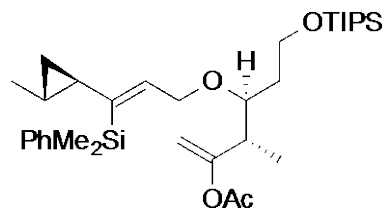
(3*S*,4*S*)-3-Methyl-4-(3-((1*R*,2*R*)-2-methylcyclopropyl)prop-2-ynyloxy)-6-(triisopropylsilyloxy)hex-1-en-2-yl acetate (3.37)

A mixture of Na_2CO_3 (13 mg, 0.12 mmol), $[(p\text{-cymene})\text{RuCl}_2]_2$ (20 mg, 0.033 mmol), tri(2-furyl)phosphine (0.08 equiv), acetic acid (190 μL , 3.3 mmol), and 1-decyne (300 μL , 1.67 mmol) in toluene (1 mL) was heated to 80 $^\circ\text{C}$ and stirred for 1 h. The alkyne substrate (311 mg, 0.83 mmol) was dissolved in toluene (1 mL) and added to the mixture. The reaction was stirred at 80 $^\circ\text{C}$ for 6 h. The crude mixture was concentrated and purified by flash chromatography (5% EtOAc in hexane) to give the desired product (357 mg, 55%). ^1H NMR (400 MHz, CDCl_3) δ 4.78 (s, br, 2H), 4.11 – 4.05 (m, 2H), 3.73 (dd, $J = 7.5, 4.8$ Hz, 3H), 2.70 (dd, $J = 6.8, 4.7$ Hz, 1H), 2.09 (s, 3H), 1.68 – 1.61 (m, 1H), 1.57 – 1.50 (m, 1H), 1.10 – 0.94 (m, 27H), 0.89 – 0.83 (m, 1H), 0.79 – 0.73 (m, 1H), 0.49 – 0.44 (m, 1H); ^{13}C NMR (101 MHz, CDCl_3) δ 169.2, 157.5, 102.5, 89.4, 76.2, 72.2, 60.2, 58.0, 40.3, 33.4, 21.3, 18.5, 18.3, 16.9, 16.6, 12.2, 7.8; $[\alpha]_{\text{D}}^{20} -24.4$ (c 0.8, CHCl_3); IR (thin film, neat) 2943, 2866, 1762, 1661, 1463, 1368, 1220, 1180, 1097, 1057, 882 cm^{-1} ; HRMS (ESI) calcd for $\text{C}_{25}\text{H}_{44}\text{NaO}_4\text{Si}$ $[\text{M}+\text{Na}]^+$: 459.2907, found: 459.2948.



(3S,4S)-4-(((E)-3-Acetoxy-3-((1R,2R)-2-methylcyclopropyl)allyl)oxy)-3-methyl-6-((triisopropylsilyl)oxy)hex-1-en-2-yl acetate (3.38)

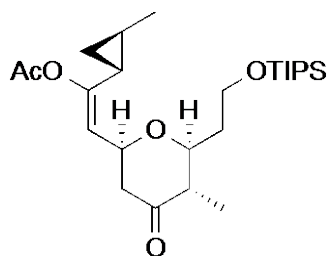
A mixture of Na_2CO_3 (40 mg, 0.36 mmol), $[(p\text{-cymene})\text{RuCl}_2]_2$ (52 mg, 0.085 mmol), tri(2-furyl)phosphine (40 mg, 0.17 mmol), acetic acid (495 μL , 8.54 mmol), and 1-decyne (610 μL , 2.85 mmol) was stirred at 80 $^\circ\text{C}$ for 1 h. The ether (536 mg, 1.42 mmol) was added and the reaction was stirred for 12 h at 80 $^\circ\text{C}$. The mixture was purified by flash chromatography (20% EtOAc in hexane) to give the desired product (487 mg, 69%). ^1H NMR (500 MHz, CDCl_3) δ 5.30 (t, $J = 7.3$ Hz, 1H), 4.84 (app d, $J = 4.9$ Hz, 1H), 4.23 (dd, $J = 11.6$, 7.3 Hz, 1H), 4.15 – 4.10 (m, 1H), 3.83 – 3.75 (m, 2H), 3.73 (ddd, $J = 9.6$, 4.8, 2.6 Hz, 1H), 2.79 – 2.73 (m, 1H), 2.13 (s, 3H), 2.08 (s, 3H), 1.74 – 1.67 (m, 1H), 1.59 – 1.52 (m, 1H), 1.44 – 1.39 (m, 1H), 1.14 – 1.03 (m, 27H), 1.02 – 0.94 (m, 1H), 0.77 – 0.73 (m, 1H), 0.48 (dt, $J = 8.7$, 5.1 Hz, 1H); ^{13}C NMR (126 MHz, CDCl_3) δ 169.4, 169.3, 157.6, 151.4, 114.9, 102.5, 76.3, 64.9, 60.1, 40.3, 33.6, 21.3, 21.0, 19.1, 18.6, 18.3, 13.7, 13.6, 12.2, 12.1; $[\alpha]_{\text{D}}^{20}$ -21.3 (c 0.31, CHCl_3); IR (thin film, neat) 2943, 2866, 1761, 1663, 1463, 1369, 1218, 1178, 1098, 1068, 882 cm^{-1} ; HRMS (ESI) calcd for $\text{C}_{27}\text{H}_{48}\text{O}_6\text{Si}$ $[\text{M}+\text{Na}]^+$: 519.3118, found: 519.3097.



(3S,4S)-4-(((Z)-3-(Dimethyl(phenyl)silyl)-3-((1R,2R)-2-methylcyclopropyl)allyl)oxy)-3-methyl-6-((triisopropylsilyl)oxy)hex-1-en-2-yl acetate (3.39)

To a solution of with enol acetate ether **3.37** (8 mg, 0.02 mmol) and dimethylphenylsilane (5 μL , 0.02 mmol) in acetone (0.5 mL) was added $[\text{Cp}^*\text{Ru}(\text{MeCN})_3]\text{PF}_6$ (0.2 mg, 0.0004 mmol). The

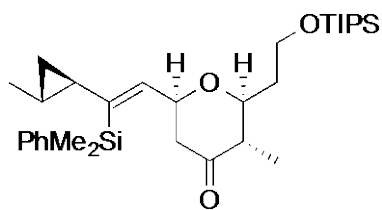
mixture was stirred for 3 h then was purified by flash column chromatography (5% ether in hexane) to provide the desired product (7.4 mg, 71%). ¹H NMR (400 MHz, CDCl₃) δ 7.52 – 7.48 (m, 2H), 7.35 – 7.31 (m, 3H), 5.98 (td, *J* = 6.6, 1.6 Hz, 1H), 4.77 (s, 2H), 3.91 (dd, *J* = 12.1, 6.9 Hz, 1H), 3.77 – 3.74 (m, 1H), 3.71 (dd, *J* = 7.6, 4.4 Hz, 2H), 3.48 (ddd, *J* = 9.6, 4.6, 2.6 Hz, 1H), 2.48 (qd, *J* = 6.9, 4.4 Hz, 1H), 2.06 (s, 3H), 1.61 (dtd, *J* = 10.3, 7.7, 2.6 Hz, 1H), 1.55 – 1.43 (m, 1H), 1.04 (s, 24H), 0.93 (d, *J* = 7.0 Hz, 3H), 0.90 (dd, *J* = 6.9, 4.1 Hz, 1H), 0.77 – 0.70 (m, 1H), 0.69 – 0.63 (m, 1H), 0.43 (s, 3H), 0.42 (s, 3H), 0.35 – 0.29 (m, 1H); ¹³C NMR (101 MHz, CDCl₃) δ 169.1, 157.5, 141.4, 139.3, 137.2, 133.9, 129.1, 128.1, 102.4, 69.5, 60.2, 40.2, 33.5, 26.9, 21.3, 19.3, 18.3, 15.6, 14.0, 12.2, 11.9, -0.8, -0.9; [α]_D²⁰ -11.4 (*c* 0.74, CHCl₃); IR (thin film, neat) 2944, 2866, 1761, 1462, 1368, 1220, 1179, 1098, 834 cm⁻¹; HRMS (ESI) calcd for C₃₃H₅₇O₄Si₂ [M+H]⁺: 573.3795, found: 573.3810.



(*E*)-2-((2*S*,5*S*,6*S*)-5-Methyl-4-oxo-6-(2-((triisopropylsilyl)oxy)ethyl)tetrahydro-2H-pyran-2-yl)-1-((1*S*,2*S*)-2-methylcyclopropyl)vinyl acetate (3.40)

The general cyclization reaction procedure was followed with **3.38** (90 mg, 0.18 mmol), 2,6-dichloropyridine (54 mg, 0.36 mmol), 4 Å molecular sieves (180 mg), 1,2 dichloroethane (5 mL), LiClO₄ (6 mg, 0.05 mmol), and DDQ (165 mg, 0.73 mmol). The reaction was stirred at rt for 1.5 h, then was quenched with 5% aqueous NaHCO₃. The crude mixture was extracted with CH₂Cl₂, concentrated, and purified by flash chromatography (5% EtOAc in hexane) to give the desired product (81 mg, 62%). ¹H NMR (400 MHz, CDCl₃) δ 5.25 (d, *J* = 8.3 Hz, 2H), 4.51 (ddd, *J* = 10.0, 8.2, 4.1 Hz, 1H), 3.95 – 3.84 (m, 2H), 3.58 – 3.51 (m, 1H), 2.55 – 2.50 (m, 2H), 2.40 (dq, *J* = 12.6, 6.4 Hz, 1H), 2.11 (s, 3H), 2.01 (dddd, *J* = 14.6, 8.5,

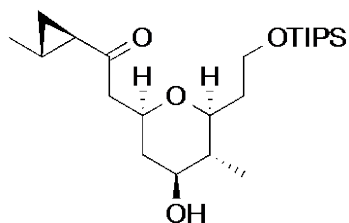
6.1, 2.1 Hz, 1H), 1.76 (app dq, dddd, $J = 8.9, 8.9, 8.9, 4.4$ Hz, 1H), 1.39 – 1.34 (m, 1H), 1.09 (d, $J = 2.4$ Hz, 3H), 1.07 (s, 24H), 1.00 – 0.89 (m, 1H), 0.87 – 0.81 (m, 1H), 0.51 (dt, $J = 8.6, 5.1$ Hz, 1H); ^{13}C NMR (101 MHz, CDCl_3) δ 208.4, 169.0, 151.3, 117.8, 79.6, 73.5, 59.5, 50.2, 48.5, 37.6, 21.0, 19.4, 18.6, 18.2, 13.9, 13.8, 12.2, 9.5; $[\alpha]_{\text{D}}^{20} -31.8$ (c 0.63, CHCl_3); IR (thin film, neat) 2943, 2867, 1762, 1717, 1462, 1369, 1209, 1098, 1067, 883 cm^{-1} ; HRMS (ESI) calcd for $\text{C}_{25}\text{H}_{44}\text{NaO}_5\text{Si}$ $[\text{M}+\text{Na}]^+$: 475.2856, found: 475.2855.



(2*S*,3*S*)-6-((*Z*)-2-(Dimethyl(phenyl)silyl)-2-((1*R*,2*R*)-2-methylcyclopropyl)vinyl)-3-methyl-2-(((triisopropylsilyloxy)ethyl)dihydro-2*H*-pyran-4(3*H*)-one
(3.41)

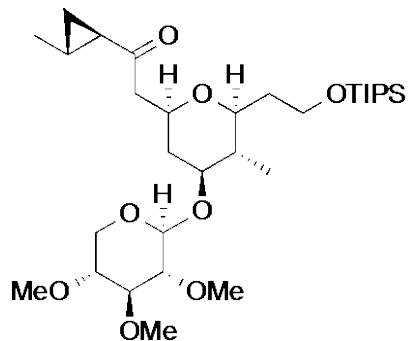
The general cyclization reaction procedure was followed with **3.39** (7.4 mg, 0.013 mmol), 2,6-dichloropyridine (16 mg, 0.11 mmol), 4 Å molecular sieves (21 mg), 1,2 dichloroethane (0.5 mL), LiClO_4 (1 mg, 0.01 mmol), and DDQ (12 mg, 0.052 mmol). The reaction was stirred at 45 °C for 4 h, then was quenched with 5% aqueous NaHCO_3 . The crude mixture was extracted with CH_2Cl_2 , concentrated, and purified by flash chromatography (5%-15% ether in hexane) to give the desired product (3.5 mg, 51%). ^1H NMR (400 MHz, CDCl_3) δ 7.50 – 7.45 (m, 2H), 7.35 – 7.31 (m, 3H), 5.81 (dd, $J = 8.9, 1.5$ Hz, 1H), 4.05 (ddd, $J = 11.4, 9.0, 2.6$ Hz, 1H), 3.84 (ddd, $J = 9.7, 6.8, 4.9$ Hz, 1H), 3.74 (ddd, $J = 10.0, 7.7, 6.0$ Hz, 1H), 3.07 (ddd, $J = 10.5, 8.5, 2.4$ Hz, 1H), 2.30 – 2.21 (m, 2H), 2.06 (dd, $J = 14.0, 2.6$ Hz, 1H), 1.87 (dtd, $J = 9.7, 7.4, 2.4$ Hz, 1H), 1.72 (ddt, $J = 14.1, 8.5, 5.5$ Hz, 1H), 1.36 – 1.24 (m, 1H), 1.13 – 1.02 (m, 24H), 0.92 (d, $J = 6.6$ Hz, 1H), 0.90 – 0.83 (m, 1H), 0.82 – 0.76 (m, 1H), 0.68 – 0.56 (m, 1H), 0.44 (s, 3H), 0.42 (s, 3H), 0.35 (dt, $J = 8.1, 4.9$ Hz, 1H); ^{13}C NMR (101 MHz, CDCl_3) δ 208.3, 144.1, 138.9, 138.1, 133.9, 129.3, 128.2, 79.5, 76.2, 60.0, 49.9, 48.0, 37.6, 26.7, 19.2, 18.3, 16.2, 14.2, 12.2, 9.5, -0.6, -0.8.

$[\alpha]_D^{20} -47.8$ (*c* 0.32, CHCl₃); IR (thin film, neat) 2944, 2865, 1717, 1462, 1250, 1096, 835, 771, 732 cm⁻¹; HRMS (ASAP+) calcd for C₃₁H₅₂O₃Si₂ [M+H]⁺: 529.3533, found: 529.3541.



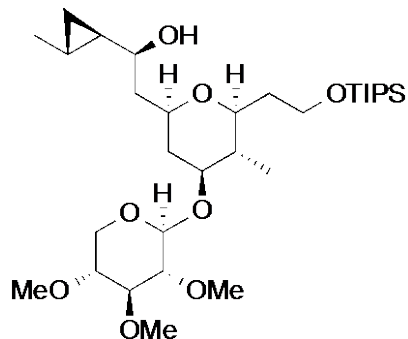
2-((2S,4S,5R,6S)-6-(2-(tert-butyldimethylsilyloxy)ethyl)-4-hydroxy-5-methyl-tetrahydro-2H-pyran-2-yl)-1-((1R,2R)-2-methylcyclopropyl)ethanone

To a solution of **3.40** (7.3 mg, 0.018 mmol) in MeOH (0.8 mL) at -10 °C was added NaBH₄ (0.5 mg, 0.01 mmol, 0.7 equiv.) in one portion. The mixture was stirred at -10 °C for 15 min, then was quenched with H₂O. After concentration, the crude product was used directly in the next step without further purification. To a solution of the ketone in MeOH (0.5 mL) at 0 °C was added K₂CO₃ (13 mg, 0.09 mmol) in one portion. The mixture was stirred for 30 min at 0 °C, then was quenched with NH₄Cl (5 mL) and extracted with Et₂O (2 x 10 mL). The combined organic layers were dried over MgSO₄ and purified by flash chromatography (15% to 25% EtOAc in hexane) to afford the desired product (6.1 mg, 81%, two steps). ¹H NMR (500 MHz, CDCl₃) δ 3.85 – 3.72 (m, 3H), 3.37 (td, *J* = 10.4, 4.7 Hz, 1H), 3.14 (td, *J* = 9.6, 2.2 Hz, 1H), 2.80 (dd, *J* = 15.6, 6.7 Hz, 1H), 2.55 (dd, *J* = 15.6, 6.0 Hz, 1H), 2.03 – 1.99 (m, 1H), 1.95 – 1.88 (m, 1H), 1.69 (dt, *J* = 8.3, 4.3 Hz, 1H), 1.61 – 1.51 (m, 1H), 1.43 – 1.36 (m, 1H), 1.28 – 1.22 (m, 4H), 1.11 (d, *J* = 6.0 Hz, 3H), 1.06 (s, br, 21H), 0.98 (d, *J* = 6.5 Hz, 3H), 0.71 (td, *J* = 7.2, 3.7 Hz, 1H); ¹³C NMR (101 MHz, CDCl₃) δ 208.3, 78.1, 73.5, 71.8, 60.2, 49.7, 43.8, 41.2, 36.5, 30.5, 20.4, 19.6, 18.3, 18.2, 13.1, 12.2; $[\alpha]_D^{20} -45.0$ (*c* 2.54, CHCl₃); IR (thin film, neat) 3443, 2942, 2866, 1693, 1463, 1404, 1381, 1094 cm⁻¹; HRMS (ESI) calcd for C₂₃H₄₅O₄Si [M+H]⁺: 413.3087, found: 413.3091.



2-((2*S*,4*S*,5*S*,6*S*)-5-Methyl-6-(2-
 ((triisopropylsilyl)oxy)ethyl)-4-(((2*S*,3*R*,4*S*,5*R*)-3,4,5-
 trimethoxytetrahydro-2*H*-pyran-2-yl)oxy)tetrahydro-2*H*-
 pyran-2-yl)-1-((1*R*,2*R*)-2-methylcyclopropyl)ethanone (3.44)

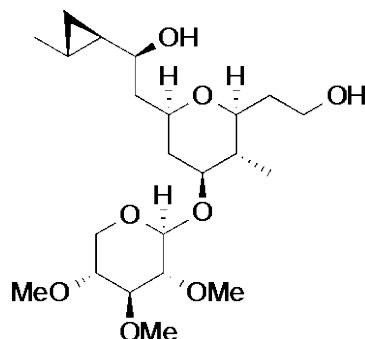
To a solution of the keto alcohol (199 mg, 0.484 mmol) in CH₂Cl₂ (13 mL) were added trichloroacetimidate **3.43** (0.5 M solution in CH₂Cl₂, 1.45 mL, 0.726 mmol) and 4Å MS (300 mg). The mixture was stirred for 30 min at rt then was cooled to -20 °C. TMSOTf (1.0 M solution in CH₂Cl₂, 65 µL, 0.063 mmol) was added dropwise. The reaction was stirred at -20 °C for 30 min then was warmed to rt slowly over 1 h. The reaction was quenched with Et₃N (5 drops) and purified by flash chromatography (25% EtOAc in hexane) to yield the desired product (148 mg, 52%). ¹H NMR (500 MHz, CDCl₃) δ 4.29 (d, *J* = 7.7 Hz, 1H), 3.97 (dd, *J* = 11.6, 5.2 Hz, 1H), 3.85 – 3.73 (m, 3H), 3.63 (s, 3H), 3.61 (s, 3H), 3.48 (s, 3H), 3.31 – 3.23 (m, 2H), 3.17 (td, *J* = 9.6, 2.2 Hz, 1H), 3.13 – 3.06 (m, 2H), 2.98 (dd, *J* = 9.1, 7.6 Hz, 1H), 2.79 (dd, *J* = 15.7, 6.9 Hz, 1H), 2.55 (dd, *J* = 15.7, 5.7 Hz, 1H), 2.16 (ddd, *J* = 12.5, 4.9, 1.9 Hz, 1H), 1.93 (dtd, *J* = 13.8, 7.6, 2.2 Hz, 1H), 1.70 (dt, *J* = 8.2, 4.2 Hz, 1H), 1.61 – 1.54 (m, 1H), 1.45 – 1.37 (m, 2H), 1.29 – 1.23 (m, 2H), 1.12 (d, *J* = 6.0 Hz, 3H), 1.06 (s, br, 21H), 1.02 (d, *J* = 6.4 Hz, 3H), 0.72 (ddd, *J* = 7.8, 6.4, 3.6 Hz, 1H); ¹³C NMR (126 MHz, CDCl₃) δ 208.3, 105.7, 85.7, 84.0, 83.6, 79.6, 78.3, 71.8, 63.4, 60.9, 60.2, 58.9, 49.7, 42.3, 40.4, 36.6, 30.5, 20.3, 19.5, 18.3, 18.2, 13.0, 12.2; [α]_D²⁰ -23.8 (*c* 0.66, CHCl₃); IR (thin film, neat) 3373, 3246, 2927, 2865, 1693, 1614, 1462, 1381, 1106, 834 cm⁻¹; HRMS (ESI) calcd for C₃₁H₅₉O₈Si [M+H]⁺: 587.3979 found: 587.3990.



(*S*)-2-((2*R*,4*S*,5*S*,6*S*)-5-Methyl-6-(2-
 ((triisopropylsilyl)oxy)ethyl)-4-(((2*S*,3*R*,4*S*,5*R*)-3,4,5-
 trimethoxytetrahydro-2*H*-pyran-2-yl)oxy)tetrahydro-2*H*-
 pyran-2-yl)-1-((1*R*,2*R*)-2-methylcyclopropyl)ethanol (**3.46**)

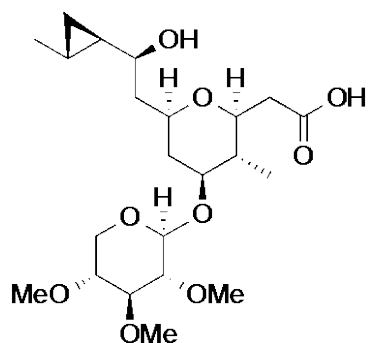
A solution of catalyst **3.45** (1M in toluene, 125 μ L, 0.049 mmol) was dried on a high vacuum pump for 1 h. The catalyst was dissolved in THF (3.5 mL) the resulting solution was cooled to -20 $^{\circ}$ C. A solution of $\text{BH}_3 \cdot \text{SMe}_2$ in THF (1M, 495 μ L, 0.495 mmol) was added. The mixture was stirred for 30 min at -20 $^{\circ}$ C, then the ketone **3.44** (144 mg, 0.245 mmol) in THF (1 mL) was added dropwise over 10 min. The reaction was stirred at -20 $^{\circ}$ C for 12h then was quenched with MeOH (5 mL, dropwise). Saturated NH_4Cl (15 mL) and EtOAc (20 mL) were added. After extraction with EtOAc (2 x 20 mL), the combined organic extracts were dried and concentrated. Purification by flash chromatography (20% EtOAc in hexane) provided the desired product (113 mg, 78%) and its diastereomer (13 mg, 9%). ^1H NMR (400 MHz, CDCl_3) δ 4.30 (d, $J = 7.6$ Hz, 1H), 3.97 (dd, $J = 11.6, 5.2$ Hz, 1H), 3.85 – 3.74 (m, 3H), 3.64 (s, 3H), 3.62 (s, $J = 1.6$ Hz, 3H), 3.49 (s, 3H), 3.29 – 3.23 (m, 4H), 3.15 – 3.09 (m, 2H), 3.00 (dd, $J = 9.1, 7.6$ Hz, 1H), 2.12 – 2.07 (m, 1H), 1.94 (tdd, $J = 8.7, 6.6, 2.5$ Hz, 1H), 1.84 – 1.74 (m, 1H), 1.74 – 1.66 (m, 1H), 1.64 – 1.56 (m, 1H), 1.53 – 1.44 (m, 2H), 1.08 (s br, 24H), 1.04 (d, $J = 6.5$ Hz, 3H), 0.81 – 0.71 (m, 1H), 0.61 (tt, $J = 8.6, 4.4$ Hz, 1H), 0.37 – 0.28 (m, 1H), 0.20 (dt, $J = 8.4, 4.8$ Hz, 1H). ^{13}C NMR (126 MHz, CDCl_3) δ 105.9, 85.8, 84.1, 83.5, 79.6, 78.4, 76.0, 75.9, 63.4, 61.0, 61.0, 59.8, 59.0, 42.9, 42.2, 41.0, 36.4, 26.4, 18.9, 18.3, , 13.1, 12.2, 11.3, 10.5. $[\alpha]_{\text{D}}^{20} -19.6$ (c 1.14, CHCl_3); IR (thin film, neat) 3490, 2942, 2866, 1731, 1463, 1369,

1162, 1095, 989, 884 cm^{-1} ; HRMS (ESI) calcd for $\text{C}_{31}\text{H}_{60}\text{O}_8\text{NaSi}$ $[\text{M}+\text{Na}]^+$: 611.3955 found: 611.3951.



**(S)-2-(((2R,4S,5S,6S)-6-(2-Hydroxyethyl)-5-methyl-4-
(((2S,3R,4S,5R)-3,4,5-trimethoxytetrahydro-2H-pyran-2-
yl)oxy)tetrahydro-2H-pyran-2-yl)-1-((1R,2R)-2-
methylcyclopropyl)ethanol**

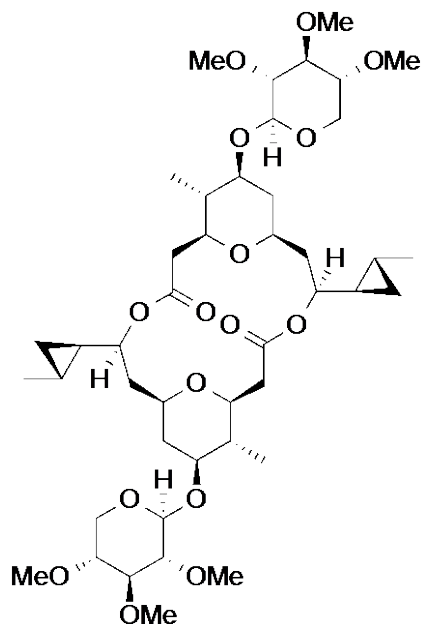
To a solution of the silyl ether **3.46** (108 mg, 0.184 mmol) in EtOH (6.4 mL) was added 1% HCl (1.95 mL). The solution was stirred at rt for 5h. The reaction was quenched with saturated NaHCO_3 (5 mL) and extracted with EtOAc (3 x 10 mL). The combined organic layers were dried over MgSO_4 and purified by flash chromatography (35% to 20% hexane in EtOAc) to afford the desired product (80 mg, 100%). ^1H NMR (400 MHz, CDCl_3) δ 4.27 (d, $J = 7.6$ Hz, 1H), 3.95 (dd, $J = 11.5, 5.2$ Hz, 1H), 3.79 – 3.72 (m, 2H), 3.61 (s, $J = 2.5$ Hz, 3H), 3.59 (s, 3H), 3.47 (s, $J = 2.7$ Hz, 3H), 3.28 – 3.20 (m, 3H), 3.12 – 3.04 (m, 3H), 2.97 (dd, $J = 9.1, 7.6$ Hz, 1H), 2.09 (ddd, $J = 12.7, 4.8, 2.0$ Hz, 1H), 1.99 – 1.88 (m, 1H), 1.81 (dt, $J = 14.4, 9.1$ Hz, 1H), 1.72 – 1.58 (m, 2H), 1.53 – 1.35 (m, 2H), 1.05 (d, $J = 5.9$ Hz, 3H), 1.00 (d, $J = 6.5$ Hz, 3H), 0.79 – 0.69 (m, 1H), 0.64 – 0.57 (m, 1H), 0.31 (dt, $J = 8.4, 4.7$ Hz, 1H), 0.22 (dt, $J = 8.3, 4.8$ Hz, 1H); ^{13}C NMR (101 MHz, CDCl_3) δ 105.8, 85.8, 84.0, 83.2, 81.1, 79.6, 76.0, 75.7, 63.5, 61.1, 61.0, 60.6, 59.1, 42.8, 42.5, 35.2, 26.9, 18.9, 14.4, 13.0, 11.4, 10.8; $[\alpha]_{\text{D}}^{20}$ –20.5 (*c* 0.57, CHCl_3); IR (thin film, neat) 3427, 2930, 1455, 1372, 1326, 1162, 1090, 988 cm^{-1} ; HRMS (ESI) calcd for $\text{C}_{22}\text{H}_{40}\text{NaO}_8$ $[\text{M}+\text{Na}]^+$: 455.2621 found: 455.2620.



2-((2*S*,3*S*,4*S*,6*R*)-6-((*S*)-2-Hydroxy-2-((1*R*,2*R*)-2-methylcyclopropyl)ethyl)-3-methyl-4-(((2*S*,3*R*,4*S*,5*R*)-3,4,5-trimethoxytetrahydro-2*H*-pyran-2-yl)oxy)tetrahydro-2*H*-pyran-2-yl)acetic acid (3.47)

To a solution of the diol (10 mg, 0.024 mmol) in CH₂Cl₂ (110 μL) was added TEMPO (0.2 mg, 0.001 mmol) and saturated NaHCO₃ (60 μL). KBr (5 μL, 0.002 mmol, 0.5M aq. stock solution) and Bu₄NCl (25 μL, 0.0017 mmol, 0.08M aq stock solution) were added subsequently and the mixture was cooled to 0 °C. To the vigorously stirring biphasic solution was added a stock solution of sat. NaHCO₃ (35 μL), brine (65 μL) and bleach (95 μL, 0.065 mmol, 0.7 M) dropwise over 45 min. The mixture was allowed to stir for an additional 30 min at 0 °C upon completion of the addition. The solution was then diluted with H₂O (5 mL) and EtOAc (5 mL). The diluted mixture was acidified with 10% citric acid (4 drops) to pH 3-4. The aqueous layer was extracted with EtOAc (3 x 5mL). The combined organic extracts were dried over MgSO₄. The crude colorless oil (8 mg, 78%) was determined pure by ¹H NMR and used without further purification. ¹H NMR (400 MHz, CDCl₃) δ 4.26 (d, *J* = 7.6 Hz, 1H), 3.94 (dd, *J* = 11.5, 5.1 Hz, 1H), 3.61 (s, 3H), 3.58 (s, 3H), 3.46 (s, 3H), 3.30 – 3.20 (m, 3H), 3.13 – 3.07 (m, 3H), 2.97 (dt, *J* = 9.0, 4.8 Hz, 1H), 2.67 (d, br, *J* = 14.7 Hz, 1H), 2.40 (m, 1H), 2.14 – 2.02 (m, 1H), 1.78 (dt, *J* = 15.0, 9.8 Hz, 1H), 1.72 – 1.65 (m, 1H), 1.55 – 1.40 (m, 2H), 1.01 (d, *J* = 6.6 Hz, 3H), 1.00 (d, *J* = 5.8 Hz, 3H), 0.92 – 0.79 (m, 1H), 0.78 – 0.68 (m, 1H), 0.57 (tt, *J* = 8.7, 4.5 Hz, 1H), 0.28 – 0.20 (m, 1H), 0.16 (dt, *J* = 8.7, 4.9 Hz, 1H); ¹³C NMR (101 MHz, CDCl₃) δ 173.7, 105.7, 85.7, 83.9, 82.6, 79.5, 78.4, 77.63, 76.9, 63.4, 61.0, 61.0, 59.0, 42.1, 41.8, 40.7, 38.7, 25.8, 18.7, 12.8, 12.0,

10.4; $[\alpha]_D^{20} -24$ (c 2.1, CHCl_3); IR (thin film, neat) 3455, 2926, 1731, 1457, 1373, 1327, 1257, 1162, 1091 cm^{-1} ; HRMS (ESI) calcd for $\text{C}_{22}\text{H}_{38}\text{NaO}_9$ $[\text{M}+\text{Na}]^+$: 469.2414 found: 469.2436.



Clavosolide A (3.1)

To the seco acid **3.47** (6.0 mg, 0.014 mmol) in THF (0.8 mL) was added Et_3N (40 μL , 0.28 mmol) and 2,4,6-trichlorobenzoyl chloride (25 μL , 0.14 mmol) dropwise. The reaction was allowed to stir for 2.5 h at rt and the $\text{Et}_3\text{N}\cdot\text{HCl}$ salt was removed by filtration. The filtrate was diluted with toluene (0.8 mL) and added dropwise over 5 h to a stirred solution of DMAP (16 mg, 0.132 mmol) in toluene (13 mL) at 90°C via a syringe pump. The reaction was cooled to rt and allowed to stir for another 12h. The reaction mixture was quenched with aq. NH_4Cl (5 mL), extracted with EtOAc (2 x 5mL) and concentrated under vacuum. Purification by flash chromatography (45% to 35% hexanes in EtOAc) provided the natural product as a white solid (2.6 mg, 44%). ^1H NMR (601 MHz, CDCl_3) δ 4.42 (td, $J = 8.9, 2.0$ Hz, 1H), 4.26 (d, $J = 7.6$ Hz, 1H), 3.95 (dd, $J = 11.6, 5.2$ Hz, 1H), 3.61 (s, 3H), 3.58 (s, 3H), 3.46 (s, 3H), 3.44 (qd, $J = 4.3, 1.4$ Hz, 2H), 3.27 – 3.21 (m, 1H), 3.09 (ddd, $J = 10.1, 7.9, 3.2$ Hz, 2H), 2.96 (dd, $J = 9.1, 7.6$ Hz, 1H), 2.54 (dd, $J = 17.4, 3.6$ Hz, 1H), 2.41 (dd, $J = 17.3, 6.6$ Hz, 1H), 2.04 (ddd, $J = 12.7, 4.8, 1.8$ Hz, 1H), 1.89 (dt, $J = 15.0, 9.0$ Hz, 1H), 1.68 (ddd, $J = 15.1, 3.5, 2.1$ Hz, 1H), 1.41 – 1.34 (m, 2H), 0.97 (d, $J = 5.1$ Hz, 3H), 0.85 – 0.78 (m, 1H), 0.71 (tt, $J = 8.8, 4.6$ Hz, 1H), 0.34 (dt, $J = 8.4, 4.7$ Hz, 1H), 0.22 (dt, $J = 8.3, 4.9$ Hz, 1H); ^{13}C NMR (151 MHz, CDCl_3) δ 171.3, 105.7, 85.8, 84.1, 83.4, 79.6, 77.5, 77.3, 75.1, 63.5, 61.0, 61.0, 59.0, 42.8, 41.5, 40.9, 39.5, 25.0, 18.7,

12.8, 12.1, 11.1; $[\alpha]_D^{20} -41.3$ (*c* 0.1, CHCl₃); IR (thin film, neat) 2945, 1734, 1165, 1089 cm⁻¹;
HRMS (ESI) calcd for C₄₄H₇₂NaO₁₆ [M+Na]⁺: 879.4716 found: 879.4739; m.p: 249-252 °C.

BIBLIOGRAPHY

- [1] R. Crabtree, H., *J. Chem. Soc., Dalton Trans.* **2001**, 2437-2450.
- [2] S. Blanksby, J., G. B. Ellison, *Acc. Chem. Res.* **2003**, *36*, 255-263.
- [3] K. Godula, D. Sames, *Science* **2006**, *312*, 67-72.
- [4] K. Chen, J. M. Richter, P. S. Baran, *J. Am. Chem. Soc.* **2008**, *130*, 7247-7249.
- [5] M. C. White, M. S. Chen, *Science* **2007**, *318*, 783-787.
- [6] A. Sharma, J. F. Hartwig, *Nature* **2015**, *517*, 600-604.
- [7] Y. Hayashi, T. Mukaiyama, *Chem. Lett.* **1987**, *16*, 1811-1814.
- [8] W. Tu, L. Liu, P. E. Floreancig, *Angew. Chem. Int. Ed.* **2008**, *47*, 4184-4187.
- [9] G. J. Brizgys, H. H. Jung, P. E. Floreancig, *Chem. Sci.* **2012**, *3*, 438-442.
- [10] Y. Cui, P. E. Floreancig, *Org. Lett.* **2012**, *14*, 1720-1723.
- [11] H. W. Whitlock, *J. Am. Chem. Soc.* **1998**, *63*, 7982-7989.
- [12] D. J. Clausen, P. E. Floreancig, *J. Org. Chem.* **2012**, *77*, 6574-6582.
- [13] Y. Cui, L. A. Villafane, D. J. Clausen, P. E. Floreancig, *Tetrahedron* **2013**, *69*, 7618-7626.
- [14] S. A. Rizvi, D. S. Courson, V. A. Keller, R. S. Rock, S. A. Kozmin, *Proc. Natl. Acad. Sci. U. S. A.* **2008**, *105*, 4088-4092.
- [15] J. Huang, J. R. Yang, J. Zhang, J. Yang, *J. Am. Chem. Soc.* **2012**, *134*, 8806-8809.

- [16] A. W. Hung, A. Ramek, Y. Wang, T. Kaya, J. A. Wilson, P. A. Clemons, D. W. Young, *Proc. Natl. Acad. Sci. U. S. A.* **2011**, *108*, 6799-6804.
- [17] Y. Ohtake, T. Sato, T. Kobayashi, M. Nishimoto, N. Taka, K. Takano, K. Yamamoto, M. Ohmori, M. Yamaguchi, K. Takami, S.-Y. Yeu, K.-H. Ahn, H. Matsuoka, K. Morikawa, M. Suzuki, H. Hagita, K. Ozawa, K. Yamaguchi, M. Kato, S. Ikeda, *J. Med. Chem.* **2012**, *55*, 7828-7840.
- [18] a) P. M. Pihko, A. J. E., *Org. Lett.* **2004**, *6*, 3849-3852; b) F. Allais, J. Cossy, *Org. Lett.* **2006**, *8*, 3655-3657; c) M. Gaunt, D. F. Hook, H. R. Tanner, S. V. Ley, *Org. Lett.* **2003**, *5*, 4815-4818.
- [19] J. S. Yadav, M. A. Rahman, N. M. Reddy, A. R. Prasad, *Tetrahedron Lett.* **2015**, *56*, 365-367.
- [20] J. Hao, C. J. Forsyth, *Tetrahedron Lett.* **2002**, *43*, 1-2.
- [21] I. E. Markó, A. Mekhafia, D. J. Bayston, H. Adams, *J. Org. Chem.* **1992**, *57*, 2211-2213.
- [22] J. M. Wurst, G. Liu, D. S. Tan, *J. Am. Chem. Soc.* **2011**, *133*, 7916-7925.
- [23] S. B. Moilanen, J. S. Potuzak, D. S. Tan, *J. Am. Chem. Soc.* **2006**, *128*, 1792-1793.
- [24] M. E. Sous, D. Ganame, P. A. Tregloan, M. A. Rizzacasa, *Org. Lett.* **2004**, *6*, 3001-3004.
- [25] M. T. Crimmins, J. D. Katz, *Org. Lett.* **2000**, *2*, 957-960.
- [26] B. Liu, J. K. De Brabander, *Org. Lett.* **2006**, *8*, 4907-4910.
- [27] S. Selvaratnam, J. H. H. Ho, P. B. Huleatta, B. A. Messerle, C. L. L. Chai, *Tetrahedron Lett.* **2009**, *50*, 1125-1127.
- [28] B. A. Messerle, K. Q. Vuong, *Pure Appl. Chem.* **2006**, *78*, 385-390.
- [29] B. B. Butler Jr, J. N. Manda, A. Aponick, *Org. Lett.* **2015**, *17*, 1902-1905.
- [30] J. S. Sperry, Y.-C. Liu, M. A. Brimble, *Org. Biomol. Chem.* **2010**, 29-38.

- [31] P. Wipf, T. D. Hopkins, *Chem. Commun.* **2005**, 3421-3423.
- [32] K. Meilert, M. A. Brimble, *Org. Biomol. Chem.* **2006**, 2184-2192.
- [33] I. Paterson, C. J. Cowden, V. S. Rahn, M. D. Woodrow, *Synlett* **1998**, 8, 915-917.
- [34] A. M. Gómez, F. Lobo, C. Uriel, J. C. López, *Eur. J. Org. Chem.* **2013**, 2013, 7221-7262.
- [35] K. Toshima, T. Ishizuka, G. Matsuo, M. Nakata, M. Kinoshita, *J. Chem. Soc., Chem. Commun.* **1993**, 704-706.
- [36] B. S. Kumar, A. Dhakshinamoorthy, K. Pitchumani, *Catal. Sci. Technol.* **2014**, 4.
- [37] K. Toshima, G. Matsuo, T. Ishizuka, Y. Ushiki, M. Nakata, S. Matsumura, *J. Org. Chem.* **1998**, 63, 2307-2313.
- [38] S. Danishefsky, T. Kitahara, *J. Am. Chem. Soc.* **1974**, 96, 7807-7808.
- [39] A. G. Dossett, T. F. Jamison, E. N. Jacobsen, *Angew. Chem. Int. Ed.* **1999**, 38, 2398-2400.
- [40] P. J. Hajduk, W. R. J. D. Galloway, *Nature* **2011**, 470, 42-43.
- [41] A. Rosiak, J. Christoffers, *Tetrahedron Lett.* **2006**, 47, 5095-5097.
- [42] R. M. Carlson, *Tetrahedron Lett.* **1978**, 19, 111-114.
- [43] B. A. Narayanan, W. H. Bunnelle, *Tetrahedron Lett.* **1987**, 28, 6161-6264.
- [44] a) A. Fujii, S. Hashiguchi, N. Uematsu, T. Ikariya, R. Noyori, *J. Am. Chem. Soc.* **1996**, 118, 2521-2522; b) Z. Fang, M. Wills, *J. Org. Chem.* **2013**, 78, 8594-8605.
- [45] E. J. Corey, C. J. Helal, *Angew. Chem. Int. Ed.* **1998**, 37, 1986-2012.
- [46] M. A. Casadei, C. Galli, L. Mandolini, *J. Am. Chem. Soc.* **1984**, 106, 1051-1056.
- [47] R. E. Ireland, M. G. Smith, *J. Am. Chem. Soc.* **1988**, 110, 854-860.

- [48] a) N. Miyaoura, T. Ishiyama, H. Sasaki, M. Ishikawa, M. Sato, A. Suzuki, *J. Am. Chem. Soc.* **1989**, *111*, 314-321; b) J. A. Marshall, B. A. Johns, *J. Org. Chem.* **1998**, *63*, 7885-7892.
- [49] a) F. Johnson, S. K. Malhotra, *J. Am. Chem. Soc.* **1965**, *87*, 5492-5493; b) F. Johnson, *Chem. Rev.* **1968**, *68*, 375-413.
- [50] H. H. Jung, P. E. Floreancig, *Tetrahedron* **2009**, *65*, 10830-10836.
- [51] D.-C. Xiong, L.-H. Zhang, X.-S. Ye, *Org. Lett.* **2009**, *11*, 1709-1712.
- [52] a) G. A. Molander, S. L. J. Trice, S. D. Dreher, *J. Am. Chem. Soc.* **2010**, *132*, 17701-17703; b) T. Leermann, F. R. Leroux, F. Colobert, *Org. Lett.* **2011**, *13*, 4479-4481.
- [53] J. L. Luche, *J. Am. Chem. Soc.* **1978**, *100*, 2226-2227.
- [54] H. C. Brown, P. K. Jadhav, *J. Am. Chem. Soc.* **1983**, *105*, 2092-2093.
- [55] K. Peng, F. Chen, X. She, C. Yang, Y. Cui, X. Pan, *Tetrahedron Lett.* **2005**, *46*, 1217-1220.
- [56] J. C. Y. Cheng, G. D. Daves, *J. Org. Chem.* **1987**, *52*, 3083-3090.
- [57] M. R. Rao, D. J. Faulkner, *J. Nat. Prod.* **2002**, *65*, 386-388.
- [58] K. L. Erickson, K. R. Gustafson, L. K. Pannell, J. R. Beutler, M. R. Boyd, *J. Nat. Prod.* **2002**, *65*, 1303-1306.
- [59] X. Fu, F. J. Schmitz, M. Kelly-Borges, T. L. McCready, C. F. B. Holmes, *J. Org. Chem.* **1998**, *63*, 7957-7963.
- [60] K. L. Erickson, K. R. Gustafson, L. K. Pannell, J. A. Beutler, M. R. Boyd, *J. Nat. Prod.* **2002**, *65*, 1303-1306.
- [61] C. S. Barry, N. Bushby, J. P. H. Charmant, J. D. Elsworth, J. R. Harding, C. L. Willis, *Chem. Commun.* **2005**, 5097-5099.

- [62] J. B. Son, S. N. Kim, N. Y. Kim, D. H. Lee, *Org. Lett.* **2006**, *8*, 661-664.
- [63] A. B. I. Smith, V. Simov, *Org. Lett.* **2006**, *8*, 3315-3318.
- [64] P. T. Seden, J. P. H. Charmant, C. L. Willis, *Org. Lett.* **2008**, *10*, 1637-1640.
- [65] A. de Meijere, *Angew. Chem. Int. Ed.* **1979**, *18*, 809-826.
- [66] a) M. Hanack, H. J. Schneider, *Angew. Chem. Int. Ed.* **1967**, *6*, 666-677; b) G. A. Olah, C. L. Jeuell, D. P. Kelly, R. D. Porter, *J. Am. Chem. Soc.* **1972**, *94*, 146-156; c) M. Saunders, K. E. Laidig, K. B. Wiberg, P. v. R. Schleyer, *J. Am. Chem. Soc.* **1988**, *110*, 7652-7659.
- [67] G. A. Olah, V. P. Reddy, G. K. S. Prakash, *Chem. Rev.* **1992**, *92*, 69-95.
- [68] a) L. Liu, P. E. Floreancig, *Org. Lett.* **2009**, *11*, 3152-3155; b) L. Liu, P. E. Floreancig, *Angew. Chem. Int. Ed.* **2010**, *122*, 3133-3136; c) L. Liu, P. E. Floreancig, *Angew. Chem. Int. Ed.* **2010**, *49*, 5894-5897.
- [69] W. C. Poon, G. B. Dudley, *J. Org. Chem.* **2006**, *71*, 3923-3927.
- [70] L. J. Goossen, J. Paetzold, D. Koley, *Chem. Commun.* **2003**, 706-707.
- [71] W. Tu, P. E. Floreancig, *Angew. Chem. Int. Ed.* **2009**, *48*, 4567-4571.
- [72] E. Anderson, D. Lim, *Synthesis* **2012**, *44*, 983-1010.
- [73] T. den Hartog, A. Rudolph, B. Maciá, A. J. Minnaard, B. L. Feringa, *J. Am. Chem. Soc.* **2010**, *132*, 14349-14351.
- [74] O. G. Kulinkovich, I. G. Tischenko, V. L. Sorokin, *Synthesis* **1985**, 1058-1059.
- [75] E. Negishi, A. O. King, W. L. Klima, W. Patterson, A. Silveira, *J. Org. Chem.* **1980**, *45*, 2526-2528.
- [76] J. A. Marshall, N. D. Adams, *J. Org. Chem.* **1998**, *63*, 3812-3813.

- [77] H. C. Aspinall, N. Greeves, W.-M. Lee, E. G. McIver, P. M. Smith, *Tetrahedron Lett.* **1997**, *38*, 4679-4682.
- [78] B. M. Trost, Z. T. Ball, *J. Am. Chem. Soc.* **2005**, *127*, 17644-17655.
- [79] R. Crabtree, H., *Acc. Chem. Res.* **1979**, *12*, 331-337.
- [80] M. Krel, J. Y. Lallemand, C. Guillou, *Synlett* **2005**, *26*, 2043-2046.
- [81] R. R. Schmidt, M. Josef, *Angew. Chem. Int. Ed.* **1980**, *19*, 731-732.
- [82] a) H. Kim, J. Hong, *Org. Lett.* **2010**, *12*, 2880-2883; b) P. T. Seden, J. P. H. Charmant, C. L. Willis, *Org. Lett.* **2008**, *10*, 1637-1640.
- [83] T. K. Chakraborty, V. R. Reddy, P. K. Gajula, *Tetrahedron* **2008**, *64*, 5162-5167.
- [84] E. J. Corey, C. J. Helal, *Tetrahedron Lett.* **1995**, *36*, 9153-9156.
- [85] P. Lucio Anelli, C. Biffi, F. Montanari, S. Quici, *J. Org. Chem.* **1987**, *52*, 2559-2562.
- [86] J. Inanaga, K. Hirata, H. Saeki, T. Katsuki, M. Yamaguchi, *Bull. Chem. Soc. Jpn.* **1979**, *52*, 1989-1993.